# UNIVERSITA' DEGLI STUDI DI PARMA

Dottorato di Ricerca in Scienze Chimiche

Ciclo XXVIII (2013-2015)

# Calix[6]arene Derivatives as Pivotal Components of Working Devices and Molecular Machine Prototypes

Coordinatore:
Chiar.mo Prof. Cammi Roberto

Tutor:
Chiar.mo Prof. Arduini Arturo

Dottorando: **Orlandini Guido**

**2016**

**Abstract**

This Ph.D. thesis describes the synthesis, characterization and study of calix[6]arene derivatives as pivotal components for the construction of molecular machine prototypes. Initially, the ability of a calix[6]arene wheel to supramolecularly assist and increase the rate of a nucleophilic substitution reaction was exploited for the synthesis of two constitutionally isomeric oriented rotaxanes. Then, the synthesis and characterization of several hetero-functionalised calix[6]arene derivatives and the possibility to obtain molecular muscle prototypes was reported. The ability of calix[6]arenes to form oriented pseudorotaxane towards dialkyl viologen axles was then exploited for the synthesis of two calixarene-based [2]catenanes. As last part of this thesis, studies on the electrochemical response of the threading-dethreading process of calix[6]arene-based pseudorotaxanes and rotaxanes supported on glassy carbon electrodes are reported.

Keywords: molecular machines, pseudorotaxanes, rotaxanes, catenanes, calix[6]arenes, viologen salts, cyclic voltammetry, glassy carbon electrodes, self-assembly, supramolecular chemistry.

# CONTENTS

**General Introduction**…… **10**

References……. 11

**Chapter 1**

**Mechanically interlocked molecules as molecular level machines: state of the art**……..…… **13**

1.1 Supramolecular Chemistry: general aspects..…..…….. 14

1.2 Mechanically interlocked molecule (MIM) architectures and their syntheses 16

1.3 MIM as molecular machines……..……... 19

1.4 Calix[6]arene-Based molecular machines and devices……..……... 24

References……... 34

**Chapter 2**

**Supramolecularly assisted synthesis of two isomeric oriented calix[6]arene-based rotaxanes**…….……...…….. **37**

2.1 Introduction……...……...……. 38

2.2 Host-Guest complex between tris(*N*-phenylureido)calix[6]arene and *N*-alkyl-4,4'-bipyridinium salts.……...……. 40

2.3 Supramolecular assistance of calix[6]arene in a nucleophilic substitution reaction..... 42

2.4 Kinetical and thermodynamical control for the synthesis of two oriented rotaxanes..... 49

**2.5 Steering the spectroscopic behavior of calix[6]arene wheels bearing naphthyl groups through pseudorotaxane formation**..... **57**

2.5.1 Introduction..... 57

2.5.2 Design and synthesis of the wheels..... 58

2.5.3 Spectroscopic and photophysical experiments on the calixarenes and their pseudorotaxanes..... 63

2.6 Conclusions and perspectives..... 72

Experimental section..... 74

References..... 80

**Chapter 3**

**Towards the synthesis of a calix[6]arene-based molecular muscle**..... **81**

3.1 Introduction..... 82

3.2 Design and synthesis of a calix[6]arene based daisy chain..... 84

3.3 Design and synthesis of [3]rotaxanes..... 105

3.4 Conclusions and perspectives..... 113

Experimental section..... 114

References…….. 122

**Chapter 4**

**Synthesis by Ring Closing Metathesis and properties of electroactive calix[6]arene [2]catenanes 125**

4.1 Introduction……...…… 126

4.2 Design and synthesis of the axle……...…… 128

4.3 Synthesis and characterization of a symmetric [2]catenane……...……... 131

4.4 Design and synthesis of an asymmetric [2]catenane…..…….. 133

4.5 Electro- and photochemical studies on a [2]catenane……...…… 138

4.6 Conclusions and perspectives……...……. 141

Experimental section……... 142

References……... 148

**Chapter 5**

**Electrochemical response of the threading-dethreading process of calix[6]arene-based pseudorotaxanes anchored on glassy carbon electrodes..** 151

5.1 Introduction……...……...…… 152

5.2 Design and synthesis of calix[6]arene derivatives suitable for GC electrodes modification……. 155

5.3 Modification of glassy carbon electrodes with pseudorotaxane systems…….. 162

5.4 Conclusions and perspectives……..……...……... 177

Experimental section……... 178

References……... 187

# PREFACE

# General Introduction

# General Introduction

Every chemical entity can be considered as specie endowed with a characteristic and peculiar asset of structural information that is responsible of its physical properties and determines its reactivity. The understanding of these properties is still a focal objective of chemical sciences and will surely contribute to the development of modern nanotechnology.

The theoretical bases of non-covalent interactions[1,2] devised by J. D. van der Waals at the beginning of the last Century, the concept of receptor formulated by Paul Ehrlich,[3] the "lock-and-key" idea by Emil Fisher[4] and the theoretical bases of coordination chemistry by Alfred Werner,[5] together with the development of synthetic chemistry, paved the way for the birth of *Supramolecular Chemistry*, pionereed by D. Cram[6], C. Pedersen[7] and J. M. Lehn. [8] The principles and methods of this highly interdisciplinary branch of chemistry brought to the extension of the concepts of molecular machine down to the molecular level as envisaged by R. Feynman[9] and applied to a supramolecular context by J. F. Stoddart.[10,11]

This thesis deals with the synthesis, characterization and study of calix[6]arene derivatives as pivotal components for the construction of molecular machine prototypes. In particular these studies have been focused on:

- *Chapter 1*: the state of the art of molecular interlocked molecules as molecular level machines and their perspectives as working devices;

- *Chapter 2*: the synthesis and characterization of two constitutionally isomeric oriented rotaxanes, exploiting the ability of a calix[6]arene wheel to supramolecularly assist and increase the rate of a nucleophilic substitution reaction.

- *Chapter 3*: the synthesis and characterization of several hetero-functionalised calix[6]arene derivatives, the study of their properties in solution and the possibility to exploit their features for the synthesis of a molecular muscle prototype.

- *Chapter 4*: the synthesis and characterization of two calix[6]arene based [2]catenanes obtained by using the synthetic strategy of an intramolecular ring closing metathesis and the study of their electro- and photochemical properties.

- *Chapter 5*: evaluating the electrochemical response of the threading-dethreading process of calix[6]arene-based pseudorotaxanes and rotaxanes supported on glassy carbon electrodes.

## References


(1) Margenau, H.; Kestner, N. R. *Theory of Intermolecular Forces*; Elsevier, 1969.

(2) Maitland, G. C.; Smith, E. B. *Chem. Soc. Rev.* **1973**, *2* (2), 181.

(3) Cay-Rüdiger Prüll. *Med. Hist.* **2003**, *47* (03), 332–356.

(4) Fischer, E. *Berichte der Dtsch. Chem. Gesellschaft* **1894**, *27* (3), 2985–2993.

(5) Constable, E. C.; Housecroft, C. E. *Chem. Soc. Rev.* **2013**, *42* (4), 1429–1439.

(6) Cram, D. J. *Angew. Chemie Int. Ed. English* **1988**, *27* (8), 1009–1020.

(7) Pedersen, C. J. *Angew. Chemie Int. Ed. English* **1988**, *27* (8), 1021–1027.

(8) Lehn, J.-M. *Angew. Chemie Int. Ed. English* **1988**, *27* (1), 89–112.

(9) Feynman, R. *Eng. Sci.* **1960**, *23*, 22.

(10) Balzani, V.; Gómez-López, M.; Stoddart, J. F. *Acc. Chem. Res.* **1998**, *31* (7), 405–414.

(11) Balzani, V.; Credi, A.; Raymo, F.; Stoddart, J. *Angew. Chem. Int. Ed. Engl.* **2000**, *39* (19), 3348–3391.

# CHAPTER 1

# Mechanically Interlocked Molecules as Molecular Level Machines: State of the Art

# Chapter 1

# Mechanically Interlocked Molecules as Molecular Level Machines: State of the Art

## 1.1 Supramolecular Chemistry: General Aspects

Since the beginning of the Industrial Era, the progress of technology was strictly connected to the construction of new working devices and machines. Over the years, together with the development of these technologies, remarkable efforts to miniaturize the components employed for the construction of devices and machines were established.

The approach employed for the miniaturization of components and the realization of new nanodevices was defined as the "top-down approach".[1] It consists in the use of suitable techniques for the miniaturization of the components needed for such devices.[2,3] However it is becoming evident that this approach is subject to intrinsic limitations for objects smaller than 100 nm.[4–6] The "bottom-up approach" seems to offer an alternative and more promising strategy for the obtainment of devices at the nanometre scale.[7] Such approach utilises nano or subnanoscale objects (atoms or molecules) to build up nanostructures endowed with specific functions.[8–11]

The principles and methods of Supramolecular Chemistry[12,13] have been considered as convenient tools to assemble the components of nanodevices and thus for the development of nanotechnologies.[14,15] Supramolecular chemistry indicates a branch of chemistry beyond the molecules and focuses on chemical systems composed by a discrete number of molecular subunits or components that spontaneously assemble

through non-covalent interactions. Differently from traditional chemistry, which gathers on the manipulation of covalent bonds, supramolecular chemistry exploits the reversible non-covalent interactions between different chemical species either charged or neutral, in the solid, liquid or gas phase. Hydrogen and halogen bonding, metal coordination, hydrophobic forces, van der Waals forces, π-π, CH-π and Coulomb interactions, are among the driving forces that hold assembled the components of a supramolecular system.[12,13] Although these interactions are particularly weak, when operating in a co-operative manner, they can afford stable supramolecular complexes, and thus they are a powerful tool to organize in space chemical species to endow the aggregates with specific functions. Within this context, a host is defined as the molecular entity possessing convergent binding sites (Lewis basic donor atoms, hydrogen bond donors, etc.), while the guest possesses divergent and complementary binding site. Usually, but not necessarily, the host is a large molecule or an aggregate such as a synthetic macrocycle or an enzyme endowed with a central hole or a cavity. The guest may be a cation, an anion, an ion pair, a neutral species or a more sophisticated molecule. [16,17]

When compared with their acyclic analogues, the complexes formed by macrocyclic hosts are endowed with an additional stability by what is traditionally defined as macrocyclic effect.[18,19] This effect relates not only to the binding of the guest by multiple sites, but also to their preorganization. Another key parameter for the modelling and designing of *Host-Guest* complex is complementarity between the host and the guest, in term of binding affinity. In order to be efficient, a host needs to complement the binding sites of the guest through a specific arrangement of its own binding functions.

The use of *Host-Guest* chemistry for the development of new supramolecular devices and machine prototype has stimulated great interest in the recent decades. Countless examples of working devices and molecular level machines endowed with specific functions were engendered through the use of well-defined and shaped molecules exploring the principles of the "bottom-up approach".[9,20,21,22]

## 1.2 Mechanically Interlocked Molecule (MIM) Architectures and their Syntheses

A peculiar class of supramolecular complexes are pseudorotaxanes. They are supramolecular assemblies constituted by a molecular species having an axial symmetry that threads a macrocycle as depicted in Figure 1. In an accepted jargon, the term "wheel" refers to the cyclic component, the term "axle" to the linear component.[15] The stability of this complex is determined by the nature and the magnitude of the intermolecular interactions between the two components. [n]Pseudorotaxane systems, whose number of components is indicated in square-brackets before the name, are considered as ideal platform for the synthesis of mechanically interlocked molecules (MIM) named rotaxanes, catenanes, etc. [23]

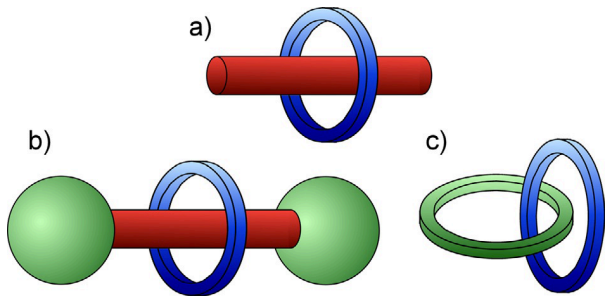


**Figure 1.** Schematic representation of (a) a [2]pseudorotaxane complex, (b) a [2]rotaxane, and (c) a [2]catenane.

Almost all the synthetic strategies so far devised for the synthesis of rotaxanes, require a [n]pseudorotaxane precursor.[24,25] For example, the following synthetic pathways have been devised for the obtainment of interlocked structures (Figure 2): *a*) end-capping of the linear component with bulky groups, a process usually called as "stoppering", results in the formation of a [2]rotaxane,[26,27] while *b*) macrocyclization of the axle component affords a [2]catenane.[28,29] Rotaxane architectures were also obtained through a "clipping" strategy, in which the macrocycle is clipped around the pre-

existing axial dumbbell.[30,31] Another promising approach for the synthesis of [n]rotaxanes is the "slippage", that consists in the separate synthesis of the rotaxane components, both the axle and the dumbbell, that are then heated in solution in a process in which the macrocycle slips over the dumbbell's stoppers to afford the thermodynamically favoured rotaxane.[32]

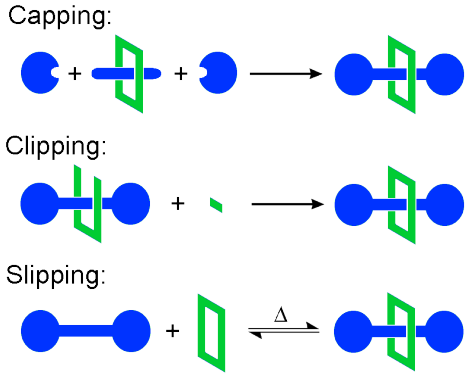


**Figure 2**. General synthetic approaches to rotaxane synthesis.

A particular kind of molecular architecture reported in literature, those belonging to the class of daisy chains, received great attentions. A molecular daisy chain is an array of identical molecules that consist of both the axial component (guest) and the macrocycle wheel (host) that are covalently bound together.[33,34] Intermolecular recognition, rather than intramolecular, may control the threading of the macrocycle by the guest section of another component (preventing self-complexation) (Figure 3). The insertion of a stopper unit prevents dethreading of these supramolecularly assembled daisy chains and converts the supramolecular association into mechanically interlocked daisy chains.

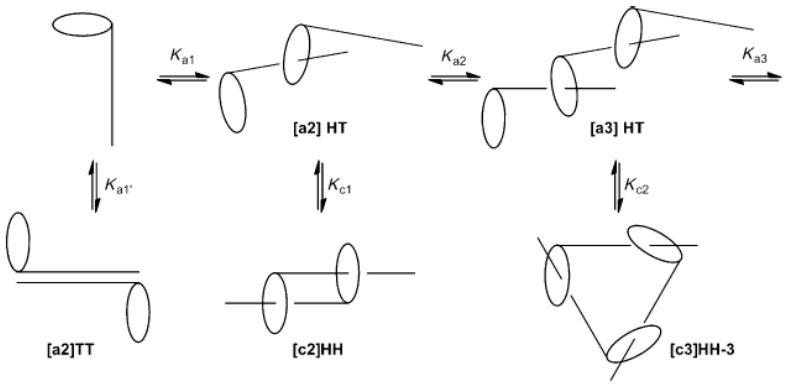


**Figure 3.** Possible aggregates formed by daisy chain monomers. Reprinted with permission from ref. 34. Copyright © Royal Society of Chemistry.

Each of these strategies requires a precise orientation of two or more molecules before the final step, in which the formation of a covalent bond fixes the shape of the molecule. Quite often, the concepts of molecular recognition and *Host-Guest* chemistry were exploited for the preorganization of the system prior to the final synthetic step. The synthetic strategy for the obtainment of these structures is thus performed under kinetical control. This latter strategy may results in the irreversible formation of undesired products, such as a non-complexed dumbbell or a non-catenated ring, with the result of a poor efficiency of the interlocking reaction.[35]

In recent years, a new thermodynamically controlled approach was established for the synthesis of MIMA's, in which side products, thanks to the use of reversible bonds, are recycled in the reactive mixture to finally afford the thermodynamically most stable product (Figure 4).[36]

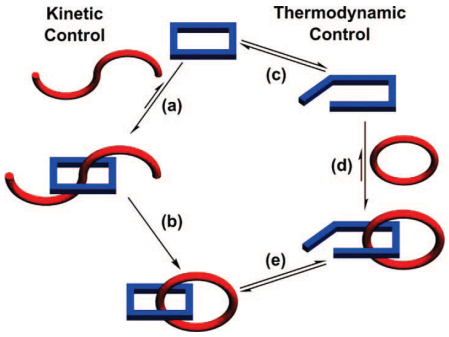


**Figure 4.** Both kinetic (left) and thermodynamic (right) control can be exercised in a catenane synthesis. Kinetically controlled reactions proceed through (a) pseudorotaxane formation, followed by (b) an irreversible ring closure. Thermodynamically controlled methods rely on (c) reversible ring opening of the blue component, followed by the (d) coordination to a complementary molecule, and finally (e) reversible ring closure. Reprinted with permission from ref. 36. Copyright © 1999-2016 John Wiley & Sons.

## 1.3 MIM as Molecular Machines

The availability of more and more examples of interlocked molecules with increasing complexity allowed their use as molecular machines, finding important applications in the field of molecular electronics, switching and nano-sized devices. The chemical information stored in the components of these devices strictly influence their working mode.[37–39] For example, if two or more binding sites are inserted in a rotaxane dumbbell, the macrocycle may interact with both of them; the rotaxane can exist as two different equilibrating coconformations whose population depends on the relative thermodynamical stability. The equilibrium between the conformations may be governed by an appropriate external stimulus (chemical, electrochemical or

photochemical), whose role is to change the affinity of the wheel for the two stations present in the linear component. As a result the wheel translates along the dumbbell to reach a more stable conformation; such structure represents a molecular shuttle (Figure 5).[40–42]

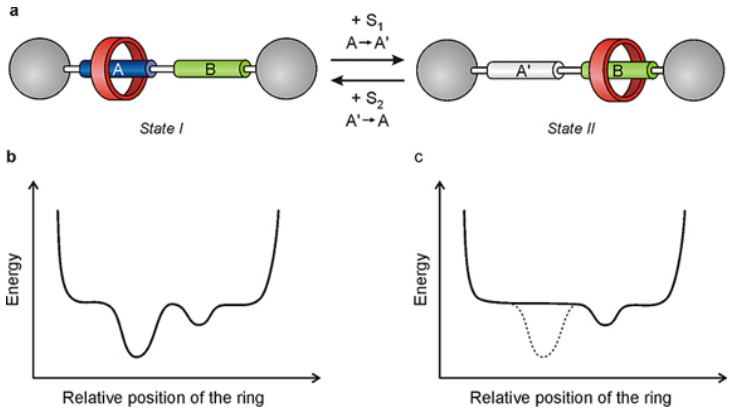


**Figure 5.** (a) Schematic representation of a two-station rotaxane and its operation as a controllable molecular shuttle. (b) A simplified representation of the potential energy of the system as a function of the position of the ring relative to the axle before (left) and after (right) switching off station A. Reprinted with permission from ref. 39. Copyright © Elsevier B.V.

Herein, some examples of molecular machines, related to the topics tackled in this thesis, are reported. J.F. Stoddart and co-workers established the first example of a rotaxane-based molecular shuttle. This interlocked compound is composed by a tetracationic "wheel" and a polyether "thread" that bears at its termini two bulky triisopropylsilyl groups that act as "stoppers". Two hydroquinol units positioned symmetrically in the polyether chain act as identical "stations". The ability of the wheel to move back and forth like a shuttle between the two stations was demonstrated to be temperature dependent and monitored through NMR techniques (Figure 6).[42]

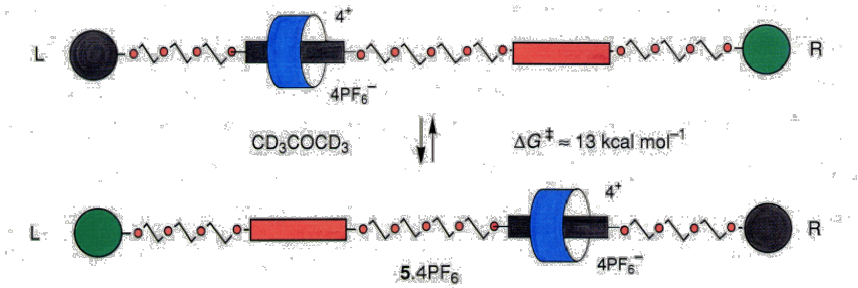


**Figure 6.** (a) Schematic representation of the first example of a [2]rotaxane molecular shuttle. Adapted with permission from ref. 42. Copyright © American Chemical Society.

After this extraordinary achievement, Stoddart and co-workers paved the way for the development of a wide series of rotaxane-based molecular switches, driven by different chemical, electrochemical and/or photochemical external stimuli. For example, a [2]rotaxane able to act as a molecular shuttle when electrochemically stimulated was described (Figure 7). The interlocked molecule is composed by an axial component, decorated with two electron-rich units, a 1,5-dioxynaphthalene (DNP) and a tetratiofulvalene (TTF), and a cyclobis(paraquat-*p*-phenylene) as wheel.[43]

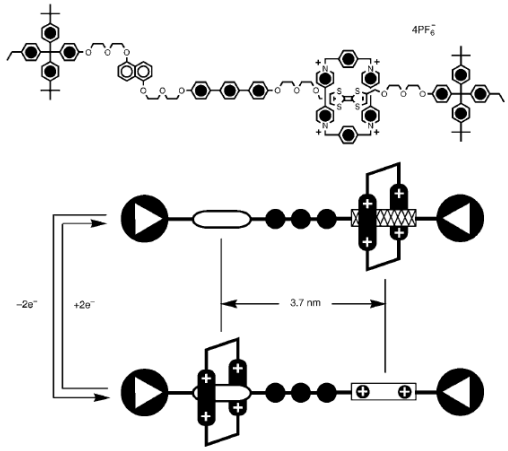


**Figure 7.** A [2]rotaxane with the TTF (hatched) and DNP (open) recognition units separated by a rigid terphenylene spacer (black circles) demonstrates a relative mechanical movement between the macrocyclic and dumbbell-shaped components. Adapted with permission from ref. 43. Copyright © 1999-2016 John Wiley & Sons.

In the ground state the macrocycle exclusively encircles the TTF station because of the strong charge transfer interactions that occur between these two species. Exploiting the redox properties of the TTF moiety, a translation movement was induced by the oxidation of the TTF to $TTF^{2+}$. The dicationic form of TTF, indeed, destabilizes this supramolecular interaction and the wheel shuttles toward the DNP station. Through NMR and UV-Vis spectroscopy the movement could be monitored. A secondary electrochemical stimulus, more precisely the reduction of $TTF^{2+}$ to the original TTF, restores the initial state by shuttling back the macrocycle.

As in the case of rotaxanes, the shuttling movement in a [2]catenane architecture was demonstrated by Stoddart and co-workers with a very similar strategy utilized for the rotaxanes.[44] First a degenerate [2]catenane was obtained in which $CBPQT^{4+}$ (cyclobis(paraquat-*p*-phenylene)) and BPP34C10 (bis-*p*-phenylene-34-crown-10) are interlocked (Figure 8). Dynamic $^1$H NMR spectroscopy performed in solution on the [2]catenane revealed, in addition to an extremely rapid rocking motion relating the two inter-locked rings, the presence of three different degenerate circumrotational processes.

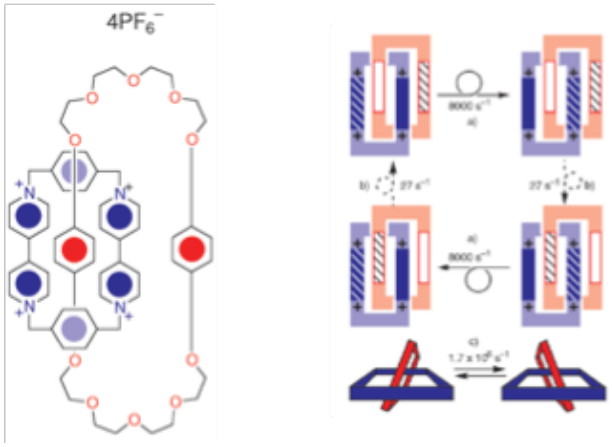


**Figure 8.** Three different degenerate co-conformational processes observed in temperature-dependent $^1$H NMR spectra of the [2]-catenane: (a) circumrotation of $CBPQT^{4+}$ through BPP34C10; (b) circumrotation of BPP34C10 through $CBPQT^{4+}$; and (c) rocking of BPP34C10 within $CBPQT^{4+}$. Adapted with permission from ref. 44. Copyright © American Chemical Society.

Thanks to this prototype, the same group designed several [2]catenane systems. For example that containing a tetrathiafulvalene (TTF) and a 1,5-dioxynaphthalene (1/5DN) units in place of the hydroquinone ones in the previously described [2]catenane (Figure 9). Since, in solution, TTF and its derivatives have strong affinity ($K_a$ > 8000 $M^{-1}$) for $CBPQT^{4+}$, while substrates incorporating 1,5-dioxynaphthalene ring systems are more weakly bound (Ka < 5000 $M^{-1}$), the wheel component would reside preferentially around the TTF unit. Upon oxidation of the TTF, the $CBPQT^{4+}$ circumrotates with respect to crown ether ring so that the 1/5DN system would occupy its cavity. UV-vis and NMR experiments demonstrated the circumrotating movement of the [2]catenane, both in solution and in the solid state. [45]

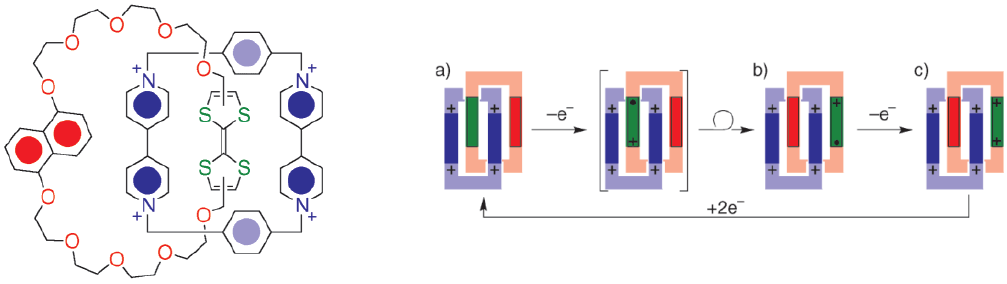


**Figure 9.** Representation of the Redox switching process of the [2]catenane endowed with tetrathiafulvalene (TTF) and a 1,5-dioxynaphthalene (1/5DN) functions. Reprinted with permission from ref. 45. Copyright © American Chemical Society.

More recently, D. Leigh and co-workers showed that a sequential and unidirectional rotation could also be induced in mechanically interlocked assemblies characterized by one small rings moving around a larger one (Figure 10).[46] The three "stations" inserted in the larger ring are *a*) a secondary amide fumaramide group; *b*), a tertiary amide fumaramide group; *c*) a succinic amide ester. All these moieties can interact with the smaller ring, a xylylene ring of the benzylic amide, but with different binding affinities ($K_a$ (*a*)> $K_a$ (*b*)> $K_a$ (*c*), respectively). The circumrotating movement of the small ring with respect to the larger one is promoted by light, heat or chemical stimuli that change the relative affinity of the macrocycle for the different binding sites.

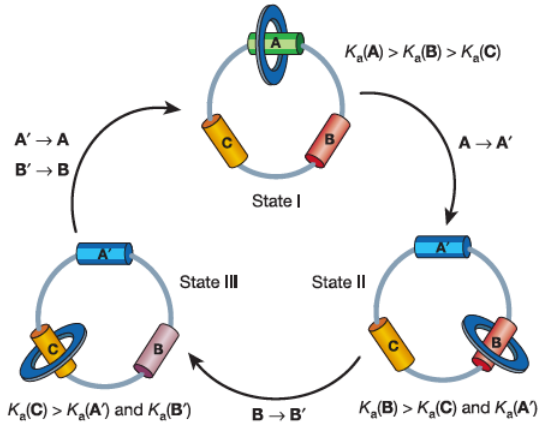


**Figure 10.** Figure 1 Stimuli-induced sequential movement of a macrocycle between three different binding sites in a [2]catenane. The larger macrocycle contains three stations, A, B and C, each with different binding affinities (association constants, $K_a$) for the smaller macrocycle. Reprinted with permission from ref. 46. Copyright © Nature Publishing Group.

Through $^1$H NMR investigations, they were able to identify the portion of the large ring threading the cavity of the small ring; furthermore, they also isolated samples of each conformer in order to confirm the position of the rings after each external stimulus.

## 1.4 Calix[6]arene-Based Molecular Machines and Devices

Calix[n]arenes are a series of synthetic macrocycles belonging to the class of metacyclophanes. These compounds are readily accessible in high yield from the base-catalyzed one-pot reaction (condensation) of p-*tert*-butylphenol and formaldehyde.[47] Because of its cup-like structure and the possibility to gain full control over its regio- and stereoselective functionalization, the calix[4]arene represents the most extensively employed molecular platform to anchor and orient in space functional groups and binding sites for the selective and efficient recognition of neutral and charged species

in the solid state, in solution, and in the gas phase.[48,49] Despite synthetic procedures for the selective (partial) functionalization of the phenolic groups of larger size calix[n]arene are usually low yielding and because of the difficulties to fix their conformation through functionalization, calix[5]arene and calix[6]arene are only recently emerging as very convenient tools to further expand the scopes of calixarene chemistry toward nanoscience and nanotechnology. It was, indeed, discovered that a guest having an axial symmetry and suitable chemical information can thread their annulus to yield supramolecular complexes belonging to the class of pseudorotaxanes or interlocked systems like rotaxanes and catenanes.

The first example of a calix[6]arene-based pseudorotaxane, depicted in Figure 11, was published when it was demonstrated that the tris(*N*-phenylureido)calix[6]arene derivative **1** is able to take up dioctylviologen diiodide (**DOV**•2I) in apolar solvents.[50]

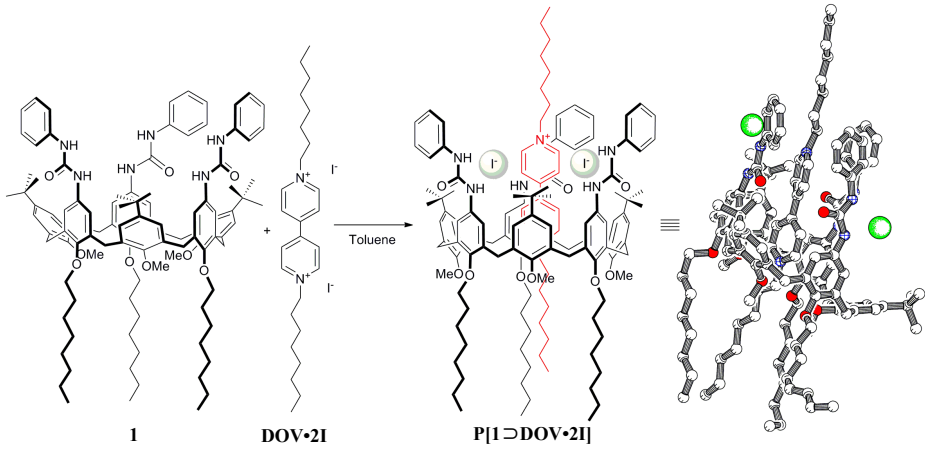


**Figure 11.** Self-assembly in toluene of calix[6]arene-based wheel **1** and viologen-based axle **DOV**·2I and X-ray structure of the solid-state structure of the resulting pseudorotaxane **P[1⊃DOV·2I]**.

The structure of this complex, analysed in solution and established in the solid state, clearly showed that the dicationic viologen threads the calix[6]arene annulus and the two iodide anions are hydrogen-bonded to the phenylureido NH of the calix upper rim. In these complexes, all the components – namely, the dicationic viologen axle, the

calix[6]arene wheel, and the two counteranions – are held together by a combination of several non-covalent interactions. Of particular importance was the observation that all the domains of the wheel (the three alkyl chains at the lower rim, the π-rich calixarene walls, and the three polar phenylureido groups at the upper rim) participate in stabilizing the complex.

A very peculiar property of calix[6]arene-based wheels is that orientational pseudorotaxane isomers can be selectively obtained when a non-symmetric axle is used as the guest. For example wheel **2**, having three ethylethoxy chains at its lower rim to simplify the NMR spectra, acts as a host for a non-symmetric dicationic axle consisting of a viologen-based unit bearing two alkyl side chains, one of which is stoppered at one terminus, forming exclusively the oriented pseudorotaxane in which the stopper of the axle is positioned in proximity of the upper rim of the wheel (Figure 12).[51]

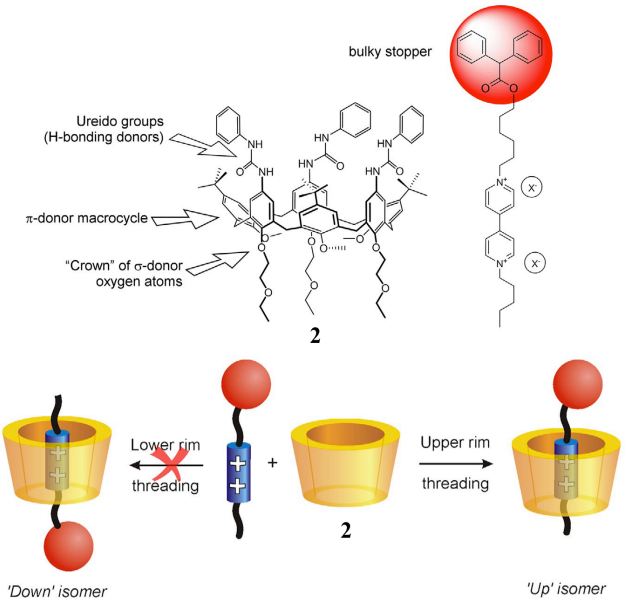


**Figure 12**. Schematic representation of the two possible pseudorotaxane isomers derived from the calix[6]arene wheel **2** and the non-symmetrical axle carrying only one stopper.

This behaviour was tentatively explained considering that: *i*) in apolar solvent the three methoxy groups of the calix occupy the cavity and disfavour the access of the axle

from the lower rim; *ii*) in apolar solvent the axle is present as a "tight" ion-pair; since the cavity of the calixarene can host only the cationic portion of the guest, a partial separation of the cation from its counteranions should take place before axle threading; iii) the ureido groups, that are potent hydrogen-bond donor group, can interact with the anions of the axle, inducing the separation of the ion-pair and thus pivoting the threading process from the upper rim of the wheel. Through UV-Vis spectroscopy, an apparent association constant of the order of $10^6$ $M^{-1}$ was calculated for these pseudorotaxane systems. [52]

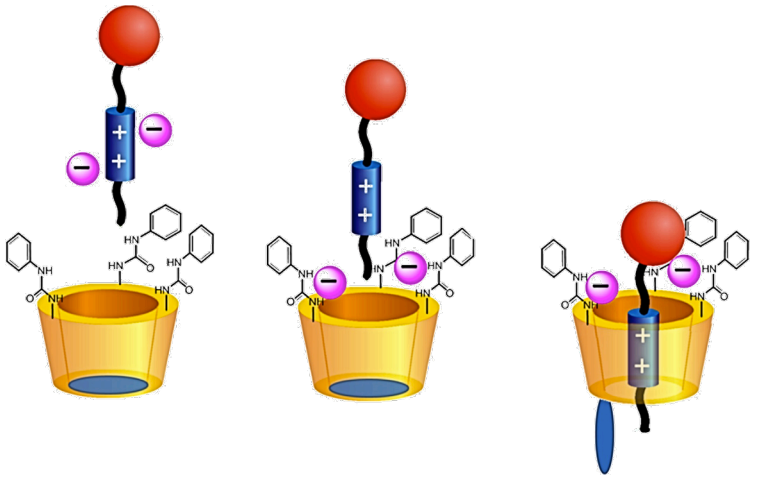

**Figure 12.** Possible threading mechanism of a viologen-based non-symmetrical axle in a tris(*N*-phenylureido)calix[6]arene based wheel: the three phenylurea moieties present on the calix[6]arene aromatic cavity coordinate the viologen counteranions by hydrogen bonding, thus pivoting threading of the dicationic axle from the upper rim of the wheel.

More recently, it was also shown that simple n-alkyl chains in dialkyl viologen-type axles (C5C8, C5C10, C5C12, and C5C18) can act as kinetic control elements in the self-assembly of calix[6]arene pseudorotaxanes (Figure 13).[53] It was indeed demonstrated, through NMR and stopped flow experiments, that the length of the alkyl chain appended to the 4,4' bipyridinium, together with the experimental conditions at which the binding process is carried out, could influence the orientation of the axle insertion within the wheel to yield oriented pseudorotaxanes. In particular it was established that, increasing the length of the alkyl chains in symmetric viologen salts

(passing from axle C5C5 to axle C18C18), the threading rate constant decreases of four order of magnitude and the stability constant decreases of two orders of magnitude. When the 4,4' bipyridinium salt bears alkyl chains of different length, it was evidenced that the axle enters the wheel selectively or exclusively through its shorter chain.

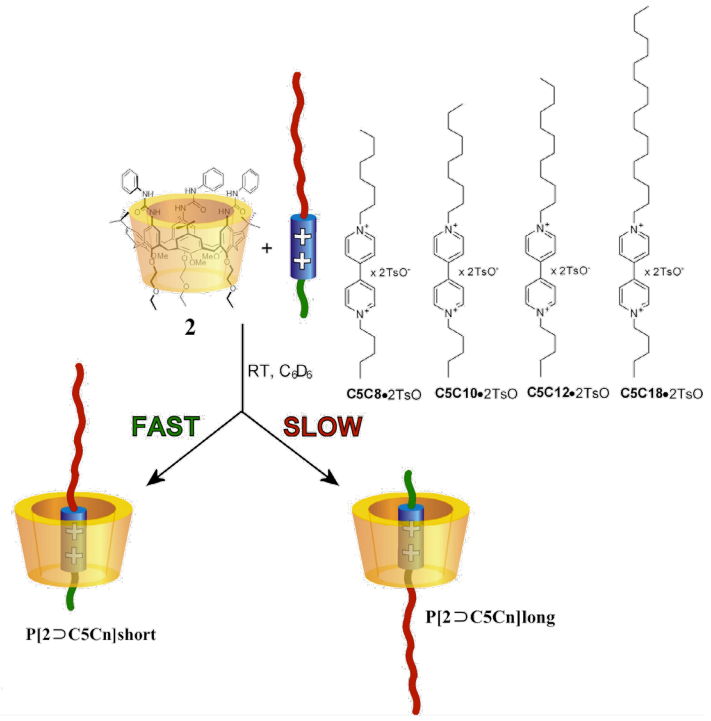


**Figure 13.** Schematic representation of the possible self-assembly processes between wheel **2** and non-symmetrical axles C5Cn (n=8, 10, 12, and 18) to yield oriented pseudorotaxane isomers $\mathbf{P[2\supset C5Cn]_{short}}$ and $\mathbf{P[2\supset C5Cn]_{long}}$.

Cyclic voltammetry (CV) measurements carried out in dichloromethane on a series of pseudorotaxanes showed that a fast (submicrosecond time-scale) dethreading takes place upon monoelectronic electrochemical reduction of the axle. [52]

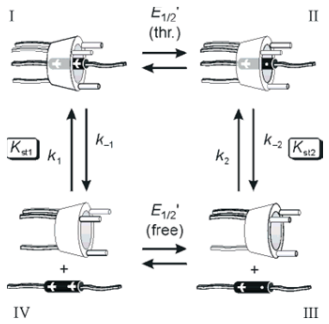


**Figure 14.** Square scheme mechanism for the one-electron reduction of **P[1⊃DOV·2I]**; I and III represent the stable states, whereas II and IV are metastable intermediates. The counteranions have been omitted for clarity.

By playing around the structural features of the groups anchored at the viologen-based unit and the experimental conditions, the solvent and light- controlled unidirectional transit of non-symmetric axles through **2** was also achieved (Figure 15).[54] A viologen axle, containing a photoisomerizable stilbene moiety at one end, was equilibrated with **2**, in apolar media, to yield the oriented pseudorotaxane depicted in Figure 15. Stoppering reaction of this pseudorotaxane with diphenylacetyl chloride gave the corresponding semi-rotaxane.

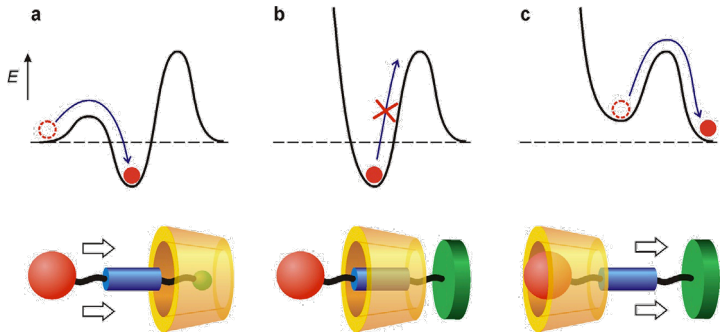


**Figure 15.** Simplified potential energy curves representing the steps that account for the unidirectional transit of the axle through the wheel. The horizontal coordinate of the diagrams represents the axle–wheel distance when they approach one another along the direction and with the orientation shown in the cartoons. (a) Threading of the axle through the upper rim of the wheel in apolar solvents. (b) The stoppering reaction to convert the pseudorotaxane into a rotaxane-like species. (c) Dethreading of the axle from the lower rim of the wheel occurring in polar solvents.

By means of NMR and UV-Vis measurements it was demonstrated that in the highly polar DMSO these complexes disassemble. Because of the presence of the bulky diphenylacetyl stopper, this process must take place through the slippage of the stilbene unit from the lower rim of the wheel. The fact that the dethreading rate constant depends on the stilbene bulkiness unambiguously evidences that this group, positioned in proximity of the upper rim, should pass through the lower calixarene annulus during the slippage.

The possibility to gain full control on the threading of a viologen salt through **2**, was exploited for the synthesis of several oriented calix[6]arene-based rotaxanes.[26,55,56] For example, interlocked systems bearing a terpyridine in the axle were synthesized with the aim to verify whether the orientation of the calix[6]arene wheel rims toward one particular stopper in rotaxanes could be employed as further structural information element to subtly modify the properties and/or the working mode of oriented pseudorotaxanes and rotaxanes.[56] The equilibration of wheel **2** with a terpyridine-based axle in toluene gave, as expected, the corresponding oriented pseudorotaxane, in which the terpyridine unit of the axial component is in positioned at the calixarene upper rim. The stoppering reaction carried out on the pseudorotaxane with diphenylacetyl chloride afforded the corresponding oriented rotaxane (Figure 16).

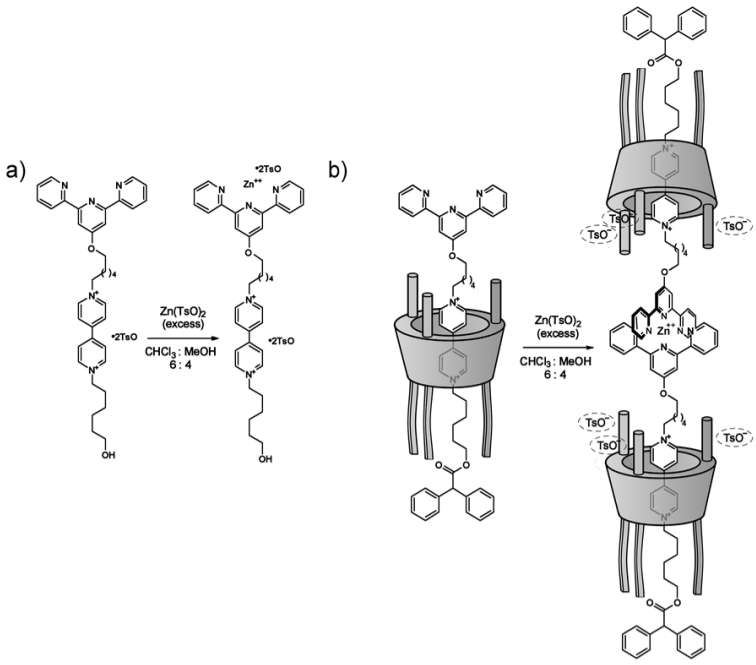


**Figure 16.** Different complexing behaviour of (a) terpyridine axle and (b) rotaxane in the presence of an excess of $Zn(TsO)_2$.

After the addition of $Zn(TsO)_2$, NMR measurements taken in $CDCl_3/CD_3OD$ (6/4) showed that, in agreement with literature data, the axle forms either 1:1 or 2:1 Zn/Axle complexes, depending on the ratio between the analytes and that these complexes are in slow exchange in the NMR timescale. On the contrary, the spectra recorded upon addition of an excess of solid $Zn(TsO)_2$ to a $C_6D_6$ solution of the pseudorotaxane showed the formation of the 1:2 Zn/Pseudo complex as the unique adduct present in solution (Figure 16), as also verified through DOSY experiments that confirmed the stoichiometry of complexation around the Zn metal ion. This 1:2 stoichiometry was observed also when the rotaxane was employed as ligand for $Zn(TsO)_2$.

To this state of the art, the natural development of these tris(*N*-phenylureido)calix[6]arene based molecular devices is the design of new working machines endowed with the specific function to promote a shuttling or circumrotating movement between the components.

Contemporaneously, Neri and coworkers reported a general mode to obtain calix[6]arene and calix[7]arene-based pseudorotaxanes (Figure 17) by employing simple alkoxy derivatives as wheels and dialkylammonium cations having the weakly coordinating tetrakis[3,5-bis(trifluoromethyl)phenyl]borate (TFPB) as the counteranion in apolar media.[57]

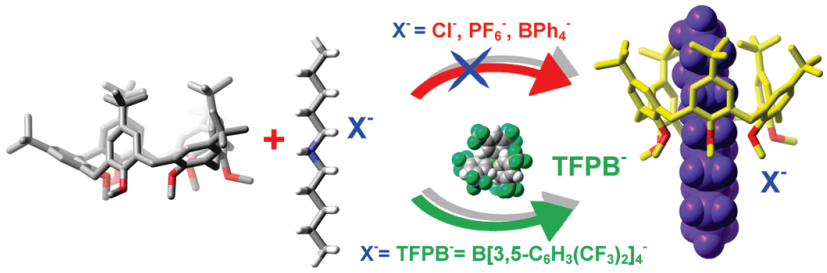


**Figure 17.** Schematic representation of calix[6]arene-based pseurotaxane formation in apolar media utilising dialkylammonium cations having the weakly coordinating tetrakis[3,5 bis(trifluoromethyl)phenyl]borate (TFPB) counteranion as guest. Reprinted with permission from ref. 57. Copyright © American Chemical Society.

It is interesting to note that, contrary to the tris(*N*-phenylureido)calix[6]arene wheels previously discussed, where anion binding and ion pair separation of the ureido moieties play a crucial and pivotal role during threading of the axle, in these simpler calixarene derivatives, it is the very weak coordinating power of the anion that, forming very loose ion pairs with the dialkylammonium cation, allows axle threading. The apparent binding constants for pseudorotaxane formation, measured through NMR techniques, experienced range between $10^2$ and $10^6$ $M^{-1}$. The potential of these systems to act as prototypes of molecular machines was demonstrated by studying the shuttling modes of rotaxanes derived from hexaalkoxycalix[6]arenes as wheels and dialkylammonium as TFPB salts as axles (Figure 18).[58] NMR structural determination confirmed that, as expected in rotaxane, the n-hexyloxycalixarene encircles the positively charged ammonium station. Deprotonation of the central cationic station gave the new rotaxanes. In this neutral species, the shuttling of the wheels along the two alkyl chains of the thread yields the two translational isomers in a 6:4 ratio,

respectively, as measured trough NMR techniques at 263 K. Acid treatment of this translational isomers mixture restored the original ammonium station that resets the system to the original situation.

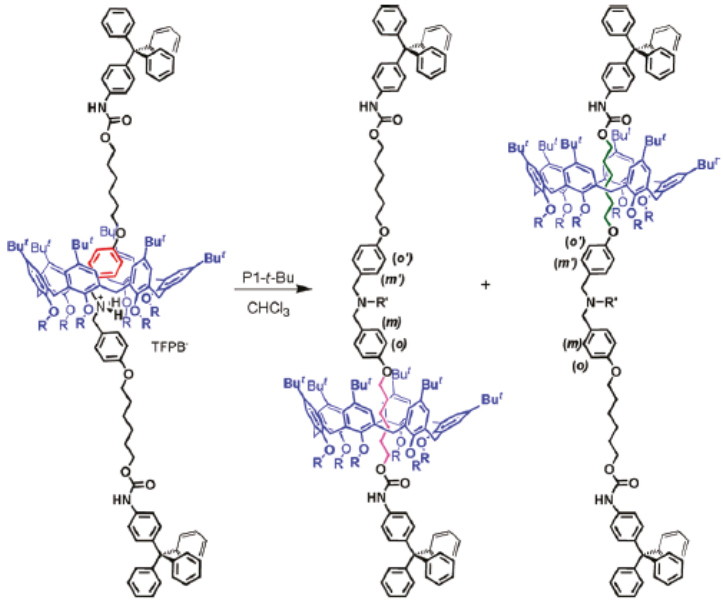


**Figure 18.** The shuttling behavior of the calix[6]arene wheel along the axle and structural formulas of calix[6]arene-based rotaxanes obtained. Adapted with permission from ref. 58. Copyright © American Chemical Society.

## References


(1) Moore, G. E. *Electronics* **1965**, *38* (8), 114.

(2) Amato, I. *Science (80-. ).* **1998**, *282* (5388), 402–405.

(3) Judy, J. W. *Smart Mater. Struct.* **2001**, *10* (6), 1115–1134.

(4) Muller, D. A.; Sorsch, T.; Moccio, S.; Baumann, F. H.; Evans-Lutterodt, K.; Timp, G. **1999**, *399* (6738), 758–761.

(5) Service, R. F. *Science (80-. ).* **2001**, *293* (5531), 785–786.

(6) Whitesides, G. M. *Sci. Am.* **2001**, 32.

(7) Feynman, R. *Eng. Sci.* **1960**, *23,* 22.

(8) Philp, D.; Stoddart, J. F. *Angew. Chemie Int. Ed. English* **1996**, *35* (11), 1154–1196.

(9) Balzani, V.; Credi, A.; Venturi, M. *Chemistry* **2002**, *8* (24), 5524–5532.

(10) Lu, W.; Lieber, C. M. *Nat. Mater.* **2007**, *6* (11), 841–850.

(11) Shimomura, M.; Sawadaishi, T. *Curr. Opin. Colloid Interface Sci.* **2001**, *6* (1), 11–16.

(12) Steed, J. W.; Atwood, J. L. *Supramolecular Chemistry*; 2013.

(13) Lehn, J.-M. *Angew. Chemie Int. Ed. English* **1990**, *29* (11), 1304–1319.

(14) Teo, B. K.; Sun, X. H. *J. Clust. Sci.* **2006**, *17* (4), 529–540.

(15) Balzani, V.; Credi, A.; Venturi, M. *Molecular Devices and Machines*; Wiley-VCH Verlag GmbH & Co. KGaA: Weinheim, Germany, 2008.

(16) Gale, P. A., Steed, J. W. *Supramolecular Chemistry*; John Wiley & Sons, Ltd: Chichester, UK, 2012.

(17) Stoddart, J. F. *Annu. Reports Sect. "B" (Organic Chem.* **1988**, *85*, 353.

(18) Melson, G. A. *Coordination Chemistry of Macrocyclic Compounds*; Springer US: Boston, MA, 1979.

(19) Becher, J. *Adv. Mater.* **1993**, *5* (10), 769–770.

(20) Kelly, T. R. *Molecular Machines*; 2005.

(21) Balzani, V. *Pure Appl. Chem.* **2008**, *80* (8).

(22) Stoddart, J. F. *Acc. Chem. Res.* **2001**, *34* (6), 410–411.

(23) Sauvage, J.-P., Dietrich-Buchecker, C. *Molecular Catenanes, Rotaxanes and Knots*; Wiley-VCH Verlag GmbH: Weinheim, Germany, 1999.

(24) Griffiths, K. E.; Stoddart, J. F. *Pure Appl. Chem.* **2008**, *80* (3), 485-506.

(25) Zhang, C.; Li, S.; Zhang, J.; Zhu, K.; Li, N.; Huang, F. *Org. Lett.* **2007**, *9* (26), 5553–5556.

(26) Arduini, A.; Bussolati, R.; Credi, A.; Pochini, A.; Secchi, A.; Silvi, S.; Venturi, M.

*Tetrahedron* **2008**, *64* (36), 8279–8286.

(27) Furusho, Y.; Sasabe, H.; Natsui, D.; Murakawa, K.; Takata, T.; Harada, T. *Bull. Chem. Soc. Jpn.* **2004**, *77* (1), 179–185.

(28) Hansen, J. G.; Feeder, N.; Hamilton, D. G.; Gunter, M. J.; Becher, J.; Sanders, J. K. M. *Org. Lett.* **2000**, *2* (4), 449–452.

(29) Weck, M.; Mohr, B.; Sauvage, J.-P.; Grubbs, R. H. *J. Org. Chem.* **1999**, *64* (15), 5463–5471.

(30) Yin, J.; Dasgupta, S.; Wu, J. *Org. Lett.* **2010**, *12* (8), 1712–1715.

(31) Wu, J.; Leung, K. C.-F.; Stoddart, J. F. *Proc. Natl. Acad. Sci.* **2007**, *104* (44), 17266–17271.

(32) Asakawa, M.; Ashton, P. R.; Ballardini, R.; Balzani, V.; Bělohradský, M.; Gandolfi, M. T.; Kocian, O.; Prodi, L.; Raymo, F. M.; Stoddart, J. F.; Venturi, M. *J. Am. Chem. Soc.* **1997**, *119* (2), 302–310.

(33) Ashton, P. R.; Parsons, I. W.; Raymo, F. M.; Stoddart, J. F.; White, A. J. P.; Williams, D. J.; Wolf, R. *Angew. Chemie Int. Ed.* **1998**, *37* (13-14), 1913–1916.

(34) Rotzler, J.; Mayor, M. *Chem. Soc. Rev.* **2013**, *42* (1), 44–62.

(35) Horn, M.; Ihringer, J.; Glink, P. T.; Stoddart, J. F. *Chem. - A Eur. J.* **2003**, *9* (17), 4046–4054.

(36) Aricó, F.; Chang, T.; Cantrill, S. J.; Khan, S. I.; Stoddart, J. F. *Chem. - A Eur. J.* **2005**, *11* (16), 4655–4666.

(37) Jones, W.; Rao, C. *Supramolecular Organization and Materials Design*; Cambridge University Press, 2008.

(38) Loeb, S. J. *Chem. Soc. Rev.* **2007**, *36* (2), 226–235.

(39) Balzani, V.; Bergamini, G.; Ceroni, P. *Coord. Chem. Rev.* **2008**, *252* (23-24), 2456–2469.

(40) Silvi, S.; Arduini, A.; Pochini, A.; Secchi, A.; Tomasulo, M.; Raymo, F. M.; Baroncini, M.; Credi, A. *J. Am. Chem. Soc.* **2007**, *129* (44), 13378–13379.

(41) Leigh, D.; Troisi, A.; Zerbetto, F. *Angew. Chem. Int. Ed. Engl.* **2000**, *39* (2), 350–353.

(42) Anelli, P. L.; Spencer, N.; Stoddart, J. F. *J. Am. Chem. Soc.* **1991**, *113* (13), 5131–5133.

(43) Tseng, H.-R.; Vignon, S. A.; Stoddart, J. F. *Angew. Chem. Int. Ed. Engl.* **2003**, *42* (13), 1491–1495.

(44) Pease, a. R.; Jeppesen, J. O.; Stoddart, J. F.; Luo, Y.; Collier, C. P.; Heath, J. R. *Acc. Chem. Res.* **2001**, *34* (6), 433–444.

(45) Balzani, V.; Credi, A.; Mattersteig, G.; Matthews, O. A.; Raymo, F. M.; Stoddart, J. F.; Venturi, M.; White, A. J. P.; Williams, D. J. *J. Org. Chem.* **2000**, *65* (7), 1924–1936.

(46) Leigh, D. A.; Wong, J. K. Y.; Dehez, F.; Zerbetto, F. *Nature* **2003**, *424* (6945), 174–179.

(47) Gutsche, C. D.; Dhawan, B.; No, K. H.; Muthukrishnan, R. *J. Am. Chem. Soc.* **1981**, *103* (13), 3782–3792.

(48) Asfari, Z.; Böhmer, V.; Harrowfield, J.; Vicens, J. *Calixarenes 2001*; Springer Science & Business Media, 2007.

(49) Mandolini, L.; Ungaro, R. *Calixarenes in Action*; World Scientific, 2000.

(50) Arduini, A.; Ferdani, R.; Pochini, A.; Secchi, A.; Ugozzoli, F. *Angew. Chemie, Int. Ed.* **2000**, *39* (19), 3453–3456.

(51) Arduini, A.; Calzavacca, F.; Pochini, A.; Secchi, A. *Chem. - A Eur. J.* **2003**, *9* (3), 793–799.

(52) Credi, A.; Dumas, S.; Silvi, S.; Venturi, M.; Arduini, A.; Pochini, A.; Secchi, A. *J. Org. Chem.* **2004**, *69* (18), 5881–5887.

(53) Arduini, A.; Bussolati, R.; Credi, A.; Secchi, A.; Silvi, S.; Semeraro, M.; Venturi, M. *J. Am. Chem. Soc.* **2013**, *135* (26), 9924–9930.

(54) Arduini, A.; Bussolati, R.; Credi, A.; Monaco, S.; Secchi, A.; Silvi, S.; Venturi, M. *Chem. - A Eur. J.* **2012**, *18* (50), 16203–16213.

(55) Arduini, A.; Ciesa, F.; Fragassi, M.; Pochini, A.; Secchi, A. *Angew. Chemie, Int. Ed.* **2005**, *44* (2), 278–281.

(56) Arduini, A.; Bussolati, R.; Masseroni, D.; Royal, G.; Secchi, A. *European J. Org. Chem.* **2012**, *2012* (5), 1033–1038, S1033/1–S1033/12.

(57) Gaeta, C.; Troisi, F.; Neri, P. *Org. Lett.* **2010**, *12* (9), 2092–2095.

(58) Pierro, T.; Gaeta, C.; Talotta, C.; Casapullo, A.; Neri, P. *Org. Lett.* **2011**, *13* (10), 2650–2653.

# CHAPTER 2

# Supramolecularly Assisted Synthesis of Two Isomeric Oriented Calix[6]arene-based Rotaxanes

# Chapter 2

# Supramolecularly Assisted Synthesis of Two Isomeric Oriented Calix[6]arene-based Rotaxanes

## 2.1 Introduction

In the previous chapter, the ability of a tris(*N*-phenylureido)calix[6]arene derivative (**1**, Scheme 1) to act as heteroditopic receptor for *N,N'*-Dialkyl-4,4'-bipyridinium ion pairs that in low polar solvent is able to form stable oriented pseudorotaxanes was reported. The unidirectional threading process of the axle into the electron-rich cavity was accurately described and the recent studies on the kinetic control on the orientational outcome given by the length of simple alkyl chains appended to the viologen axle paved the way for new challenges. In fact, the total control on the threading/dethreading process of the axle may allow the development of new molecular devices endowed with a wider set of properties and possible applications. Indeed, from those studies, it clearly emerged that the exclusive synthesis of a pseudorotaxane bearing the longer alkyl chain of a non-symmetric viologen axle protruding from the lower rim of the calix[6]arene wheel, was not possible.[1] To overcome this limitation, it was envisaged that, as in the case of dialkylviologen salts, **1** could also form *Host-Guest* inclusion complexes with mono-alkyl bispyridinium guests in whom, in principles, the guest can be bound with two opposite orientation (Figure 1).

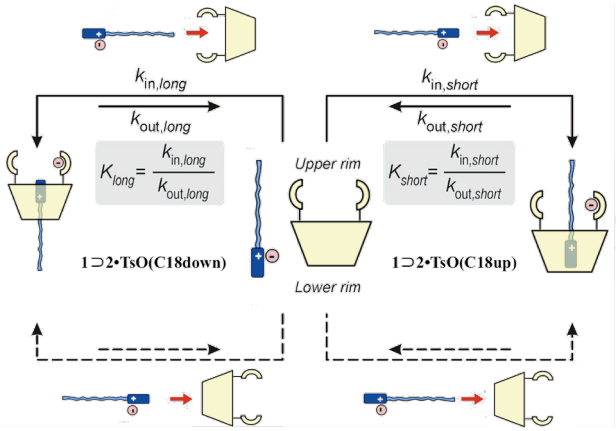


**Figure 1.** Graphical representation of the two possible orientational isomers and the four possible threading processes for the formation of *Host-Guest* complexes between tris(*N*-phenylureido)calix[6]arene and *N*-alkyl-4,4'-bipyridinium ion pairs.

In those orientational complexes, the engulfment of the positively charged guest inside the π-rich cavity could result in an increase of the nucleophilicity of the neutral nitrogen atom towards a $S_N2$ reaction with an alkylating agent and yield oriented pseudorotaxanes. With the exception of the studies reported by Rebeck and co-workers, who demonstrated the reaction rate enhancement toward the Menschutkin reaction of a quinuclidine engulfed in a cavitand (Figure 2),[2] no other explicit studies in which the electron-rich cavity of an Host plays a role on a reaction rate have been reported so far.

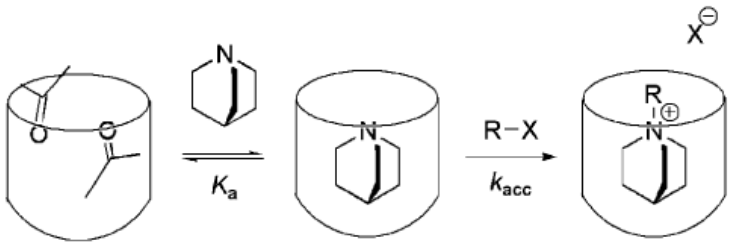


**Figure 2.** The cavitand is occupied with two molecules of acetone (solvent); through a partial unfolding mechanism, quinuclidine displaces the acetone with an association constant $K_a$ of 40 $M^{-1}$. This complex then engages an electrophile RX in an $S_N2$ reaction, accelerating the rate constant $k_{acc}$. Reprinted with permission from ref. 2. Copyright © American Chemical Society.

In this chapter, a new strategy for the synthesis of two orientational rotaxane isomers, otherwise not obtainable through the already developed protocols, will be presented.

## 2.2 Host-Guest Complex Between tris(*N*-phenylureido)calix[6]arene and *N*-alkyl-4,4'-bipyridinium Salts

Initially, the ability of **1** to form inclusion complexes with monoalkylviologen salts in apolar media and whether also, for these binding processes, the factors that govern the threading direction of guest inclusion into **1** were studied through NMR and UV-Vis techniques (Scheme 1). **2**•TsO, in which the 4,4'-bipyridyl unit is functionalized with an octadecyl chain was employed as guest.

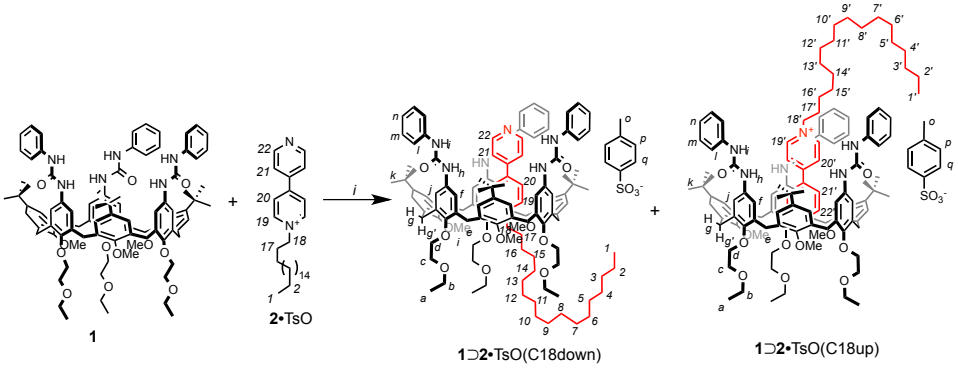


**Scheme 1.** Reagent and conditions: *i*) low polar solvent (toluene, $C_6D_6$, $CDCl_3$), r.t., 1h.

The UV-Vis data were collected at 333 K in toluene because of the poor solubility of **2**•TsO at room temperature. The apparent binding constant relative to the complex formed by host **1** and **2**•TsO as the guest was evaluated by titrating a 240 μM solution of **2**•TsO with a 24 μM solution of **1**. Fitting the absorbance values at 370 nm at different [H]/[G] values, a binding constant of 8.1 x $10^4$ $M^{-1}$ was calculated (Figure 3).

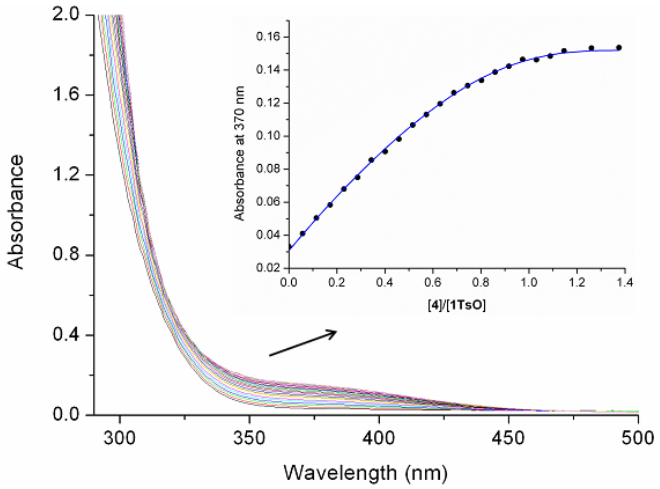


**Figure 3.** Absorption spectra (toluene, 333 K) of **2**•TsO upon titration with calix[6]arene **1**. Inset: plot of the absorption changes at 370 nm vs equivalents of calix and fitting of the data (solid line).

The complexation reaction was also studied through a $^1$H NMR experiment by adding an equivalent of **2**•TsO to a 27 mM solution of **1** in $C_6D_6$ at room temperature. The formation of **1**⊃**2**•TsO was confirmed by the dissolution of the guest, otherwise insoluble at r.t.; a color change of the solution, from colorless to orangish, also suggests the successful capture of **2**•TsO by **1**. The broad signals displayed in the $^1$H NMR spectrum (300 MHz, $CDCl_3$, 295K) suggest that a high conformational fluxionality of the complex is taking place on the NMR timescale. In order to gain insights about the orientation of **2**•TsO inside **1**, 2D NMR experiments in $CDCl_3$ at low temperature (253 K) were carried out. The engulfment of **2**•TsO into **1** was inferred by the strong upfields shift experienced by the protons of the guest alkyl chain. In particular, the $-CH_2-$ protons adjacent to the viologen unit undergo to a Δδ of about 1.3 ppm (resonance *18* in Figure 3, see also Scheme 1 for protons' labelling). Information about the threading of the axle were also collected monitoring the shift relative to the aromatic protons of the bipyridinium unit; the significant shift to upper fields (Δδ = 3.26 ppm) suffered by protons *20* (Figure 3, protons' label in Scheme 1) is remarkable if compared to the minor one (Δδ = 0.03 ppm) endured by protons *22* (Figure 3,

protons' label in Scheme 1). The same shielding effects were also observed for the chemical shift of the aromatic protons in *orto* position respect to the viologen nitrogen: proton *19* undergoes a shift of about 3.5 ppm due to its inclusion in the cavity, while proton *22* is almost unaffected by the presence of **1**. From these data it is possible to conceive that **2**•TsO threads the macrocycle with the alkyl chain, placing the cationic ring in the electron-rich cavity of **1** while leaving the neutral nitrogen of the other ring protruding from the wider rim of the macrocycle.

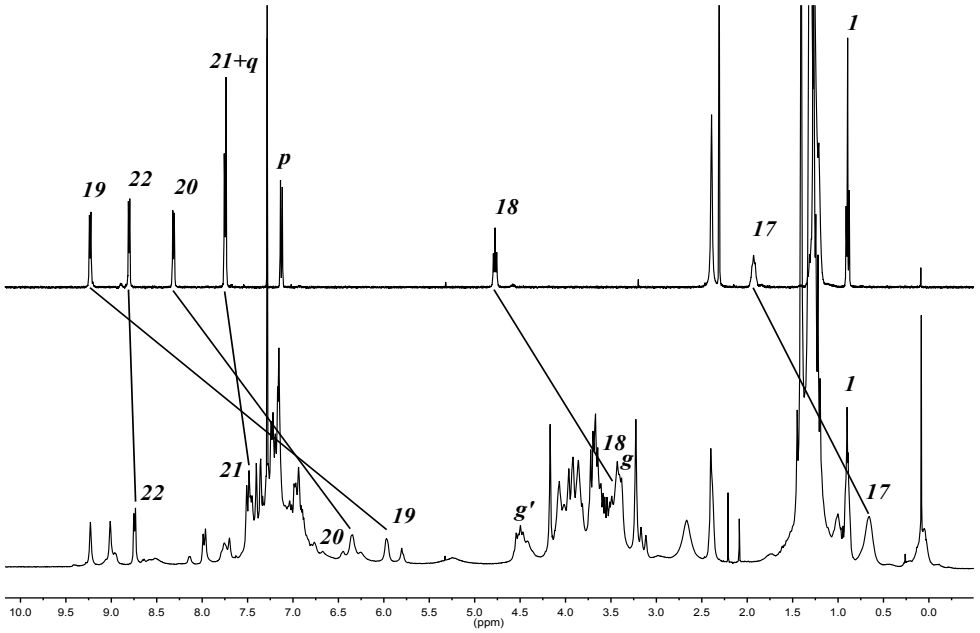


**Figure 3.** $^1$H NMR ($CDCl_3$, 300 MHz) spectrum of: a) **2**•TsO at 273 K; b) **1**⊃**2**•TsO at 253 K.

## 2.3 Supramolecular Assistance of Calix[6]arene in a Nucleophilic Substitution Reaction

The engulfment of **2**•TsO into the cavity of **1** and its orientation was then exploited for oriented pseudorotaxane synthesis; indeed, since the cationic site of **2**•TsO is stabilized by the electron-rich cavity of the macrocycle, the nucleophilicity of its neutral nitrogen

could be enhanced. To demonstrate this hypothesis, a nucleophilic substitution reaction, in which **2**•TsO reacts with an alkylating agent in toluene at 60°C, was carried out, with and without the presence of **1**. Pentyl 4-methylbenzenesulfonate (**3**) was used as alkylating agent and UV-Vis measurements were used to monitor the reaction. Two distinct reactions (**Reaction A** and **B** represented in Scheme 2), were carried on; the progress of the reactions were monitored through the following strategies:

- **A)** to a 1.66 mM solution of **1** in toluene, an equimolar amount of **2**•TsO (**2**•TsO is not completely soluble at r.t.) was added to form pseudorotaxane **1**⊃**2**•TsO(C18down); a 20:1 excess of **3** was then added and the mixture heated at 60°C. To determine the reaction kinetic, the formation of **1**⊃**4**•2TsO was quantified by monitoring absorbance at 470 nm, where the typical band for the pseudorotaxane formation between **1** and *N,N'*-dialkyl-4,4'-bipyridinium salt is observed.
- **B)** to a 1.66 mM solution of **2**•TsO at 60°C in toluene, a 20:1 excess of **3** was added. Since in this solvent **4**•2TsO is not appreciably soluble, the reaction rate for **4**•2TsO formation was monitored by adding an equimolar amount of **1**, with respect to **2**•TsO, at different times to one out of ten separated and parallel reactions between **2**•TsO and **3**. Twenty minutes after the addition of **1**, the solution turns homogeneous, because of the formation of a pseudorotaxane either **1**⊃**4**•2TsO or **1**⊃**2**•2TsO, depending on the species in the mixture. The amount of **4**•2TsO formed is then monitored by observing the increase of absorbance at 470 nm.

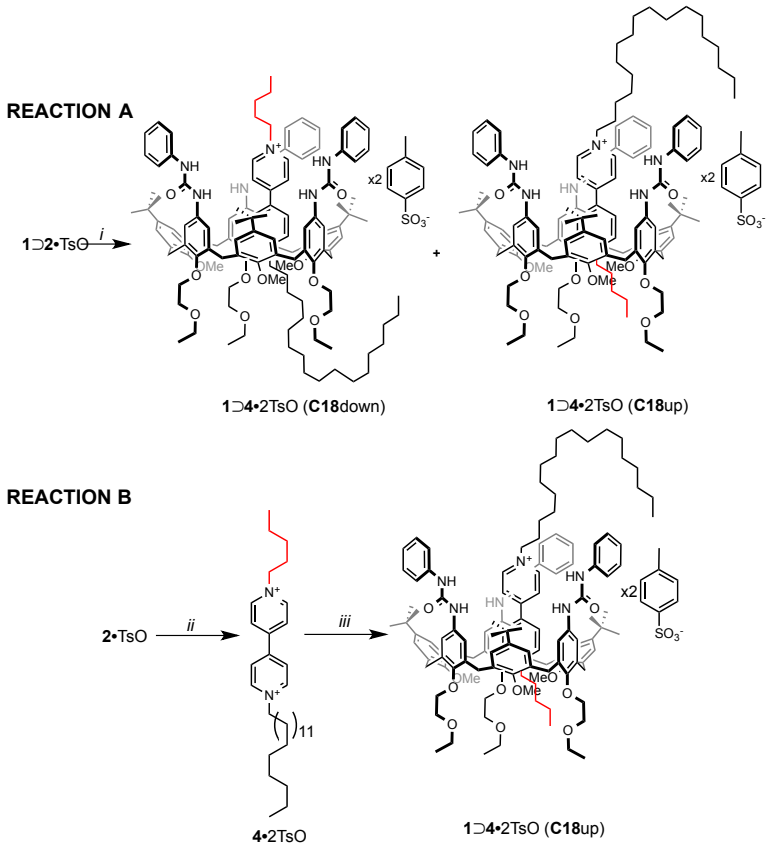


**Scheme 2.** Reagents and conditions: *i*) pentyl 4-methylbenzenesulfonate (**3**), Toluene, 60°C, 4 days; *ii*) pentyl 4-methylbenzenesulfonate (**3**), toluene, 60°C, 4 days; *iii*) **1**, toluene, 60°C, 20 min.

In **Reaction A**, the absorption band at λ= 470 nm relative to **1⊃4•**2TsO considerably increased within few days. The formation of **1⊃4•**2TsO can also be observed by the solution color, that turns from yellowish to red. From the data analysis, a kinetic constant of $k$ = 1.4 x $10^{-4}$ $M^{-1}$ $s^{-1}$ for the formation of **1⊃4•**2TsO was then calculated. Experimental data are in agreement with a $S_N2$ reaction mechanism (see Figure 4a). In **Reaction B**, gradually monitored with the method previously explained, the band intensity at λ= 470 nm increases less significantly respect than **Reaction A**. The data were processed considering **B** as a $S_N2$ reaction; a kinetic constant of 8.6 x $10^{-6}$ $M^{-1}$ $s^{-1}$ for the formation of **4•**2TsO was calculated (Figure 4b). Comparing the two kinetic

constant, an increment by 16 times in the reaction rate was established (see Figure 5) when **1** is present in the mixture.

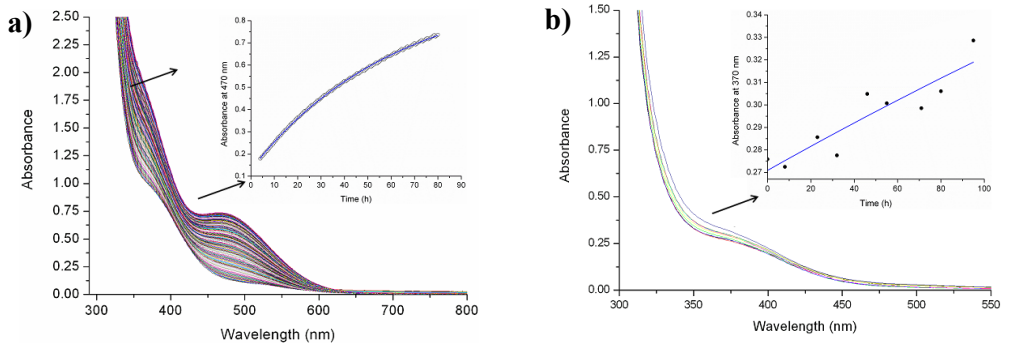


**Figure 4.** Absorption spectra of: a) **Reaction A** (toluene, 333 K) at different time. The inset shows the enhancement of the absorbance band at λ= 470 nm with the proceeding of the reaction; b) **Reaction B** at different time after the addition of one equivalent of **1** and an equilibration time of 20 min. The inset shows the enhancement of the absorbance band at λ= 470 nm with the proceeding of the reaction.

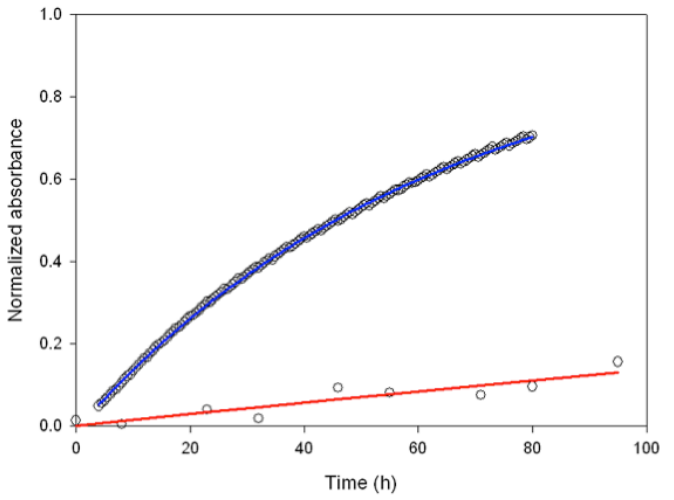


**Figure 5.** Comparison of the absorbance at 470 nm with reaction time in **Reaction A** (blue) and **Reaction B** (red).

The rate enhancement so far measured could be ascribed to the following factors:

a) The pseudorotaxane **1⊃2**•TsO formation strongly enhances the nuclephilicity of the neutral nitrogen in the non alkylated pyridine ring thanks to the charge delocalization of the positive nitrogen induced by the electron-rich cavity of the macrocycle (**Cavity effect**);

b) The phenylureido groups at the upper rim could reasonably have a pivoting role in the threading process of **2**•TsO into **1**. Because of this orientation, in which the free nitrogen of **2**•TsO is in proximity of the ureido moieties of **1**, they could accelerate the reaction by binding the tosylate leaving group at the transition state level (**Phenylureido effect**).

To establish which of these effects do play a dominant role, in particular to verify the role of the phenylureido groups in this reaction, a new reaction **Reaction C** (see Scheme 3) was devised: **2**•TsO (27 mM in $C_6D_6$) was reacted with an excess of **3** (81 mM) in presence of 1,3-diphenylurea (81 mM) at 60° C and the outcome was monitored by NMR spectroscopy.

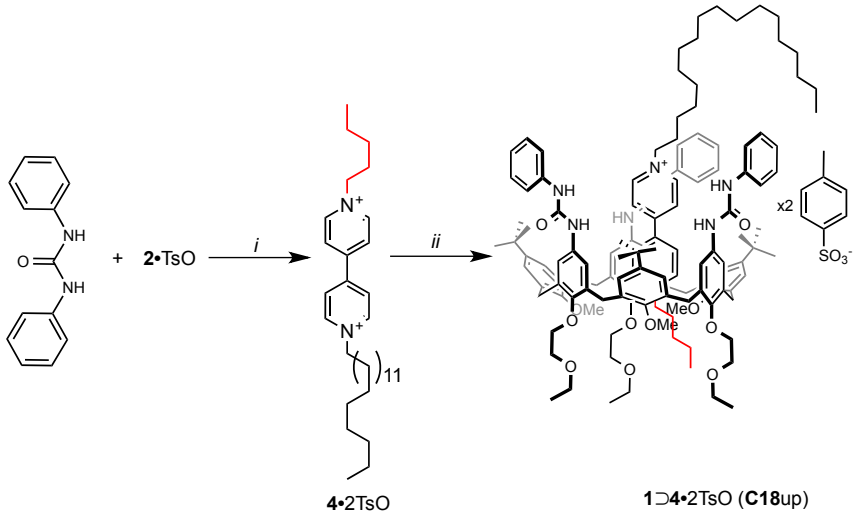


**Scheme 3.** Reagents and conditions: i) Pentyl 4-methylbenzenesulfonate (**3**), $C_6D_6$, 60°C, 4 days; ii) 1 eq. of **1**, $C_6D_6$, 60°C, 20 min.

After four days, an equimolar ratio of **1**, with respect to **2**•TsO, was added to the mixture in order to monitor the amount of **4**•2TsO formed; no traces of the product was evidenced. In fact, in the spectrum collected, the typical signal pattern of **Reaction A** at time zero, with the addition of the signals ascribable to the diphenylurea protons was observed (see Figure 7). From this experiment, it can be inferred that the phenylureido groups alone are not sufficient to accelerate the $S_N2$ reaction between **2**•TsO and **3**.

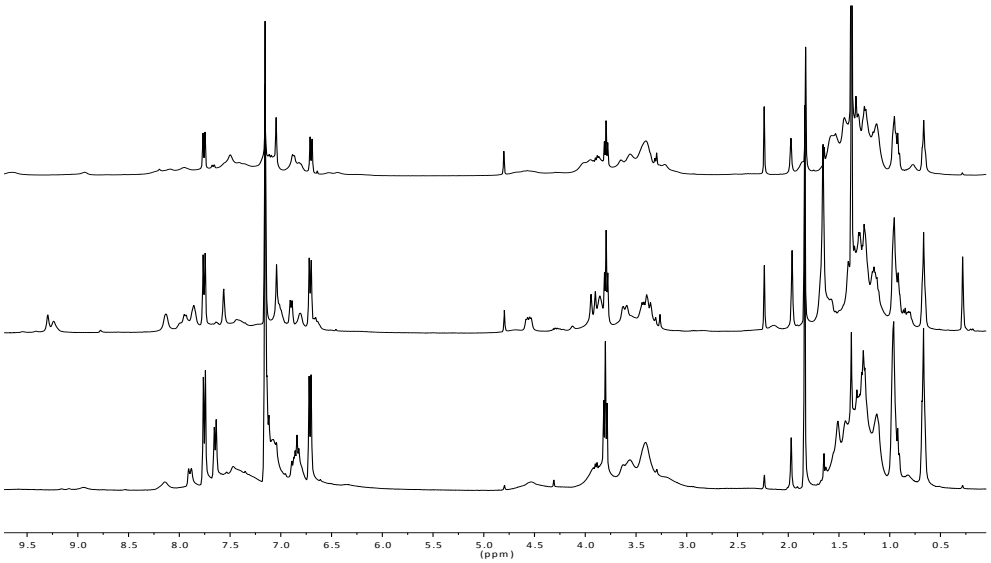


**Figure 7.** All spectra recorded in $C_6D_6$, 400 MHz: a) **Reaction A**, t=0; b) **Reaction A**, t= 4 days; c) **Reaction C** + 1 eq. of **1**, t= 4 days.

With the intent to study the possibility wether the reaction rate enhancement is only due to the presence of the electron-rich cavity, calix[6]arene **1b** was synthesized from **1** after the complete methylation of its NH groups at the upper rim.[3] The ability of this new wheel to act as receptor in low polar solvents for *N*-alkyl-4,4'-bipyridinium axles was examined by stirring a solution of **1b** in $C_6D_6$ at room temperature in presence of **2**•TsO as guest. In the collected $^1$H NMR spectrum, only the signals ascribable to the host **1b** are present (see Figure 8), while the guest remains undissolved. This suggests that **1b**, that lacks the ureido NH, is not able to form complexes with **2**•TsO as guest.

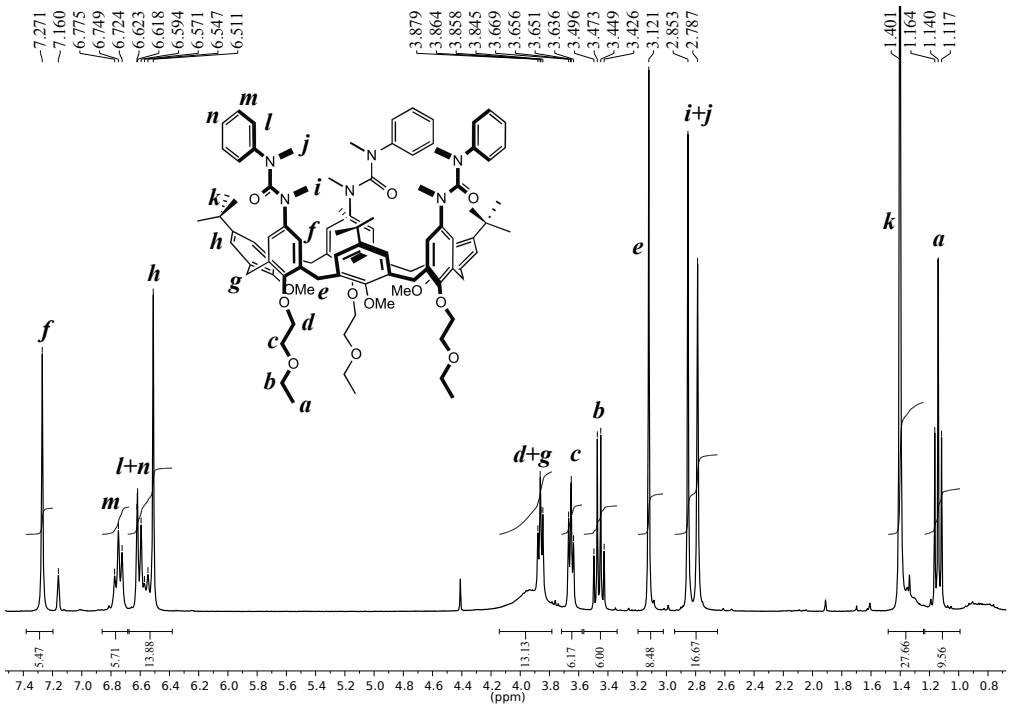


**Figure 8.** $^{1}$H NMR ($C_6D_6$, 400 MHz, 295 K) of **1b** in presence of **2**•TsO.

Afterwards, wheel **1b** was used in place of **1** for a reaction between **2**•TsO and **3** carried out in the same conditions of **Reaction A** (Scheme 4). NMR clearly showed that **1b** does not play any appreciable role in this reaction (see Figure 9).

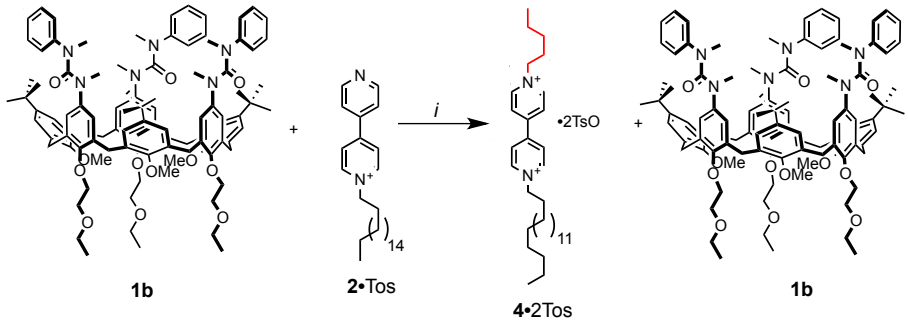


**Scheme 4.** Reagents and conditions: *i*) **3**, $C_6D_6$, 60°C, 4 days.

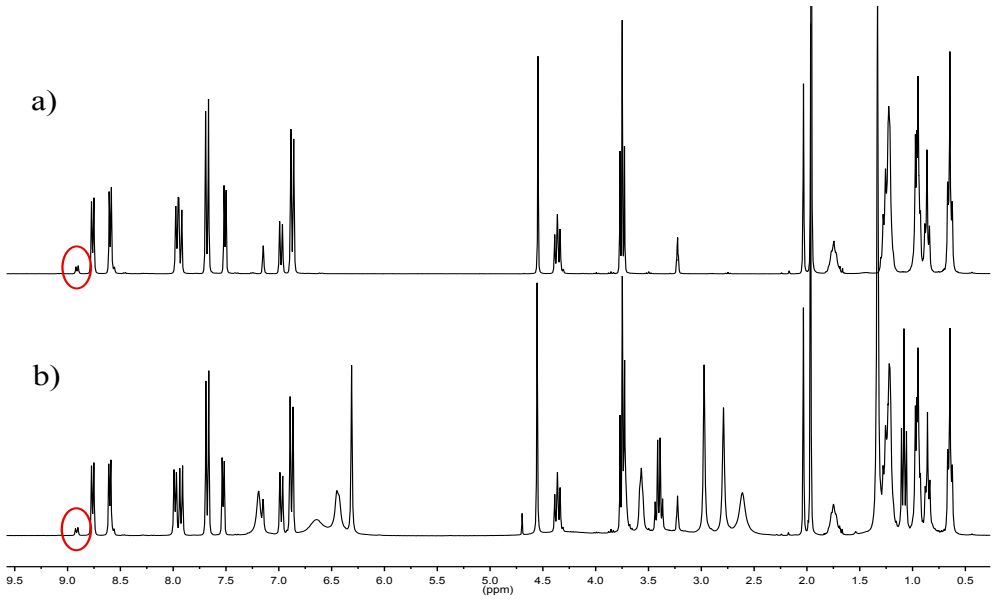


**Figure 9.** $^1$H NMR ($C_6D_6$+ MeOD, 400 MHz) of: a) **Reaction B**, t=4 days; b) **Reaction A** (with **1b**), t= 4 days. The red circles indicate the slight formation of **4**•2TsO in both of the mixture.

From these experiments, it is demonstrated that only the simultaneous presence of both the electron-rich cavity and the phenylureido groups at the upper rim of **1** confers to the wheel the ability to form oriented pseudorotaxanes with **2**•TsO and to accelerate the $S_N2$ reaction between **2**•TsO and **3**.

## 2.4 Kinetical and Thermodynamical Control for the Synthesis of Two Oriented Rotaxanes

As previously reported, the length of the alkyl chains appended to viologen salts, together with the experimental conditions at which the threading into **1** is carried out, could be considered as control elements to govern the orientation of the axle insertion within **1** to yield oriented pseudorotaxanes.[1] For example, mixing an equimolar ratio of **1** and **4**•2TsO in $C_6D_6$, only one orientational isomer is obtained, **1⊃4**•2TsO **($C18_{up}$)** (Figure 10). The chemical shift of the methoxy groups at the lower rim of **1** was

exploited to investigate the orientational output. Refluxing the solution for ten days, the ratio between the two orientational isomers changes from 100(**C18$_{up}$**):0(**C18$_{down}$**) to 70(**C18$_{up}$**):30(**C18$_{down}$**); this latter ratio was estimated as the equilibrium distribution of the two isomers.

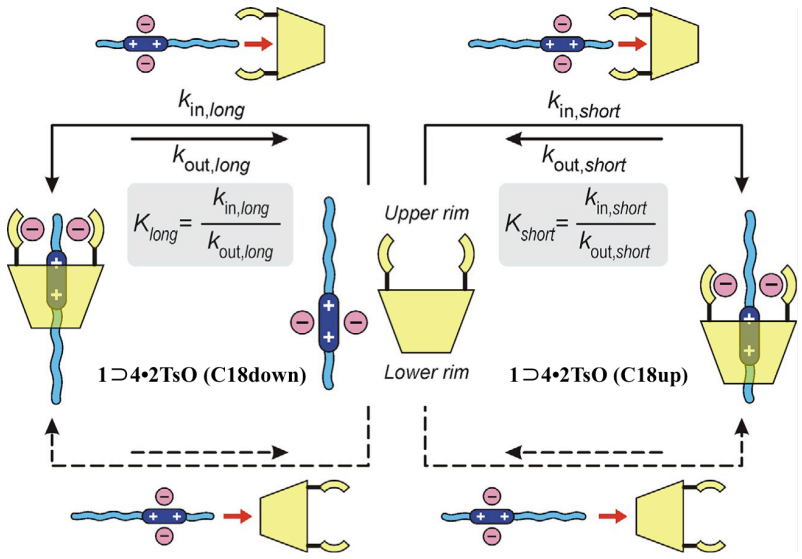


**Figure 10.** Threading–dethreading equilibriums of the two pseudorotaxane isomers**1⊃4**•2TsO **(C18$_{down}$)** and **1⊃4**•2TsO **(C18$_{up}$)**. Dashed lines represent lower-rim threading processes that do not occur under our conditions.

Since it was established that the most favoured orientational isomer of **1⊃2**•TsO is **C18$_{down}$**, the possibility to yield selectively, after a $S_N2$ reaction, the opposite orientational isomers of **1⊃4**•2TsO (**C18$_{up}$**) was investigated. The exclusive obtainment of one out of the two possible pseudorotaxane isomers of **1⊃4**•2TsO is exclusively possible if one of the two possible orientational isomers of **1⊃2**•TsO is more reactive than the other at high temperature; if the two possible orientational isomers of **1⊃2**•TsO have the same reactivity, a 50(**C18$_{up}$**):50(**C18$_{down}$**) ratio of **1⊃4**•2TsO should be expected (Scheme 5).

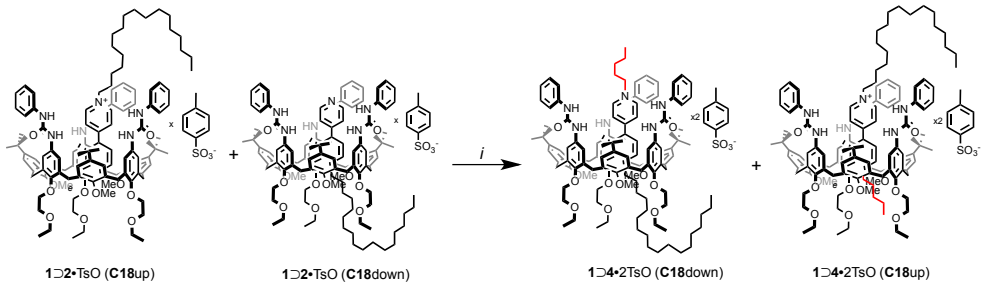


**Scheme 5.** All the orientational isomers of **1⊃2•**TsO are plausible reactants in Reaction A, while all the orientational isomers of **1⊃4•**2TsO are possible products. Reagents and conditions: i) **3**, $C_6D_6$, 60°C, 4 days.

**Reactions A** and **B** were carried out in $C_6D_6$ at 60°C and monitored through $^1$H NMR spectroscopy; after 4 days, in the spectrum of **Reactions B**, the same pattern of signals verified for **Reactions A** at zero time was observed (see Figure 7). On the contrary, after 24h, the $^1$H NMR spectrum of **Reactions A** shows sharper signals, typical of pseudorotaxanes (Figure 11).

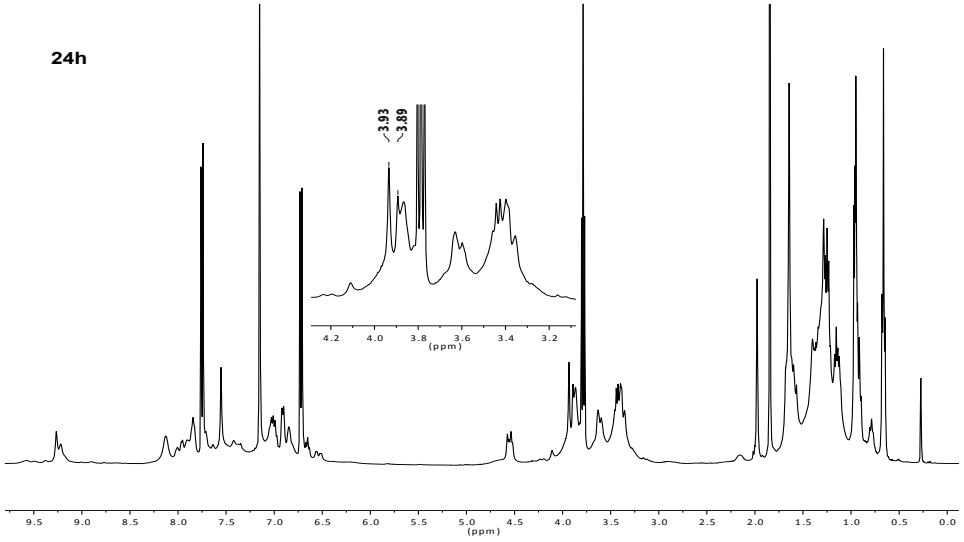


**Figure 11.** $^1$H NMR spectrum ($C_6D_6$, 400 MHZ, 295 K) of **Reactions A**, t= 4 days. The inset shows the two singlets amenable to the two orientational isomers of **1⊃4•**2TsO**($C18_{down}$)** and **($C18_{up}$)** at $\delta$= 3.93 ppm and $\delta$= 3.89 ppm, respectively.

This spectrum also showed that two distinct signals for the methoxy groups of **1** are present, suggesting the presence of two orientational isomers in the reaction mixture (see inset in Figure 10). Based on our previous studies,[1] the signal at $\delta$= 3.93 ppm was ascribed to the orientational isomer **1⊃4**•2TsO**(C18$_{down}$)**, while that at $\delta$= 3.88 ppm to **1⊃4**•2TsO**(C18$_{up}$)**. The presence of both isomers, in different and opposite ratio with respect to previous studies, derives from two parallel and competing reaction routes: *i*) one in which **3** reacts with **1⊃2**•TsO that, being the kinetically stable pseudorotaxane, does not scramble to the opposite isomer or *ii*) because the reaction between **3** and **2**•TsO takes place outside the calixarene cavity yielding **1⊃4**•2TsO**(C18$_{up}$)** that, as previously evidenced,[1] threads **1** through its shorter chain.

In order to verify whether the orientational outcome for pseudorotaxane formation was affected by the structural informations present in the monoalkyl viologen guest, the complexes formed between **6**•TsO,[4] where 4,4'-bipyridyl is decorated with only one hexyl chain terminating with a diphenylacetyl stopper, and **1** was employed. In fact, in **6**•TsO, the presence of the stopper at the terminus of the alkyl chain bonded to the charged nitrogen of the 4,4'-bipyridine imposes its threading into **1** through a different mode, since the guest should enter the calixarene cavity through its neutral nitrogen atom (Scheme 6).

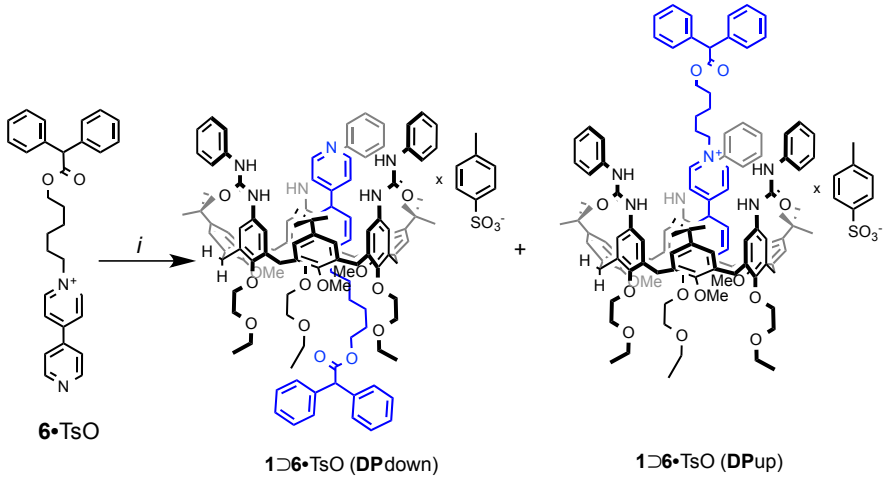


**Scheme 6.** Reagents and conditions: *i*) **1**, toluene-$d_8$, r.t., 1h.

Contrary to what observed for the system **1⊃2**•TsO, the $^1$H NMR spectrum of the solution obtained by mixing **1** and **6**•TsO in toluene-$d_8$ at room temperature, at 253 K and at 355 K showed very broad signals (Figure 12). Nevertheless, 2D NMR measurements carried out at 355K suggested the formation of both the orientational complexes **1⊃6**•TsO(**DP$_{down}$**) and **1⊃6**•TsO(**DP$_{up}$**).

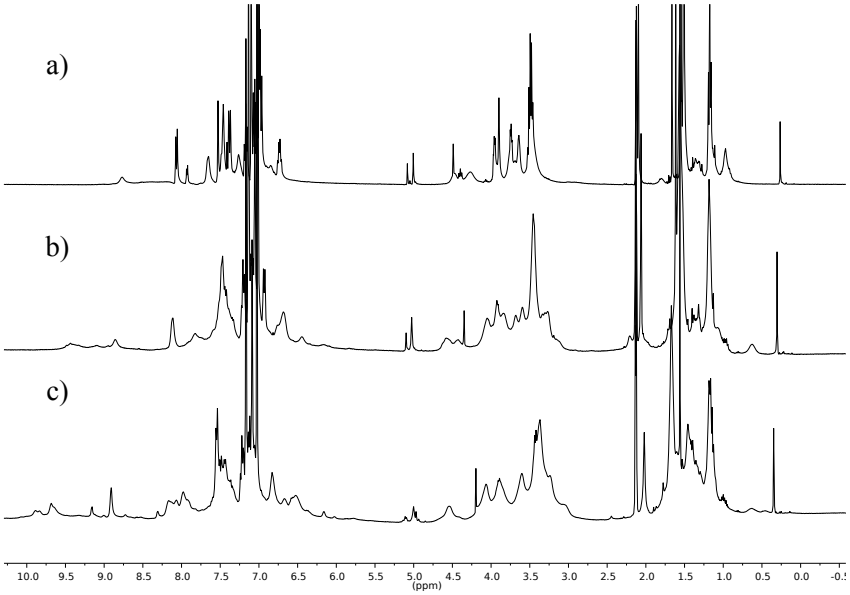


**Figure 12.** $^1$H NMR (toluene-$d_8$, 400 MHz) spectrum of **1⊃6**•TsO at: a) 353 K; b) 295 K and c) 253 K.

In these two isomers, the free nitrogen of **6**•TsO engulfed into **1** does have an opposite orientation with respect to the calixarene rims. The mixture of **1⊃6**•TsO**(DP$_{down}$)** and **1⊃6**•TsO**(DP$_{up}$)** was reacted with the long 12-hydroxydodecyl 4-methylbenzenesulfonate (Scheme 7).

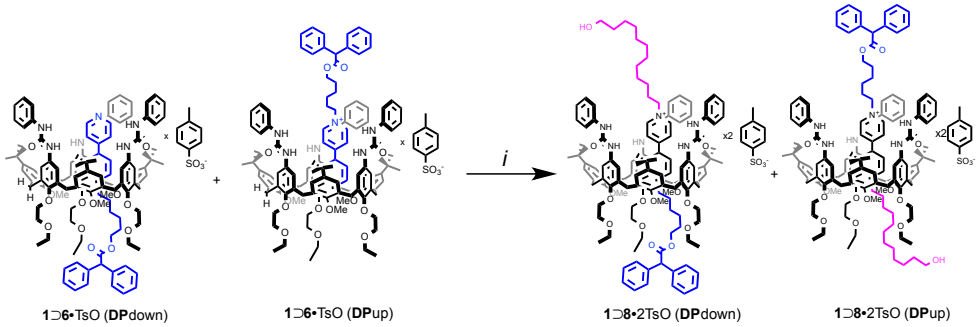


**Scheme 7.** Reagents and conditions: *i*) 12-hydroxydodecyl 4-methylbenzenesulfonate, toluene, reflux, 4 days.

After four days**,** the mixture was cooled to room temperature and diphenylacetyl chloride and triethylamine were added in order to stopper the pseudorotaxanes formed (**1⊃8**•2TsO**(DP$_{down}$)** and/or **1⊃8**•2TsO**(DP$_{up}$)**) to yield the corresponding rotaxanes (**9a**•2TsO and/or **9b**•2TsO) (Scheme 8)).

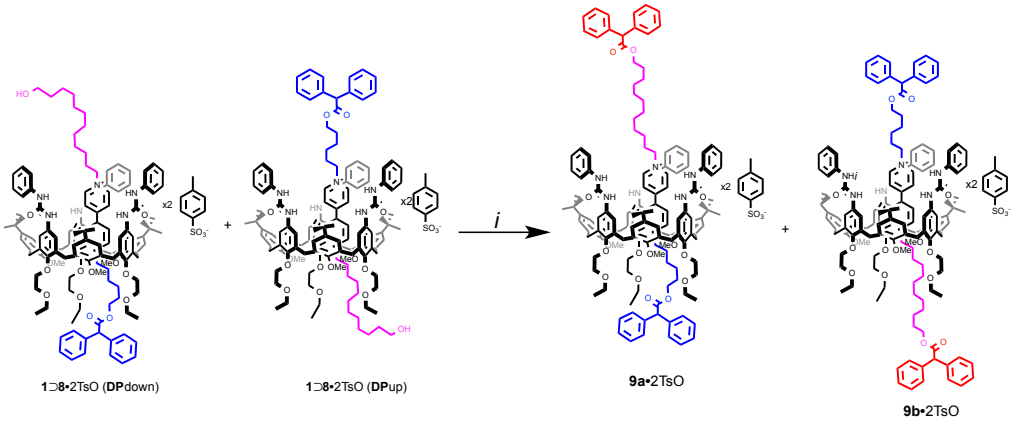


**Scheme 8.** Reagents and conditions: *i*) diphenylacetyl chloride, toluene, r.t., 16h

NMR investigations were carried out to establish the structure of the reaction products. The $^{1}$H NMR (Figure 13) clearly showed the presence of only one out of two possible rotaxanes **9a**•2TsO and **9b**•2TsO. In fact, the presence of only one signal for the wheel methoxy groups at $\delta$= 3.88 ppm, only one triplet for $\alpha$ and $\alpha'$ at $\delta$= 4.32 and $\delta$= 4.04 ppm respectively, clearly demonstrates the exclusive formation of rotaxane **9a**•2TsO.

This suggests that reaction between **1⊃6**•TsO and 12-hydroxydodecyl 4-methylbenzenesulfonate took place only on the orientational complex **1⊃6**•TsO(**DP$_{down}$**) and that the stoppering reaction occurred only on pseudorotaxane **1⊃8**•2TsO(**DP$_{down}$**). 2D NMR spectra confirmed the relative orientation of the two arms of the dumbbell in **9a**•2TsO.

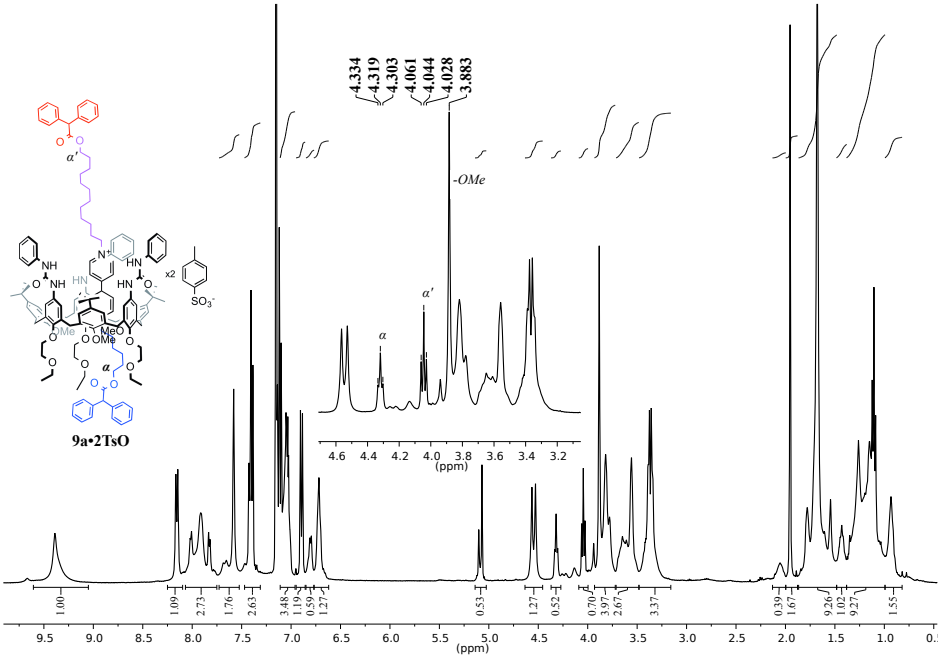


**Figure 13.** $^{1}$H NMR ($C_6D_6$, 400 MHz) spectrum of rotaxane **9a**•2TsO. The inset shows the diagnostic chemical shifts for a rotaxane bearing a short alkyl chain at the lower rim of **1**.

This strictly orientational outcome was also indirectly confirmed by synthesising the opposite orientational rotaxane isomer **9b**•2TsO. Pseudorotaxane **1⊃7**•TsO, obtained in toluene by mixing **1** and **7**•TsO, was refluxed with an excess of 6-(tosyloxy)hexyl 2,2-diphenylacetate (**5**) for four days.

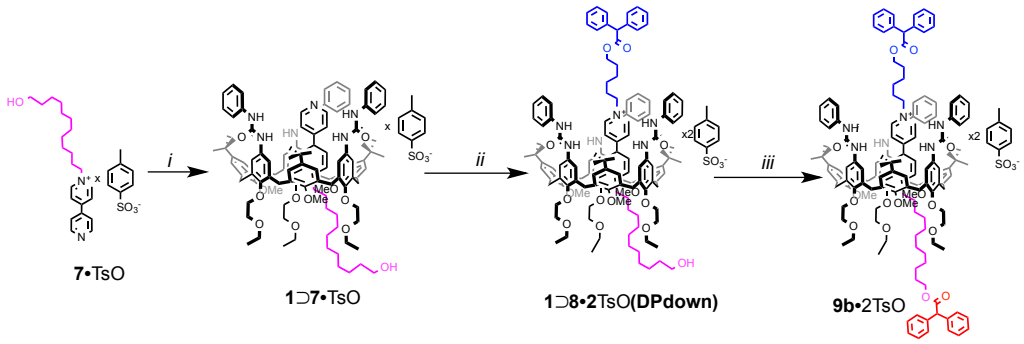


**Scheme 9.** Reagents and conditions: *i*) **1**, toluene, r.t., 1h; *ii*) 6-(tosyloxy)hexyl 2,2-diphenylacetate (**5**), toluene, reflux, 4 days; *iii*) diphenylacetyl chloride, toluene, r.t., 16h.

The reaction mixture was then brought to room temperature and diphenylacetyl chloride and triethylamine were added. After 16h the reaction product was isolated and characterized through NMR techniques in $C_6D_6$. In the $^1$H NMR spectrum (Figure 14), the chemical shift of the wheel methoxy groups, that resonate at $\delta$= 3.95 ppm, the overlapping of the signals attributed to protons $\alpha$ and $\alpha'$, together with the presence of the two singlets for the methyne protons of the two diphenylacetyl stoppers, are in agreement with the structure of rotaxane **9b**•2TsO (64% yield), in which the non symmetrical dumbbell has the opposite orientation with respect to **9a**•2TsO.

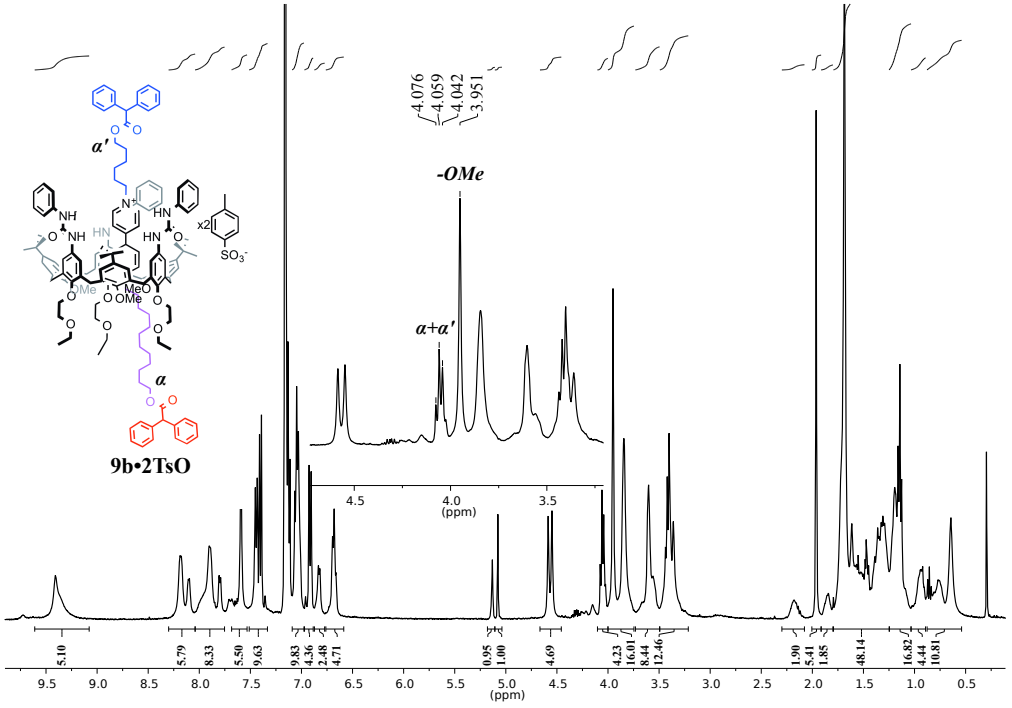


**Figure 14.** $^{1}$H NMR ($C_6D_6$, 400 MHz) spectrum of rotaxane **9b**•2TsO. The inset shows the diagnostic chemical shifts for a rotaxane bearing a long alkyl chain at the lower rim of **1**.

## 2.5 Steering the Spectroscopic Behavior of Calix[6]arene Wheels Bearing Naphthyl Groups through Pseudorotaxane Formation

### *2.5.1 Introduction.*

In view of our current interest in the design and synthesis of molecular machine prototypes based on calix[6]arene endowed with working modes governed and monitored through a wider set of control tools, we envisaged that the incorporation of photoactive and quite extensively employed naphthyl moieties onto the calixarene skeleton could provide either a deeper insights into their working modes as wheels and potentially exploit them as "photoresponsive" groups to further signal/monitor the functions of new working devices.[5–7] Therefore, the synthesis, structural

characterization and study of the photophysical behavior of two new calix[6]arene wheels decorated with three naphthyl groups anchored to the upper or lower rim of their phenylureido calix[6]arene platform was tackled.

### 2.5.2 *Synthesis and design of the wheels.*

In order to study whether the photochemical properties of the naphthalene group can be affected by its position within a defined supramolecular system, we designed to synthesize the calix[6]arene-based derivatives **15** and **18** (Figure 15), which are characterized by the different position of their naphthyl groups with respect to the aromatic cavity of the macrocycle.

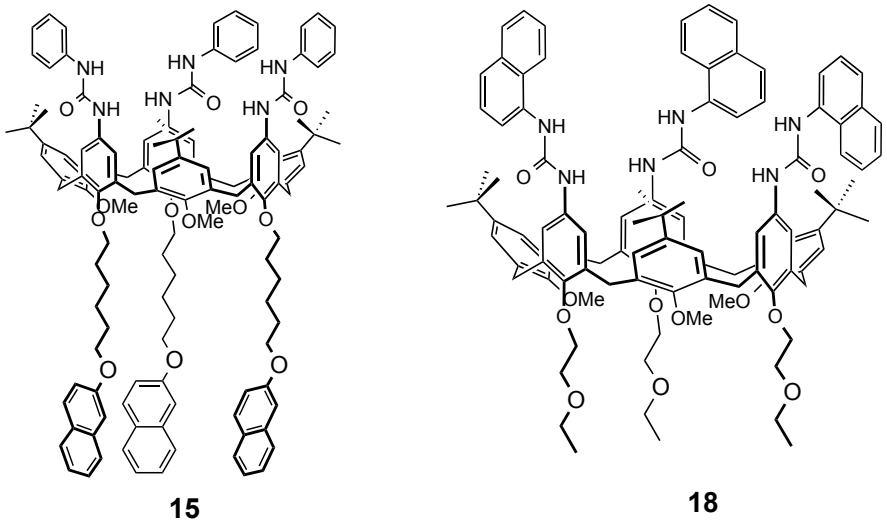


**Figure 15**. Calix[6]arene whee1s, **15** and **18**, used in this study.

The three *β*-naphthyloxy groups of **15** are linked to the three phenolic groups present at the macrocycle lower rim through a C6 alkyl chain acting as a spacer, while in **18** these units are directly attached to the three urea moieties present on the host upper rim. These two derivatives present all the structural features necessary to maintain the recognition properties of the simpler **1**, in low polar solvents, towards molecular axles derived from the *N*,*N*'-dialkyl-4,4'-bipyridinium (viologen) unit namely a pre-organized electron-rich aromatic cavity, necessary to stabilize the dicationic unit of the

axle and ureido groups that, acting as hydrogen bond donor groups, bind the two counter-anions.[8,9]

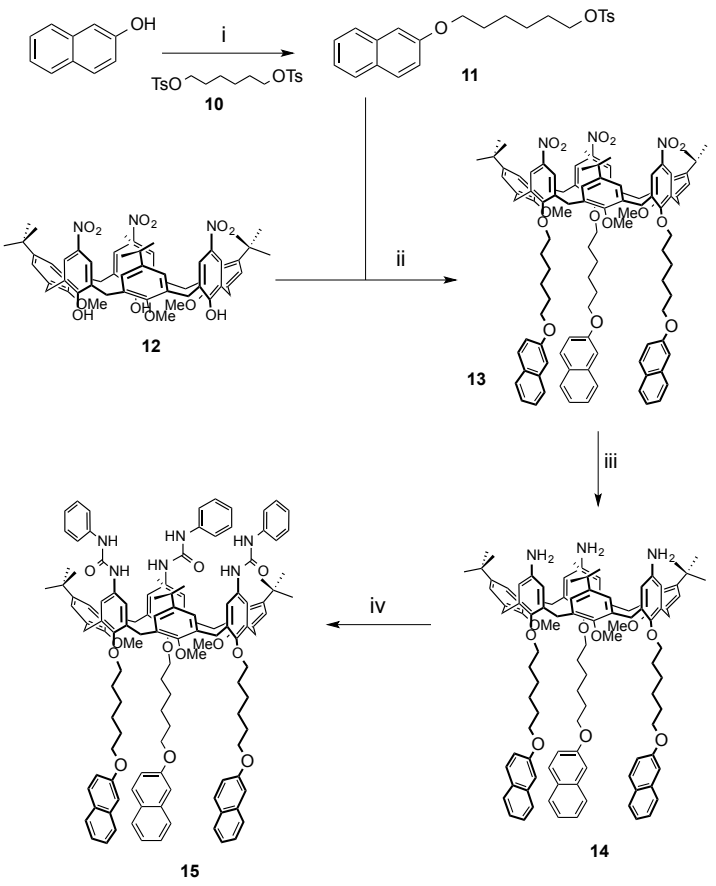


**Scheme 10.** Reagents and Conditions: *i*) 2-naphthol, $K_2CO_3$, $CH_3CN$, reflux, 48h; *ii*) $K_2CO_3$, $CH_3CN$, reflux, 72h; *iii*) $NH_2NH_2 \cdot H_2O$, MeOH, reflux, 6h; *iv*) $C_6H_5NCO$, $CH_2Cl_2$, r.t., 2h.

Calixarene **15** was obtained through a convergent synthetic approach (see Scheme 10); the alkylating agent **11** was obtained in high yields by reacting 2-naphthol with a molar excess of 1,6-hexanediol ditosylate (**10**) in refluxing acetonitrile. A similar procedure has been adopted to functionalize the phenolic groups at the lower rim of the known calix[6]arene **12**, to yield **13**. The three nitro groups of **13** were then quantitatively reduced to amino in refluxing methanol using hydrazine monohydrate as the reducing agent and Pd/C as the catalyst. The phenylureido moieties were finally inserted on the macrocycle upper rim by reacting **14** with phenyl isocyanate in dry dichloromethane to

yield **15** with 16% of overall yield. Calixarene **18** was synthesized in two steps starting from the known trinitro calix[6]arene derivative **16** (see Scheme 11). The nitro groups of this compound were quantitatively reduced using the same approach used for **13**. The resulting triamino derivative **17** was immediately reacted with 1-naphthyl isocyanate to obtain **18** in 48% of overall yield.

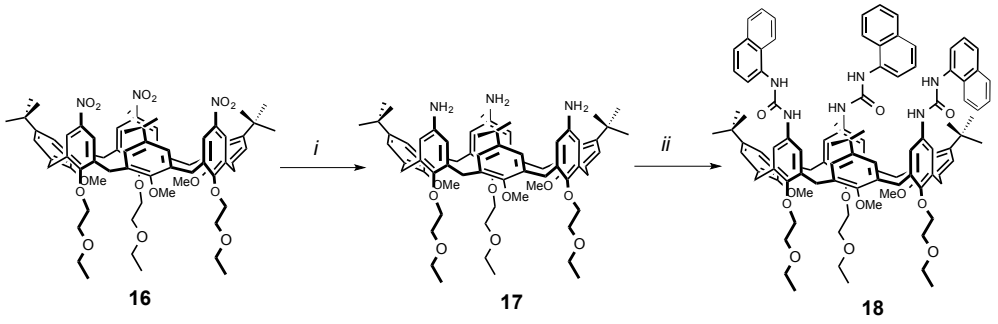


**Scheme 11.** Reagents and Conditions: *i*) $NH_2NH_2 \bullet H_2O$, MeOH, reflux, 6h; *ii*) $C_{10}H_7NCO$, $CH_2Cl_2$, r.t., 2h.

The common features of the $^1H$ NMR spectra taken respectively in $CD_2Cl_2$ and $CDCl_3$ on the novel derivatives **15** and **18**, respectively, are that in these solvent they adopt a pseudo *cone* conformation on the NMR timescale, as suggested by the signal of the methoxy groups at the lower rim that, being oriented inward the cavity in the NMR timescale, resonate at $\delta$ = 2.80 ppm (Figure 16).

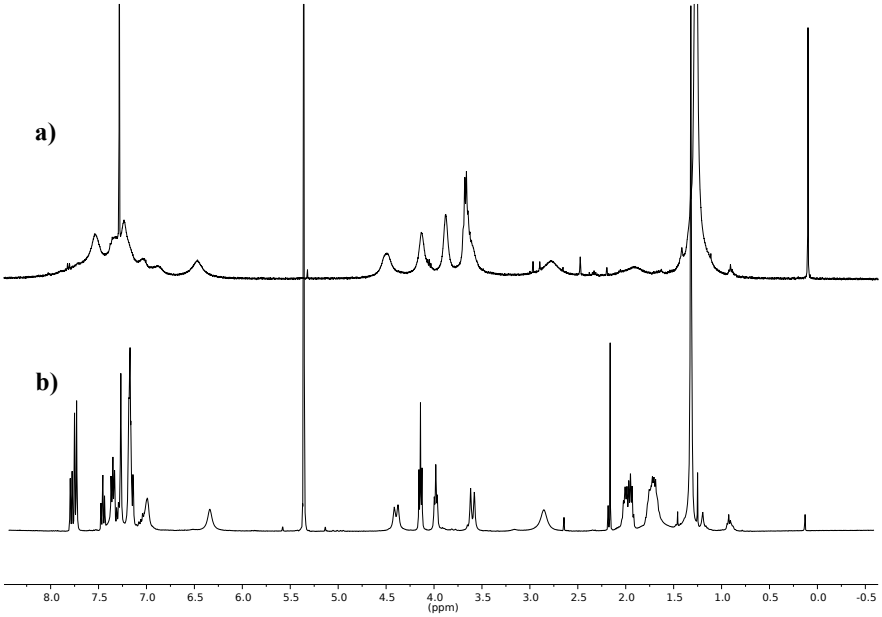


**Figure 16.** $^{1}$H NMR (400 MHz) spectra of: a) **18** in $CDCl_3$; b) **15** in $CD_2Cl_2$.

Other signals that confirm the pseudo *cone* conformation are the two doublet at $\delta$= 4.4 and 3.6 ppm ($J$ = 15.6 Hz) related to the bridging methylene groups of the macrocycle. Despite these conformational evidences, the $^{1}$H NMR spectrum of **18** (see Figure 16b) in $CDCl_3$ gives rise to several very broad resonances, which evidence the high conformational mobility of this host in chloroform solution. Contrariwise, in $CD_2Cl_2$, **15** presents very sharp NMR signals, indicating its lower mobility with respect to **18**.

The ability of **15** and **18** to form pseudorotaxanes towards **DOV**•2TsO as the axle was evaluated and monitored through NMR techniques. For both **15** and **18**, the downfield shift experienced by their methoxy groups that, because of their expulsion from the cavity upon complex formation, now resonate at $\delta$= 3.95 ppm, the downfield shift of the ureido moieties of about 3 ppm, the appearance of the typical AX quartet of the bridging methylene protons of the calixarene skeleton and the upfield shift of about 3 ppm of the *N*-$CH_2$- protons of the axle due to its inclusion, demonstrated that the presence of the naphthyl groups does not substantially affect their binding abilities (Figure 17).

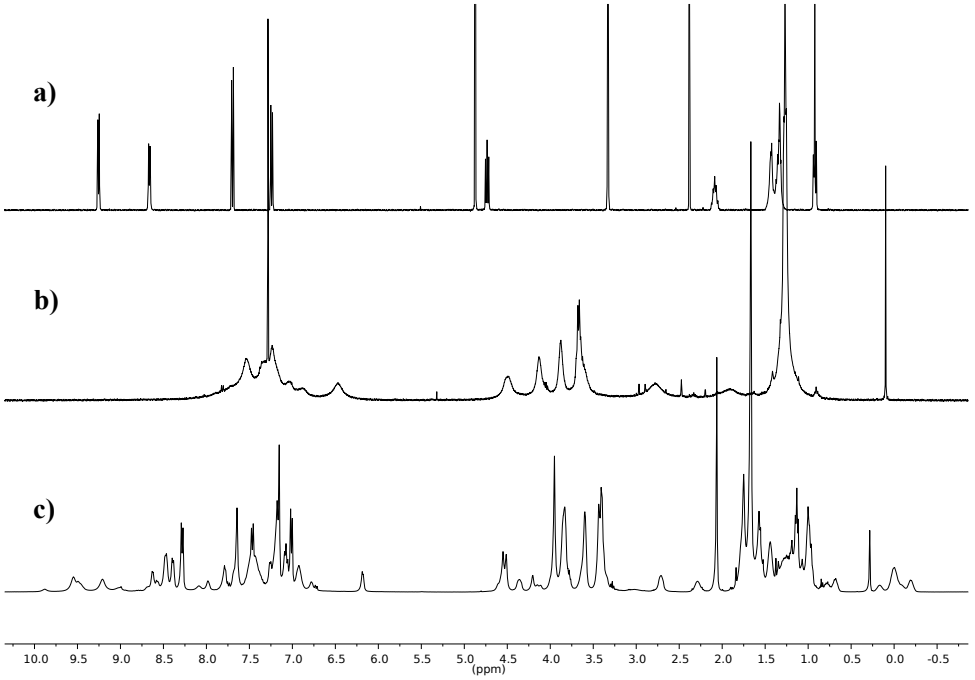


**Figure 17.** $^1$H NMR (400 MHz) spectra of: a) **DOV**•2TsO in MeOD; b) **18** in $CDCl_3$; c) pseudorotaxane **18**⊃**DOV**•2TsO in $C_6D_6$.

The association of **15** with **DOV**•2TsO could also be probed by electrochemical techniques. The voltammetric pattern of calixarene **15** exhibits no reduction processes and several chemically irreversible oxidation processes with onset at ca. +1.1 V versus the saturated calomel electrode (SCE), assigned to the oxidation of the alkoxynaphthalene pendant units and the alkoybenzene rings of the calixarene skeleton. Because of their irreversible nature, these processes will not be further discussed. **DOV**•2TsO shows the typical reversible monoelectronic reductions of the 4,4′-bipyridinium unit ($E_{1/2}'$ = –0.27 V, $E_{1/2}''$ = –0.81 V vs SCE) and no oxidation[10]. The inclusion of **DOV**•2TsO into **15** causes a large negative shift of the first reduction potential, while the second process occurs at the same potential as for the free guest. These results indicate that *i*) the bipyridinium unit becomes more difficult to reduce because it is stabilized inside the calixarene wheel, and *ii*) the one-electron reduction of **DOV**•2TsO promotes its dethreading from **7**, in line with the behavior of several related bipyridinium-containing pseudorotaxanes.[9] The large peak-to-peak separation

and the scan-rate dependence of the first reduction process of the [**15**⊃**DOV**•2TsO] complex indicate that the complexation/decomplexation reactions occur on the voltammetric time scale; these aspects have been discussed in detail elsewhere.[9]
The spectroscopic and photophysical properties of **15** and **18** and their pseudorotaxanes were then preliminary evaluated by Prof. A. Credi and his group of the University of Bologna.

### *2.5.3 Spectroscopic and photophysical experiments on the calixarenes and their pseudorotaxanes.*

The absorption and luminescence data for the calixarene host **15**, the guest **DOV**•2TsO, their pseudorotaxane, and the models compound for the calixarene scaffold (**1**) and the naphthalene chromophore (2-methoxynaphthalene, **2-MN**) are reported in Table 1. The UV-visible absorption spectrum of **15** in $CH_2Cl_2$ (Figure 18) shows the bands typical of the aromatic systems of the calixarene ring in the 240-300 nm region, while the features occurring between 280 and 340 nm are assigned to π-π* transitions of the 2-alkoxynaphthalene units. The absorption spectrum of **15** matches well with the sum of the absorption spectra of its chromophoric components (**1** + 3×**2-MN**) in the 280-340 nm region, indicating the absence of interactions between the pendant naphthalene units in the ground state. On the other hand, the absorption of **15** is substantially more intense than the sum of its chromophoric components in the 240-280 nm region. As the naphthalene units and the wheel skeleton are electronically insulated by the long alkyl chains, we hypothesize that the change in the calixarene absorption bands arises from conformational effects exerted on the diphenylureido units of the wheel by the bulky substituents at the lower rim.

| | Absorption | | Luminescence | | |
|---|---|---|---|---|---|
| Compound | $\lambda_{max}$ (nm) | $\varepsilon$ ($M^{-1}$ $cm^{-1}$) | $\lambda_{max}$ (nm) | $\Phi$ | $\tau$ (ns) |
| **1** [a] | 250 [b] | 60000 [b] | 340 | 0.0025 | < 1 [c] |
| **2-MN** | 327 | 1900 | 348 | 0.12 | 4.8 |
| **15** | 327<br>250 [b] | 5200<br>63000 [b] | 350 | 0.12 | 5.0 |
| **DOV**•2TsO [a] | 270 | 24000 | — | — | — |
| [**15**⊃**DOV**•2TsO] | 460 | 600 | 350 | 0.006 | < 1 [c] |

**Table 1.** Absorption and luminescence data for the calixarene host **15**, the guest **DOV**•2TsO, their pseudorotaxane, and the model compounds for the chromophoric units (air equilibrated $CH_2Cl_2$, r.t.). [a] Data from ref. 9. [b] Shoulder on the lower energy side of an intense band. [c] The lifetime value is shorter than the time resolution of the equipment.

In $CH_2Cl_2$ at room temperature, compound **15** shows a luminescence band ($\lambda_{max}$ = 350 nm) that is safely assigned to the fluorescence of the alkoxynapthalene units (Table 1 and Figure 18, inset). The emission quantum yield ($\Phi$ = 0.12) and lifetime ($\tau$ = 5.0 ns) values are identical within errors to those of the **2-MN** model. In rigid matrix at 77K, **7** shows both the structured fluorescence ($\lambda_{max}$ = 350 nm) and phosphorescence ($\lambda_{max}$ = 465 nm) bands of the alkoxynaphthalene units.

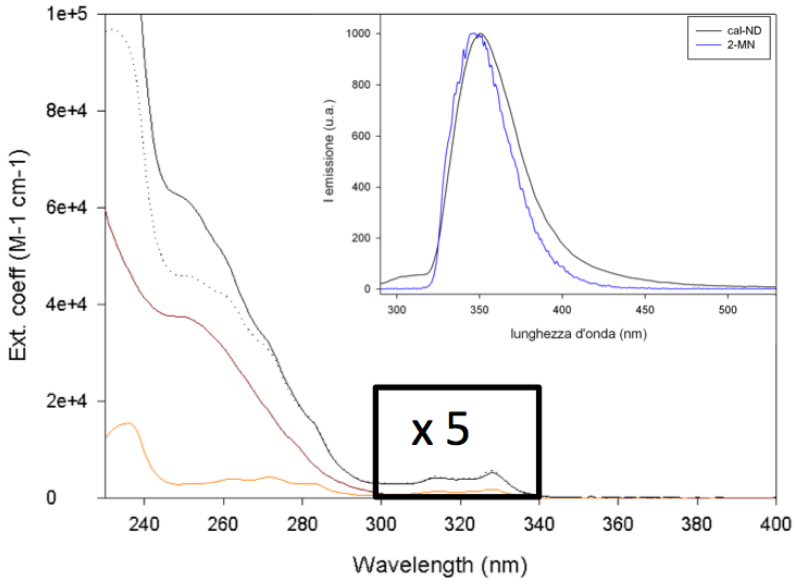


**Figure 18.** Absorption spectra of multichromophoric calixarene **15**(full line), calixarene **1** (red line), **2-MN** (orange line). The sum of the absorption spectra of the chromophoric components of **15** (dotted line) is also shown for comparison. Inset: normalized emission spectra ($\lambda_{exc}$ = 315 nm) of **15** (black line) and **2-MN** (blue line). Conditions: air equilibrated $CH_2Cl_2$, room temperature.

The corrected excitation spectrum of **15** ($\lambda_{em}$ = 350 nm) at room temperature matches with the absorption spectrum of the same compound only between 310 and 340 nm, while it is significantly weaker in the 230-310 nm region. Conversely, the excitation spectrum of **15** exhibits a good overlap with the absorption spectrum of **2-MN** in the whole spectral region monitored (Figure 19).

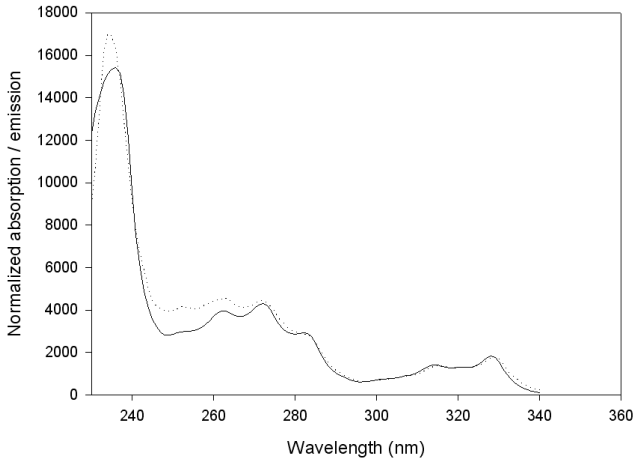


**Figure 19.** The corrected excitation spectrum of **15** (dotted line) and **2-MN** (full line). Conditions: air equilibrated $CH_2Cl_2$, room temperature.

This observation indicates that the energy transfer from the excited states located on the calixarene skeleton to the excited singlet level of the pendant naphthalene units is inefficient. Unfortunately an estimation of the residual fluorescence intensity arising from the calixarene annulus ($\lambda_{max}$ = 340 nm, Table 1) is prevented because such an emission band is covered by the much more intense naphthalene-type fluorescence ($\lambda_{max}$ = 350 nm). The application of the Förster model[11] suggests that the low energy-transfer efficiency is determined by the very poor overlap between the calixarene-type (donor) emission and the naphthalene-type (acceptor) absorption, together with the small quantum yield of the calixarene-type emission. In summary, the naphthalene units appended at the lower rim of the wheel as in **15** are photophysically independent both on one another and on the calixarene chromophore.

The addition of **DOV**•2TsO to a solution of **15** causes changes in the UV absorption bands of the molecular components and the appearance of broad absorption features in the 350-600 nm region ($\lambda_{max}$ = 460 nm, Table 1), arising from charge-transfer (CT) interactions between the π-electron rich aromatic units of the calixarene and the π-electron poor 4,4′-bipyridiniun moiety of the guest.[9] In the same experiment the fluorescence band of **15** is quenched as a function of the amount of **DOV**•2TsO added (Figure 20). The absorption and luminescence data collected in the titration

experiments could be satisfactorily fitted with a 1:1 binding model, yielding a value of the association constant log$K$ = (7.0±0.2). These results are consistent with the NMR data and with previous observations on related compounds,[9] and confirm the formation of a pseudorotaxane in with **DOV**•2TsO is threaded into the cavity of **15** with its bipyridinium unit located close to the aromatic units of the calixarene.

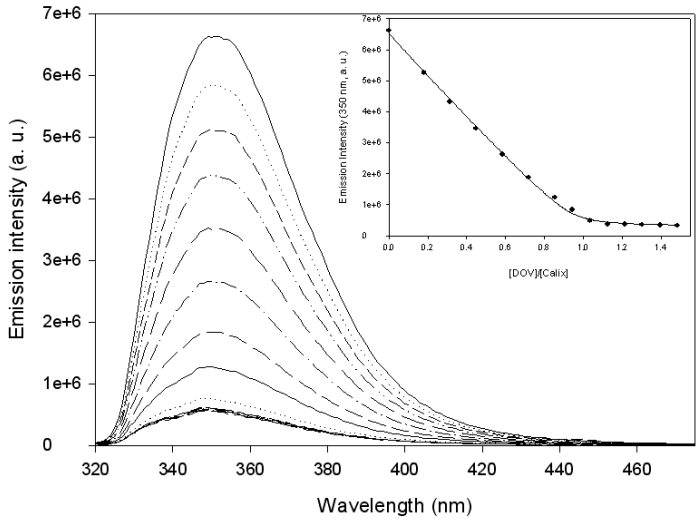


**Figure 20.** Luminescence spectral changes ($\lambda_{exc}$ = 315 nm) upon addition of increasing amounts of **DOV**•2TsO to a $3.0\times10^{-5}$ M solution of **15**. The inset shows the titration curve obtained by plotting the emission intensity at 350 nm as a function of the **DOV**•2TsO equivalents; the full line is the data fitting corresponding to a 1:1 binding model. Conditions: air equilibrated $CH_2Cl_2$, room temperature.

In the light of these observations, it is worth discussing the effect of the **DOV**•2TsO guest on the photophysics of the calixarene. From the residual emission intensity of **15** at the end of the titration one can calculate the quenching rate constant according to eq. 1:

$$k_q = 1/\tau_0\,(\Phi_0/\Phi - 1) \qquad (1)$$

in which $\tau_0$ and $\Phi_0$ are the luminescence lifetime and quantum yields of **15** in the absence of **DOV**•2TsO, and $\Phi$ is the luminescence quantum yield of the complex.

According to the data listed in Table 1, $k_q = 3.8\times10^9$ $s^{-1}$. The quenching of the naphthalene-type emission of **15** by **DOV**•2TsO can involve two distinct mechanisms: *i*) energy transfer from the singlet excited state localized on an alkoxynaphthalene unit to the lower lying charge-transfer levels due to the calixarene-bipyridinium interaction, and *ii*) electron transfer from the alkoxynaphthalene singlet excited state to the encapsulated bipyridinium unit. Because of the good overlap between the naphthalene emission and the visibile charge-transfer absorption and the large luminescence quantum yield of the donor, the Förster radius (i.e. the donor-acceptor distance at which the energy-transfer efficiency is 50%) results to be as long as 5.4 nm. Considering that the maximum distance between the naphthalene substituents and the center of the calixarene cavity is 1.5 nm, the energy-transfer process (mechanism *ii*) is expected to be very efficient. On the other hand, from the available excited state energy and the potential values for oxidation of the donor and reduction of the acceptor (vide supra), one can estimate that the photoinduced electron transfer (mechanism *i*) is highly exoergonic ($\Delta G° < -1.8$ eV).

To gain more insight into the luminescence quenching mechanism we performed emission experiments in rigid matrix at 77 K. Under these conditions the solvent reorganization energy is small and highly exoergonic electron-transfer processes such as that mentioned above, that may fall into the Marcus inverted region, can become slow. Both the naphthalene-type fluorescence and phosphorescence bands observed for **15** in $CH_2Cl_2$:$CHCl_3$ 1:1 at 77 K are absent in the spectrum of the [**15**⊃**DOV**•2TsO] complex. The occurrence of such a strong quenching in a rigid medium at low temperature is consistent with an energy transfer from the naphthalene excited singlet to the CT levels. Laser flash photolysis experiments with ns excitation pulses, carried out in solution at room temperature, revealed no trace of the bipyridinium radical cation, which would be a product of the electron-transfer reaction. It cannot be excluded, however, that a fast back-electron transfer process prevents the accumulation of the bipyridinium radical cation on the ns time scale.

The absorption and luminescence data for the calixarene host **18**, the guest **DOV**•2TsO, their pseudorotaxane, and the model chromophoric compound for the

calixarene (N-1-naphthyl-N′-phenylurea, **1-NPU**) are reported in Table 2. The absorption spectrum of **18** in $CH_2Cl_2$ (Figure 22) shows the bands typical of the napthyl-phenylureido chromophore in the near UV region. The spectrum is very similar to the sum of the spectra of its chromophoric components (3×**1-NPU**), which suggests that the interactions between the pendant naphthalene units are negligible in the ground state.

| | Absorption | | Luminescence | | |
|---|---|---|---|---|---|
| Compound | $\lambda_{max}$ (nm) | ε ($M^{-1}$ $cm^{-1}$) | $\lambda_{max}$ (nm) | Φ | τ (ns) |
| **1-NPU** | 295 | 7500 | 360 | 0.18 | 1.6 |
| **18** | 295 | 24000 | 410 | 0.11 | 2.8 [a]<br>18 [a] |
| **DOV**•2TsO [b] | 270 | 24000 | — | — | — |
| [**18**⊃**DOV**•2TsO] | 450 [c] | 200 [c] | 360 | - | 2.9 |

**Table 2.** Absorption and luminescence data for the calixarene host **18**, the guest **DOV**•2TsO, their pseudorotaxane, and the model chromophoric compound **1-NPU** (air equilibrated $CH_2Cl_2$, r.t.). [a] Biexponential decay. [b] Data from ref. 9 [c] Shoulder on the lower energy side of an intense band. [d] The lifetime value is shorter than the time resolution of the equipment.

The luminescence band of **18** in $CH_2Cl_2$ at room temperature is less intense, much broader and shifted to longer wavelengths in comparison with that of the **1-NPU** model (Table 2 and Figure 22, inset). The excitation spectrum of **18** ($\lambda_{em}$ = 410 nm, Figure 21) is similar to its absorption spectrum.

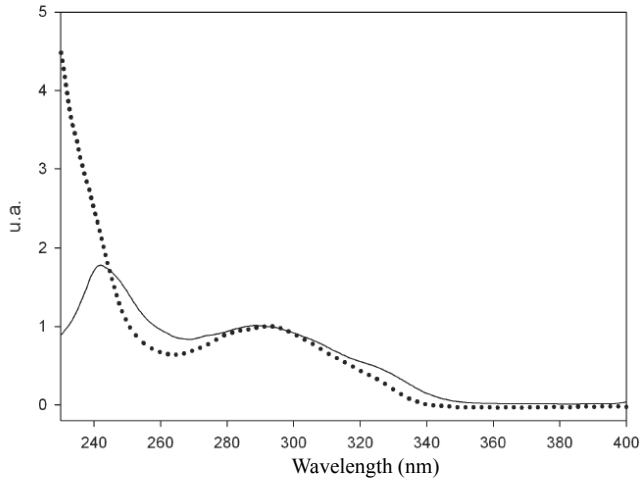


**Figure 21.** The corrected excitation spectrum (full line) and the absorption spectrum (dotted line) of **18**. Conditions: air equilibrated $CH_2Cl_2$, room temperature.

The emission band, however, shows a biexponential decays with $\tau_1$ = 2.8 ns and $\tau_2$ = 18 ns. The shorter lifetime is comparable with that of **1-NPU** ($\tau$ = 1.6 ns) and its contribution to the overall decay decreases as the monitored emission wavelength is moved towards the lower energy side (Figure 22, inset). On the basis of these observations and in the light of the structure of **18**, it can be concluded that its emission has a dual nature: a higher energy and shorter lived component assigned to the individual naphthyl-phenylureido chromophores, and a lower energy and longer lived component attributed to the formation of excimers between the pendant naphthalene moieties. This hypothesis is confirmed by the fact that in rigid matrix at 77 K, in which the formation of excimers is prevented, both the fluorescence and phosphorescence bands of **18** coincide with those of **1-NPU**.

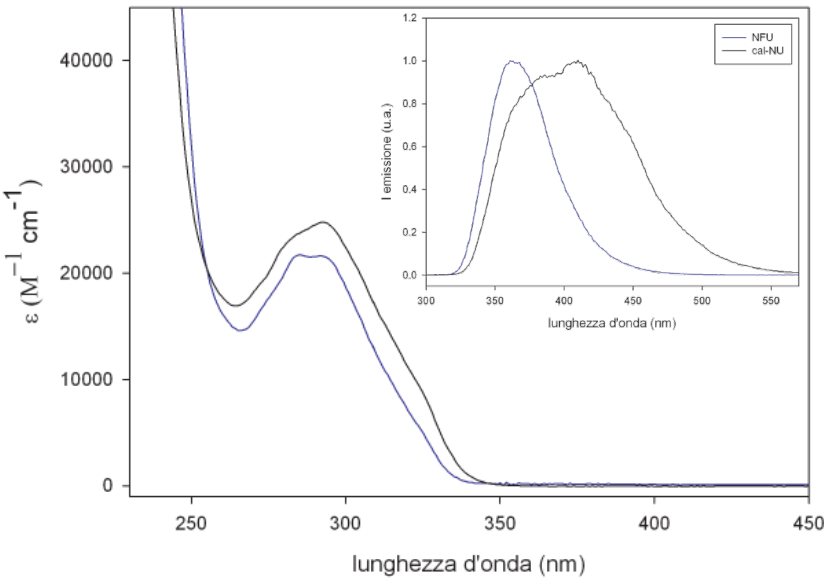


**Figure 22.** Absorption spectrum of calixarene **18** (black line) and sum of the absorption spectra of its **1-NPU** chromophoric components (blue line). Inset: normalized emission spectra ($\lambda_{exc}$ = 300 nm) of **18** (black line) and **1-NPU** (blue line). Conditions: air equilibrated $CH_2Cl_2$, room temperature.

The addition of **DOV**•2TsO to a solution of **18** causes absorption spectral changes consistent with the formation of a 1:1 complex, as discussed above for host **15**. In particular, a weak shoulder on the lower energy side of the more intense UV bands, assigned to calixarene-bipyridinium CT interactions, is observed (Table 2). The emission changes of **18** upon titration with **DOV**•2TsO (Figure 23) consist in a decrease of the band intensity accompanied by a change in shape; namely, the band becomes sharper and its maximum exhibits a blue shift. From the titration curves obtained from absorption and luminescence data and fitted with a 1:1 binding model, a lower limiting value of the association constant log$K$ > 7.5 was obtained. Once again, these findings are consistent with the NMR results and confirm that **DOV**•2TsO is threaded into wheel **18** in a pseudorotaxane fashion.

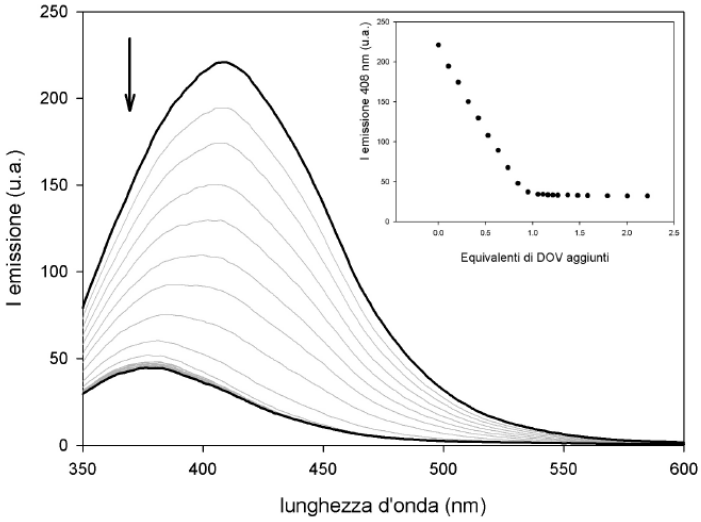


**Figure 23.** Luminescence spectral changes ($\lambda_{exc}$ = 315 nm) upon addition of increasing amounts of **DOV**•2TsO to a $3.0\times10^{-5}$ M solution of **18**. The inset shows the titration curve obtained by plotting the emission intensity at 350 nm as a function of the **DOV**•2TsO equivalents. Conditions: air equilibrated $CH_2Cl_2$, room temperature.

It should be noted that at the end of the titration the residual emission band has the same shape as that of **1-NPU**. In summary, in the case of calixarene **18** the pendant naphthalene units do not exchange electronic energy with the calixarene skeleton; the DOV•2TsO guest, however, enables photoinduced energy and/or electron transfer processes from the peripheral chromophores to the cavity.

## 2.6 Conclusion and Perspectives

Taken all together these data confirm that the formation of a *Host-Guest* complex between tris(*N*-phenylureido) calix[6]arene derivatives and *N*-monoalkyl-4,4'-bipyridinium salt enhances the nucleophilicity of the neutral nitrogen present in the guest scaffold. Furthermore, an appropriate selection of the alkyl chain appended to the guest and of the alkylating agent allows to govern the orientation of the pseudorotaxanes afforded in the reaction. Thanks to the data collected, the synthesis of

two oriented rotaxanes was achieved with increased yields and simplified synthesis with respect to literature procedures. This confident synthetic strategy paves the way for the obtainment of new and more sophisticated molecular devices. In our group, the natural development of these studies is currently undergoing: the synthesis of two calix[6]arene-based rotaxanes, bearing an ammonium unit on the axle scaffold. These two rotaxane prototypes, represented in Figure 24, if opportunely stimulated, may work as molecular shuttle. It would be important to induce the shuttling movement in two different rotaxanes where the ammonium station is positioned at the two opposite rims in order to understand the favourite direction of slippage of the wheel along the dumbbell of these interlocked systems. Furthermore, from the data collected by the experiments carried out on naphthyl-calixarene derivatives, a better understanding of the working modes of calix[6]arene-based molecular devices may be achieved by the insertion of photoactive functional groups in the calixarene scaffold.

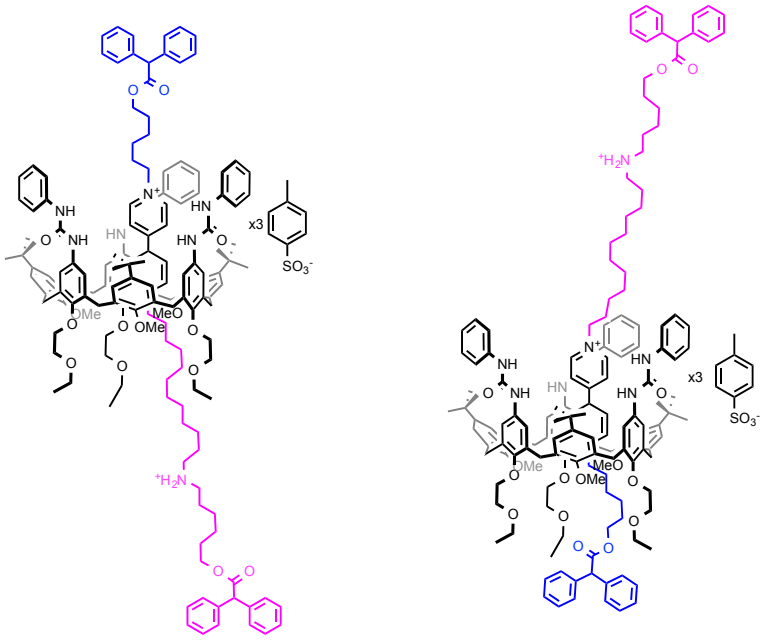

**Figure 24.** Two prototypes of calix[6]arene-based, electrochemically and pH-driven, molecular shuttles. These two latter molecules are orientational isomers.

# Experimental Section

**Materials.** All solvents were dried using standard procedures; all other reagents were of reagent grade quality obtained from commercial suppliers and were used without further purification. NMR spectra were recorded at 400 MHz for $^{1}$H and 100 MHz for $^{13}$C. Melting points are uncorrected. Chemical shifts are expressed in ppm ($\delta$) using the residual solvent signal as internal reference (7.16 ppm for $C_6H_6$; 7.26 ppm for $CHCl_3$ and 3.31 for $CH_3OH$). Mass spectra were recorded in ESI mode. Calix[6]arenes **1**,[8] **1b**,[3] **12**,[12] **16**[13] and **17**,[13] axle **DOV•2**TsO[14] and **6**•TsO,[4] alkylating agents octadecyl 4-methylbenzenesulfonate,[15] 12-hydroxydodecyl 4-methylbenzenesulfonate[16] and **10**[17] were synthesised according to published procedures. Deuterated benzene was used as the solvent in most NMR experiments because a better resolution of the signals, especially in the low fields portion of the spectra, is afforded.

## Synthetic Procedures

**Salt 2•**TsO**.** In a 100 ml round-bottomed flask octadecyl 4-methylbenzenesulfonate (1.0 g, 2.4 mmol) and 4,4'-dipyridyl (1.1 g, 7.1 mmol) were dissolved in $CH_3CN$ (50ml) and the solution was refluxed for 24h. Then the solvent was evaporated at reduced pressure and the residue obtained was triturated with EtOAc (3x 20 ml) until the product precipitated as a solid compound and was recovered by suction filtration to afford 1.0 g of product **2•**TsO as a white solid (64%). M.p. = 97-99 °C. $^{1}$H NMR (400MHz, $CD_3OD$) $\delta$ = 9.12 (d, 2H, *J* = 6.0 Hz), 8.85 (d, 2H, *J* = 6.8 Hz), 8.52 (d, 2H, *J*= 5.6 Hz), 7.99 (d, 2H, *J*= 6.4 Hz), 7.72 (d, 2H, *J*= 7.6 Hz), 7.24 (d, 2H, *J*= 8.0 Hz), 4.68 (t, 2H, *J* = 7.6 Hz), 2.37 (s, 3H), 2.18 (t, 2H, *J* = 6.8 Hz), 1.4-1.3 (m, 30H), 0.92 (t, 3H, *J* = 6.0 Hz). $^{13}$C NMR (100 MHz) $\delta$ = 153.9, 150.4, 142.3, 142.2, 140.2, 128.4, 125.7, 125.6, 122.1, 61.4, 31.7, 31.1, 29.4, 29.3, 29.2, 29.1, 28.7, 25.8, 22.3, 19.9, 13.0. MS (ESI): m/z: 409.3 $[M- Tos]^{+}$.

**Salt 7•**TsO. In a 100 ml round-bottomed flask, 12-hydroxydodecyl 4-methylbenzenesulfonate (1.0 g, 2.8 mmol) and 4,4'-dipyridyl (1.1 g, 7.1 mmol) were dissolved in $CH_3CN$ (50ml) and the solution was refluxed for 24h. Then the solvent was evaporated at reduced pressure and the residue obtained was triturated with EtOAc (3x 20 ml) until the product precipitated as a solid compound and was recovered by suction filtration to afford 1.0 g of product **7•**TsO as a white solid (69%). M.p. = 74-75°C; $^1$H NMR ($CD_3OD$, 400 MHz) $\delta$ = 9.12 (d, 2H, $J$ = 7.2 Hz), 8.84 (dd, 2H, $J$ = 6.4 Hz, 2.0 Hz), 8.51 (d, 2H, $J$ = 6.8 Hz), 8.00 (dd, 2H, $J_1$ = 6.4 Hz, $J_2$ =, 2.0 Hz), 7.71 (d, 2H, $J$= 8.0 Hz), 7.24 (d, 2H, $J$= 8.0 Hz), 4.68 (t, 2H, $J$= 7.6 Hz), 3.55 (t, 2H, $J$ = 6.8 Hz), 2.37 (s, 3H), 2.1 (bs, 2H), 1.6-1.2 (m, 18H). $^{13}$C NMR (100 MHz): $\delta$ = 153.6, 150.4, 145.1, 142.3, 142.2, 140.2, 128.4, 125.7, 125.6, 122.2, 61.6, 61.4, 32.3, 31.1, 29.3, 29.2, 29.1, 28.7, 25.8, 25.5, 19.9. MS (ESI): m/z: 341.2 $[M- Tos]^+$.

**Rotaxane 9a•**2TsO**.** To a solution of wheel **1** (0.1 g, 0.07 mmol) in toluene (20 ml), an equimolar ratio of axle **7•**Ts (0.04 g, 0.07 mmol) and an excess of 6-(tosyloxy)hexyl 2,2-diphenylacetate (**5**) (0.1 g, 0.21 mmol) were added. The orangish solution was refluxed for 4 days; afterwards, the mixture was cooled to room temperature and diphenylacetyl chloride (0.03 g, 0.14 mmol) and triethylamine (0.01 g, 0.1 mmol) were added. The solution was stirred at r.t. for 16h; then, the solvent was evaporated under reduced pressure and the solid residue was purified by column chromatography (Dichloromethane/Methanol= 95:5) to afford 0.05 g of rotaxane **9a•**2TsO as a red solid (63%). $^1$H NMR ($C_6D_6$, 400 MHz) $\delta$ = 9.4 (bs, 6H), 8.16 (d, 4H, $J$ = 7.6 Hz), 8.1-7.8 (m, 8H), 7.83 (d, 2H, $J$ = 6.0 Hz), 7.58 (s, 6H), 7.5-7.3 (m, 10H), 7.2-7.1 (m, 10H), 7.1-7.0 (m, 10H), 6.90 (d, 4H, $J$ = 8.0 Hz), 6.81 (d, 2H, $J$ = 6.0 Hz), 6.8-6.6 (m, 5H), 5.10 (s, 1H), 5.07 (s, 1H), 4.56 (d, 6H, $J$ = 14.8 Hz), 4.33 (t, 2H, $J$ = 6.2 Hz), 4.04 (t, 2H, $J$ = 6.6 Hz), 3.88 (s, 9H), 3.8 (bs, 6H), 3.7-3.5 (m, 10H), 3.5-3.2 (m, 12H), 2.1 (bs, 2H), 1.95 (s, 6H), 1.9-0.6 (m, 83H). $^{13}$C NMR (100 MHz): $\delta$ = 172.0, 171.9, 153.5, 152.9, 148.1, 147.9, 144.4, 143.3, 143.0, 141.3, 139.4, 139.3, 139.0, 137.5, 133.8, 132.2, 129.3, 128.7, 128.6, 128.5, 127.8, 127.6, 127.3, 127.1, 126.5, 125.6, 124.8, 121.1, 118.1, 116.7, 72.4, 69.9, 66.3, 64.9, 61.3, 61.0, 60.7, 57.3, 34.6, 31.5, 29.9, 29.8,

29.7, 29.6, 29.5, 29.3, 28.8, 28.6, 27.8, 26.1, 26.0, 25.8, 22.8, 20.8, 15.2, 14.0. MS (ESI): m/z: 1148.3 $[M\text{-}2TsO]^{2+}$.

**Rotaxane 9b•**2TsO**.** To a solution of wheel **1** (0.1 g, 0.07 mmol) in toluene (20 ml), an equimolar ratio of axle **7•**Ts (0.03 g, 0.07 mmol) and an excess of alkylating agent **6** (0.1 g, 0.21 mmol) were added. The orangish solution was refluxed for 4 days; afterwards, the mixture was cooled to room temperature and diphenylacetyl chloride (0.03 g, 0.14 mmol) and triethylamine (0.01 g, 0.1 mmol) were added. The solution was stirred at r.t. for 16h; then, the solvent was evaporated under reduced pressure and the solid residue was purified by column chromatography (Dichloromethane/Methanol= 95:5) to afford 0.04 mg of rotaxane **9b•**2TsO as a red solid (54%). $^{1}$H NMR ($C_6D_6$, 400 MHz) $\delta$ = 9.4 (bs, 6H), 8.3-8.0 (bs, 6H), 8.0-7.7 (m, 10H), 7.59 (s, 6H), 7.45 (d, 4H, $J$ = 7.6 Hz), 7.41 (d, 4H, $J$ = 7.2 Hz), 7.2-7.1 (m, 6H), 7.1-7.0 (m, 10H), 6.92 (d, 4H, $J$ = 8.0 Hz), 6.83 (d, 2H, $J$ = 6.0 Hz), 6.68 (t, 6H, $J$ = 6.8 Hz), 5.13 (s, 1H), 5.08 (s, 1H), 4.58 (d, 6H, $J$ = 15.2 Hz), 4.1-4.0 (m, 4H), 3.95 (s, 9H), 3.9-3.7 (m, 8H), 3.7-3.5 (m, 8H), 3.5-3.2 (m, 12H),, 2.2 (bs, 2H), 1.96 (s, 6H), 1.8 (bs, 2H), 1.8-1.5 (m, 70H). $^{13}$C NMR (100 MHz): $\delta$ = 172.0, 171.9, 153.5, 152.8, 148.2, 147.9, 144.4, 142.9, 141.2, 139.2, 139.2, 137.5, 133.8, 132.1, 129.3, 128.7, 128.7, 128.6, 128.6, 128.5, 128.3, 127.9, 127.8, 127.7, 127.6, 127.5, 127.2, 127.1, 127.0, 126.5, 125.7, 124.7, 121.2, 118.1, 116.7, 72.4, 70.0, 66.3, 64.7, 60.9, 60.5, 57.4, 57.3, 34.6, 31.5, 30.0, 29.7, 29.2, 28.6, 28.3, 25.8, 25.5, 24.9, 20.8, 15.2. MS (ESI): m/z: 1148.3 $[M\text{-}2TsO]^{2+}$.

**6-(naphthalen-2-yloxy)hexyl tosylate (11)**. In a 250 ml round bottom flask, to a solution of 2-naphthol (1.5 g, 10.4 mmol) and 1,6-hexanediol ditosylate **10** (13.3 g, 31.2 mmol) in $CH_3CN$ (100 ml), $K_2CO_3$ (2.9 g, 20.8 mmol) was added. The resulting heterogeneous reaction mixture was refluxed for 36 hours. After cooling at room temperature, the solvent was evaporated to dryness under reduced pressure and the sticky residue was taken up with ethyl acetate (100 ml). The resulting organic phase was washed with a 10% w/v solution of HCl (100 ml) and twice with distilled water (2

x 100 ml), then dried with anhydrous sodium sulfate and evaporated to dryness under reduced pressure. The oily residue was purified by column chromatography on silica gel (n-hexane/ethyl acetate 7:3) to yield 3.0 g of **11** (72%) as a white solid. M.p. = 71-72 °C; $^{1}$H NMR ($CDCl_3$, 400 MHz) $\delta$ = 7.80 (d, 2H, $J$ = 7.6 Hz), 7.46 (t, 2H, $J$ = 8.0 Hz), 7.36 (d, 2H, $J$ = 7.6 Hz), 7.28 (s, 1H), 7.14 (d, 1H, $J$ = 7.2 Hz), 4.1-4.0 (m, 4H), 2.41 (s, 3H), 1.76 (m, 2H, $J$ = 9.2 Hz), 1.68 (m, 2H, $J$ = 9.2 Hz), 1.5-1.4 (m, 4H); $^{13}$C NMR (100 MHz) $\delta$= 157.0, 144.7, 134.6, 133.2, 129.8, 129.3, 128.9, 127.9, 127.6, 126.7, 126.3, 123.5, 118.9, 106.6, 70.5, 67.7, 29.0, 28.8, 25.5, 25.2, 21.6; MS (ESI) m/z: 421.3 $[M+ Na]^+$.

**Calix[6]arene 13**. In a 100 ml sealed glass autoclave, a heterogeneous mixture of compounds **12** (0.8 g, 0.8 mmol), **11** (1.0 g, 2.5 mmol) and $K_2CO_3$ (0.5 g, 3.7 mmol) in $CH_3CN$ (60 ml) was refluxed under vigorous stirring for 72 h. After cooling to room temperature, the solvent was evaporated to dryness under reduced pressure. The solid residue was taken up with ethyl acetate (80 ml) and the resulting organic phase washed with a 10% w/v solution of HCl (80 ml) and water (2x 80 ml). The separated organic phase was dried over anhydrous sodium sulfate, filtered to remove the drying agent and the solvent evaporated to dryness under reduced pressure. The residue was purified by column chromatography on silica gel (hexane/ethyl acetate 8:2) to yield 0.58 g of **13** (43%) as a pale yellow solid. M.p.= 108-109 °C; $^{1}$H NMR ($CDCl_3$, 400 MHz) $\delta$ = 7.8-7.6 (m, 15H), 7.44 (dt, 3H, $J_1$ =7.2, $J_2$= 1.2 Hz), 7.33 (dt, 3H, $J_1$ =7.2, $J_2$ = 1.2 Hz), 7.2 (bs, 3H), 7.14 (d, 3H, $J$ = 2.4 Hz), 7.12 (s, 6H), 4.4 (bs, 6H), 4.09 (t, 6H, $J$ = 6.4 Hz), 3.9 (bs, 6H), 3.6 (bs, 6H), 2.89 (s, 9H), 1.9 (bs, 12H), 1.63 (m, 12H), 1.3-1.2 (m, 27H); $^{13}$C NMR (100 MHz): $\delta$ = 159.9, 157.0, 154.4, 146.9, 143.7, 135.7, 134.6, 132.2, 129.3, 128.9, 128.0, 127.8, 127.6, 127.3, 126.7, 126.3, 125.5, 123.5, 123.2, 119.0, 106.5, 73.8, 67.7, 59.9, 34.3, 31.5, 31.0, 30.3, 30.2, 30.1, 29.7, 29.4, 29.2, 26.1, 25.9; MS (ESI) m/z: 1684.1 $[M+ Na]^+$.

**Calix[6]arene 14**. In a 100 ml round bottom flask kept under nitrogen atmosphere, a tip of spatula of Pd/C catalyst was cautiously added to a suspension of compound **13**

(0.40 g, 0.25 mmol) in methanol (50 ml), then hydrazine monohydrate (1.03 g, 20 mmol) was added dropwise. The resulting heterogeneous mixture was refluxed for 6 h, cooled to room temperature and then filtered, under nitrogen atmosphere, through a celite pad to remove the Pd/C catalyst. The filtered solution was evaporated to dryness under reduced pressure to yield 0.38 g of **14** (98%) as a white solid. Because of its instability to air, compound **6** was employed in the following synthetic step without any further purification.

**Calix[6]arene 15**. In a 50 ml round bottom flask kept under nitrogen atmosphere, to a solution of **14** (0.38 g, 0.24 mmol) in dichloromethane (20 ml), phenyl isocyanate (0.18 g, 1.44 mmol) was added dropwise. The reaction mixture was stirred for two hours at room temperature, then the solvent was evaporated to dryness under reduced pressure and the residue was purified by column chromatography on silica gel (hexane/ethyl acetate 65:35) to yield 0.18 g of **15** (38%) as a pale yellow solid. M.p. = 147-149 °C; $^{1}$H NMR ($CDCl_3$, 400 MHz) $\delta$ = 7.8-7.6 (m, 9H), 7.44 (t, 3H, $J$ = 7.8 Hz), 7.33 (t, 3H, $J$ = 7.8 Hz), 7.23 (s, 6H), 7.15 (d, 3H, $J$ = 2.4 Hz), 7.13 (s, 6H), 7.1-7.0 (m, 15H), 7.0-6.9 (m, 3H), 6.30 (s, 6H), 4.42 (d, 6H, $J$ =15.6 Hz), 4.12 (t, 6H, $J$ = 15.2 Hz), 2.82 (s, 9H), 1.93 (m, 12H, $J$ = 7.2 Hz), 1.7 (bs, 12H), 1.3-1.2 (m, 27H). $^{13}$C NMR (100 MHz): $\delta$ = 157.1, 155.0, 154.6, 152.3, 146.8, 138.2, 135.7, 134.6, 133.0, 132.4, 129.3, 129.1, 129.0, 128.9, 127.7, 127.6, 126.7, 126.3, 123.5, 123.4, 123.1, 120.6, 119.0, 107.7, 106.6, 72.8, 67.9, 60.2, 34.2, 31.5, 31.1, 30.5, 29.7, 29.2, 26.2, 26.1; MS (ESI) m/z: 1951.3 $[M+ Na]^+$.

**Calix[6]arene 18**. In a 50 ml round bottom flask, under nitrogen atmosphere, to a solution of **9** (0.33 g, 0.25 mmol) in dichloromethane (25 ml), α-naphthyl isocyanate (0.23 g, 1.25 mmol) was added dropwise. The reaction mixture was stirred for two hours at room temperature, then the solvent was evaporated to dryness under reduced pressure and the residue was purified by column chromatography on silica gel (hexane/ethyl acetate 6:4) to yield 0.23 g of **17** (48%) as a purple solid. M.p. = 162-163 °C; $^{1}$H NMR ($CDCl_3$, 400 MHz) $\delta$ = 7.5 (bs, 9H), 7.4 (bs, 3H), 7.2 (bs, 15H), 7.0 (bs,

3H), 6.8 (bs, 3H), 6.5 (bs, 6H), 4.5 (bs, 6H), 4.2 (bs, 6H), 3.9 (bs, 6H), 3.7-3.6 (m, 12H), 2.8 (bs, 9H), 1.3-1.2 (m, 36H). $^{13}$C NMR (100 MHz) $\delta$ = 155.9, 154.7, 146.6, 135.9, 133.9, 133.1, 128.0, 127.9, 127.8, 125.8, 125.6, 125.4, 125.0, 123.4, 121.3, 120.7, 72.3, 69.3, 66.9, 60.2, 34.2, 31.5, 31.10. MS (ESI) m/z: 1638.7 $[M+ Na]^+$.

## References


(1) Arduini, A.; Bussolati, R.; Credi, A.; Secchi, A.; Silvi, S.; Semeraro, M.; Venturi, M. *J. Am. Chem. Soc.* **2013**, *135* (26), 9924–9930.

(2) Purse, B. W.; Gissot, A.; Rebek, J. *J. Am. Chem. Soc.* **2005**, *127* (32), 11222–11223.

(3) Arduini, A.; Credi, A.; Faimani, G.; Massera, C.; Pochini, A.; Secchi, A.; Semeraro, M.; Silvi, S.; Ugozzoli, F. *Chem. - A Eur. J.* **2008**, *14* (1), 98–106.

(4) Arduini, A.; Ciesa, F.; Fragassi, M.; Pochini, A.; Secchi, A. *Angew. Chemie, Int. Ed.* **2005**, *44* (2), 278–281.

(5) Suresh, M.; Mandal, A. K.; Kesharwani, M. K.; Adarsh, N. N.; Ganguly, B.; Kanaparthi, R. K.; Samanta, A.; Das, A. *J. Org. Chem.* **2011**, *76* (1), 138–144.

(6) Mandal, A. K.; Gangopadhyay, M.; Das, A. *Chem. Soc. Rev.* **2015**, *44* (3), 663–676.

(7) van Dongen, S. F. M.; Cantekin, S.; Elemans, J. A. A. W.; Rowan, A. E.; Nolte, R. J. M. *Chem. Soc. Rev.* **2014**, *43* (1), 99–122.

(8) Arduini, A.; Calzavacca, F.; Pochini, A.; Secchi, A. *Chem. - A Eur. J.* **2003**, *9* (3), 793–799.

(9) Credi, A.; Dumas, S.; Silvi, S.; Venturi, M.; Arduini, A.; Pochini, A.; Secchi, A. *J. Org. Chem.* **2004**, *69* (18), 5881–5887.

(10) Arduini, A.; Bussolati, R.; Credi, A.; Pochini, A.; Secchi, A.; Silvi, S.; Venturi, M. *Tetrahedron* **2008**, *64* (36), 8279–8286.

(11) Tod Rieger, P.; Palese, S. P.; Dwayne Miller, R. J. *Chem. Phys.* **1997**, *221* (1-2), 85–102.

(12) Casnati, A.; Domiano, L.; Pochini, A.; Ungaro, R.; Carramolino, M.; Oriol Magrans, J.; M. Nieto, P.; López-Prados, J.; Prados, P.; de Mendoza, J.; G. Janssen, R.; Verboom, W.; N.Reinhoudt, D. *Tetrahedron* **1995**, *51* (46), 12699–12720.

(13) Gonzalez, J. J.; Ferdani, R.; Albertini, E.; Blasco, J. M.; Arduini, A.; Pochini, A.; Prados, P.; De Mendoza, J. *Chem. - A Eur. J.* **2000**, *6* (1), 73–80.

(14) Arduini, A.; Ferdani, R.; Pochini, A.; Secchi, A.; Ugozzoli, F. *Angew. Chemie, Int. Ed.* **2000**, *39* (19), 3453–3456.

(15) Boccia, A.; Lanzilotto, V.; Zanoni, R.; Pescatori, L.; Arduini, A.; Secchi, A. *Phys. Chem. Chem. Phys.* **2011**, *13* (10), 4444–4451.

(16) Ballot, S.; Noiret, N. *Tetrahedron Lett.* **2003**, *44* (49), 8811–8814.

(17) Bouzide, A.; Sauvé, G. *Org. Lett.* **2002**, *4* (14), 2329–2332.

# CHAPTER 3

# Towards the Synthesis of a Calix[6]arene-based Molecular Muscle

# Chapter 3

# Towards the Synthesis of a Calix[6]arene-based Molecular Muscle

## 3.1 Introduction

In the last decades, one of the most strenuous challenges in the field of molecular machines was the construction of devices able to emulate the relaxation/contractive process of biological muscle.[1] Several examples of these supramolecular systems have been reported so far in which the contraction/relaxation process is guided by an appropriate external stimulus of different nature (electrochemical,[2] photochemical,[3] pH,[4]…). Among the several prototypes reported, those based on the class of pseudorotaxanes and rotaxanes seem to be the most promising for the construction of real devices. Giuseppone and co-workers showed a very interesting pH-driven molecular muscle (Figure 1); thanks to the use of stoppers that can also bind to metal ions they were able to create coordination polymers, extending the contractile/relaxation process to the macroscopic scale. The integrated translational motion of the supramolecular polymer chain, indeed, is the product of the individual contractions and extensions of each molecular machine by the degree of polymerization.[4]

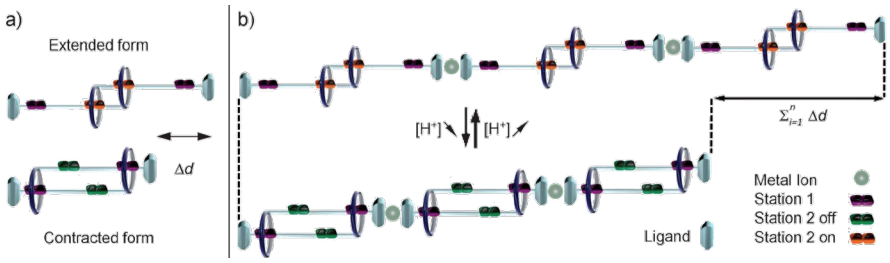


**Figure 1.** General principle of a) a bistable [c2]daisy chain rotaxane and b) the supramolecular polymer. Adapted with permission from ref. 4. Copyright © 1999-2016 John Wiley & Sons.

From the perusal of the literature it appeared us that several interlocked molecule architectures, like [3]rotaxanes (Figure 2), [*c*2]daisy chains or simple [2]rotaxanes, that have been commonly used for nano-scale muscle prototypes,[1,5,6] could be constructed employing a calix[6]arene component.

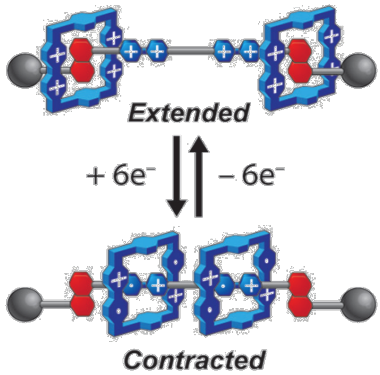


**Figure 2.** Graphical representation of the relative motion of the ring components, which undergoes to a redox-stimulated contraction and expansion in a doubly bistable palindromic [3]rotaxane. Adapted with permission from ref. 2. Copyright © Royal Society of Chemistry.

A functional structural unit frequently employed in these types of interlocked molecules is the 4,4'-bipyridine, since its redox and UV-Vis properties can be very helpful features to monitor the working modes of molecular switches, devices or shuttles. The ability of the viologen group to promote mechanical work upon

electrochemical stimulation is well documented in the literature.[7] For example, G. Royal and co-workers demonstrated that, upon electrochemical stimulation, two suitably spanned viologen units, linked through an alkyl chain, can efficiently and reversibly rearrange a molecule from an "open" charge-repelled conformation into a "closed" cofacial arrangement. In this system, also called tweezer, the "closed" conformation is stabilized by the π-stacking interactions between the radical-cationic state of the two viologen units (Scheme 1).[8,9]

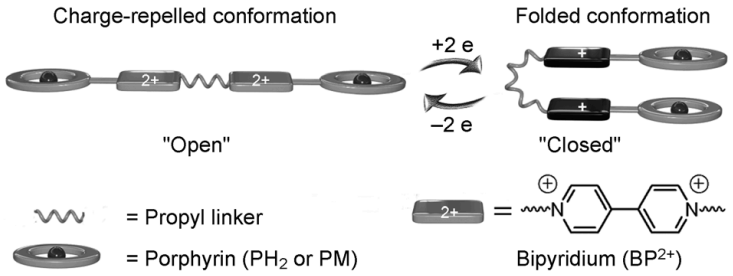


**Scheme 1.** The electroactivation of a bisporphyrin architecture between "open" and "closed" conformation. Adapted with permission from ref. 8. Copyright © 1999-2016 John Wiley & Sons.

## 3.2 Design and Synthesis of a Calix[6]arene-based Daisy Chain

As shown in the previous chapters, the calix[6]arene is a very promising platform for the construction of working devices and molecular machine prototypes belonging to the class of pseudorotaxanes.[10,11] In order to expand the scopes of these devices, we designed a calix[6]arene-based derivative which could potentially act as a molecular muscle. To this aim, we initially considered that a calix[6]arene-based daisy chain[12] structure could experience a contractive-relaxation motion upon electrochemical stimulation of the viologen unit, directly attached to the upper rim of the calix (Figure 3).

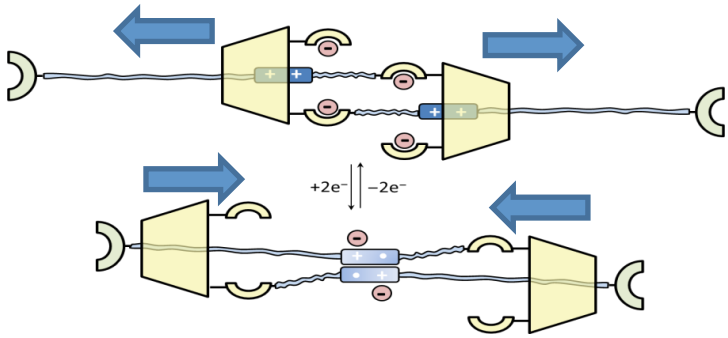


**Figure 3.** Prototype of a calix[6]arene-based molecular muscle envisaged in a [*c*2]daisy chain architecture.

In a perspective view, this reversible electrochemically-driven process could be extended to a macroscopic scale through the insertion of bulky metal-ligands as stopper for [*c*2]daisy chain architectures. The metal coordination could allow the formation of a supramolecular polymer (Figure 4).

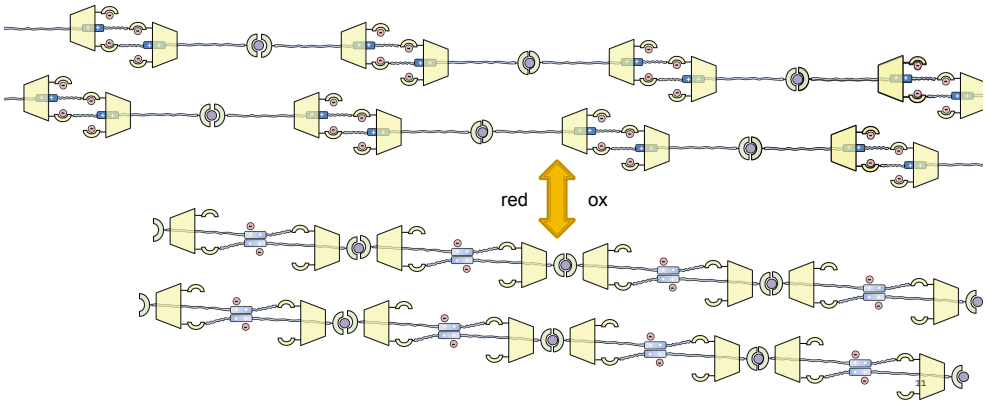


**Figure 4.** The use of ligands for metal ion as stoppers may encourage the spontaneous formation of supramolecular reversibly contractile polymers.

Following a design strategy already reported in the literature,[13–15] the synthesis of a calix[6]arene phenylureido derivative decorated with a viologen unit at its upper rim was tackled (Figure 5).

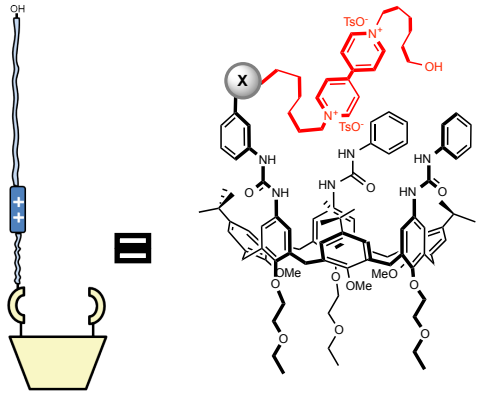

**Figure 5.** Schematic representation of the envisaged molecular target. X represents a connecting point between the calixarene scaffold and the viologen derivative.

**1**•2TsO was synthesised through a convergent synthetic strategy in which a calix[6]arene derivative (**5a**), functionalized with an anchoring group on one of the tris(*N*-phenylureido) groups, was reacted with a suitably functionalized viologen unit (**6**•2TsO) (Scheme 2). The synthetic challenge was thus the synthesis of a calixarene wheel monofunctionalized at one of the three phenylureido moieties at the upper rim and the selection of the anchoring group for the connection of the calixarene "host" domain to the viologen "guest" unit.

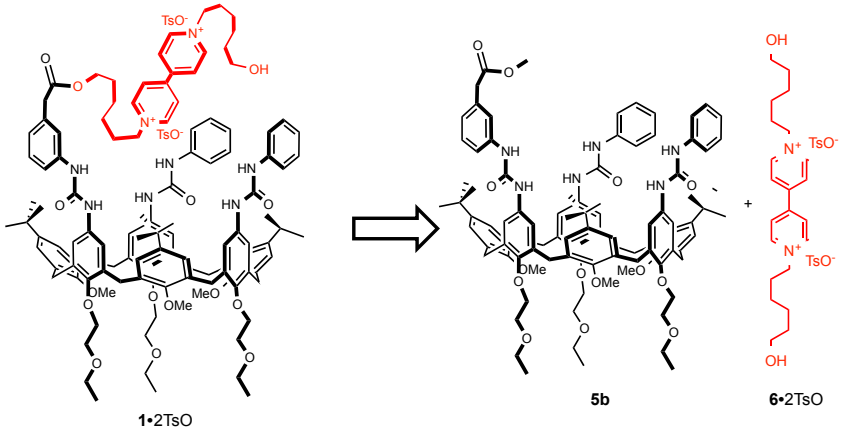


**Scheme 2.** Target molecule **1**•2TsO designed for the obtainment of a [*c*2]daisy chain structure. The *Host* component (**5b**) is represented in black, while the *Guest* portion **6**•2TsO in red. An ester function was imagined as connecting point.

Attempts to synthesize in a selective manner the calix[6]arene component, that were initially pursued by reacting the triamino calix[6]arene (**2**)[16] with a mixture of two different phenylisocyanates, one of which bears a methyl ester function in its 4 position, considering that the different reactivity of these two isocyanate groups toward the amino functions of **2** could have been exploited as control element for the selective monofunctionalization of **2**, failed.

After several unsuccessful attempts, **5b** could be obtained by reacting **2** with a mixture of phenyl isocyanate (**3**) and methyl 2-(4-isocyanatophenyl)acetate (**4**). After a systematic study aimed to study the best molar ratio between **2**, **3** and **4**, 38% of **5b**, 24% of **5a**, 17% of **5c** and trace amount of **5d** could be isolated (optimized conditions descripted in Scheme 3). Any variation of the reaction parameters (see experimental part) gave lower to negligible yields of **5b**. The above products distribution appears in agreement with a statistic distributions, thus suggesting an identical reactivity of the two isocyanates **3** and **4** towards the three identical amino groups of **2**.

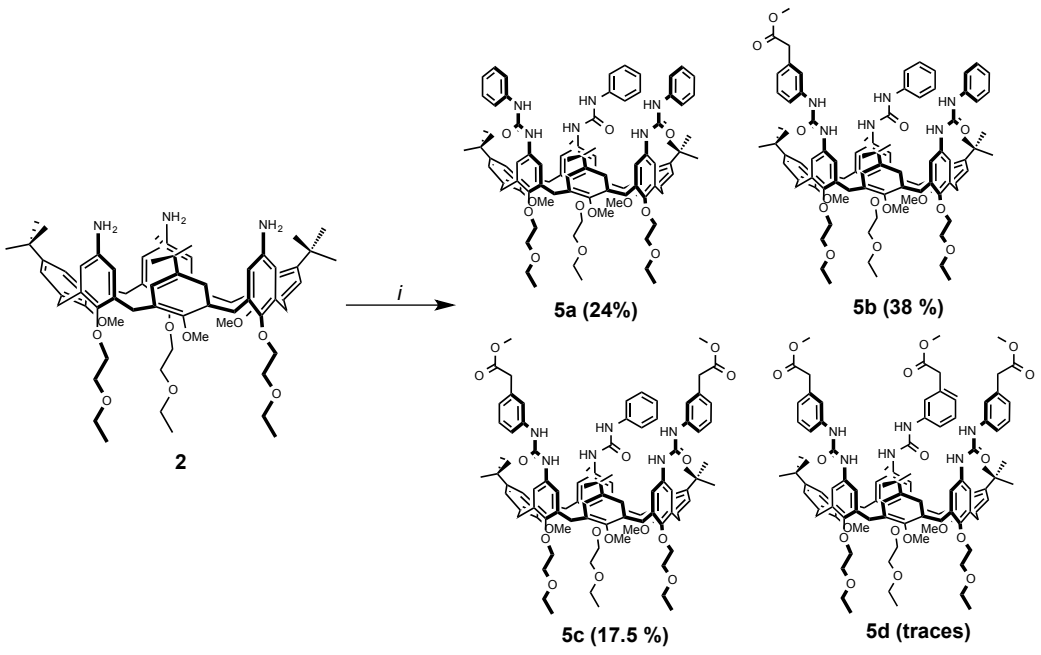


**Scheme 3.** Reagents and Conditions: *i*) Isocyanates **3** and **4** (molar ratio 3 and 2, respectively, with respect to **2**), $CH_2Cl_2$, 1h, r.t.; calculate experimental yield in bracket for each product.

NMR and MS analysis demonstrated the identity of wheel **5b**. The $^{1}$H NMR (400 MHz, $CDCl_3$) spectrum of **5b** (Figure 6) showed very broad signals; nevertheless, the presence of diagnostic signals such as the broad singlet at $\delta$ = 2.9 ppm for the methoxy groups suffering the shielding effect of the electron-rich cavity, and the two broad signals at $\delta$ = 4.4 and $\delta$ = 3.5 ppm for the axial and equatorial protons of the bridging methylene units, respectively, are in agreement with a calix[6]arene adopting a *pseudo* cone conformation on the NMR timescale. The two diagnostic signals of the methyl phenylacetate group, that is a singlet for the methyl ester and one for the benzyl methylene protons on the *para*-substituted phenylurea at ca. $\delta$ = 3.5 and $\delta$ = 3.7 ppm, respectively, could not be identified in the $^{1}$H NMR spectrum due to their overlapping with other signals. However, $^{1}$H-$^{13}$C 2D HSQC experiment (Figure 7, protons' label is also present in Figure 7) confirmed the presences of these groups: for example, the correlation displayed at $\delta$ = 3.50; 40.4 ppm is assignable to the presence of the methylene unit *p*, while the methyl ester signal (*q*) is visible at $\delta$ = 3.68; 52.0 ppm. Mass spectrometry experiments in the ESI-MS mode confirmed the identity of the molecule exhibiting a mass peak at 1560.7 m/z for the adduct formed by **5b** and $Na^{+}$.

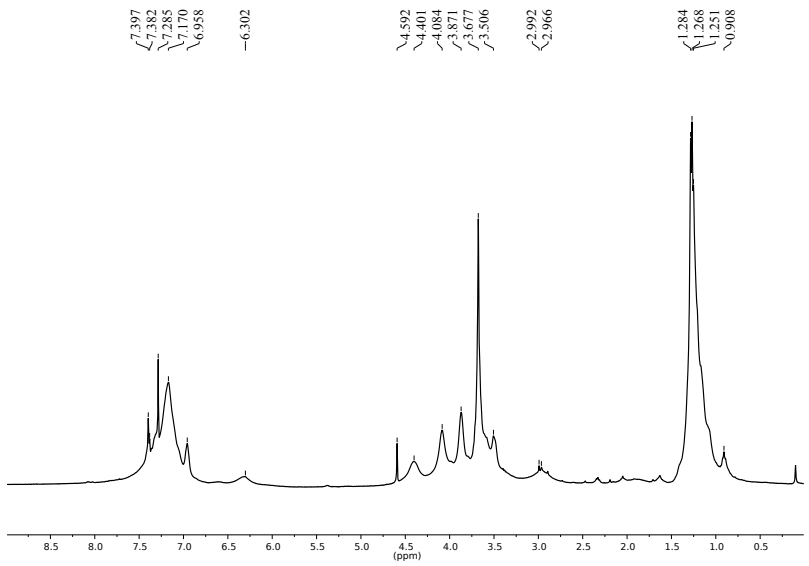


**Figure 6.** $^{1}$H NMR (400 MHz) of **5b** in $CDCl_3$ (protons label in Figure 7).

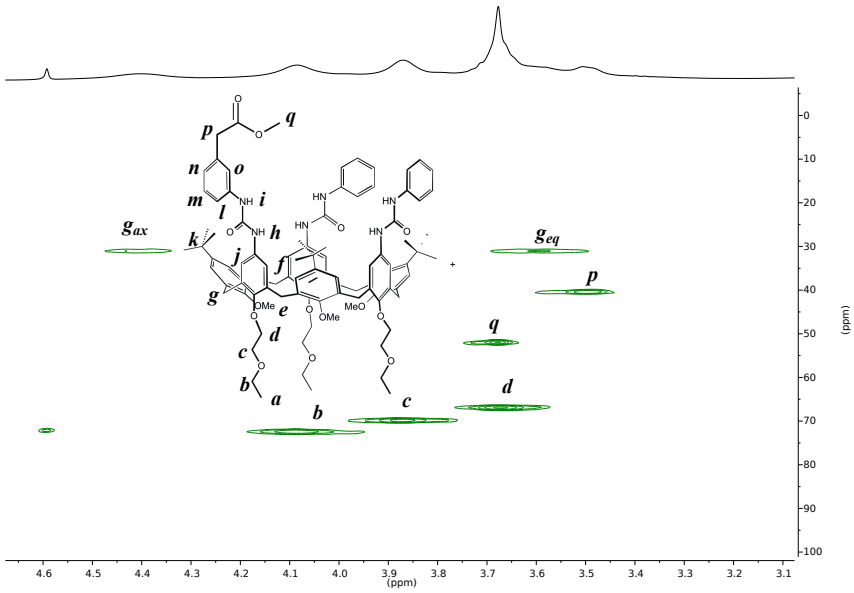


**Figure 7.** $^{1}H$-$^{13}C$ 2D HSQC (400 MHz) (expanded region) of **5b** in $CDCl_3$.

To verify the hypothesis that the products distribution is governed by statistic, **2** was reacted with a solution containing an excess of phenyl isocyanate (**3**) and 4-*tert*-butylphenyl isocyanate (**7**) in the same ratio. Since the reactivity of these two molecules is comparable, a $–NH_2$ group would react indifferently with one of them, yielding four differently functionalized products (see Scheme 4). The theoretical ratio between the four reaction products should be (yields calculated on the total conversion of **2**): 12.5% for each of the two calixarenes bearing identical phenylureido groups (**5a** or **8d**), 37.5% for each of the two calixarenes having phenylureido moieties differently functionalized (**8b** or **8c**). The yield, calculated after column chromatography (hexane/ethyl acetate = 6:4), closely reflected the value predicted by statistic. In fact, wheel **5a** represents the 14.3%, **8b** the 39.3, **8c** the 35.0% and **8d** the 11.4% of the converted triamino derivative.

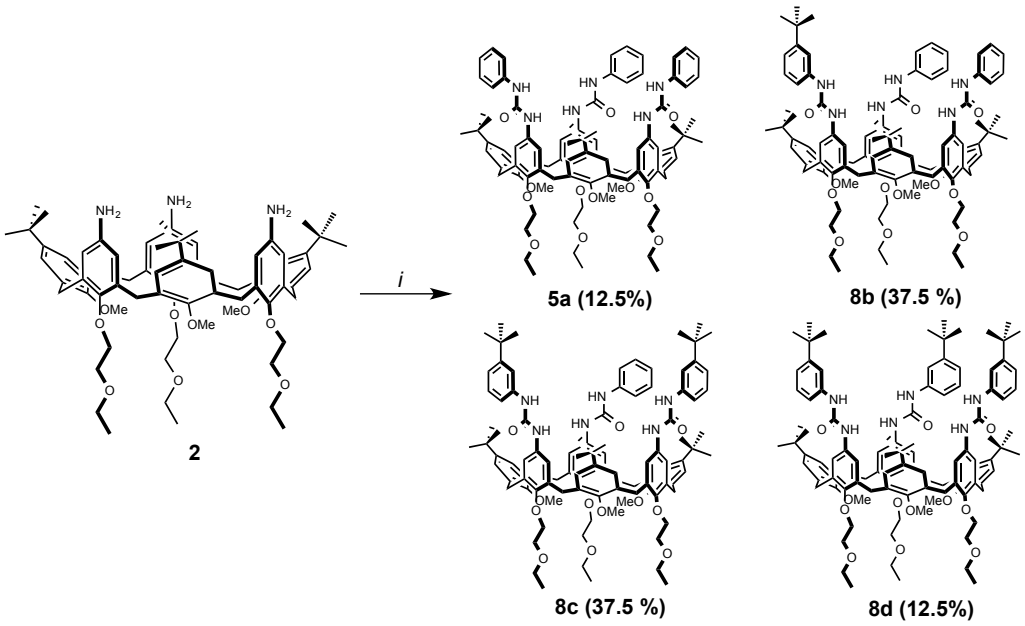


**Scheme 4.** Reagents and Conditions: *i*) Isocyanates **3** and **7** (molar ratio 3 and 3, respectively, with respect to **2**), $CH_2Cl_2$, 1h, r.t.; the statistical prediction for the yield of each product is presented in the bracket.

The methyl ester function present in the 4 position in one of the ureido groups of **5b** was reacted with dialkylviologen salt to yield the corresponding daisy chain pseudorotaxane **1**•2TsO. Initially, **5b** was reacted with **6**•2TsO,[17] which bears two terminal OH groups. Since **6**•2TsO should form, in apolar media, a pseudorotaxane with **5b**, the hydroxyl groups of the thread positioned at the upper rim of the wheel could react with the ester function of **5b** in a transesterification reaction, while the other OH terminal group of the axle, oriented toward the lower rim, could be amenable for a subsequent stoppering reaction. As expected, equilibration of **5b** with **6**•2TsO in $CDCl_3$ yielded the corresponding pseudorotaxane **5b⊃6**•2TsO (Scheme 5). The $^1H$ NMR spectrum of **5b⊃6**•2TsO shows the typical chemical shifts pattern of the hydrogens of both the components in a pseudorotaxane. In fact, the two doublets at $\delta$ = 3.5 and $\delta$ = 4.5 ppm, assigned to the bridging methylene groups of the wheel, $g_{eq}$ and $g_{ax}$ respectively, the downfield shift from $\delta$ = 2.9 to $\delta$ = 3.9 ppm of the methoxy groups

and the substantial downfield shift of the NH protons of the ureido groups are in agreement with a rigidified calix[6]arene structure. In addition, the inclusion of the viologen was inferred by the upfield shift ($\Delta\delta \sim 2.6$ and 2.4 ppm) observed for the resonances of protons *8'* and *7'* (Figure 8) and the upfield shift endured by the *N*-$CH_2$ protons *6* and *6'* of the axle (Figure 8).

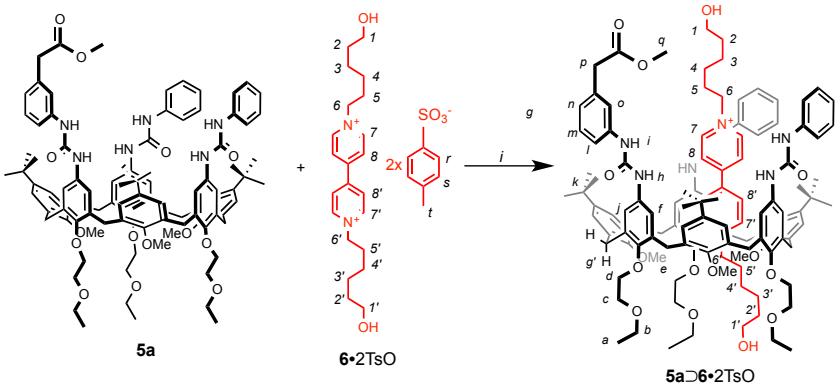


**Scheme 5.** Reagents and Conditions: *i*) $CDCl_3$, 1h, r.t.

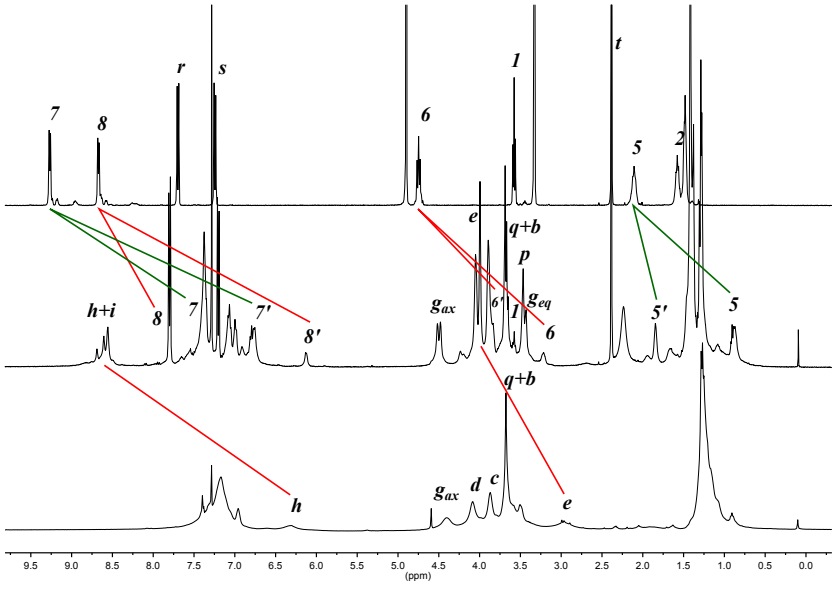


**Figure 8.** $^1$H NMR (400 MHz) stack plot of a) **6**•2TsO in $CD_3OD$, b) pseudorotaxane **5b⊃6**•2TsO in $CDCl_3$, and c) wheel **5b** in $CDCl_3$ showing the most important protons assignments (for protons labels see Scheme 5).

$CDCl_3$ was then removed from the NMR sample and the solid residue dissolved in toluene. A catalytic amount of *p*-toluenesulfonic acid was then added as catalyst and the resulting mixture was refluxed for 16h (Scheme 6). After column chromatography (DCM/MeOH = 95:5), **1**•2TsO was isolated in 65% yields and fully characterized through NMR and MS analysis.

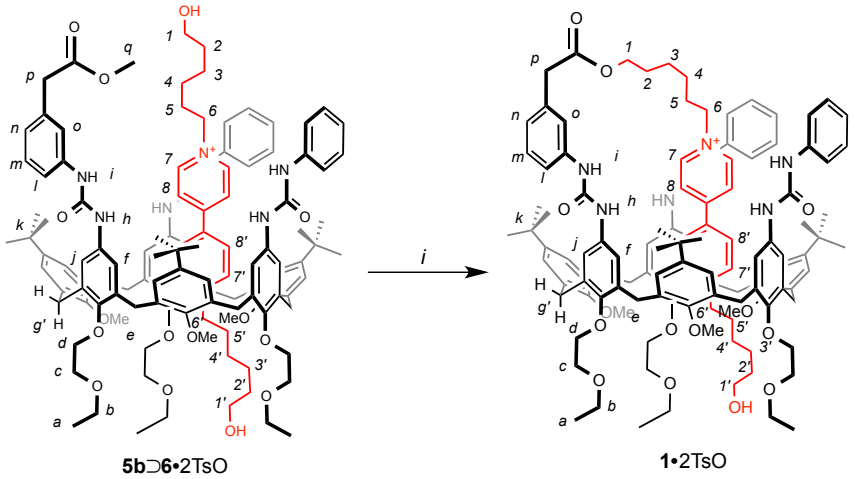


**Scheme 6.** Reagents and Conditions: *i*) *p*-Toluenesulfonic acid, Toluene, 16h, reflux.

Albeit the $^1$H NMR spectra of **1**•2TsO is very similar to that of **5b⊃6**•2TsO ($^1$H NMR stack plot shown in Figure 9), the comparison between the $^1$H-$^{13}$C HSQC spectra of **5b⊃6**•2TsO and **1**•2TsO, revealed that in the latter the signal assigned to the methyl group of the ester function in **5b⊃6**•2TsO ($\delta$ = 3.69; 52.0 ppm, *q* in Figure 9 and 10, for protons label see Scheme 6) is not present, while the cross-peak of the methylene group in **5b⊃6**•2TsO ($\delta$ = 3.58-62.1 ppm, signal *1* in Figure 9 and 10, see Scheme 6 for protons label), because of its connection to the ester function of the wheel, now resonates at $\delta$ = 4.16-63.2 ppm.

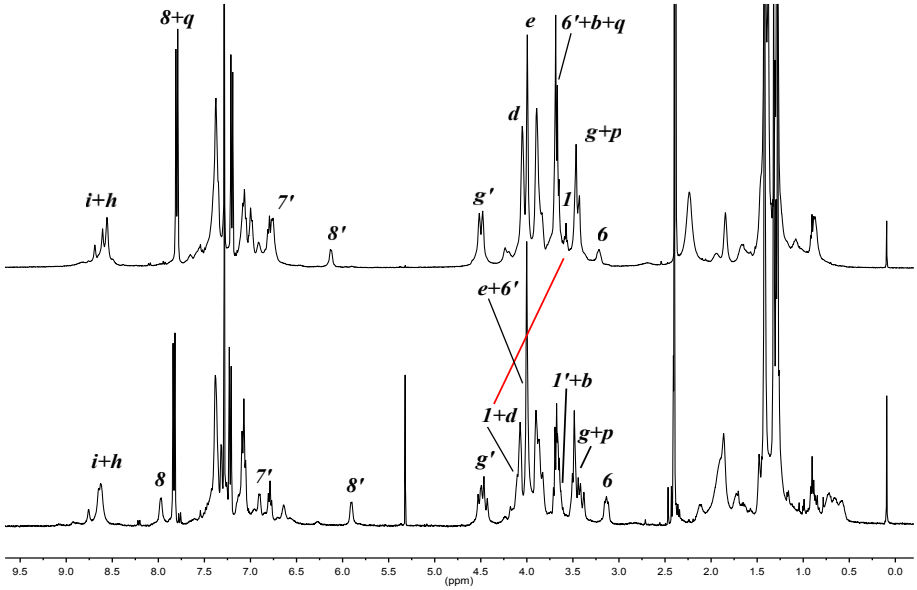


**Figure 9.** $^{1}$H NMR (400 MHz) stack plot of pseudorotaxane **5b⊃6**•2TsO (top) in and **1**•2TsO (bottom) in $CDCl_3$ showing the most important protons assignments (for protons labels see Scheme 6).

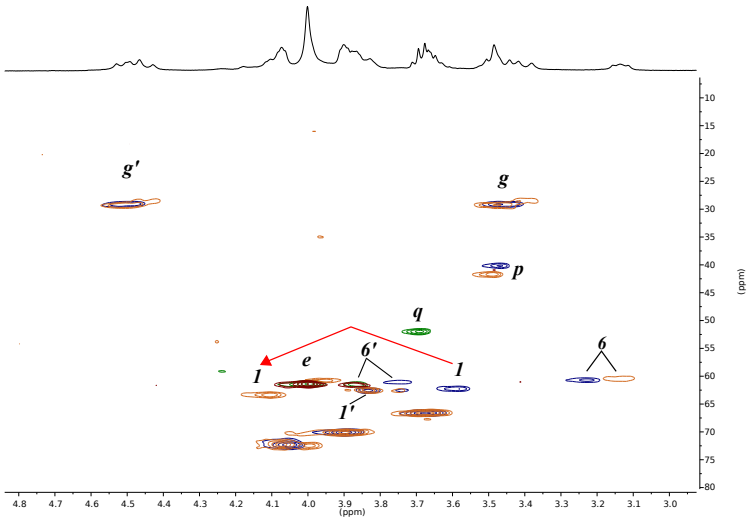


**Figure 10.** Superimposed $^{1}$H-$^{13}$C 2D HSQC (400 MHz) (expanded region) spectra of **5b⊃6**•2TsO (blue for $-CH_2-$ and green for –CH- and $-CH_3-$) and **1**•2TsO (orange for $-CH_2-$ and red for –CH- and $-CH_3-$) in $CDCl_3$. Most important protons assignments are shown (for protons labels see Scheme 6).

MS spectrometry confirmed the identity of the molecule exhibiting a peak at 932.1 m/z; the isotopic distribution of the signals suggests that z=2.

Inspired by a work of Strutt et al.,[15] DOSY NMR experiments were carried out on **1**•2TsO at four different concentrations, between 7.0 mM and 0.03 M, in $C_6D_6$ with the aim to understand its aggregation properties in solution. The diffusion coefficients measured for **1**•2TsO were compared to that of **5a⊃DOV**•2TsO[18] (Figure 11) that possesses a similar molecular weight (**DOV**= dioctylviologen). Diffusion coefficients were measured according to Stokes-Einstein equation[19] (Equation 1):

$$D = \frac{k_B T}{6\pi\eta r} \quad \text{(Eq.1)}$$

Where $k_B$ is the Boltzmann constant, $T$ is the temperature, $\eta$ is the viscosity of the solvent and $r$ the hydrodynamic radius of the molecule.

The first experiment, carried out at the concentration of 7.0 mM, gave very similar diffusion coefficient for **1**•2TsO and **5a⊃DOV**•2TsO: $D$ = 3.11•10$^{-10}$ and 3.07•10$^{-10}$ m$^2$s$^{-1}$ respectively (Figure 11). These values suggest that, at this concentration, the structure of **1**•2TsO is that of a [*c*1]daisy chain structure. In this architecture, the alkylviologen unit appended to upper rim of the macrocycle threads intramolecularly the electron-rich calixarene cavity. The experiment performed with a 12.0 mM solution of **1**•2TsO displayed a very similar diffusion coefficient ($D$ = 2.97•10$^{-10}$ m$^2$s$^{-1}$), clearly indicating that this increase of concentration does not affect the aggregation behaviour.

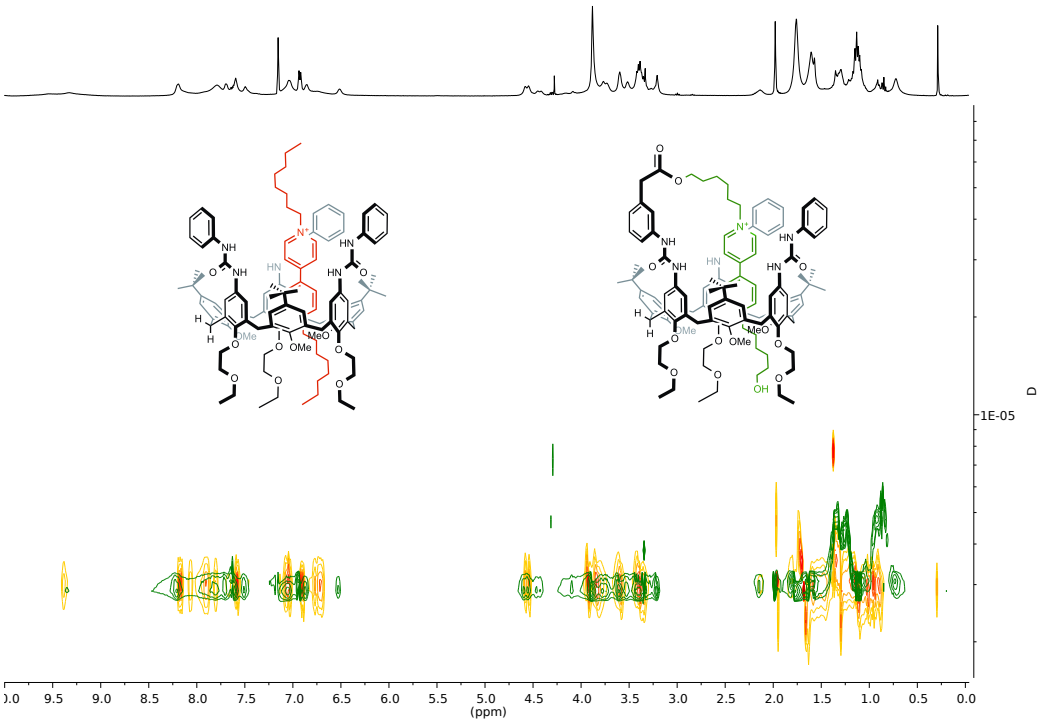


**Figure 11.** Superimposed DOSY (400 MHz) spectra of a 7.0 mM solution of **5a⊃DOV**•2TsO (orange) and **1**•2TsO (green) in $C_6D_6$.

On the contrary, the experiment carried out at 22.0 mM showed a different coefficient diffusion value for **1**•2TsO, $D = 2.51 \cdot 10^{-10}$ $m^2s^{-1}$ (Figure 12).

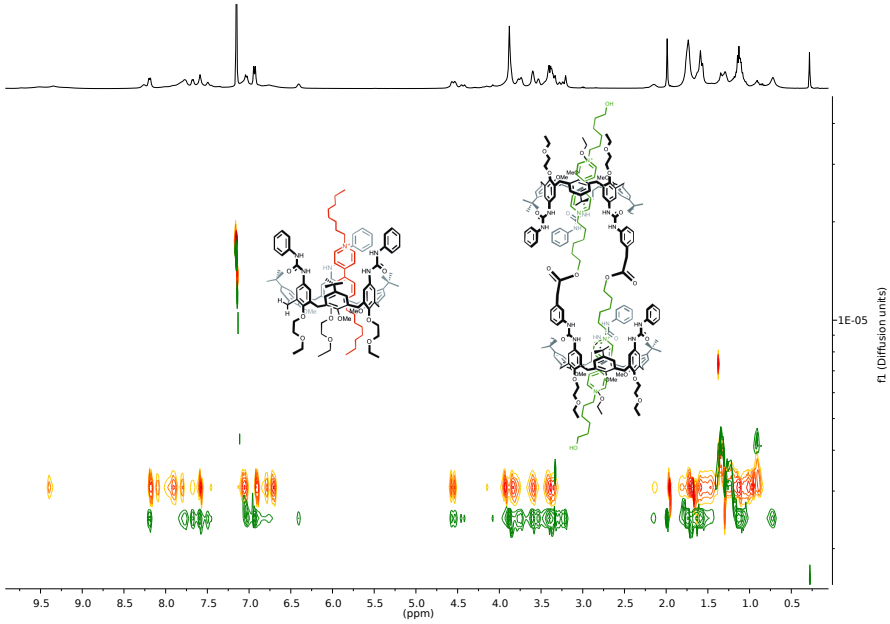


**Figure 12.** Superimposed DOSY (400 MHz) spectra of a 22.0 mM solution of **5a⊃DOV**•2TsO (orange) and **1**•2TsO (green) in $C_6D_6$.

Coefficient diffusion measurements carried out at a concentration of 30 mM for **1**•2TsO ($D$ = 2.53•10$^{-10}$ m$^2$s$^{-1}$), confirmed a substantial difference for the diffusion coefficient values of the system. Thanks to a formula for spherical-shape molecules, derived from the Stoke-Einstein equation (Equation 2), the molecular weight of the molecular complex was calculated:[19]

$$\frac{D_{exp}}{D_{ref}} = \sqrt[3]{\frac{M.W._{ref}}{M.W._{exp}}} \quad \text{(Eq. 2)}$$

The calculated M.W. of the **1**•2TsO aggregate in solution is 3627, a value that approach the double molecular weigth of **5a⊃DOV**•2TsO; thus indicating that the intermolecular aggregation of **1**•2TsO is now favoured and the desired [*c*2]daisy chain architecture is now the favourite state (Scheme 7).

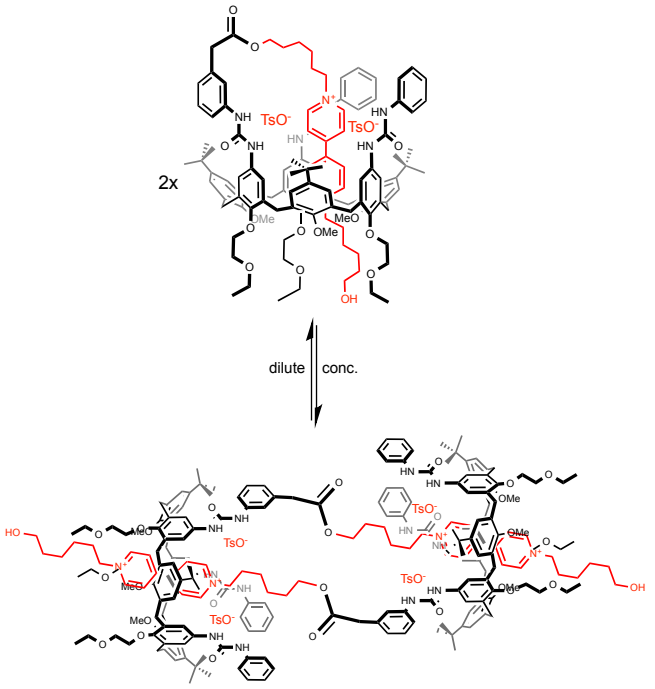


**Scheme 7.** Concentration dependant behaviour of **1**•2TsO aggregation properties in $C_6D_6$.

It was then envisaged that, carrying out a stoppering reaction of **1**•2TsO at a concentration of about 0.03M, a [*c*2]daisy chain rotaxane could be obtained; to this aim, to a 0.03M solution of **1**•2TsO in dichloromethane, an excess of diphenylacetyl chloride and triethylamine was added in order to stopper the [*c*2]daisy chain architecture (Scheme 8).

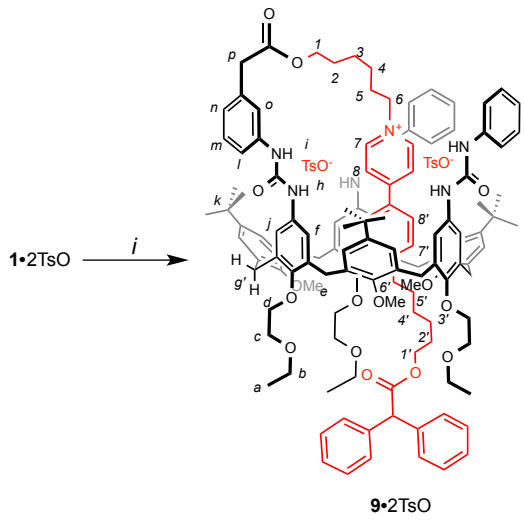


**Scheme 8.** Reagents and Conditions: *i*) 0.03M in toluene, Diphenylacetyl Chloride, Triethylamine, r.t., 16h.

The red solid product (**9**•2TsO) isolated from the mixture in 52% yield was characterized and the following NMR studies ($CDCl_3$, 400 MHz) gave us information on the successful stoppering of **1**•2TsO (see Figure 13, protons label in Scheme 8). The downfield shift ($\Delta\delta$ = 0.7 ppm) relative to the signal of proton *1'* indicates the formation of the diphenylacetyl ester. The esterification reaction is confirmed by the presence of a singlet at $\delta$ = 5.07 ppm, typical of a methyne proton of the diphenylacetyl ester group (proton λ in Figure 13, proton label in Scheme 8). The other main features of the spectrum resemble that of **1**•2TsO spectrum except the window from $\delta$ = 7.0 to $\delta$ = 7.5 ppm due to the presence of signals assignable to the aromatic protons of the stopper.

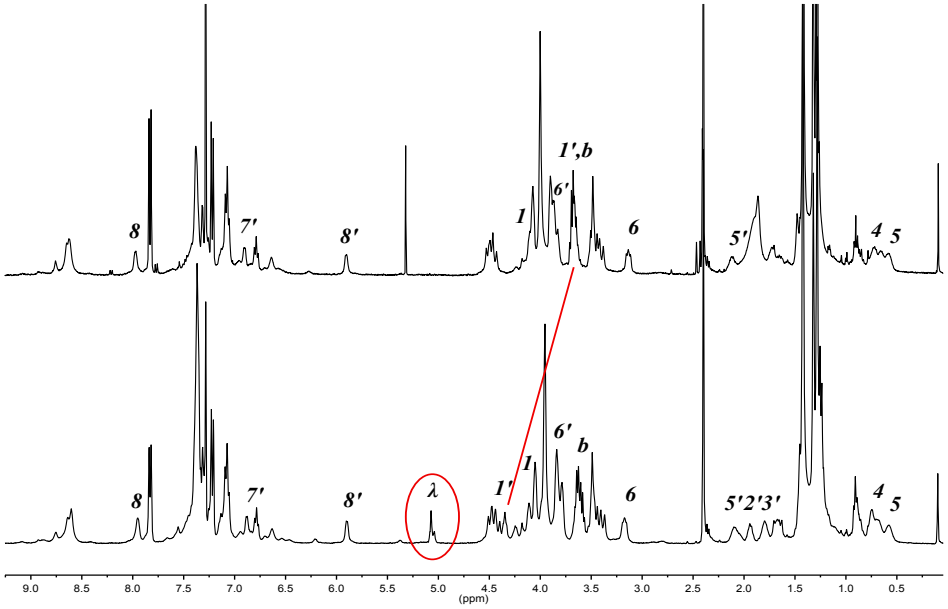


**Figure 13.** $^{1}$H NMR (400 MHz) stack plot of **1**•2TsO (top) in and **9**•2TsO (bottom) in $CDCl_3$ showing the most important protons assignments (for protons label see Scheme 7 and 8).

DOSY experiments (400 MHZ) were carried out on **9**•2TsO in $CDCl_3$; the calculated diffusion coefficient was compared to the one of the known rotaxane (**10**, structure present in Figure 14)[17]. A very similar diffusion coefficient was found for the two compounds. This clearly indicates that **2**•2TsO structure is a [*c*1]daisy chain where the viologen arm is complexed inside its own electron-rich cavity.

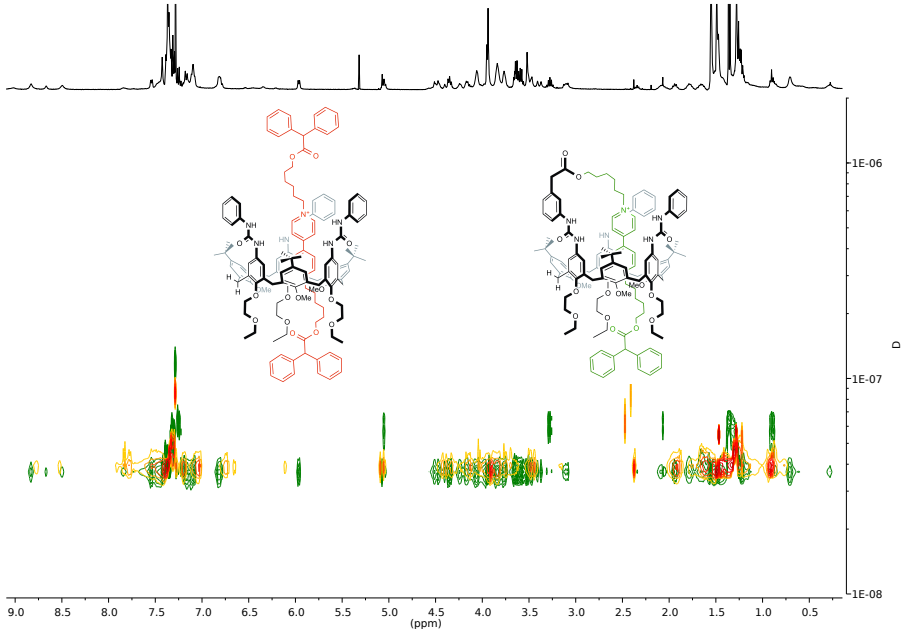


**Figure 14.** Superimposed DOSY (400 MHz) spectra of a 22.0 mM solution of **10**•2TsO (orange) and **9**•2TsO (green) in $CDCl_3$.

A further confirmation of the molecular architecture of this interlocked molecule was given by high resolution Mass Spectroscopy: the isotopic distribution of the peaks clearly indicates that **9**•2TsO has a self-assembled structure (Figure 15). The peak at 102.565778 m/z, assigned to **9**•2TsO without anions, shows only signals with z=2.

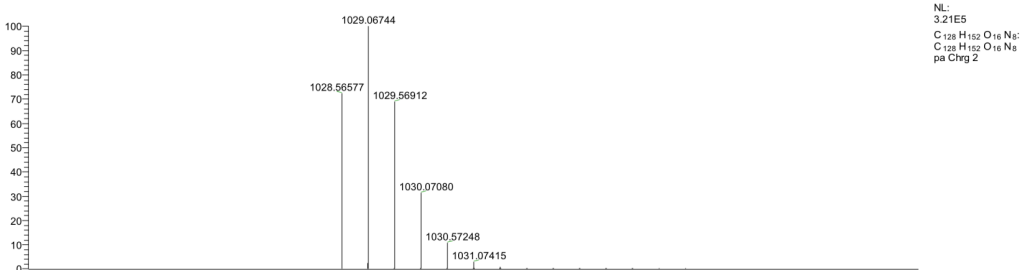


**Figure 15.** High resolution mass spectrum (orbitrap LQ) of **9**•2TsO; the experimental isotope distribution pattern of the doubly charged (z = 2) molecular ion is shown.

Unfortunately, also by carrying out the reaction at higher concentration, the only product isolated was the [*c*1]daisy chain architecture, thus suggesting that this reaction is entropically driven.

Therefore, a different synthetic approach was developed to prevent the intramolecular reaction between the OH group of the axle and the ester function of the wheel in a preformed pseudorotaxane (Scheme 9).

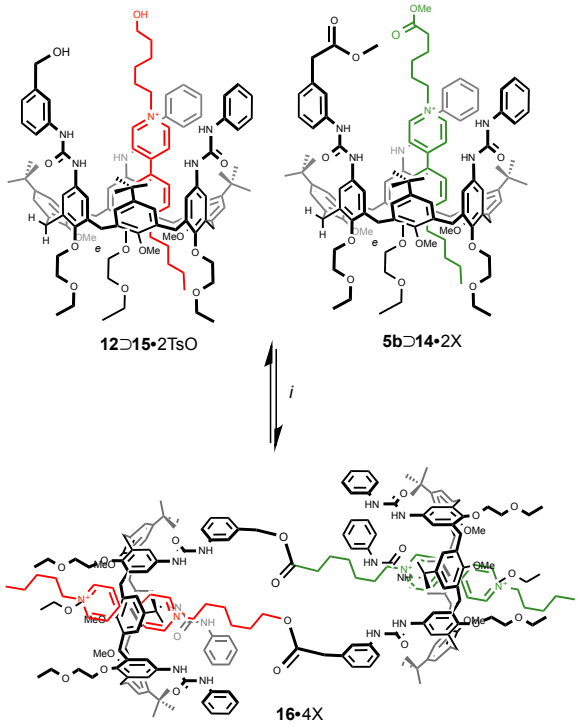


**Scheme 9.** Reagents and Conditions: *i*) Toluene, reflux, 16h.

The strategy adopted was to utilize two different pseudorotaxanes whose components bear the same functional group on the same rim of the wheel. Specifically, one pseudorotaxane, **12⊃15**•2TsO, having two hydroxyl groups at the upper rim and one, **5b⊃14**•2X, bearing two methyl ester functions in the same spatial domain. The working hypothesis was that a double transesterification reaction between the two

different pseudorotaxanes **12⊃15**•2TsO and **5b⊃14**•2X could minimize the yielding of the self-included daisy chain **1**•2TsO.

**5b⊃14**•2X was obtained equilibrating an equimolar amount of **5b** and **14**•2X in toluene (Scheme 10).

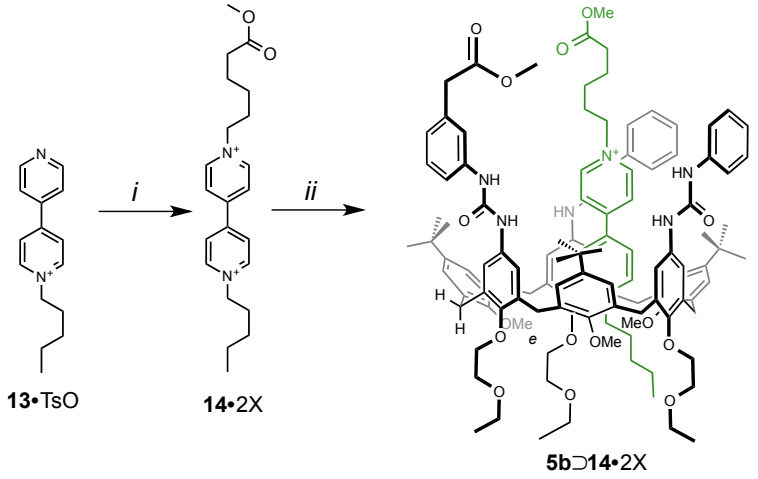


**Scheme 10.** Reagents and Conditions: *i*) methyl 6-bromohexanoate, $CH_3CN$, reflux, 4 days; *ii*) toluene, r.t., 1h.

The formation of **12⊃15**•2TsO required the synthesis of a new mono-functionalised calix[6]arene bearing a hydroxyl moiety on the upper rim; the statistical approach optimized for the synthesis of **5b** was adopted for the obtaining of compound **12**. To a solution of calixarene **2** in dichloromethane, a mixture of phenylisocyanate and tert-butyl((4-isocyanatobenzyl)oxy)dimethylsilane (**11**), synthesized from a known procedures,[20] was added in a 3:2 ratio with respect to **2**. Wheel $\mathbf{12_{pr}}$ was isolated in 27% yield. The protecting group tert-butyldimethylsilyl (TBDMS) was removed with tetrabutylammonium fluoride (TBAF) and acetic acid to afford the final compound **12** in 69% yield (Scheme 11).

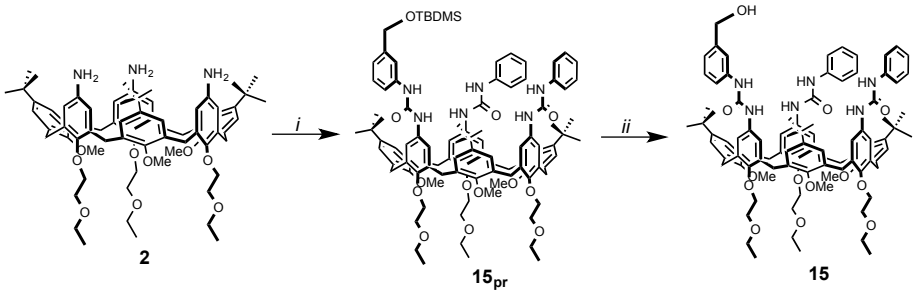


**Scheme 11.** Reagents and Conditions: *i*) Phenylisocyanate (**3**), *tert*-butyl((4-isocyanatobenzyl)oxy) dimethylsilane (**11**), (molar ratio 3 and 2, respectively, with respect to **2**), $CH_2Cl_2$, 1h, r.t.; *ii*) Acetic acid, TBAF, THF, r.t., 16h.

NMR investigations (300 MHz, $CDCl_3$) on **12** showed the typical spectra of a tris(*N*-phenylureido) calix[6]arene (Figure 16). In the $^1$H NMR spectrum of **12**, the removal of the TBDMS protecting group is evidenced by the absence of two singlet at $\delta = 0.08$ (6H) ppm and $\delta = 0.9$ (9H) ppm (protons *q* and *r* respectively in Figure 16, protons label in Figure 16), which are instead present in the $^1$H NMR spectrum of $\mathbf{12_{pr}}$ (Figure 16a).

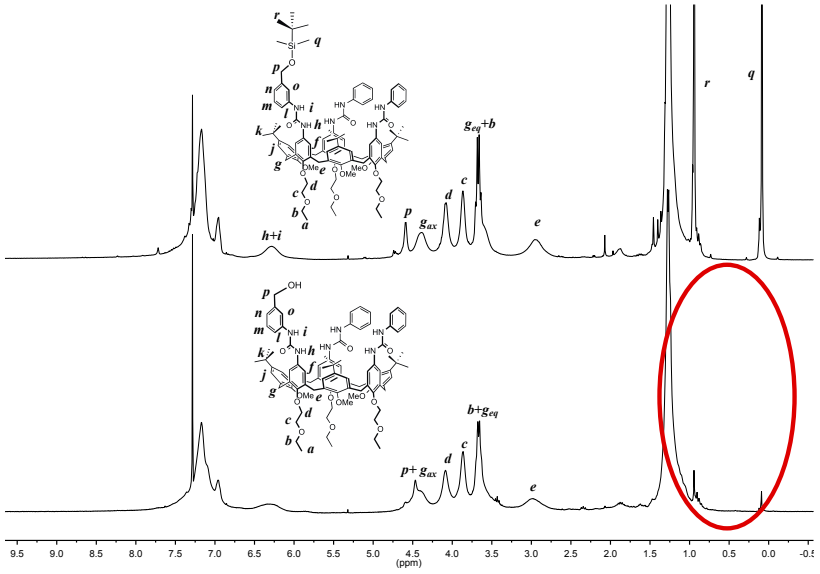


**Figure 16.** $^1$H NMR (300 MHz) stack plot of $\mathbf{12_{pr}}$ (top) and **12** (bottom) in $CDCl_3$ showing the most important protons assignments.

MS measurements confirmed the identity of the two molecules: $\mathbf{12_{pr}}$ spectrum shows a signal of at m/z= 1633.1, for the adduct formed by $\mathbf{12_{pr}}$ and $Na^+$; **12** spectrum showed a peak at m/z= 1518.1, also formed by **12** and $Na^+$. The difference in mass between the two signals is 115.0, exactly the molecular weight of the TBDMS protective group. Pseudorotaxane **12⊃15**•2TsO was then obtained by equilibrating **12** and an equimolar amount of **15**•2TsO, in toluene (Scheme 12).

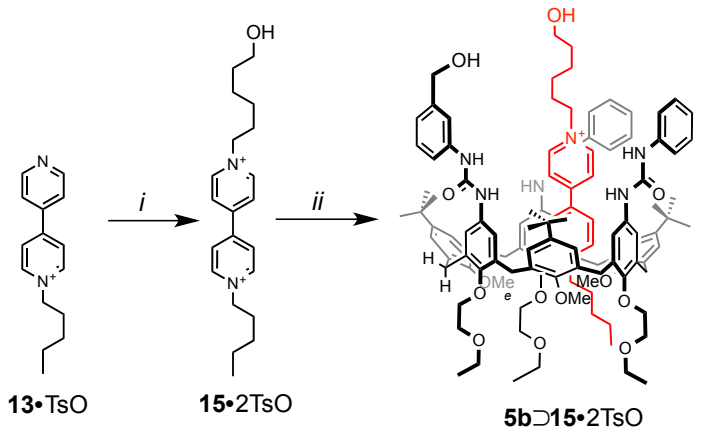


**Scheme 12.** Reagents and Conditions: *i*) 6-hydroxyhexyl 4-methylbenzenesulfonate, $CH_3CN$, reflux, 4 days; *ii*) toluene, r.t., 1h.

The solutions of the two different pseudorotaxanes **12⊃15**•2TsO and **5b⊃14**•2TsO were mixed in a 1:1 ratio and a catalytic amount of *p*-toluenesulfonic acid was added. The mixture was refluxed for 16h (Scheme 9).

After column chromatography, a red solid was isolated in 12% yield. $^1$H NMR of compound **16**•2X shows a very similar set of signals if compared to **1**•2TsO, suggesting that esterification has occurred. Unfortunately, DOSY NMR experiments ($C_6D_6$, 400 MHz) carried out on this latter product gave a diffusion coefficient very similar ($D$ = 2.97•10$^{-10}$ m$^2$s$^{-1}$) to that of pseudorotaxane **5a⊃DOV**•2TsO ($D$ = 3.07•10$^{-10}$ m$^2$s$^{-1}$), again suggesting a self-assembled aggregation of **16**•2X in apolar media (Figure 17).

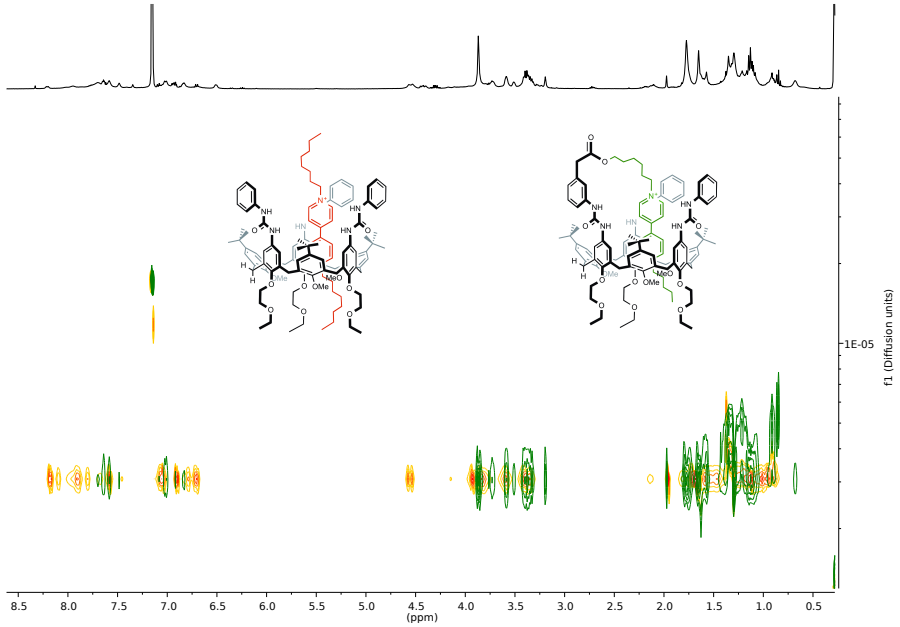


**Figure 17.** Superimposed DOSY (400 MHz) spectra of a solution of **5a⊃DOV**•2TsO (orange) and **16**•2X (green) in $C_6D_6$.

## 3.3 Design and Synthesis of [3]Rotaxanes

Since the daisy chain approach was not useful for the construction of a molecular muscle prototype, the development of a new synthetic strategy for the obtainment of a calix[6]arene based muscle-like structure was devised (Scheme 13). Among all the possible molecular architectures, that of a [3]rotaxane prototype was considered a better candidate, since this architecture was already exploited to emulate the process of a biological muscle.[2,3,5]

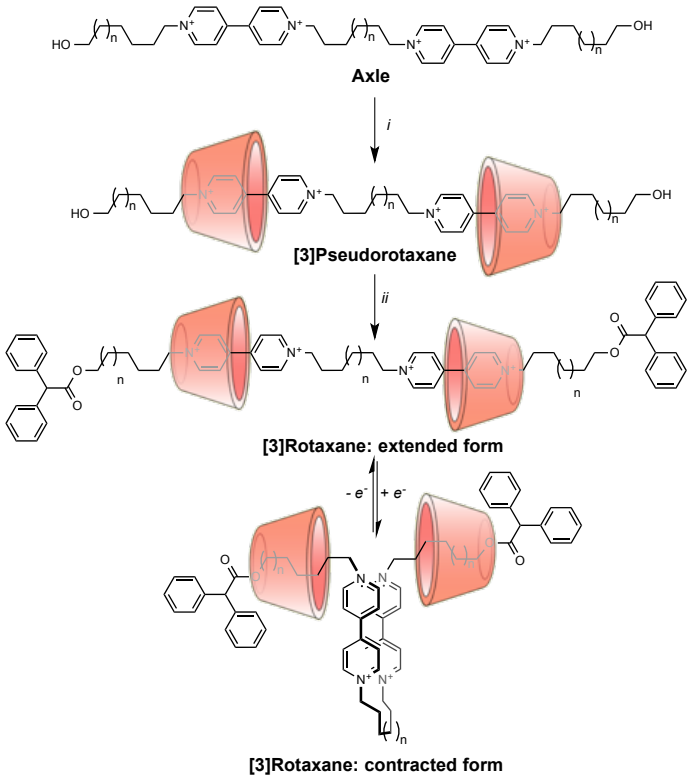


**Scheme 13.** Prototype of a [3]rotaxane acting as a molecular muscle. Reagents and Conditions: *i*) **5a**, toluene, r.t., 24h; : *ii*) Diphenylacetyl chloride, triethylamine, toluene, r.t., 16h;

The important structural features needed for the axial components of [3]rotaxanes were the suitable length of the alkyl chain that spans the two viologen units and the distance between these units and their terminal sidearms. In fact, a short distance between the two viologen sites could sterically prevent the formation of a [3]pseudorotaxane. In addition, during the electrochemically guided contraction of the molecule, the wheel requires a suitable space for its sliding movement along the two dumbbells. A short spacer between the lower rim of **5a** and the diphenylacetic stoppers may prevent the stacking of the two mono-reduced viologen moieties. Therefore, four tetra-charged viologen derivatives, functionalized with alkyl chains of variable length, were synthetized through a common procedure. Already available *N*-alkyl-4,4'-bipyridinium tosylate salts, bearing a variable length alkyl chain with a $\omega$-hydroxylic function

(**17**•TsO, **18**•TsO), were reacted with a 0.5 molar ratio of ditosylates of *α,ω*-diol of variable length (**19, 20**), as depicted in Scheme 14.

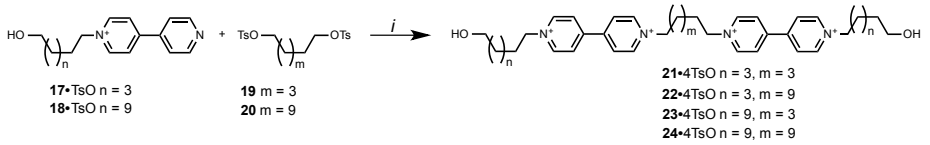


**Scheme 14.** Reagents and Conditions: *i*) $CH_3CN$, reflux, 4 days.

All the products were isolated by recrystallization in yields from 56% to 65% as white powders. $^1$H NMR investigations confirmed the identities of all the four products synthetized. As an example, the $^1$H NMR (400 MHz) spectrum of **22**•4TsO in $CD_3OD$ is reported (Figure 18). The relative integration of the signals of the *N*-$CH_2$- ($\delta$ = 4.72 ppm, 8H), -$CH_2$-*OH* ($\delta$ = 3.55 ppm, 4H) and the bipyridyl aromatic protons ($\delta$ = 9.25 and $\delta$ = 8.66 ppm, 16H) gave clear indications about the structure of the molecule.

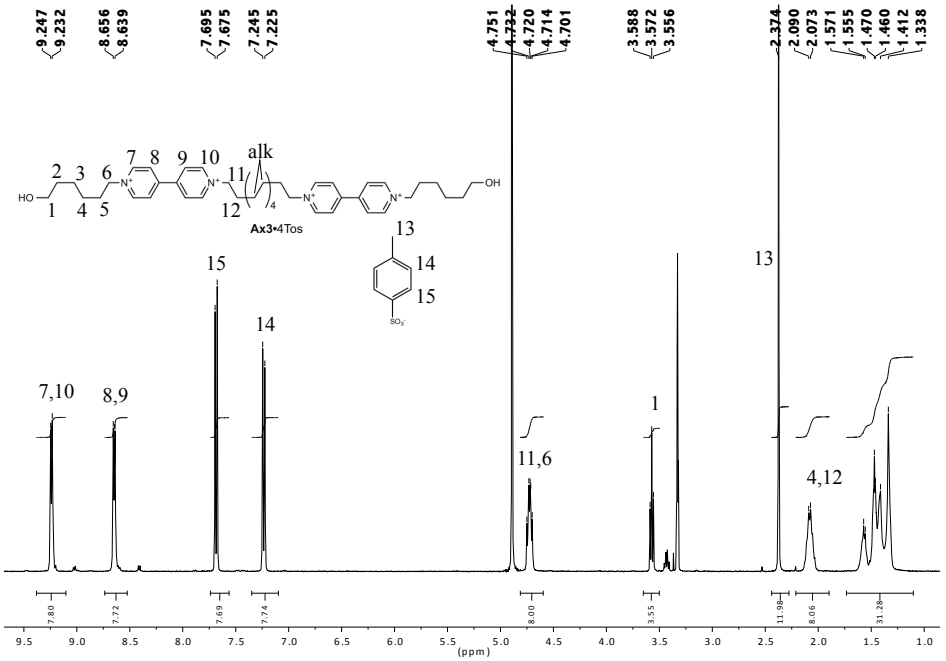


**Figure 18.** $^1$H NMR (400 MHz) of **22**•4TsO (n= 3, m= 9) in $CD_3OD$ showing the most important protons assignments.

In order to establish whether the viologen derivatives are suitable axles for the [3]pseudorotaxane syntheses in low polarity media using wheel **5a** as host, in separated experiments, axle **23**•4TsO and **24**•4TsO were equilibrated in $C_6D_6$ with two equivalent of **5a**. After 24h of stirring, only the solution with **24**•4TsO manifested a quantitative formation of the [3]pseudorotaxane, since the amount of undissolved guest was negligible and the colour of the solution turned deep red. Contrariwise, the mixture with **23**•4TsO showed a copious amount of undissolved guest and a pale orange colour, suggesting a non-quantitative complexation of **23**•4TsO by **5a**. After removal of the undissolved salt through filtration, NMR investigations were performed for all the complexation experiments. The $^1$H NMR spectra of both pseudorotaxanes displayed the typical pattern of signals of a complex having **5a** as the wheel and a viologen salt as the axle. Nevertheless, the presence of broad signals in the spectrum of [3]**5a**⊃**23**•4TsO (Figure 19c) reveals that the complex is not totally formed and a large amount of wheel **5a** is still present in solution. The low percentage of the complex formation is probably determined by the short (C6) span between the two viologens that prevent the threading of **23**•4TsO into two molecule of **5a** because of the steric hindrance of the phenylureido groups at the upper rim. The $^1$H NMR spectrum of [3]**5a**⊃**24**•4TsO (Figure 19b) displayed sharper peaks that allowed further investigations.

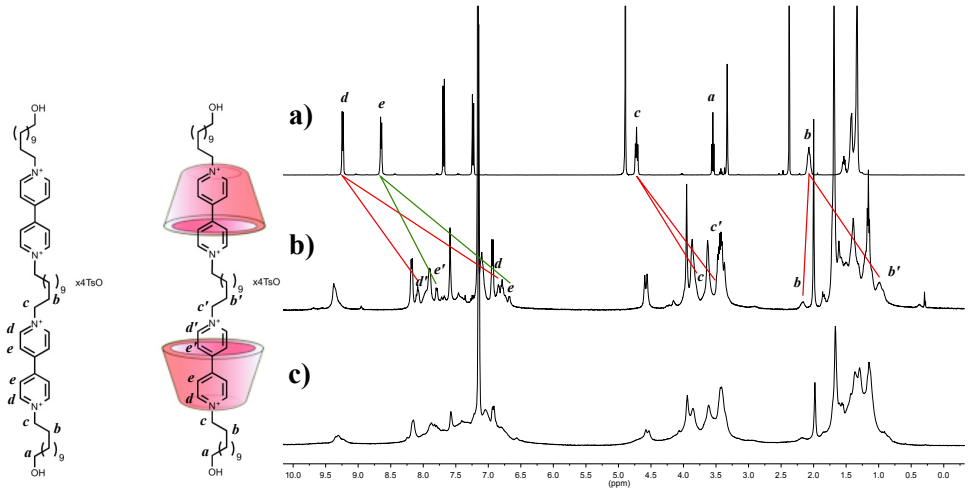


**Figure 19.** $^1$H NMR (400 MHz) stack plot of: a) **24**•4TsO in $CD_3OD$; b) [3]**5a⊃24**•4TsO in $C_6D_6$ and c) [3]**5a⊃23**•4TsO in $C_6D_6$ showing the most important protons assignments.

In the $^1$H NMR spectrum ($C_6D_6$, 400 MHz) of [3]**5a⊃24**•4TsO several diagnostic signals indicate the successful threading of axle **24**•4TsO into two molecules of **5a**. The inclusion of the axle is manifested by the upfield shift of the N-$CH_2$- protons (protons *c* in Figure 19a, protons label in Figure 19) induced by their engulfment in the electron-rich cavity, from $\delta = 4.72$ (in $CD_3OD$) to $\delta = 3.80$ and 3.47 ppm, signal *c* and *c'* respectively in Figure 19b. The splitting of the triplet into two signals indicates the different magnetic field, depending by their position in the wheel, suffered by protons *b*. Another indication about the inclusion of the axle is the splitting of the bipyridyl doublet at $\delta = 9.25$ ppm ($CD_3OD$, protons *d* in Figure 19a), and its concurrent shift to stronger fields, into two signals at $\delta = 7.99$ at $\delta = 6.73$ ppm (protons *d'* and *d*, respectively, in Figure 19b); their different position in the electron-rich cavity determined their different chemical shifts. Thanks to these indications, the synthesis of [3]rotaxanes with axle **22**•4TsO and **24**•4TsO was tackled. A suspension of the axle (**24**•4TsO or **22**•4TsO) in toluene was stirred with a two-fold molar amount of **5a** until the solution became homogeneous and red-coloured. Diphenylacetyl chloride and triethylamine were then added in excess. After 24 hours, a red solid was purified through column chromatography to obtain a [3]rotaxane (yields of **25**•4TsO and

**26**•4TsO, 15% and 21% respectively). The identity of these two latter compounds was then confirmed by NMR spectroscopy ($C_6D_6$, 400 MHz) and high resolution mass spectrometry (HRMS). The complete assignments of the NMR peaks was not possible because of the extensive overlapping of several signals, particularly in the high field region of the spectra, nevertheless several diagnostic signals gave information about the formation of the rotaxanes and, most important, of the relative orientation of the wheels with respect to the axle. For example, in the $^1$H NMR spectrum of **25**•4TsO (shown in Figure 20a), the triplet at $\delta$ = 4.33 ppm gave clear indication of the ester formation with diphenylacetic group. The singlet at $\delta$ = 5.10 ppm, assigned to the methyne carbon with the diphenylacetic group, also demonstrates the formation of the ester bond between the axle and the stopper. The head-to-head position of the calixarenes is also supported by the presence of the methoxy singlet at $\delta$ = 3.89 ppm. In fact, when **5a** is threaded by longer alkyl chain the signal undergoes a shift to lower field of about 0.04 ppm, as shown in the $^1$H NMR spectrum of **26**•4TsO (Figure 20b), where the singlet resonates at $\delta$ = 3.95 ppm. Furthermore, in this spectrum, the triplet of the protons adjacent to the new generated ester functions also undergoes to a shift, now at higher fields of $\delta$ = 0.28 ppm, due to the longer alkyl chain that connects the viologens to the stoppers.

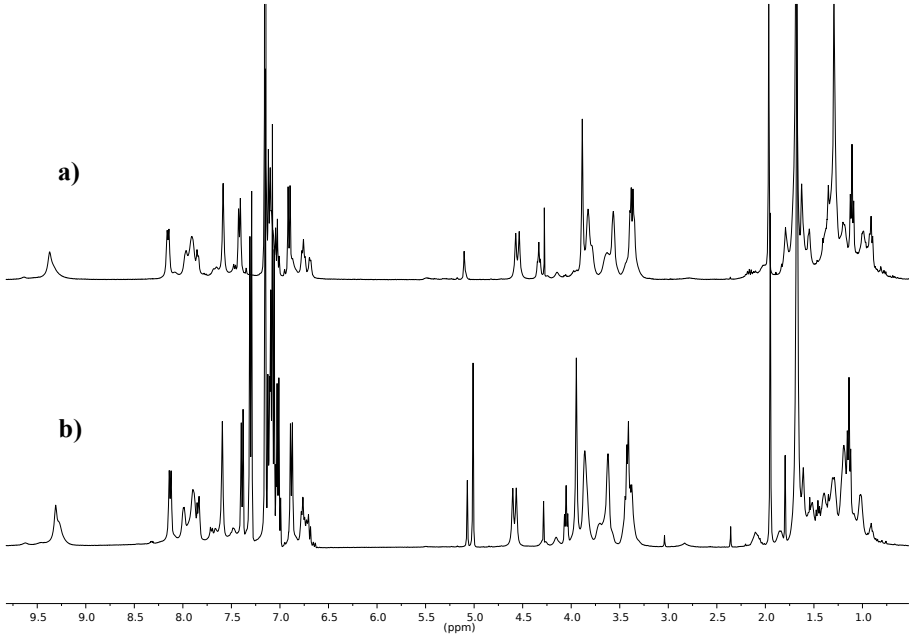


**Figure 20.** $^{1}$H NMR (400 MHz) stack plot of: a) **25**•4TsO and b) **26**•4TsO (down) in $C_6D_6$.

HR-MS measurements (ORBITRAP LQ) finally confirmed the formation of rotaxanes **25**•4TsO and **26**•4TsO. The mass spectrum of **25**•4TsO depicted in Figure 21 shows a very intense doubly charged ion with a monoisotopic peak at m/z = 2171.14411 given by the adduct generated by the tetra-charged rotaxane and two tosylate counter-anions.

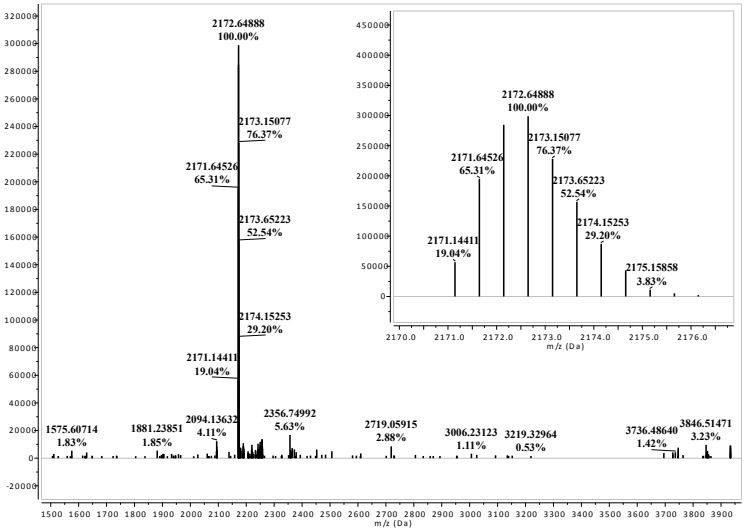


**Figure 21**. High resolution mass spectrum (Orbitrap LQ) of rotaxane **25**•4TsO. In the inset is shown the experimental isotope distribution pattern of the doubly charged (z = 2) molecular ion.

Mass spectrum of **26**•4TsO (Figure 22) displays a triple-charged intense peak at m/z = 1446.48779 assignable the adduct formed by the [3]rotaxane with one tosylate as counterion.

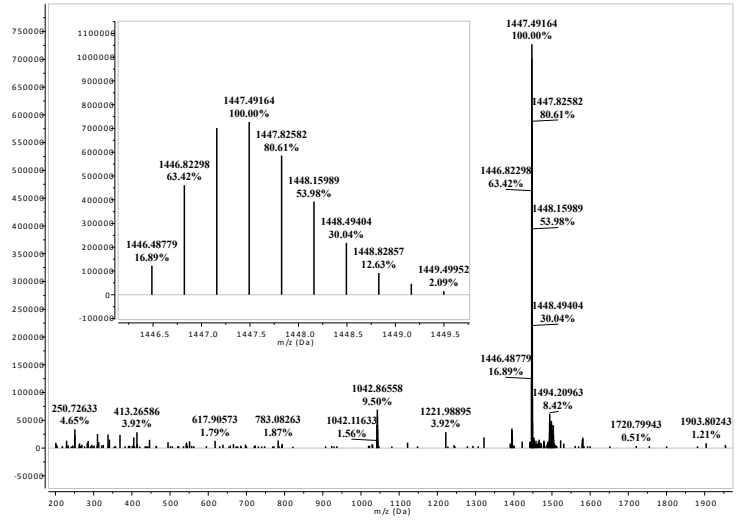


**Figure 22**. High resolution mass spectrum (Orbitrap LQ) of rotaxane **26**•4TsO. In the inset is shown the experimental isotope distribution pattern of the triply charged (z = 3) molecular ion.

## 3.4 Conclusions and Perspectives

In this chapter, several important information about the reactivity of calixarene derivatives were established. New synthetic strategies for the obtainment of hetero-functionalised tris(phenylureido) calix[6]arene were optimized; these latter macrocycles, in some cases, were also further functionalized with viologen derivatives through supramolecularly assisted reaction. A self-aggregating molecule, able to modify the association properties depending on its concentration in apolar media, was synthesized. The first example of calix[6]arene [*c*1]daisy chain was synthesized and characterized. This prototype of molecular machines paves the way for the synthesis of more sophisticated working devices in which appropriate external stimuli may open or close the ring defined by the self-engulfed viologen bracket; this kind of working device is called molecular "lasso" and only few examples are known in literature.[21,22] Finally, the obtainment of two [3]rotaxanes was tackled; with the aim to understand whether these molecules may reproduce the reversible contractile process of biological muscle, electrochemical studies are currently undergoing in our laboratories. In case of successful results, the natural development of this work may be the synthesis of new calix[6]arene based [3]rotaxanes decorated with ligands for metal ions as stoppers. The subsequent creation of supramolecular polymers may transfer the contractile process of the muscle to a macroscopic scale.

# Experimental section

**Reagents and methods.** All solvents were dried using standard procedures; all other reagents were of reagent grade quality obtained from commercial suppliers and were used without further purification. NMR spectra were recorded at 400 MHz for $^{1}H$ and 100 MHz for $^{13}C$. Melting points are uncorrected. Chemical shifts are expressed in ppm ($\delta$) using the residual solvent signal as internal reference (7.16 ppm for $C_6H_6$; 7.26 ppm for $CHCl_3$ and 3.31 for $CH_3OH$). Mass spectra were recorded in ESI mode. Calix[6]arenes **2**,[16] axle **6•2**TsO,[17] **13•**TsO,[23] **17•**TsO and **18•**TsO,[24] alkylating agents 6-hydroxyhexyl 4-methylbenzenesulfonate,[25] methyl 6-bromohexanoate,[26] hexane-1,6-diyl bis(4-methylbenzenesulfonate) **(19)**,[27] dodecane-1,12-diyl bis(4-methylbenzenesulfonate) (**20**)[28] and tert-butyl((4-isocyanatobenzyl)oxy) dimethylsilane (**11**)[20] were synthesised according to published procedures. Deuterated benzene was used as the solvent in most NMR experiments because a better resolution of the signals, especially in the low fields portion of the spectra, is afforded.

## Synthetic Procedures

**Methyl 2-(4-isocyanatophenyl)acetate (4)**. A triphosgene (0.52 g, 2.1 mmol) solution in dry dichloromethane (10 ml) was added dropwise to a solution at 0° C of methyl (4-aminophenyl)acetate (1.00 g, 6.1 mmol) and triethylamine (0.6 g, 6.1 mmol) in dry dichloromethane (25 ml) under nitrogen atmosphere. The reaction mixture was stirred for 30 min at room temperature. The solvent was removed under reduced pressure and the pure product was extracted from the mixture with n-hexane (3x25 ml). The solvent was removed under reduced pressure to yield 0.64 g of product **1** as colorless oil in 55% yield. $^{1}H$ NMR ($CDCl_3$, 400 MHz) $\delta$= 7.26 (d, 2H, $J$ = 8.0 Hz), 7.08 (d, 2H, $J$ =8.0 Hz), 3.72 (s, 2H), 3.63 (s, 2H); $^{13}C$ NMR (100 MHz) $\delta$= 171.7, 132.4, 131.6, 130.5, 124.8, 52.2, 40.5.

**Calixarene 5b**. In a 50 ml round bottom flask, at a solution of **2** (0.15 mg, 0.13 mmol) in dichloromethane (20 ml) under nitrogen atmosphere, a solution of dichloromethane containing phenylisocyanate (0.06 g, 0.54 mmol) and **3** (0.05 g, 0.26 mmol) was added dropwise. The reaction mixture was stirred for two hours at room temperature. The solvent was removed under reduced pressure and the mixture was purified by silica gel chromatography column, using dichloromethane/ethyl acetate (85:15) as eluent to yield 0.08 g of product **5b** as a pale yellow solid in 38% yield. $^{1}$H NMR ($CDCl_3$, 400 MHz) $\delta$= 7.4-6.6 (m, 26H), 6.0 (bs, 6H), 4.4 (bs, 6H), 3.9 (bs, 6H), 3.7-3.6 (m, 11H), 3.5 (bs, 6H), 2.9 (bs, 9H), 1.3-0.9 (m, 27H); $^{13}$C NMR (100 MHz) $\delta$= 172.2, 154.6, 151.8, 146.7, 135.7, 133.0, 129.7, 128.9, 128.4, 127.8, 127.6, 122.6, 120.1, 72.4, 72.1, 69.9, 66.9, 60.3, 52.0, 40.5, 34.2, 31.5, 31.2, 31.0, 29.7, 15.3, 14.1. MS (ESI): m/z: 1560.8 $[M+ Na]^{+}$.

**Pseudorotaxane 5b⊃6•2TsO.** In a 50 ml two-necked round bottom flask, calix[6]arene wheel **5b** (0.10 g, 0.07 mmol) was dissolved in toluene (20 ml) under nitrogen atmosphere and axle **6•2TsO** (0.05 g, 0.08 mmol) was added. The resulting heterogeneous solution was stirred for two hours at room temperature, during which it gradually turned homogeneous and deep red color. After this period, the solution was filtered and the solvent was evaporated under reduced pressure to obtain **5b⊃6•2TsO** as a red solid. $^{1}$H NMR ($CDCl_3$, 400 MHz) $\delta$= 8.7-8.5 (m, 6H), 7.8-7.7 (m, 6H), 7.6-7.3 (m, 14H), 7.21 (d, 4H, $J$ = 8.4 Hz), 7.1-6.6 (m, 16H), 6.1 (bs, 2H), 4.52 (d, 6H, $J$ = 14.8 Hz), 4.1-3.9 (m, 15H), 3.9-3.8 (m, 8H), 3.8-3.5 (m, 13H), 3.5-3.3 (m, 8H), 3.2 (bs, 2H), 2.38 (s, 6H), 1.9 (bs, 2H), 1.8 (bs, 4H), 1.7 (bs, 2H), 1.5-1.0 (m, 48H), 0.9-0.7 (m, 4H). $^{13}$C NMR (100 MHz): $\delta$= 153.2, 152.5, 148.0, 144.2, 142.8, 141.9, 140.1, 136.5, 133.8, 131.9, 129.6, 128.9, 128.8, 128.7, 126.7, 126.1, 125.2, 124.2, 121.4, 117.7, 116.6, 77.3, 77.2, 77.0, 76.7, 72.3, 70.1, 66.6, 62.6, 62.3, 61.4, 52.0, 40.1, 34.5, 33.3, 31.9, 31.4, 29.7, 29.1, 25.5, 22.7, 21.4, 15.3, 14.1. MS (ESI): m/z: 948.2 $[M-2TsO]^{2+}$.

**1•2TsO.** In a 50 ml two-necked round bottom flask, to a solution of pseudorotaxane **5b⊃6•2TsO** (0.15 g, 0.07 mmol) in refluxing toluene (20 ml), *p*-Toluenesulfonic acid monohydrate (0.002 g, 0.01 mmol) was added. The resulting homogeneous solution

was refluxed for two hours. After this period, the solvent was evaporated under reduced pressure and the solid residue purified over chromatography column (DCM/MeOH= 95:5) to afford 0.97 g of **1**•2TsO as a red solid in 65% yield. $^{1}$H NMR ($CDCl_3$, 400 MHz) $\delta$= 8.7-8.5 (m, 6H), 7.9 (bs, 2H), 7.82 (d, 4H, $J$ = 8.0 Hz), 7.6-7.3 (m, 12H), 7.2-6.6 (m, 16H), 7.20 (d, 4H, $J$ = 8.0 Hz), 7.2-7.0 (m, 8H), 7.0-6.4 (m, 9H), 5.9 (bs, 2H), 4.6-4.3 (m, 6H), 4.1-3.7 (m, 21H), 3.7-3.5 (m, 6H), 3.5-3.3 (m, 8H), 3.1 (bs, 2H), 2.38 (s, 6H), 2.1 (bs, 2H), 1.8 (bs, 4H ), 1.7 (bs, 2H), 1.5-1.0 (m, 48H), 1.0-0.7 (m, 6H). $^{13}$C NMR (100 MHz): $\delta$= 171.6, 153.0, 152.1, 148.1, 144.3, 142.7, 142.1, 140.2, 140.0, 139.2, 139.1, 136.7, 134.3, 131.8, 129.8, 129.7, 129.1, 128.8, 127.8, 127.6, 126.1, 125.4, 124.1, 121.5, 117.7, 116.8, 116.6, 77.3, 77.2, 77.0, 76.7, 70.1, 66.6, 62.5, 61.4, 41.7, 34.5, 34.3, 31.3, 29.7, 29.3, 22.7, 21.5, 21.4, 15.3, 14.1.; MS (ESI): m/z: 932.2 $[M\text{-}2TsO]^{2+}$.

**9•2TsO.** In a 10 ml two-necked round bottom flask, to a solution of daisy chain **1•2TsO** (0.050 g, 0.02 mmol) in toluene (0.6 ml) at room temperature, diphenylacetyl chloride (0.008 g, 0.04 mmol) and triethylamine (0.008 g, 0.04 mmol) were added. The resulting homogeneous solution was stirred overnight. Afterwards, the solvent was evaporated under reduced pressure and the solid residue purified over chromatography column (DCM/MeOH= 97:3) to afford 0.025 g of **2**•2TsO as a red solid in 52% yield. $^{1}$H NMR ($CDCl_3$, 400 MHz) $\delta$= 9.0-8.5 (m, 6H), 7.9 (bs, 2H), 7.84 (d, 4H, $J$ = 8.0 Hz), 7.6-7.3 (m, 24H), 7.3-7.2 (m, 6H), 7.2-7.0 (m, 8H), 7.0-6.7 (m, 6H), 6.6 (bs, 2H), 5.9 (bs, 2H), 5.07 (s, 1H), 4.6-4.4 (m, 6H), 4.35 (t, 2H, $J$ = 6.8 Hz), 4.3-4.0 (m, 6H), 4.0-3.9 (m, 11H), 3.8 (bs, 6H), 3.7-3.5 (m, 6H), 3.5-3.3 (m, 8H), 3.2 (bs, 2H), 2.38 (s, 6H), 2.1 (bs, 2H), 1.9 (bs, 2H ), 1.8 (bs, 2H), 1.7 (bs, 4H), 1.5-1.0 (m, 50H), 0.8-0.4 (m, 6H). $^{13}$C NMR (100 MHz): $\delta$= 172.5, 171.6, 152.9, 152.5, 148.1, 144.3, 142.8, 142.2, 140.3, 140.0, 138.6, 136.7, 133.8, 133.6, 131.9, 131.8, 129.7, 129.1, 128.8, 128.7, 128.6, 128.6, 128.5, 128.1, 127.8, 127.6, 127.4, 126.1, 125.4, 124.0, 121.5, 117.7, 116.8, 116.6, 77.2, 72.7, 72.4, 70.0, 66.6, 65.0, 63.4, 61.3, 60.4, 57.1, 41.7, 34.5, 34.3, 31.9, 31.3, 29.7, 29.7, 29.5, 29.4, 29.2, 28.5, 27.7, 26.0, 24.8, 22.7, 21.4, 15.4, 14.1. HR-MS (ESI, Orbitrap LQ) calculated for $C_{128}H_{152}N_8O_{16}$ m/z (z = 2): 1028.56577 (72),

1029.06744 (100), 1029.56912 (68), 1030.07080 (31), 1030.57248 (11), 1031.07415 (3).

**Calixarene $12_{pr}$.** In a 50 ml round bottom flask, at a solution of **2** (0.35 g, 0.32 mmol) in dichloromethane (20 ml) under nitrogen atmosphere, a solution of dichloromethane containing phenylisocyanate (0.11 g, 0.96 mmol) and isocyanate **11** (0.17 g, 0.64 mmol) was added dropwise. The reaction mixture was stirred for two hours at room temperature. The solvent was removed under reduced pressure and the mixture was purified by silica gel chromatography column, using hexane/ethyl acetate (65:35) as eluent to yield 0.14 g of product $\mathbf{12_{pr}}$ as a pale yellow solid in 27% yield. $^{1}$H NMR ($CDCl_3$, 300 MHz) $\delta$= 7.4-6.6 (m, 26H), 6.3 (bs, 6H), 4.6 (bs, 2H), 4.4 (bs, 6H), 4.0 (bs, 6H), 3.8 (bs, 6H), 3.7-3.4 (m, 12H), 2.9 (bs, 9H), 1.3-1.0 (m, 36H), 0.94 (s, 9H), 0.08 (s, 6H); $^{13}$C NMR (75 MHz): $\delta$= 154.8, 153.3, 152.1, 146.7, 139.2, 135.8, 133.0, 132.4, 128.9, 128.8, 127.6, 126.8, 125.5, 123.1, 122.5, 120.2, 119.3, 72.4, 69.9, 66.9, 64.6, 60.3, 34.2, 31.5, 31.4, 30.9, 30.3, 29.7, 29.4, 26.0, 18.4, 15.3, -5.2. MS (ESI): m/z: 1633.1 $[M+ Na]^+$.

**Calixarene 12.** In a 25 ml round bottom flask, at a solution of $\mathbf{12_{pr}}$ (0.05 g, 0.03 mmol) and acetic acid (0.01 g, 0.15 mmol) in dry THF (10 ml) at 0°C, 5 ml of a solution of tetrabutylammonium fluoride (0.02 g, 0.05 mmol) was added dropwise. The solution was then stirred at room temperature for 16h and diluted with ethyl acetate (50 ml); the organic phase was washed twice with a saturated solution of $NaHCO_3$ (2x 50 ml) and water (2x 50). The solvent was then evaporated under reduced pressure and the mixture was purified by silica gel chromatography column, using dichloromethane/methanol (97:3) as eluent to yield 0.03 g of product **12** as a pale yellow solid in 69% yield. $^{1}$H NMR ($CDCl_3$, 300 MHz) $\delta$= 7.4-6.6 (m, 26H), 6.3 (bs, 6H), 4.7-4.5 (bs, 8H), 4.1 (bs, 6H), 3.9 (bs, 6H), 3.7-3.4 (m, 12H), 2.9 (bs, 9H), 1.3-1.0 (m, 36H); $^{13}$C NMR (75 MHz): $\delta$= 154.8, 153.3, 152.1, 146.7, 139.2, 135.8, 133.0, 132.4, 128.9, 128.8, 127.6, 126.8, 125.5, 123.1, 122.5, 120.2, 119.3, 72.4, 69.9, 66.9, 64.6, 60.3, 34.2, 31.5, 31.4, 30.9, 30.3, 29.7, 29.4, 26.0, 18.4. MS (ESI): m/z: 1518.1 $[M+ Na]^+$.

**Axle 14•2X.** In a sealed 100 ml glass autoclave, a solution of **3**•TsO (0.5 g, 1.2 mmol) and methyl-6-brohexanoate (0.7 g, 3.6 mmol) in $CH_3CN$ (30 ml) was refluxed for 4 days. Afterwards, the solution was evaporated to dryness under reduced pressure. The solid residue was purified through recrystallization from $CH_3CN$ to afford 0.5 g of product **4**•2X as a yellow solid in 62% yield. $^1$H NMR ($CD_3OD$, 400 MHz) $\delta$= 9.23 (d, 4H, *J* = 6.8 Hz), 8.63 (d, 4H, *J* = 6.8 Hz), 7.70 (d, 4H, *J*= 8.4 Hz), 7.24 (d, 2H, *J*= 8.0 Hz), 4.8-4.7 (m, 4H), 3.67 (s, 3H), 2.4-2.3 (m, 6H), 2.1 (bs, 4H), 1.68 (m, 2H, *J*= 7.6 Hz), 1.5-1.3 (m, 6H), 0.96 (t, 3H, *J* = 6.8 Hz). $^{13}$C NMR (100 MHz): $\delta$= 149.7, 145.7, 142.4, 140.4, 128.6, 126.9, 125.6, 61.8, 61.3, 31.9, 31.1, 30.8, 27.9, 25.6, 25.4, 25.0, 21.8, 20.0, 12.9; MS (ES): m/z: 527.5.1 $[M- TsO]^+$.

**Axle 15•2X.** In a sealed 100 ml glass autoclave, a solution of **3**•TsO (0.5 g, 1.2 mmol) and 6-hydroxyhexyl 4-methylbenzenesulfonate (1.0 g, 3.6 mmol) in $CH_3CN$ (30 ml) was refluxed for 4 days. Afterwards, the solution was evaporated to dryness under reduced pressure. The solid residue was purified through recrystallization from $CH_3CN$ to afford 0.4 g of product **5**•2X as a white solid in 50% yield. $^1$H NMR ($CD_3OD$, 400 MHz) $\delta$= 9.24 (d, 4H, *J* = 6.4 Hz), 8.63 (d, 4H, *J* = 6.8 Hz), 7.70 (d, 4H, *J*= 8.4 Hz), 7.24 (d, 2H, *J*= 8.4 Hz), 4.8-4.7 (m, 4H), 3.57 (t, 2H, *J* = 6.4 Hz), 2.36 (s, 6H), 2.2-2.0 (m, 4H), 1.6 (bs, 2H), 1.5-1.3 (m, 10H), 0.97 (t, 3H, *J* = 6.8 Hz). $^{13}$C NMR (100 MHz): $\delta$= 174.1, 149.7, 145.7, 142.5, 140.4, 128.6, 126.9, 125.6, 61.8, 61.6, 50.8, 33.0, 30.9, 30.7, 27.9, 25.2, 23.9, 21.8, 20.1, 12.9; MS (ES): m/z: 499.5 $[M-TsO]^+$.

**Axle 21•4TsO.** In a sealed 100 ml glass autoclave, a solution of **17**•TsO (0.3 g, 0.6 mmol) and hexane-1,6-diyl bis(4-methylbenzenesulfonate) (0.1 g, 0.3 mmol) in $CH_3CN$ (40 ml) was refluxed for 4 days. Afterwards, the solution was evaporated to dryness under reduced pressure. The solid residue was purified through recrystallization from MeOH/$CH_3CN$ to afford 0.3 g of product **21•4TsO** as a white solid (67%). $^1$H NMR ($CD_3OD$, 400 MHz) $\delta$= 9.3-9.2 (m, 8H), 8.60 (d, 8H, *J* = 6.4 Hz), 7.69 (d, 8H, *J*= 8.0 Hz), 7.24 (d, 8H, *J*= 8.0 Hz), 4.8-4.7 (m, 8H), 3.57 (t, 4H, *J* = 6.4 Hz), 2.35 (s, 12H), 2.2-2.0 (m, 8H), 1.6-1.4 (m, 18H). $^{13}$C NMR (100 MHz): $\delta$= 150.6, 149.7, 149.6, 145.7, 145.6, 143.9, 142.4, 140.4, 128.6, 128.4, 126.8, 126.8,

126.5, 125.6, 125.3, 70.3, 61.8, 61.5, 61.3, 31.9, 31.1, 30.6, 29.2, 25.8, 25.6, 25.4, 25.0, 24.9, 20.1; MS (ES): m/z: 1111.8 $[M- TsO]^+$.

**22•4TsO.** In a sealed 100 ml glass autoclave, a solution of **17**•TsO (0.3 g, 0.6 mmol) and dodecane-1,12-diyl bis(4-methylbenzenesulfonate) (0.1 g, 0.3 mmol) in $CH_3CN$ (40 ml) was refluxed for 4 days. Afterwards, the solution was evaporated to dryness under reduced pressure. The solid residue was triturated with $CH_3CN$ to afford 0.3 g of product **8** as a white solid (63%). M.p. = 156-158 °C. $^1$H NMR ($CD_3OD$, 400 MHz) $\delta$= 9.25 (d, 8H, $J$ = 5.6 Hz), 8.66 (d, 8H, $J$ = 6.4 Hz), 7.70 (d, 8H, $J$= 8.4 Hz), 7.25 (d, 8H, $J$= 8.0 Hz), 4.8-4.7 (m, 8H), 3.57 (t, 4H, $J$ = 5.6 Hz), 2.37 (s, 12H), 2.1-2.0 (m, 8H), 1.5-1.3 (m, 28H). $^{13}$C NMR (100 MHz): $\delta$= 149.8, 145.6, 142.3, 140.3, 128.5, 126.9, 125.5, 61.9, 61.8, 61.2, 31.8, 31.2, 31.1, 29.2, 29.1, 28.8, 25.8, 25.7, 25.6, 25.0, 19.9. MS (ES): m/z: 1195.9 $[M-TsO]^+$.

**23•4TsO.** In a sea.led 100 ml glass autoclave, a solution of **18**•TsO (0.3 g, 0.6 mmol) and hexane-1,6-diyl bis(4-methylbenzenesulfonate) (0.15 g, 0.3 mmol) in $CH_3CN$ (40 ml) was refluxed for 4 days. Afterwards, the solution was evaporated to dryness under reduced pressure. The solid residue was triturated with $CH_3CN$ to afford 0.3 g of product **23•4TsO** as a white solid (65%). $^1$H NMR ($CD_3OD$, 400 MHz) $\delta$= 9.3-9-2 (m, 8H), 8.62 (d, 8H, $J$ = 6.4 Hz), 7.69 (d, 8H, $J$= 8.0 Hz), 7.24 (d, 8H, $J$= 8.0 Hz), 4.8-4.7 (m, 8H), 3.55 (t, 4H, $J$ = 6.8 Hz), 2.36 (s, 12H), 2.2-2.0 (m, 8H), 1.6-1.3 (m, 40H). $^{13}$C NMR (100 MHz): $\delta$= 149.8, 149.7, 145.7, 145.6, 142.3, 140.3, 128.6, 126.9, 126.9, 125.6, 61.9, 61.6, 61.5, 32.3, 31.2, 30.6, 29.4, 29.3, 29.2, 29.1, 28.8, 25.8, 25.6, 24.9, 20.0; MS (ES): m/z: 1279.1 $[M-TsO]^+$.

**24•4TsO.** In a sealed 100 ml glass autoclave, a solution of **18**•TsO (0.3 g, 0.6 mmol) and dodecane-1,12-diyl bis(4-methylbenzenesulfonate) (0.15 g, 0.3 mmol) in $CH_3CN$ (40 ml) was refluxed for 4 days. Afterwards, the solution was evaporated to dryness under reduced pressure. The solid residue was purified through recrystallization from MeOH/$CH_3CN$ to afford 0.3 g of product **24•4TsO** as a white solid (62%). M.p. = 196-198 °C; $^1$H NMR ($CD_3OD$, 400 MHz) $\delta$= 9.25 (d, 8H, $J$ = 6.8 Hz), 8.66 (d, 8H, $J$ = 6.4 Hz), 7.70 (d, 8H, $J$= 8.0 Hz), 7.25 (d, 8H, $J$= 8.0 Hz), 4.72 (t, 8H, $J$= 7.6 Hz), 3.55 (t,

4H, *J* = 7.0 Hz) 2.37 (s, 12H), 2.1 (bs, 8H), 2.0-1.9 (m, 4H), 1.53 (t, 4H, *J*= 6.8 Hz), 1.5-1.3 (m, 48H). $^{13}$C NMR (100 MHz): $\delta$= 149.8, 145.6, 142.3, 140.3, 128.5, 126.9, 70.5, 61.9, 61.6, 32.2, 31.2, 29.3, 29.2, 29.1, 28.8, 28.7, 25.8, 25.5, 19.9. MS (ES): m/z: 341.6 $[M\text{-}3TsO]^{3+}$.

**General procedure for the synthesis of [3]Rotaxane.** A suspension of the appropriate axle (0.03 mmol) and wheel **5a** (0.1 g, 0.06 mmol) in toluene (25 ml) was stirred for 24h at room temperature. When the mixture turned in a deep red homogeneous solution, diphenylacetyl chloride (0.03 g, 0.12 mmol) and triethylamine (0.03g, 0.12 mmol) were added. After being stirred at r.t. for 16h, the solvent was evaporated under reduced pressure.

**Rotaxane 25•4TsO.** The resulting red solid residue was purified through column chromatography (DCM/MeOH 95:5) to afford 0.05 g of **25•4TsO** as red solid compound **(**15**%)**. $^{1}$H NMR ($C_6D_6$, 400 MHz) $\delta$= 9.4 (bs, 12H), 8.16 (d, 12H, *J* = 8.0 Hz), 8.0-7.8 (m, 10H), 7.58 (s, 12H), 7.43 (d, 8H, *J* = 7.2 Hz), 7.1-7.0 (m, 12H), 6.9-6.8 (m, 12H), 6.8-6.6 (m, 10H), 5.10 (s, 2H), 4.57 (d, 12H, *J* = 14.4 Hz), 4.33 (t, 4H, *J* = 6.4 Hz), 4.0-3.7 (m, 30H), 3.7-3.5 (m, 20H), 3.5-3.2 (m, 24H), 2.1-1.9 (m, 16H), 1.8-1.5 (m, 82H), 1.4-0.8 (m, 126H). $^{13}$C NMR (100 MHz): $\delta$= 172.1, 153.6, 152.9, 148.2, 147.9, 144.4, 143.3, 143.0, 141.2, 139.4, 139.1, 137.5, 133.8, 132.2, 129.3, 128.8, 128.6, 128.4, 127.9, 127.8, 127.7, 127.6, 127.4, 127.2, 126.5, 124.9, 121.1, 118.1, 116.7, 72.4, 69.9, 66.3, 60.9, 60.8, 59.7, 57.3, 38.2, 34.6, 32.0, 31.5, 31.3, 29.8, 29.8, 29.7, 29.4, 29.0, 26.2, 22.8, 20.8, 15.2, 14.0. HR-MS (ESI, Orbitrap LQ) calculated for $C_{266}H_{316}N_{16}O_{34}S_2$ m/z (z = 2): 2171.14602 (25), 2171.64769 (70), 2172.14937 (100), 2172.65105 (95), 2173.15273 (68), 2173.65440 (38), 2174.15608 (18), 2174.65776 (7), 2175.15944 (3).

**Rotaxane 26•4TsO.** The resulting red solid residue was purified through column chromatography (DCM/MeOH 95:5) to afford 0.07 g of **26•4TsO** as red solid compound **(**21**%)**. $^{1}$H NMR ($C_6D_6$, 400 MHz): $\delta$= 9.3 (bs, 12H), 8.14 (d, 12H, *J* = 8.0 Hz), 8.1-7.8 (m, 16H), 7.59 (s, 12H), 7.40 (d, 8H, *J* = 7.2 Hz), 7.31 (d, 20H, *J* = 7.2 Hz), 7.1-7.0 (m, 50H), 6.82 (m, 12H), 6.8-6.6 (m, 10H), 5.07 (s, 2H), 5.01 (s, 5H) 4.60

(d, 12H, *J* = 14.8 Hz), 4.05 (t, 4H, *J* = 6.8 Hz), 4.0-3.8 (m, 30H), 3.7-3.5 (m, 20H), 3.5-3.2 (m, 24H), 2.1 (bs, 4H), 1.8 (bs, 4H) 1.95 (s, 12H), 1.7-0.8 (m, 140H).$^{13}$C NMR (100 MHz): $\delta$= 176.9, 172.0, 153.6, 152.9, 148.2, 148.0, 147.5, 144.4, 143.0, 143.0, 141.1, 140.1, 139.5, 139.2, 138.7, 137.5, 133.8, 132.8, 132.2, 129.5, 129.3, 128.8, 128.7, 128.6, 128.5, 127.9, 127.8, 127.7, 127.6, 127.4, 127.1, 127.0, 126.5, 125.6, 124.9, 121.2, 118.1, 116.7, 72.4, 71.4, 70.0, 66.4, 64.7, 61.6, 60.9, 60.8, 57.3, 57.1, 53.0, 34.6, 32.0, 31.5, 30.8, 30.1, 30.0, 29.9, 29.8, 29.8, 29.7, 29.5, 29.2, 29.1, 28.6, 26.2, 25.8, 22.8, 20.8, 20.7, 15.2, 14.0. HR-MS (ESI, Orbitrap LQ) calculated for $C_{271}H_{333}N_{16}O_{31}S$ m/z (z = 3): 1446.48779 (17), 1446.82298 (63), 1447.15735 (97), 1447.49164 (100), 1447.82582 (81), 1448.15989 (54), 1448.49404 (30), 1448.82857 (13), 1449.16442 (6), 1449.49952 (2).

## References


(1) Bruns, C. J.; Stoddart, J. F. *Nat. Nanotechnol.* **2013**, *8* (1), 9–10.

(2) Witus, L. S.; Hartlieb, K. J.; Wang, Y.; Prokofjevs, A.; Frasconi, M.; Barnes, J. C.; Dale, E. J.; Fahrenbach, A. C.; Stoddart, J. F. *Org. Biomol. Chem.* **2014**, *12* (32), 6089–6093.

(3) Dawson, R. E.; Lincoln, S. F.; Easton, C. J. *Chem. Commun. (Camb).* **2008**, No. 34, 3980–3982.

(4) Du, G.; Moulin, E.; Jouault, N.; Buhler, E.; Giuseppone, N. *Angew. Chem. Int. Ed. Engl.* **2012**, *51* (50), 12504–12508.

(5) Bruns, C. J.; Stoddart, J. F. *Acc. Chem. Res.* **2014**, *47* (7), 2186–2199.

(6) Liu, Y.; Flood, A. H.; Bonvallet, P. a.; Vignon, S. a.; Northrop, B. H.; Tseng, H. R.; Jeppesen, J. O.; Huang, T. J.; Brough, B.; Baller, M.; Magonov, S.; Solares, S. D.; Goddard, W. a.; Ho, C. M.; Fraser Stoddart, J. *J. Am. Chem. Soc.* **2005**, *127* (27), 9745–9759.

(7) Credi, A.; Silvi, S.; Venturi, M. *Molecular Machines and Motors: Recent Advances and Perspectives*; Springer, 2014.

(8) Iordache, A.; Retegan, M.; Thomas, F.; Royal, G.; Saint-Aman, E.; Bucher, C. *Chem. - A Eur. J.* **2012**, *18* (25), 7648–7653.

(9) Duclos, M.; Lemaire, M.; Kahlfuss, C.; Me, E.; Bucher, C.; Oltean, M.; Milet, A. *Comptes Rendus Chim.* **2014**, *17*, 505–511.

(10) Arduini, A.; Ferdani, R.; Pochini, A.; Secchi, A.; Ugozzoli, F. *Angew. Chemie, Int. Ed.* **2000**, *39* (19), 3453–3456.

(11) Arduini, A.; Ciesa, F.; Fragassi, M.; Pochini, A.; Secchi, A. *Angew. Chemie, Int. Ed.* **2005**, *44* (2), 278–281.

(12) Rotzler, J.; Mayor, M. *Chem. Soc. Rev.* **2012**, 44–62.

(13) Rotzler, J.; Drayss, S.; Hampe, O.; Häussinger, D.; Mayor, M. *Chemistry* **2013**, *19* (6), 2089–2101.

(14) Rebilly, J.-N.; Hessani, A.; Colasson, B.; Reinaud, O. *Org. Biomol. Chem.* **2014**, *12* (39), 7780–7785.

(15) Strutt, N. L.; Zhang, H.; Giesener, M. A.; Lei, J.; Stoddart, J. F. *Chem. Commun.* **2012**, *48* (11), 1647–1649.

(16) Gonzalez, J. J.; Ferdani, R.; Albertini, E.; Blasco, J. M.; Arduini, A.; Pochini, A.;

Prados, P.; De Mendoza, J. *Chem. - A Eur. J.* **2000**, *6* (1), 73–80.

(17) Arduini, A.; Bussolati, R.; Credi, A.; Pochini, A.; Secchi, A.; Silvi, S.; Venturi, M. *Tetrahedron* **2008**, *64* (36), 8279–8286.

(18) Credi, A.; Dumas, S.; Silvi, S.; Venturi, M.; Arduini, A.; Pochini, A.; Secchi, A. *J. Org. Chem.* **2004**, *69* (18), 5881–5887.

(19) Schalley, C. *Analytical Methods in Supramolecular Chemistry*; Wiley-VCH Verlag GmbH & Co. KGaA: Weinheim, Germany, 2006.

(20) El Alaoui, A.; Schmidt, F.; Monneret, C.; Florent, J.-C. *J. Org. Chem.* **2006**, *71* (26), 9628–9636.

(21) Clavel, C.; Romuald, C.; Brabet, E.; Coutrot, F. *Chemistry* **2013**, *19* (9), 2982–2989.

(22) Romuald, C.; Ardá, A.; Clavel, C.; Jiménez-Barbero, J.; Coutrot, F. *Chem. Sci.* **2012**, *3* (6), 1851.

(23) Boccia, A.; Lanzilotto, V.; Di, C. V.; Zanoni, R.; Pescatori, L.; Arduini, A.; Secchi, A. *Phys. Chem. Chem. Phys.* **2011**, *13* (10), 4452–4462.

(24) Arduini, A.; Bussolati, R.; Credi, A.; Faimani, G.; Garaudee, S.; Pochini, A.; Secchi, A.; Semeraro, M.; Silvi, S.; Venturi, M. *Chem. - A Eur. J.* **2009**, *15* (13), 3230–3242.

(25) Tatsuta, K.; Nakagawa, A.; Maniwa, S.; Kinoshita, M. *Tetrahedron Lett.* **1980**, *21* (15), 1479–1482.

(26) Neve, F.; Crispini, A.; Loiseau, F.; Campagna, S. *J. Chem. Soc. Dalt. Trans.* **2000**, No. 9, 1399–1401.

(27) Burns, D. H.; Chan, H.; Miller, J. D.; Jayne, C. L.; Eichhorn, D. M. *J. Org. Chem.* **2000**, *65* (17), 5185–5196.

(28) Fear, E. J. P.; Thrower, J.; Veitch, J. *J. Chem. Soc.* **1958**, 1322.

# CHAPTER 4

# Synthesis by Ring Closing Metathesis and Properties of Electroactive Calix[6]arene [2]Catenanes

# Chapter 4

# Synthesis by Ring Closing Metathesis and Properties of Electroactive Calix[6]arene [2]Catenanes

## 4.1 Introduction

In view of our current interest in the development of new calix[6]arene-based devices, we envisaged that the structural and chemical information stored in the three-phenylureido calix[6]arene **1** and the possibility to control the threading rate and direction of the viologen axles,[1] validated with the synthesis of oriented pseudorotaxanes and rotaxanes, could be exploited for the preparation of catenanes with the perspective to construct stimuli responsive unidirectional rotary motors.[2] In spite of the scientific interest, since only few examples of these mechanically interlocked systems have been reported in literature so far (Figure 1).[3–5]

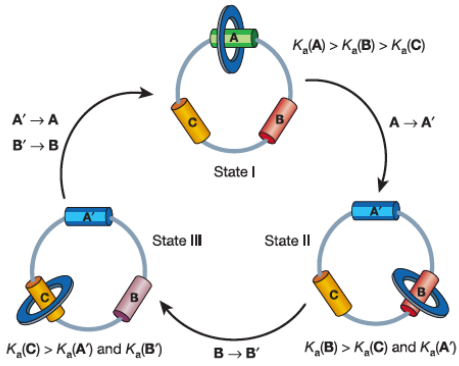


**Figure 1.** Stimuli-induced sequential movement of a macrocycle between three different binding sites in a [2]catenane. Reprinted with permission from ref. 2. Copyright © Nature Publishing Group.

The idea to use a calix[6]arene as component for catenane synthesis was pursued by Neri and co-workers, who have recently reported the synthesis of the first example of [2]catenanes in which the calix[6]arene macrocycle is one of the rings of the interlocked molecule (Figure 2).[6] The synthetic strategy adopted for the catenation step consisted in the reaction of a α,ω di-isocyanate with the terminal OH groups of the axial component of a preformed calix[6]arene-based pseudorotaxane.

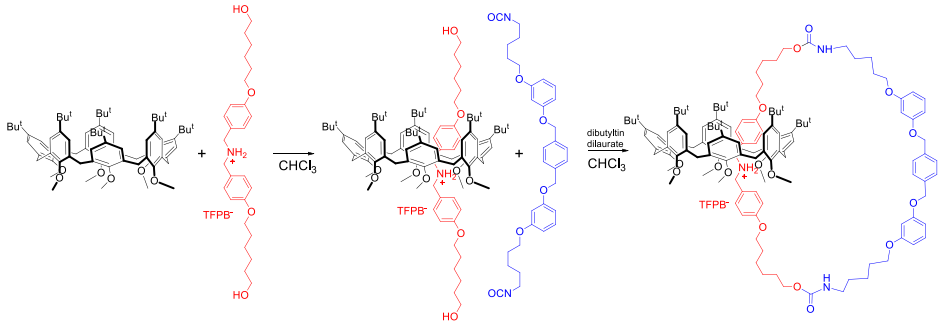


**Figure 2.** The first example of through-the-annulus catenated calixarene (calix[2]catenane), obtained by exploiting the "superweak anion" approach that allows the threading of the calix cavity with functionalized dialkylammonium axles. Reprinted with permission from ref. 6. Copyright © American Chemical Society.

In this chapter, the synthesis of two tris(*N*-phenylureido) calix[6]arene-based [2]catenanes by using the synthetic strategy of an intra-molecular Ring Closing Metathesis (RCM) between the two alkene groups present at the termini of the axial component on a preformed pseudorotaxane will be discussed. The synthesis of the first [2]catenane presented in this chapter is a preliminary study on the possibility to adopt RCM as suitable reaction to obtain a catenane. In the second calix[6]arene-based [2]catenane, the use of an asymmetric viologen axle, together with its unidirectional threading into **1** (Scheme 2), gave the possibility to obtain a non-symmetric catenane. As working hypothesis, the insertion of an asymmetric element in the catenated ring could promote a unidirectional rotation of the components after electrochemical stimulation.

## 4.2 Design and Synthesis of the Axle

Simple molecular modelling studies indicated that a suitable length of the axle bearing two alkene functions at its termini for the catenation reaction around **1** should not be shorter than 40 carbon atoms. In addition, the following requirements must be present in the axle: *i*) the dicationic viologen unit is mandatory for the molecular recognition at the basis of the formation of a very stable pseudorotaxane complex with the calixarene wheel; *ii*) the alkyl chains appended to the viologen core must bear a $\omega$-alkene function, necessary for the RCM; *iii*) these $\omega$-alkenyl chains should be long enough to allow the intramolecular RCM reaction, but not too long in order to minimize its intermolecular oligomerization processes. On the basis of these considerations, axle **5**•2TsO, whose 4,4'-bipyridyl unit is alkylated at both ends with $C_{12}$ chains bearing a *p*-allyloxy hydroquinone unit at their termini, was synthesized as depicted in Scheme 1. The alkylating agent **4** was obtained by reacting 4-(allyloxy)phenol **2** with dodecane-1,12-diyl bis(4-methylbenzenesulfonate) **3** in refluxing acetonitrile. 4,4'-bipyridine was then reacted with a large excess of **4** to yield **5**•2TsO in 45%yield overall.

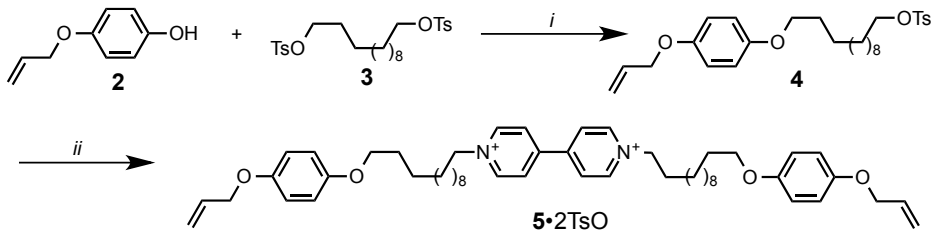


**Scheme 1.** Reagents and conditions: *i*) $K_2CO_3$, $CH_3CN$, reflux, 24h, 63%; *ii*) 4,4'-bipyridyl, $CH_3CN$, reflux, 4 days, 72%.

The capability of the calix[6]arene wheel **1** to form a pseudorotaxane with axle **5**•2TsO was then evaluated by equilibrating a $10^{-2}$ M solution of **1** in $C_6D_6$ for two hours at room temperature in the presence of a large excess of the axle as a solid salt. After

filtration of the deep red suspension to remove the excess of undissolved salt, a series of NMR experiments were carried out to confirm the formation of the pseudorotaxane **1⊃5**•2TsO (Scheme 2). According to previous studies on analogue systems,[7,8] the presence of several diagnostic signals in the NMR spectra confirms the formation of a stable pseudorotaxane complex, which is in slow exchange on the NMR timescale. In particular, the $^1$H NMR spectrum of the complex **1⊃5**•2TsO (Figure 3b) shows that the hydrogen-bonding interactions between the ureido groups of the wheel with the tosylate counter ions of the axle induce a significant downfield shift for the N–H signal (resonances *i*+*h* in Figure 3b, see also Scheme 2 for protons' labelling). Another indication of the inclusion of the axle into the wheel is given by the shift at lower fields of the methoxy groups at the lower rim of the calix[6]arene macrocycle that upon axle threading are expelled from the calixarene cavity and resonate as a sharp singlet downfield shifted of about $\Delta\delta$= 0.6 ppm (resonance *e*, Figures 3a and 3c).

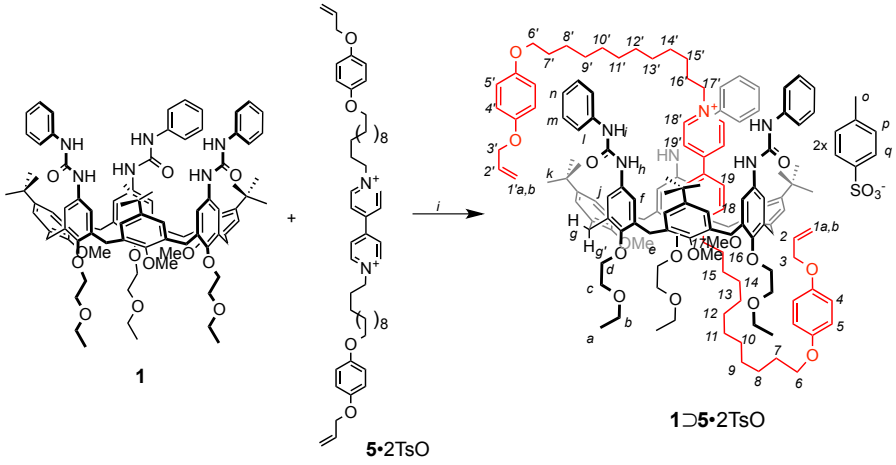


**Scheme 2.** Reagents and conditions: i) 1, toluene, r.t., 2h;

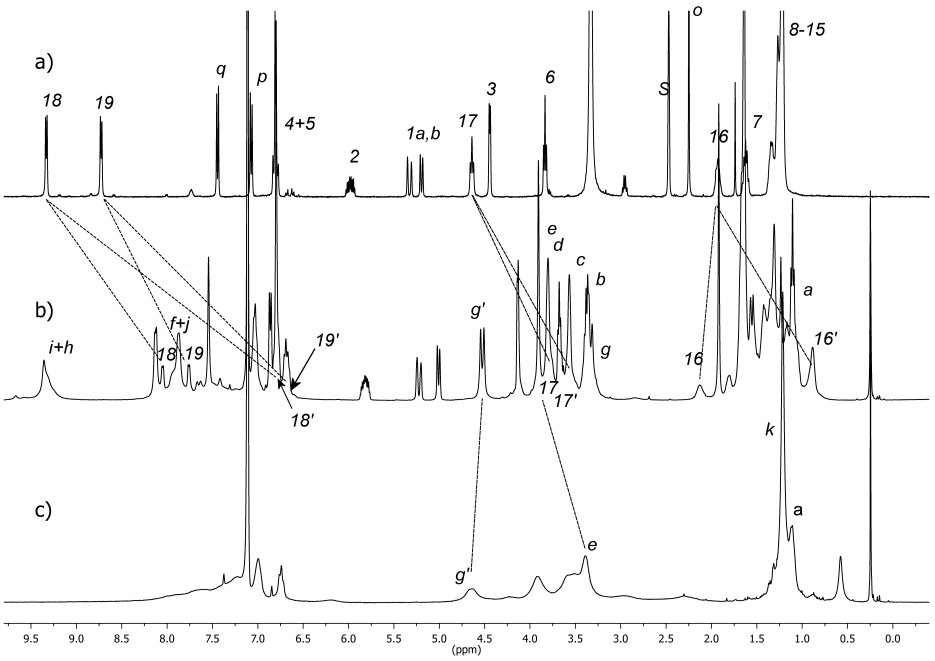


**Figure 3.** $^{1}$H NMR (400 MHz) stack plot of a) **5**•2TsO in DMSO-*d6*, b) pseudorotaxane **1⊃5**•2TsO in $C_6D_6$, and c) wheel **1** in $C_6D_6$ showing the most important protons assignments (for protons labels see Scheme 2).

As expected, the presence of the axle inside the calixarene cavity results in the rigidification of the calixarene skeleton as evidenced, for example, by the resonances of the bridging methylene groups of the calixarene that resonate as two doublets at $\delta$= 3.4 and $\delta$= 4.5 ppm for the six *pseudo*-equatorial and six *pseudo*-axial protons, respectively, with a coupling constant of $J$= 14.8 Hz (resonances *g* and *g'*, Figures 3b and 3c). In the $^{1}$H NMR spectral region between $\delta$= 5.0 and $\delta$= 6.0 ppm of **1⊃5**•2TsO (Figure 3b) the signals of the two alkene terminal groups of the axle resonate as a typical terminal vinyl group and are only slightly shifted as consequence of their orientation with respect to the two distinct rims of the calixarene wheel, as confirmed by the comparison of their chemical shift with that of the unthreaded **5**•2TsO (resonances *1a,b* and *2*, Figures 3a and 3b). On the contrary, the protons of the two chains bonded to the viologen unit of the axial component in **1⊃5**•2TsO undergo an up-field shift of about $\Delta\delta$=1.9-1.3 ppm (depending on their position along the alkyl

chain and with respect to the calix[6]arene wheel), thus further confirming that the viologen unit is included into the electron-rich cavity of **1** ( resonance 16', Figures 3a and 3b). The complexation of **5**•2TsO was also confirmed by the upfield shift endured by the *N*-$CH_2$ protons *17* and *17*' of the axle caused by the strong shielding effect of the calix[6]arene wheel aromatic cavity ($\Delta\delta$~1 ppm and $\Delta\delta$=1.1 ppm for protons *17* and *17'*, respectively). As expected, the highest up-field shift ($\Delta\delta$~2.8 ppm and $\Delta\delta$= 1.2 ppm) was observed for the resonances belonging to the bis-pyridinium aromatic ring deeply engulfed inside the calix[6]arene cavity (resonance *18'* and *19'*, Figures 3a and 3b).

## 4.3 Synthesis and Characterization of a Symmetric Catenane

The synthesis of catenane **6** was undertaken by initially suspending in toluene **5**•2TsO with **1**. To the deep red homogeneous solution the 1st generation Grubb's catalyst was then added. In order to maximize the intra-molecular reaction, several reaction conditions were explored. Indeed, the concentration of pseudorotaxane **1⊃5**•2TsO and the molar ratio of the catalyst strongly influence the yield of the catenation reaction. In agreement with literature data,[9,10,11] we succeeded in the intra-molecular RCM reaction by keeping the concentration of the pseudorotaxane solution below 1 mM and using a 5% molar ratio of catalyst.

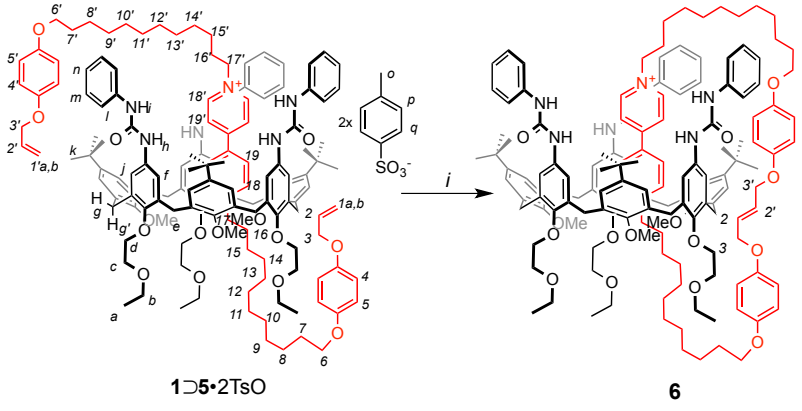


**Scheme 3.** Reagents and conditions: *i*) Grubb's 1st gen. catalyst, toluene, r.t, 24h, 17%.

After 24 hours, a red solid was isolated in moderate yield (15%) and characterized by NMR spectroscopy in $C_6D_6$ and high resolution mass spectrometry (HRMS) that confirmed the formation of catenane **6**. Even if a complete assignment of all protons was not possible because of the extensive overlapping of several signals, particularly in the high field portion of the spectra, in the $^1$H NMR spectrum (Figure 4) the signal of the protons of the olefin terminal methylene groups of the pseudorotaxane disappeared, according to the RCM mechanism that requires the loss of an ethylene molecule during the catalytic cycle. Moreover, the pattern of signals present in this spectrum resembles, under several aspects, that observed in the $^1$H NMR spectrum of pseudorotaxane of **1⊃5**•2TsO, thus suggesting that the catenation of the axle occurred through the annulus of the calix[6]arene.

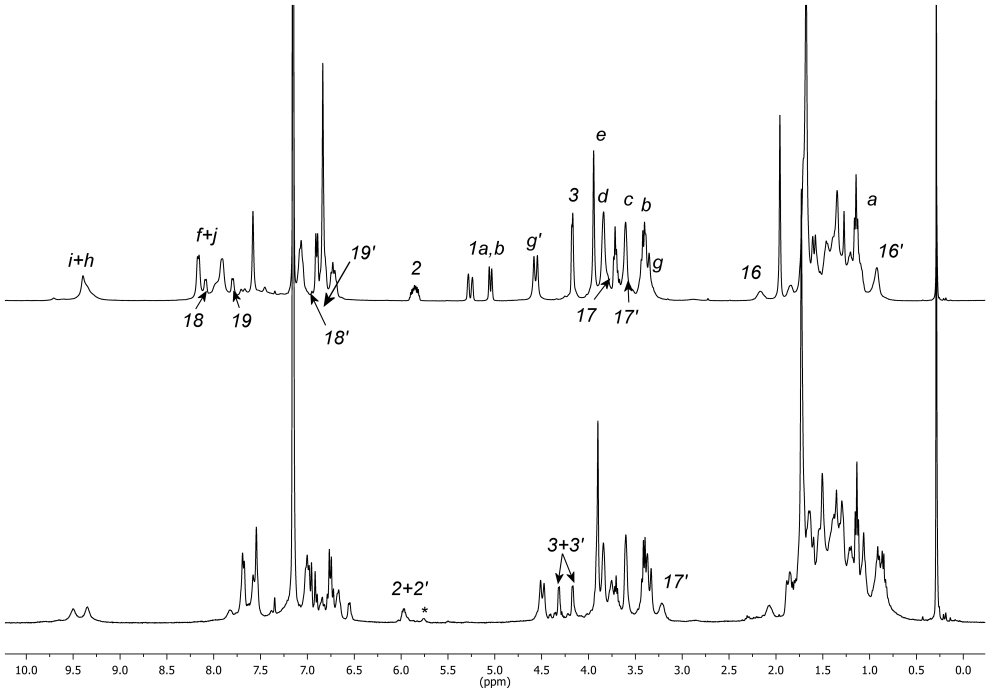


**Figure 4**. $^1$H NMR (400 MHz, $C_6D_6$) stack plot of pseudorotaxane (top) **1⊃5**•2TsO and catenane **6** (bottom). The most important protons assignments are shown on the spectra (for protons labels see Scheme 2 and 3).

HR-MS measurements (ORBITRAP LQ) finally confirmed the formation of catenane **6**. The mass spectrum depicted in Figure 5 shows a very intense doubly charged molecular ion with a monoisotopic peak at m/z = 1113.66953 (see inset of Figure 5).

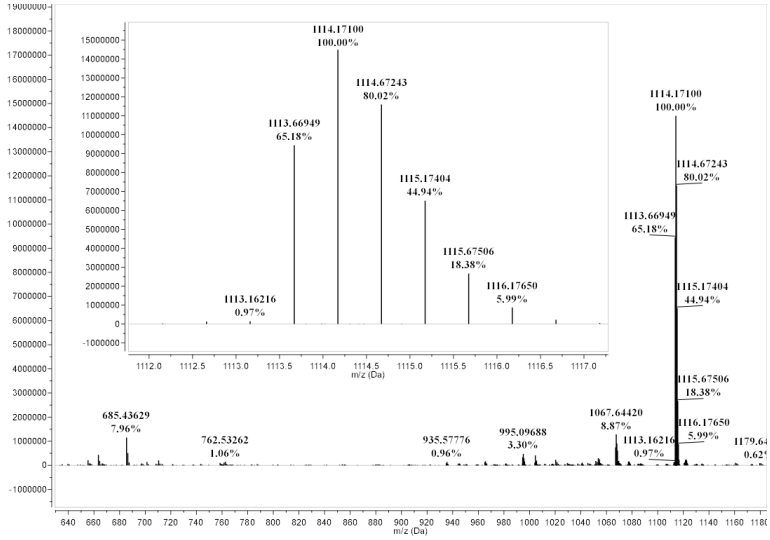


**Figure 5**. High resolution mass spectrum (Orbitrap LQ) of catenane **6**. In the inset is shown the experimental isotope distribution pattern of the doubly charged (z = 2) molecular ion.

## 4.4 Design and Synthesis of an Asymmetric Catenane

The synthetic procedure for the synthesis of catenane **6** was extended to the synthesis of an asymmetric catenane by using **10**•2X as the thread. Axle **10**•2X was synthesized with a sequential approach (Scheme 4); hydroquinone derivative **7** was reacted with dodecane-1,12-diyl bis(4-methylbenzenesulfonate) in refluxing acetonitrile, using $K_2CO_3$ as base, yielding tosylate **8**. This alkylating agent and an excess of 4,4'-bipyridil were refluxed in acetonitrile, to obtain monoalkyl viologen salt **9**•TsO; axle **10**•2X was then obtained refluxing **9**•TsO with an excess of 5-bromo-1-pentene in acetonitrile.

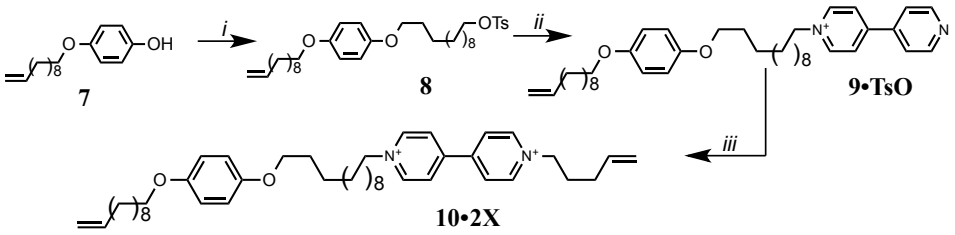


**Scheme 4.** Reagents and conditions: *i*) dodecane-1,12-diyl bis(4-methylbenzenesulfonate) (**3**), $K_2CO_3$, $CH_3CN$, reflux, 48h, 80%; *ii*) 4,4'-bipyridyl, $CH_3CN$, reflux, 18h, 61%; *iii*) 5-Bromo-1-pentene, $CH_3CN$, reflux, 5 days, 60%.

In the $^1$H NMR spectrum of **10•**2X, recorded in $CD_3OD$ (Figure 6), the pyridyl protons *26*, *6'* and *27*, *7'* resonate as two sets of signals at $\delta$= 9.16 and 8.88 ppm, respectively. The signals of protons *25* and *5'* resonate, partially overlapped, at $\delta$= 4.68 ppm while protons *2'* and *2* resonate at $\delta$= 5.81 ppm. Multiplets assignable to protons *1* and *1'* are present between $\delta$= 5.11 and 4.86 ppm, while the aromatic protons of hydroquinone (*12*, *13*) resonate as a sharp singlet at $\delta$= 6.77 ppm.

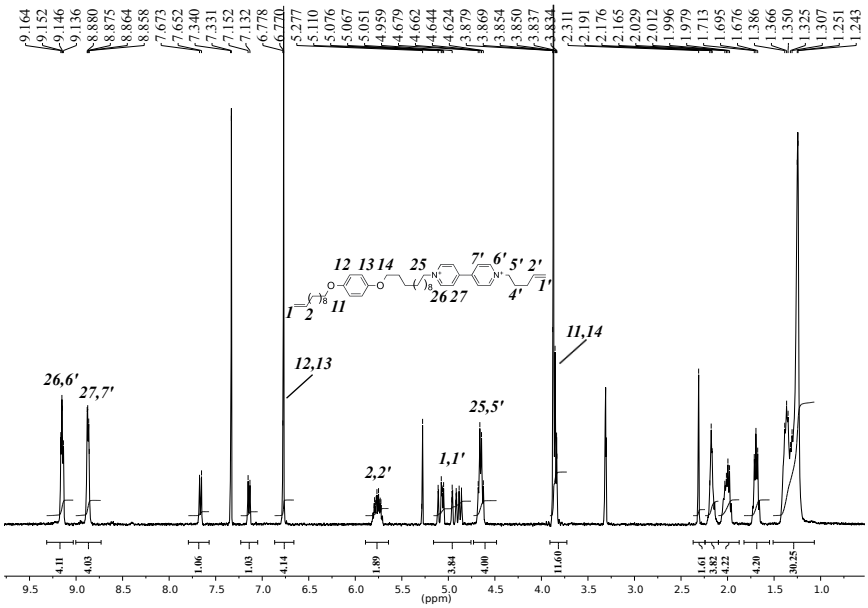


**Figure 6**. $^1$H NMR (400 MHz, MeOD) of **10•**2X. The most important protons assignments are shown on the spectra.

With the objective of verify the hypothesis that the pentene alkyl chain of **10**•2X can act as a kinetic control element during the threading process, wheel **1** and a slight excess of the corresponding axle **10**•2X were equilibrated in $C_6D_6$ at room temperature (Scheme 5).

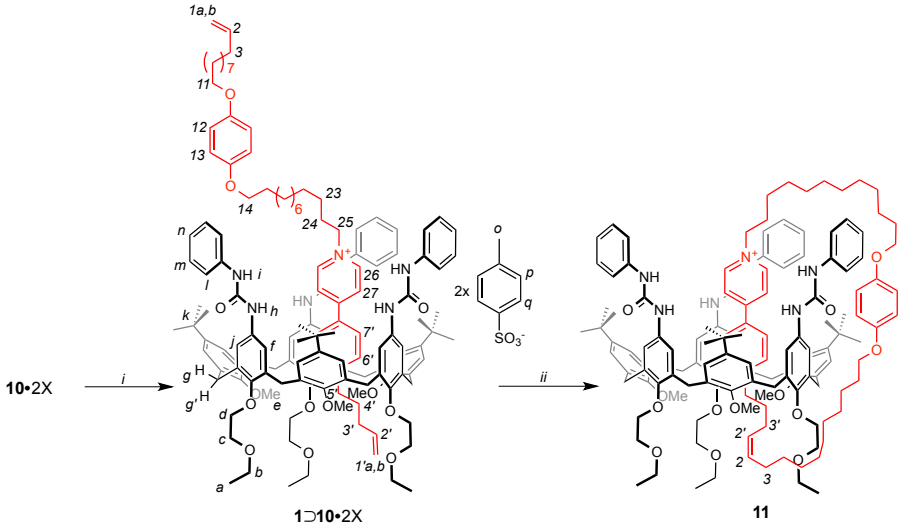


**Scheme 5.** Reagents and conditions: *i*) **1**, toluene, r.t., 2h; *ii*) Grubb's 2nd gen. catalyst, toluene, r.t, 24h, 12%.

The deep red solution, obtained after removal of the excess of undissolved axle, was characterized through NMR techniques. The $^1$H NMR and 2D NMR spectra indicate that only one pseudorotaxane isomer had formed and that the two different alkyl chains appended to the viologen generate two different sets of signals. The inclusion of axle **10**•2X into **1** results in a splitting of the overlapped multiplets of protons *2* and *2'* into two separated multiplets that now resonate at $\delta$= 6.27 and 5.81 ppm for *2* and *2'* respectively (Figure 7). Also protons *1* and *1'* resonate as two separate multiplets at $\delta$= 5.37 and 5.07 ppm respectively (Figure 7b). Protons *24* and *23* resonate at $\delta$= 0.83 and 1.05 ppm because of their confinement in the electron-rich domain of the calix[6]arene, while *3'* and *4'* resonate at $\delta$= 2.42 and 2.15 ppm due to their position right below the lower rim of the wheel. The presence of only one sharp singlet at $\delta$= 3.86 ppm (Figure 7b), for the methoxy groups at the calixarene lower rim, indicates that the guest

threaded **1** only by its shorter alkyl chain.[1] The presence of only one set of signal for the aromatic protons of the axle and for the two different alkyl chains, together with the presence of only one signal assignable to the methoxy groups, suggested the presence of only the orientational pseudorotaxane isomer in which the longer arm of the axle is oriented towards the upper rim of the calixarene wheel.

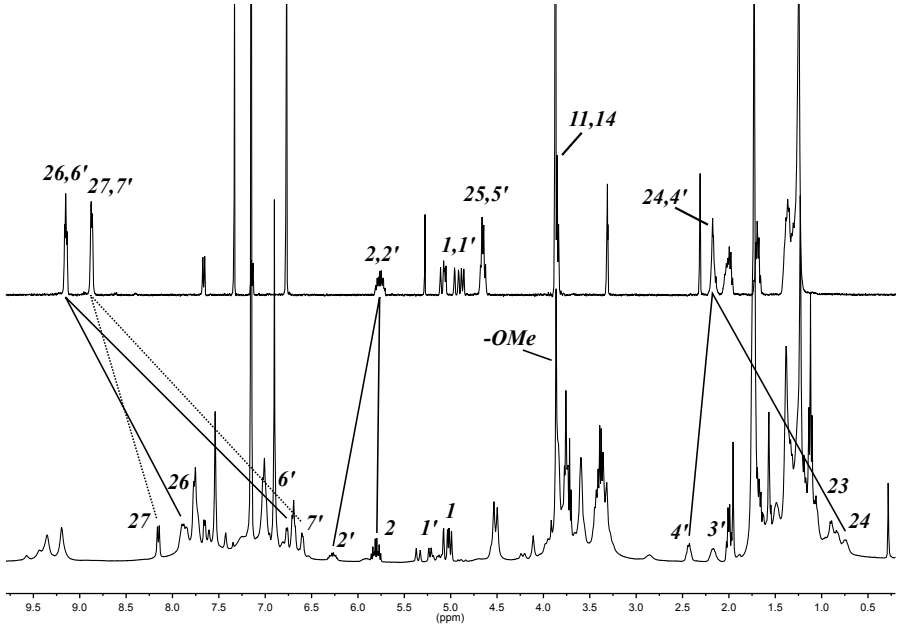


**Figure 7.** $^1$H NMR (400 MHz) stack plot of a) **10**•2X in MeOD and b) pseudorotaxane **1⊃10**•2X in $C_6D_6$ showing the most important protons assignments (for protons labels see Scheme 5).

Catenane **11** was synthesized by equilibrating axle **10**•2X with an equimolar amount of wheel **1** in toluene at room temperature; the concentration of the pseudorotaxane solution was maintained at 1 mM and a 5% molar ratio of 2$^{nd}$ generation Grubb's catalyst was added to the solution. After 24h, catenane **11** was isolated from the mixture in 12% yield and characterized through NMR and MS analysis.

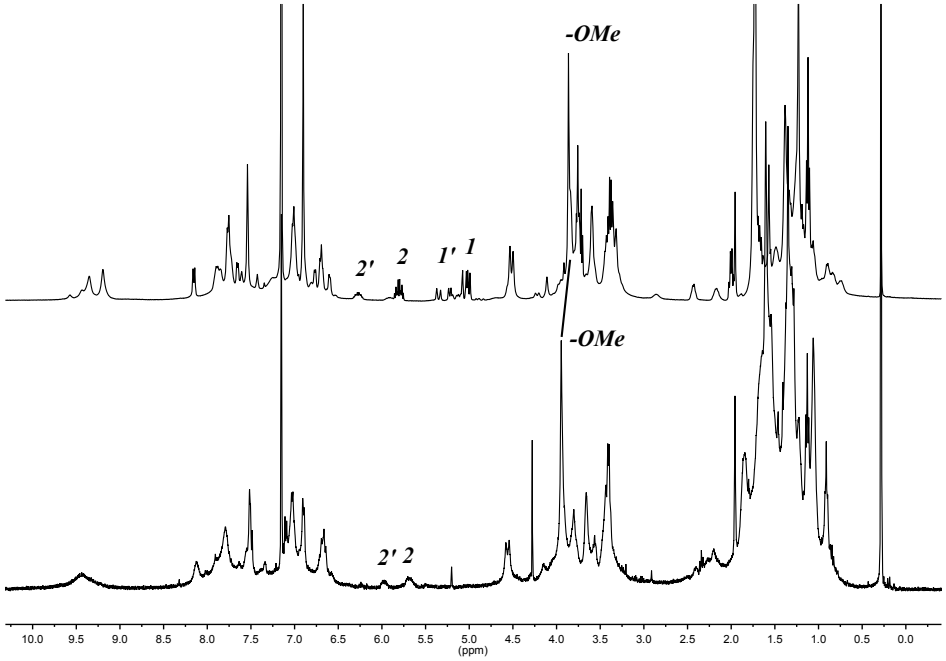


**Figure 8.** $^{1}$H NMR (400 MHz, $C_6D_6$) spectra of pseudorotaxane **1⊃10**•2X (top), and catenane **11**•2X (bottom).

The $^{1}$H NMR spectrum of the isolated red compound evidenced the successful through the calixarene annulus catenation, for example by the loss of protons *1* and *1'*, as expected according to the RCM mechanism that requires the loss of an ethylene molecule during the catalytic cycle (Figure 8). Moreover, the singlet of the methoxy groups of the calixarene undergoes to a shift from $\delta$= 3.86 to 3.95 ppm suggesting that the alkyl chain that now threads **1** is longer respect than in the pseudorotaxane. The intra-molecular catenation of the axle, that generates a long alkyl chain at the lower rim, could explain this event. Furthermore, the pattern of signals present in this spectrum resembles, under several aspects, to that observed in the $^{1}$H NMR spectrum of pseudorotaxane **1⊃10**•2X, thus suggesting that the catenation of the axle ring occurred through the annulus.

Finally, the identity of **11** was confirmed by HR-MS measurements (ORBITRAP LQ); the monoisotopic peak at m/z = 1045.64001 clearly confirms the formation of the

asymmetric catenane (Figure 9). The presence of other intense peaks in the mass spectrum is given by the combination of molecular weight with different counteranions.

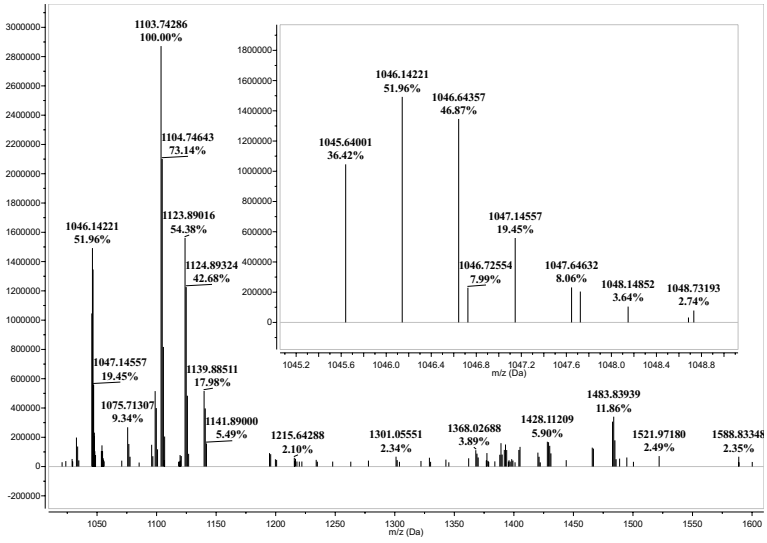


**Figure 9**. High resolution mass spectrum (Orbitrap LQ) of catenane **11**. In the inset is shown the experimental isotope distribution pattern of the doubly charged (z = 2) molecular ion.

## 4.5 Electro- and Photochemical Studies on a [2]Catenane

Electrochemical investigations were initially performed, on Ar-purged acetonitrile solutions, by cyclic and differential pulse voltammetric techniques, on the symmetric catenane **6**; this latter compound shows two reversible monoelectronic reduction processes at –0.60 and –1.13 V versus the standard calomel electrode, SCE (Figure 10), which are assigned to the first and second reduction of the viologen unit. Both reduction potentials are shifted to more negative values with respect to a free viologen-based axle (like a dioctylviologen derivative, for which $E_{1/2}^{I}$ =–0.42 V vs SCE and $E_{1/2}^{II}$ =–0.87 V vs SCE),[12] in analogy with related rotaxane systems.[13]

The shift of the first reduction potential is ascribed to a charge transfer interaction between the viologen moiety and the phenylureido groups on the calixarene upper rim. In related pseudorotaxanes wherein a viologen-based axle is threaded into the calix[6]arene wheel, the second viologen reduction occurs at the same potential observed for the free axle, demonstrating the dissociation of the molecular components upon monoreduction of the viologen unit.[13] In the present system dissociation cannot occur and, indeed, the shift of the second reduction process indicates that no dethreading of the viologen unit takes place after the first reduction and suggests that a residual interaction exists between the viologen radical cation and the calixarene.

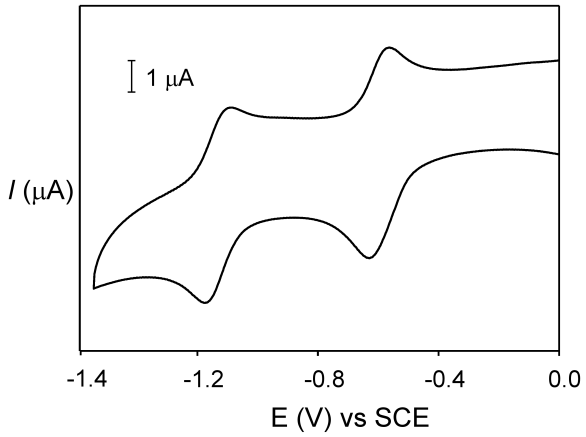


**Figure 10**. Cyclic voltammogram (anodic scan) of an argon-purged acetonitrile solution of catenane **6**. [**6**]=$3\times10^{-4}$ M, [$TEAPF_6$]= $3\times10^{-2}$ M, scan rate 100 mV/s.

Catenane **6** was studied by UV-visible absorption spectroscopy in acetonitrile. The absorption spectrum of the catenane (Figure 11A) shows the bands previously observed in related rotaxanes,[13,14] namely, an intense band in the UV region ($\lambda_{max}$= 260 nm, ε = 86000 $M^{-1}$ $cm^{-1}$) and a weaker band in the visible region ($\lambda_{max}$ = 470 nm, ε = 600 $M^{-1}$ $cm^{-1}$). In particular the latter band is ascribed to the charge transfer interaction between the viologen unit and the calixarene. The monoreduced form of catenane **6** was generated by photocatalytic reduction and subsequently investigated by absorption spectroscopy. An acetonitrile solution of the catenane was irradiated with visible light in the presence of $Ru(bpy)_3^{2+}$ (bpy = 2,2'-bipyridine) as a photosensitizer and

triethanolamine as a sacrificial reductant.[15] The appearance of a sharp band at 400 nm and a broad and structured band between 500 and 800 nm (Figure 11B) confirms the formation of the viologen radical cation. The main difference with respect to the absorption spectrum of a free viologen radical cation is the loss of the vibronic structure of the band at 400 nm in the catenane. This feature can be possibily ascribed to the different environment experienced by the interlocked viologen moiety with respect to a free model compound. In summary, both spectroscopic and electrochemical experiments suggest that, in the mechanically interlocked system, no substantial rearrangement takes place after monoreduction of the viologen unit.

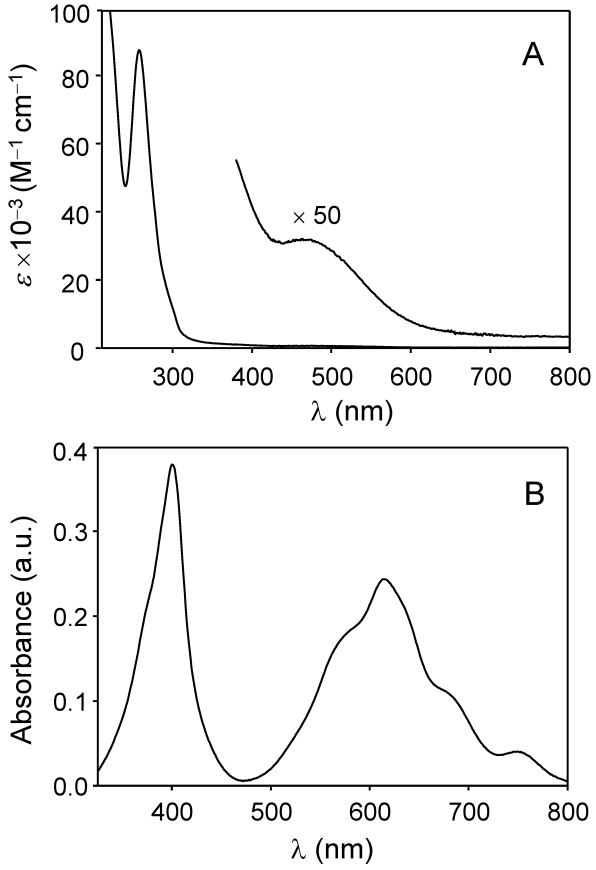


**Figure 11**. (A) Absorption spectrum of **6** in $CH_3CN$, and (B) absorption spectrum of an irradiated ($\lambda$ > 400 nm) solution of **6** ($2\times10^{-4}$ M) in presence of $Ru(bpy_3)^{2+}$ ($3.2\times10^{-4}$ M) and triethanolamine (0.1 M) in $CH_3CN$, obtained upon subtraction of the spectrum of $Ru(bpy_3)^{2+}$ to the spectrum of the irradiated solution.

# 4.6 Conclusions and Perspectives

In this chapter some preliminary studies for the synthesis of a calix[6]arene-based unidirectional rotary rotor were presented. The synthesis of catenane **6** was necessary in order to optimize all the parameters needed for the obtaining of a through the annulus calix[6]arene-based catenane through an intra-molecular RCM reaction. Afterwards, asymmetric catenane **11** was synthesized exploiting the ability of axle **10**•2X to form only one orientational pseudorotaxane isomer when equilibrated with calix[6]arene **1**. Upon electrochemical reduction of the viologen unit, unfortunately, no movement of the wheel along the ring takes place. With the final aim to obtain a unidirectional rotary motor, an additional station, able to induce a shift of the wheel along the ring, after the first reduction of the viologen, need to be inserted on the catenated guest. The synthesis of a catenane bearing an ammonium station in the catenated ring, positioned in proximity of the lower or the upper rim of the calixarene, is actually undergoing in our laboratory.

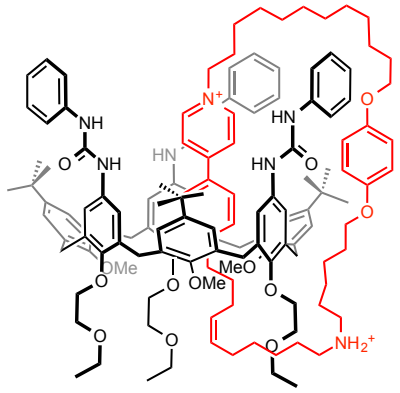


**Figure 12.** Prototype of a calix[6]arene-based [2]catenane able to shuttle from the viologen to the ammonium station upon electrochemical reduction of the bypiridyl function.

# Experimental Section

**Reagents and methods.** All solvents were dried using standard procedures; all other reagents were of reagent grade quality obtained from commercial suppliers and were used without further purification. NMR spectra were recorded at 400 MHz for $^{1}H$ and 100 MHz for $^{13}C$. Melting points are uncorrected. Chemical shifts are expressed in ppm ($\delta$) using the residual solvent signal as internal reference (7.16 ppm for $C_6H_6$; 7.26 ppm for $CHCl_3$, 3.31 for MeOH and 2.50 for DMSO). Mass spectra were recorded in ESI mode. Calix[6]arenes **1**,[16] *p*-allyloxy hydroquinone **2**,[17] dodecane-1,12-diyl bis(4-methylbenzenesulfonate) **3**[18] and *p*-hydroxyphenyl undec-10-en-1-yl ether **7**[19] were synthesised according to published procedures.

**Electrochemical measurements.** Cyclic voltammetric (CV) experiments were carried out at room temperature in argon-purged acetonitrile (Romil Hi-Dry) with an Autolab 30 multipurpose instrument interfaced to a PC. The working electrode was a glassy carbon electrode (Amel; 0.07 $cm^2$); its surface was routinely polished with a 0.3 μm alumina-water slurry on a felt surface. The counter electrode was a Pt wire, separated from the solution by a frit; an Ag wire was employed as a quasi-reference electrode, and ferrocene (Fc) was present as an internal standard ($E_{Fc+/Fc}$ = +0.395 V vs SCE). Ferrocene was added from a concentrated acetonitrile solution (typically 0.1 M). Tetraethylammonium hexafluorophosphate was added as supporting electrolyte. Cyclic voltammograms were obtained at sweep rates varying typically from 0.05 to 1 V $s^{-1}$. The IR compensation implemented within the Autolab 30 was used, and every effort was made throughout the experiments to minimize the resistance of the solution. In any instance, the full electrochemical reversibility of the voltammetric wave of ferrocene was taken as an indicator of the absence of uncompensated resistance effects. Differential pulse voltammograms (DPV) were performed with a scan rate of 20 mV $s^{-1}$, a pulse height of 75 mV, and a duration of 40 ms.

**UV-Visible Spectroscopy and Photochemistry.** Absorption spectra were recorded with a Perkin Elmer Lambda45 spectrophotometer, on air equilibrated acetonitrile

solutions at room temperature (ca. 20°C), with concentrations ranging from $1\times10^{-5}$ to $2\times10^{-4}$ M. Solutions were examined in 1-cm spectrofluorimetric quartz cells. The experimental error on the wavelength values was estimated to be ±1 nm. Photochemical reaction was performed on argon-purged acetonitrile solutions at room temperature (ca. 20 °C), by using a 150 W tungsten halogen lamp equipped with a cutoff filter ($\lambda > 400$ nm). Samples were irradiated in a sealed 1-mm cuvette.

## Synthetic Procedures

**12-[4-(allyloxy)phenoxy]dodecyl tosylate (4)**. In a 250 ml round bottom flask, to a solution of **1** (0.3 g, 0.9 mmol) and dodecane-1,12-diyl bis(4-methylbenzenesulfonate) **3** (1.4 g, 2.7 mmol) in $CH_3CN$ (50 ml), $K_2CO_3$ (0.3 g, 1.8 mmol) was added. The resulting heterogeneous mixture was refluxed for 24 hours. After cooling at room temperature, the solvent was evaporated to dryness under reduced pressure and the sticky residue was taken up with ethyl acetate (100 ml). The resulting organic phase was washed with a 10% w/v solution of HCl (100 ml) and twice with distilled water (2 × 100 ml), then dried with anhydrous sodium sulfate and evaporated to dryness under reduced pressure. The oily residue was purified by column chromatography on silica gel (*n*-hexane/ethyl acetate 8:2) to yield 0.4 g (63%) of product **4** as a white solid. M.p.: 29-30 °C; $^1$H NMR ($CDCl_3$, 400 MHz): $\delta$= 7.82 (d, 2H, $J$ = 6.8 Hz), 7.38 (d, 2H, $J$ = 8.0 Hz), 6.9-6.8 (m, 4H), 6.1-6.0 (bs, 1H), 5.44 (dd, 1H, $J$ = 17.2, 1.6 Hz), 5.30 (dd, 1H, $J$ = 10.4, 1.2 Hz), 4.6-4.5 (m, 2H), 4.06 (t, 2H, $J$ = 6.6 Hz), 3.94 (t, 2H, $J$ = 6.6 Hz), 2.5-2.4 (m, 4H), 1.77 (m, 2H, $J$ = 7.2 Hz), 1.66 (t, 2H, $J$ = 7.2 Hz), 1.6-1.2 (m, 16H); $^{13}$C NMR (100 MHz): $\delta$= 153.4, 152.6, 144.6, 133.6, 133.2, 129.8, 127.9, 117.5, 115.6, 115.3, 70.7, 69.5, 68.6, 29.6, 29.5, 29.4, 28.9, 28.8, 26.1, 25.3, 21.7; MS (ESI): m/z: 511.1 $[M+ Na]^+$.

**Axle 5•2TsO.** A solution of tosylate **4** (1.0 g, 2.0 mmol) and 4,4'-bipyridyl (0.1 g, 0.5 mmol) in $CH_3CN$ (40 ml) was sealed in a 100 ml glass autoclave and refluxed for 4 days. Afterwards, the solution was evaporated to dryness under reduced pressure. The solid residue was triturated with $CH_3CN$ to afford 0.5 g of **5**•2TsO as a white solid

(72%). M.p.: 145-146 °C; $^1$H NMR (DMSO-$d_6$, 400 MHz) $\delta$= 9.38 (d, 2H, $J$ = 6.4 Hz), 8.77 (d, 2H, $J$ = 6.4 Hz), 7.49 (d, 4H, $J$ = 8.0 Hz), 7.12 (d, 4H, $J$= 8.0 Hz), 6.9-6.8 (m, 8H), 6.1-5.9 (m, 2H), 5.39 (d, 2H, $J$ = 17.2Hz), 5.25 (d, 2H, $J$ = 10.4 Hz), 4.70 (t, 4H, $J$ = 7.2 Hz), 4.49 (d, 4H, $J$ = 5.2 Hz), 3.89 (t, 4H, $J$ = 6.2 Hz), 2.29 (s, 6 H), 2.0 (bs, 4H), 1.70 (q, 4H, $J$ = 6.4 Hz), 1.4-1.2 (m, 32H). $^{13}$C NMR (100 MHz): $\delta$= 153.3, 152.6, 146.2, 145.8, 138.0, 134.5, 128.5, 127.1, 126.0, 117.6, 116.0, 115.7, 69.1, 68.3, 29.5, 29.4, 29.2, 28.9, 26.9, 26.0, 25.9, 23.0, 21.2; MS (ESI): m/z: 789.6 $[M-H]^+$.

**Pseudorotaxane 1⊃5•**2TsO**.** In a 50 ml two-necked round bottom flask, calix[6]arene wheel **1** (0.10 g, 0.07 mmol) was dissolved in toluene (20 ml) under nitrogen atmosphere and axle **5•2TsO** (0.08 g, 0.08 mmol) was added. The resulting heterogeneous solution was stirred for two hours at room temperature, during which it gradually turned homogeneous and deep red color. After this period, the solution was filtered and the solvent was evaporated under reduced pressure to obtain **1⊃5•**2TsO as a red solid. $^1$H NMR ($C_6D_6$, 400 MHz) $\delta$= 9.4-9.2 (m, 6H), 8.2-8.0 (m, 6H), 7.9-7.7 (m, 8H), 7.6-7.3 (m, 10H), 7.1 (bs, 8H), 7.0-6.7 (m, 5H), 6.8 (bs, 8H), 6.7-6.6 (m, 4H), 5.9-5.8 (m, 2H), 5.28 (dd, 2H, $J_1$ = 19.0 Hz, $J_2$ = 1.8 Hz), 5.05 (dd, 2H, $J_1$ = 10.5 Hz, $J_2$ = 1.6 Hz), 4.58 (d, 6H, $J$ = 14.8 Hz), 4.2 (m, 4H), 3.94 (s, 9H), 3.8 (bs, 6H), 3.7-3.5 (m, 16H), 3.4-3.3 (m, 16H), 3.06 (q, 4H, $J$ = 6.7 Hz), 2.2 (bs, 2H), 1.96 (s, 6H), 1.8-0.9 (m, 4H,), 1.4-1.2 (m, 76H). $^{13}$C NMR (100 MHz): $\delta$= 153.8, 153.7, 153.5, 153.1, 153.0, 152.8, 148.1, 148.0, 144.4, 143.2, 143.0, 141.2, 139.5, 137.5, 134.0, 133.9, 133.8, 132.2, 129.2, 128.8, 128.7, 127.8, 127.6, 127.0, 126.5, 125.7, 124.7, 121.2, 118.1, 116.8, 116.4, 116.3, 115.7, 115.4, 115.3, 72.4, 70.0, 69.0, 68.2, 68.1, 68.0, 66.3, 60.9, 60.7, 34.6, 31.5, 30.7, 30.0, 29.9, 29.8, 29.8, 29.7, 29.6, 29.5, 29.2, 28.8, 28.4, 26.3, 26.2, 20.8, 15.2; MS (ESI): m/z (z= 2): 1128.3 $[M]^{2+}$.

**Catenane 6.** In a 100 ml rounded bottom flask, pseudorotaxane **1⊃5•**2TsO (0.15 g, 0.07 mmol) was dissolved in toluene (70 ml) and Grubb's 1$^{st}$ generation catalyst (0.004 g, $4.9\times10^{-3}$ mmol) was added. The solution was stirred for 24 h at room temperature. Afterwards, the solution was evaporated to dryness under reduced pressure and the solid residue was purified by column chromatography on silica gel ($CH_2Cl_2$/MeOH

95:5) to yield 0.03 g (17%) of product **6** as a red solid. $^{1}$H NMR ($C_6D_6$, 400 MHz): $\delta$= 9.5 (bs, 3H), 9.3 (bs, 3H), 7.8 (bs, 2H), 7.7-7.3 (m, 16H), 7.0-6.7 (m, 22H), 6.6 (bs, 2H), 6.0 (bs, 2H), 5.8 (bs), 4.51 (d, 6H, $J$ = 15.2 Hz), 4.3 (bs, 4H), 4.2 (bs, 4H), 3.90 (s, 9H), 3.8 (bs, 6H), 3.75-3.70 (m, 8H), 3.6 (bs, 6H), 3.43-3.33 (m, 12H), 3.2 (bs, 3H), 2.1 (bs, 3H), 1.8-0-8 (m, 76H). $^{13}$C NMR (100 MHz): $\delta$= 203.4, 153.9, 153.3, 153.0, 152.8, 148.3, 148.1, 143.8, 142.9, 140.8, 136.8, 133.9, 132.1, 130.4, 129.3, 128.9, 128.7, 127.9, 127.7, 127.6, 127.4, 124.8, 124.2, 121.0, 117.5, 116.4, 115.7, 115.6, 115.2, 72.5, 67.0, 68.4, 68.1, 68.0, 67.7, 67.5, 66.3, 61.3, 61.0, 60.7, 59.7, 38.8, 35.5, 34.9, 34.7, 32.0, 31.6, 31.3, 30.5, 29.8, 29.8, 29.7, 29.5, 29.3, 29.0, 28.9, 28.8, 28.5, 27.9, 26.8, 26.7, 26.3, 26.2, 26.1, 25.9, 25.5, 23.8, 23.0, 22.8, 15.2, 14.0, 13.9, 10.8. HR-MS (ESI, Orbitrap LQ) calculated for $C_{140}H_{178}N_8O_{16}$ m/z (z = 2): 1113.66749 (63), 1114.16920 (100), 1114.67065 (80), 1115.17236 (43), 1115.67390 (17), 1116.17532 (6), 1116.67704 (2); found: 1113.66953 (64), 1114.17106 (100), 1114.67233 (78), 1115.17409 (43), 1115.67513 (18), 1116.17654 (6), 1116.67879 (1).

**12-(4-(undec-10-en-1-yloxy)phenoxy)dodecyl 4-methylbenzenesulfonate (8)**. In a 250 ml round bottom flask, to a solution of *p*-hydroxyphenyl undec-10-en-1-yl ether (**7**) (0.5 g, 1.9 mmol) and dodecane-1,12-diyl bis(4-methylbenzenesulfonate) **3** (3.0 g, 5.7 mmol) in $CH_3CN$ (100 ml), $K_2CO_3$ (0.5 g, 3.8 mmol) was added. The resulting heterogeneous mixture was refluxed for 48 hours. After cooling at room temperature, the solvent was evaporated to dryness under reduced pressure and the sticky residue was taken up with ethyl acetate (100 ml). The resulting organic phase was washed with a 10% w/v solution of HCl (100 ml) and twice with distilled water (2 × 100 ml), then dried with anhydrous sodium sulfate and evaporated to dryness under reduced pressure. The oily residue was purified by column chromatography on silica gel (*n*-hexane/dichloromethane 6:4) to yield 0.4 g (80%) of product **8** as a white solid. M.p. = 66-68 °C; $^{1}$H NMR ($CDCl_3$, 400 MHz): $\delta$ = 7.82 (d, 2H, $J$ = 7.6 Hz), 7.37 (d, 2H, $J$ = 8.0 Hz), 6.84 (s, 4H), 5.9-5.8 (m, 1H), 5.04 (d, 1H, $J$ = 16.8 Hz), 4.96 (d, 1H, $J$ = 10.4 Hz), 4.06 (t, 2H, $J$ = 6.4 Hz), 3.93 (t, 2H, $J$ = 6.6 Hz), 2.47 (s, 3H), 2.07 (q, 2H, $J$ = 7.2 Hz), 1.8-1.2 (m, 34H); $^{13}$C NMR (100 MHz): $\delta$ = 153.2, 139.2, 133.3, 129.8, 127.9,

115.4, 114.1, 70.7, 68.7, 33.8, 29.5, 29.4, 29.3, 29.1, 28.9, 28.8, 26.0, 25.3, 21.6; MS (ESI): m/z: 601.2 $[M+ H]^+$, 623.2 $[M+ Na]^+$.

**Salt 9•TsO.** In a 100 ml round-bottomed flask, a solution of 12-(4-(undec-10-en-1-yloxy)phenoxy)dodecyl 4-methylbenzenesulfonate (0.2 g, 0.3 mmol) and 4,4'-dipyridyl (0.2 g, 1.3 mmol) in $CH_3CN$ (50ml) was refluxed for 18h. Then, the solvent was evaporated at reduced pressure and the residue obtained was triturated with EtOAc (2x 20 ml) until the product precipitated as a solid compound and was recovered by suction filtration to afford 0.15 g of product **10** as a white solid (61%). M.p. = 89-90°. $^1$H NMR (400MHz, $CD_3OD$): $\delta$ = 9.12 (d, 2H, *J* = 5.6 Hz), 8.85 (d, 2H, *J* = 5.2 Hz), 8.52 (d, 2H, *J*= 5.6 Hz), 8.00 (d, 2H, *J*= 5.2 Hz), 7.73 (d, 2H, *J*= 7.6 Hz), 7.25 (d, 2H, *J*= 8.0 Hz), 6.82 (s, 4H), 5.9-5.7 (m, 1H), 5.04 (d, 1H, *J* = 17.2 Hz), 4.70 (t, 2H, *J* = 7.6 Hz), 3.92 (t, 4H, *J* = 6.6 Hz), 2.38 (s, 3H), 2.07 (m, 4H, *J* = 7.2 Hz), 1.76 (m, 4H, *J* = 7.2 Hz), 1.5-1.3 (ms, 28H). $^{13}$C NMR (100 MHz) $\delta$ =150.4, 142.2, 140.2, 138.7, 128.4, 125.7, 125.5, 122.1, 115.1, 115.0, 113.3, 68.2, 33.5, 31.0, 29.2, 29.1, 29.0, 28.8, 28.7, 28.6, 25.7, 19.9; MS (ES): m/z: 585.3 $[M- TsO]^+$.

**Axle 10•2X.** In a sealed 100 ml glass autoclave, a solution of **9•TsO** (0.3 g, 0.4 mmol) and 5-Bromo-1-pentene (0.2 g, 1.2 mmol) in $CH_3CN$ (30 ml) was refluxed for 5 days. Afterwards, the solution was cooled to 70°C; the precipitate was separated from the solution by suction filtration to afford 0.8 g of product **10•2X** as a yellow solid (60%). M.p. = 196-198°. $^1$H NMR (MeOD, 400 MHz) $\delta$ = 9.1-9.0 (m, 4H), 8.8-8.7 (m, 4H), 7.60 (d, 1H, *J*= 8.4 Hz), 7.08 (d, 1H, *J*= 8.0 Hz), 6.70 (s, 4H), 5.8-5.6 (m, 2H), 5.0-4.9 (m, 2H), 4.9-4.8 (m, 2H), 4.6-4.5 (ms, 4H), 2.24 (s, 1.5H), 2.1 (bs, 4H), 2.0-1.9 (m, 4H), 1.66 (m, 4H, *J* = 7.2 Hz), 1.3-1.1 (ms, 28H). $^{13}$C NMR (100 MHz): $\delta$ = 153.1, 149.3, 145.6, 139.1, 135.3, 128.8, 127.8, 125.6, 117.0, 115.4, 113.9, 77.5, 77.4, 77.2, 76.8, 68.7, 62.4, 61.6, 49.5, 49.3, 49.0, 48.8, 48.6, 48.4, 48.2, 33.7, 31.4, 30.2, 29.8, 29.4, 29.3, 29.24, 29.0, 28.9, 28.8, 26.1, 25.9, 21.1. MS (ESI): m/z: 327.4$[M]^{2+}$.

**Pseudorotaxane 1⊃10•2X.** In a 50 ml two-necked round bottom flask, calix[6]arene wheel **1** (0.10 g, 0.07 mmol) was dissolved in toluene (20 ml) under nitrogen

atmosphere and axle **10•2X** (0.07 g, 0.08 mmol) was added. The resulting heterogeneous solution was stirred for two hours at room temperature, during which it gradually turned homogeneous and deep red color. After this period, the solution was filtered and the solvent was evaporated under reduced pressure to obtain **1⊃10•**2X as a red solid. $^1$H NMR ($C_6D_6$, 400 MHz) $\delta$ = 9.4-9.2 (m, 6H), 8.16 (d, 2H, $J$ = 7.6 Hz), 7.9-7.7 (m, 8H), 7.6-7.3 (m, 10H), 7.1 (bs, 8H), 7.0-6.7 (m, 5H), 6.9 (bs, 4H), 6.7-6.6 (m, 4H), 6.3 (bs, 1H), 5.8-5.7 (m, 1H), 5.37 (d, 1H, $J$ = 17.2 Hz), 5.3-4.9 (m, 4H), 4.53 (d, 6H, $J$ = 14.8 Hz), 3.86 (s, 9H), 3.8 (bs, 12H), 3.7-3.5 (m, 6H), 3.4-3.3 (m, 18H), 2.4 (bs, 2H), 2.2 (bs, 2H), 1.99 (q, 2H, $J$ = 7.6 Hz), 1.96 (s, 2H), 1.8-0.9 (m, 42H,), 0.9-0.7 (m, 6H); MS (ESI): m/z (z= 2): 1060.2 $[M]^{2+}$.

**Catenane 11.** In a 100 ml rounded bottom flask, pseudorotaxane **1⊃10•**2X (0.2 g, 0.13 mmol) was dissolved in toluene (100 ml) and Grubb's 2$^{nd}$ generation catalyst (0.01 g, $6.5\times10^{-3}$ mmol) was added. The solution was stirred for 24 h at room temperature. Afterwards, the solution was evaporated to dryness under reduced pressure and the solid residue was purified by column chromatography on silica gel ($CH_2Cl_2$/MeOH 95:5) to yield 0.03 g (12%) of product **11** as a red solid. $^1$H NMR ($C_6D_6$, 400 MHz) $\delta$ = 9.4 (bs, 6H), 8.1 (bs, 2H, $J$ = 7.6 Hz), 7.9-7.7 (m, 8H), 7.6-7.3 (m, 10H), 7.1 (bs, 8H), 7.0-6.7 (m, 5H), 6.9 (bs, 4H), 6.7-6.6 (m, 4H), 6.0 (bs, 1H), 5.7 (bs, 1H), 4.58 (d, 6H, $J$ = 14.4 Hz), 3.95 (s, 9H), 3.8 (bs, 12H), 3.7-3.5 (m, 6H), 3.4-3.3 (m, 18H), 2.4-2.0 (m, 6H), 1.8-0.7 (m, 46H); $^{13}$C NMR (100 MHz): $\delta$ = 153.4, 152.7, 148.2, 148.1, 146.3, 144.5, 143.0, 142.9, 141.0, 140.9, 140.4, 134.0, 132.2, 129.1, 126.5, 121.1, 117.9, 116.7, 115.6, 115.0, 72.6, 67.0, 68.0, 66.4, 62.2, 61.2, 61.1, 58.0, 54.9, 53.0, 34.5, 32.0, 31.5, 29.8, 29.6, 29.5, 29.1, 28.0, 26.8, 26.3, 26.0, 25.3, 22.7, 20.7, 15.2, 14.0. HR-MS (ESI, Orbitrap LQ) calculated for $C_{132}H_{170}N_8O_{14}$ m/z (z = 2): 1045.64001 (36), 1046.14221 (52), 1046.64357 (47), 1047.14557 (19), 1047.64632 (8), 1048.14852 (4), 1048.68464 (1).

## References:


(1) Arduini, A.; Bussolati, R.; Credi, A.; Secchi, A.; Silvi, S.; Semeraro, M.; Venturi, M. *J. Am. Chem. Soc.* **2013**, *135* (26), 9924–9930.

(2) Arduini, A.; Bussolati, R.; Credi, A.; Monaco, S.; Secchi, A.; Silvi, S.; Venturi, M. *Chem. - A Eur. J.* **2012**, *18* (50), 16203–16213.

(3) Hernández, J. V; Kay, E. R.; Leigh, D. A. *Science* **2004**, *306* (5701), 1532–1537.

(4) Leigh, D. A.; Wong, J. K. Y.; Dehez, F.; Zerbetto, F. *Nature* **2003**, *424* (6945), 174–179.

(5) Kelly, T. R.; De Silva, H.; Silva, R. A. *Nature* **1999**, *401* (6749), 150–152.

(6) Gaeta, C.; Talotta, C.; Mirra, S.; Margarucci, L.; Casapullo, A.; Neri, P. *Org. Lett.* **2013**, *15* (1), 116–119.

(7) Arduini, A.; Calzavacca, F.; Pochini, A.; Secchi, A. *Chem. - A Eur. J.* **2003**, *9* (3), 793–799.

(8) Arduini, A.; Ferdani, R.; Pochini, A.; Secchi, A.; Ugozzoli, F. *Angew. Chemie, Int. Ed.* **2000**, *39* (19), 3453–3456.

(9) Kidd, T. J.; Leigh, D. A.; Wilson, A. J. *J. Am. Chem. Soc.* **1999**, *121* (7), 1599–1600.

(10) Weck, M.; Mohr, B.; Sauvage, J.-P.; Grubbs, R. H. *J. Org. Chem.* **1999**, *64* (15), 5463–5471.

(11) Guidry, E. N.; Cantrill, S. J.; Stoddart, J. F.; Grubbs, R. H. *Org. Lett.* **2005**, *7* (11), 2129–2132.

(12) Ballardini, R.; Credi, A.; Gandolfi, M. T.; Giansante, C.; Marconi, G.; Silvi, S.; Venturi, M. *Inorganica Chim. Acta* **2007**, *360* (3), 1072–1082.

(13) Credi, A.; Dumas, S.; Silvi, S.; Venturi, M.; Arduini, A.; Pochini, A.; Secchi, A. *J. Org. Chem.* **2004**, *69* (18), 5881–5887.

(14) Arduini, A.; Bussolati, R.; Credi, A.; Pochini, A.; Secchi, A.; Silvi, S.; Venturi, M. *Tetrahedron* **2008**, *64* (36), 8279–8286.

(15) Semeraro, M.; Secchi, A.; Silvi, S.; Venturi, M.; Arduini, A.; Credi, A. *Inorganica Chim. Acta* **2014**, *417*, 258–262.

(16) Casnati, A.; Domiano, L.; Pochini, A.; Ungaro, R.; Carramolino, M.; Oriol Magrans, J.; M. Nieto, P.; López-Prados, J.; Prados, P.; de Mendoza, J.; G. Janssen, R.; Verboom, W.; N.Reinhoudt, D. *Tetrahedron* **1995**, *51* (46), 12699–12720.

(17) Gautier, A.; Mulatier, J.-C.; Crassous, J.; Dutasta, J.-P. *Org. Lett.* **2005**, *7* (7), 1207–

1210.

(18) Fear, E. J. P.; Thrower, J.; Veitch, J. *J. Chem. Soc.* **1958**, 1322.

(19) Ornelas, C.; Méry, D.; Cloutet, E.; Ruiz Aranzaes, J.; Astruc, D. *J. Am. Chem. Soc.* **2008**, *130* (4), 1495–1506.

# CHAPTER 5

# Electrochemical Response of the Threading-Dethreading Process of Calix[6]arene-based Pseudorotaxanes Anchored on Glassy Carbon Electrodes

# Chapter 5

# Electrochemical Response of the Threading-Dethreading Process of Calix[6]arene-based Pseudorotaxanes Anchored on Glassy Carbon Electrodes

## 5.1 Introduction

During these last decades, the tremendous advance in the comprehension of molecular recognition processes has allowed the transfer of the principles and methods of Supramolecular Chemistry to the construction of new nanodevices and functional materials by supporting Host-Guest systems onto solid surfaces.[1–3] Relatively less explored is how the functioning mode of a prototype of molecular machine is affected by its anchoring on a solid support or by the nature of the solid support.[4] This is particularly true in those cases where these systems should operate under the action of electrochemical stimulation and the nature of the interaction between the anchored active coating and the solid support can, unpredictably, modify the response. Cooke an co-workers, for example, reported that the reversibility of an electrochemically responsive pseudorotaxane self-assembled monolayer (SAM) obtained by anchoring tetrathiafulvalene derivatives on gold is significantly and adversely modified with respect to that observed in solution,[5] while Beer et al. reported that redox-active bis-ferrocenyl rotaxanes, exploited in solution for chemical sensing, maintain their property when organized as SAMs on gold electrodes (Figure 1).[6] On the other hand, in

a related work, the same authors reported that a [2]catenane, able to selectively bind chloride ions in solution, looses its binding properties when anchored to a gold electrode.[7]

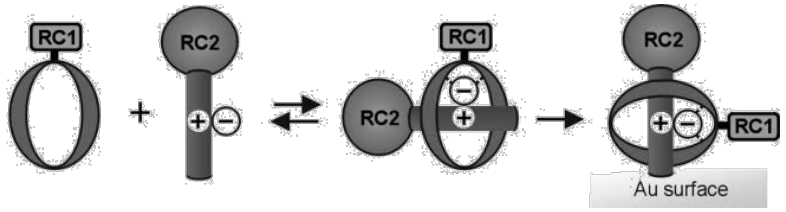


**Scheme 1**. Example reported by Beer and co-workers of a redox-active rotaxane SAM formation on Au by surface stoppering (RC = redox centre). Reprinted with permission from ref. 7. Copyright © Royal Society of Chemistry.

Some of us evidenced that the ability of tris(*N*-phenylureido) calix[6]arene derivatives to act as a three-dimensional heteroditopic receptors[8,9] that are able to form oriented pseudorotaxanes and rotaxanes with viologen salts is substantially unaffected when anchored on Si(100)[10] and polycrystalline Cu surfaces.[11] Furthermore, the electrochemically external stimuli promoted threading/de-threading working mode was unaffected by the nature of the inorganic surface.[12] The formation of these pseudorotaxane-based systems was also exploited for the assembly of gold nanoparticles on functionalized Si(100) surfaces.[13]

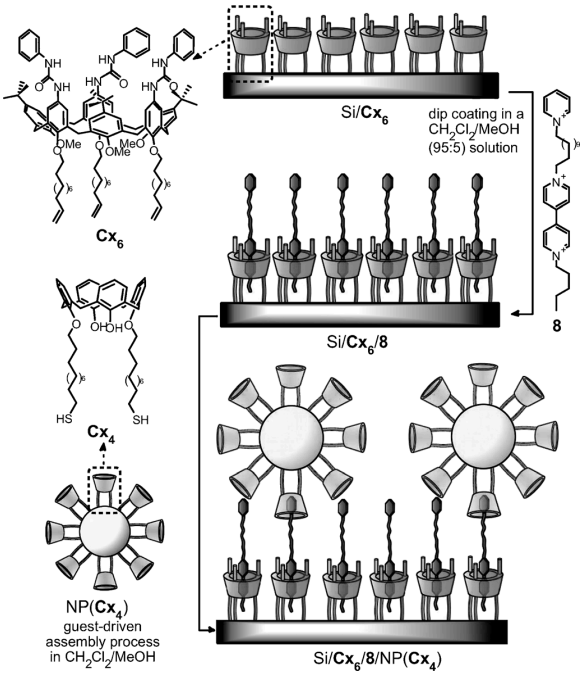


**Scheme 2**. Schematic representation of the formation of pseudorotaxane complexes at the interface between a Si (100) surface coated with calix[6]arene-based "wheels" **Cx6** and the viologen-based "axle" present in $CH_2Cl_2$/MeOH.

Glassy Carbon (GC) electrodes have been quite extensively studied as support for the anchoring of active coatings in view of analytical applications.[14,15] On the other hand, in spite of the very high electrical conductivity of GC, its stability in a wide potential windows, the possibility to directly monitor the extent of their functionalization with redox active species and the electrochemical properties conferred by the monolayer, to the best of our knowledge, no studies have been so far reported on the role of GC surface as supporting matrix on the working mode of prototype of molecular machines based on pseudorotaxanes and rotaxanes.

In this chapter, a study aimed at evaluating the electrochemical response of calix[6]arene-based pseudorotaxanes and rotaxanes supported on GC electrodes is presented.

# 5.2 Design and Synthesis of Calix[6]arene Derivatives Suitable for GC Electrodes Modification

Within the techniques available for the grafting of organic monolayers at GC surfaces,[16–19] the oxidation of primary amines at carbon electrodes represents one of the most efficient and versatile approaches.[20] It consists in the electrochemical generation of an amidyl radical at the primary amine functional group by scanning the potential of the working electrode within a precise potential window. The radical generated is then able to covalently attach to the exposed graphitic sheets that constitute the electrode surface. The advantages of such technique are: the stability of the C-N bond, the possibility to form closely packed monolayers and the introduction on solid substrates of functional groups which allow further modification through solid phase synthesis techniques (SPPS).[21]

The first method considered to covalently attach calix[6]arene derivatives to glassy carbon electrodes was to electrograft the three-amino compound **9** (Figure 1) through the oxidation of amine functions presents at the lower rim of the macrocycle.

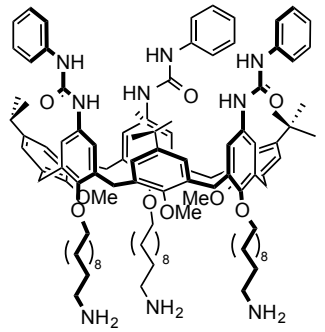


**9**

**Figure 1.** Calix[6]arene derivative (**9**) selected for the electrografting on GC electrode.

Wheel **9** was obtained with a convergent synthetic approach (see Scheme 3); the alkylating agent **4** was synthesized starting from 11-aminoundecan-1-ol (**2**), yielded following literature procedures;[22] the primary amine function was then reacted with di-

tert-butyl dicarbonate to obtain **3** in a high yield reaction. The corresponding alcohol was reacted with an excess of *p*-toluenesulfonyl chloride to obtain tosylate **4**; afterwards, this alkylating agent was used in excess to functionalise the phenolic groups at the lower rim of the known calix[6]arene derivative **5**,[23] to yield **6**. This reaction was carried out in refluxing acetonitrile, using potassium carbonate as base. The three nitro groups of **6** were quantitatively reduced to amino using hydrazine monohydrate as reducing agent and Pd/C as catalyst in refluxing methanol. The resulting triamino derivative **7** was then reacted with an excess of phenylisocyanate in dry dichloromethane to insert the phenylureido moieties on the upper rim, yielding product **8**. Finally, the three Boc protecting groups were quantitatively removed using a large excess of trifluoroacetic acid (TFA) in dichloromethane to obtain final product **9** with 21% overall yield.

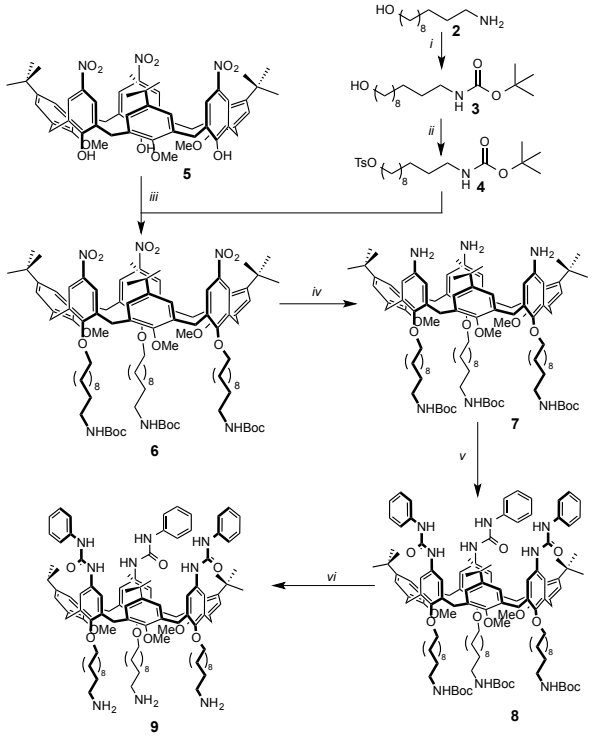

**Scheme 3.** Reagents and Conditions: *i*) di-*tert*-butyl dicarbonate, $NEt_3$, THF, r.t., 16h, 94%; *ii*) Tosyl Chloride, $NEt_3$, DMAP, $CH_2Cl_2$, r.t., 5h, 72% *iii*) $K_2CO_3$, $CH_3CN$, reflux, 72h, 32%; *iv*) $NH_2NH_2 \cdot H_2O$, Pd/C, MeOH, reflux, 6h, 98%; *v*) $C_6H_5NCO$, $CH_2Cl_2$, r.t., 2h, 69%; *vi*) TFA, $CH_2Cl_2$, r.t., 1h.

The $^{1}$H NMR spectrum (Figure 2), taken in $CDCl_3$, confirms the identity of the molecule showing the absence of signals relative to the Boc protecting groups. The presence of broad signals evidenced the high conformational mobility of this host in chloroform solution. Mass spectrometry, performed in the ESI-MS mode, exhibited a signal at m/z = 879.8, assignable to the doubly charged molecular weight.

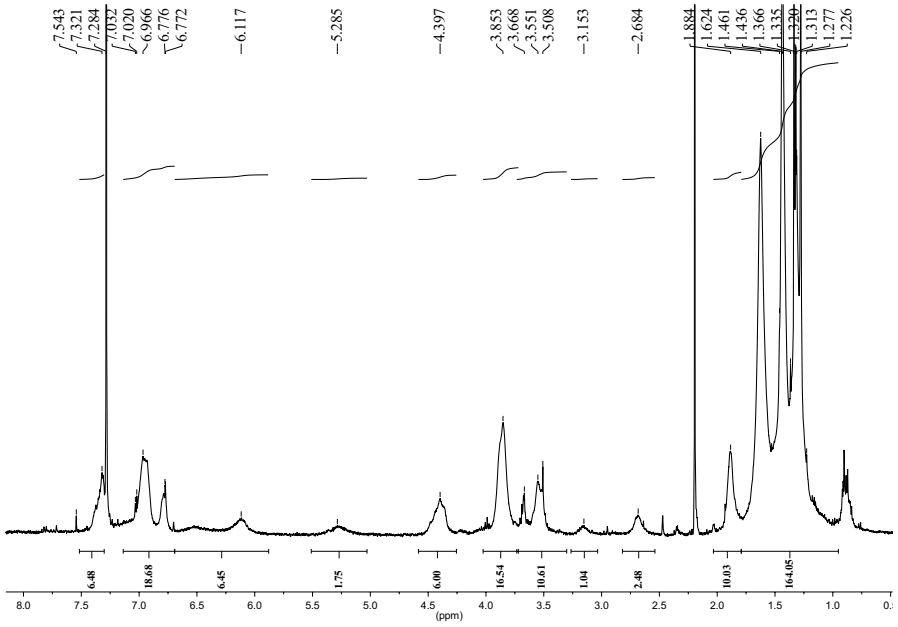


**Figure 2.** $^{1}$H NMR (400 MHz) of **9** in $CDCl_3$.

With the aim to functionalise glassy carbon electrodes through electrochemical oxidation of the three amino groups of derivative **9**, the newly obtained calixarene was dissolved in acetonitrile/water (10% $NaHCO_3$) 8:2. The presence of hydrogen carbonate anion was essential to deprotonate the amine moieties of **9**. Unfortunately, calix[6]arene **9** was not soluble at these conditions, rendering this strategy inapplicable. Therefore, an alternative strategy for the functionalization of GC electrode was imagined; it consisted in the formation of a monolayer through the electrografting of a monoprotected diamine linker; a subsequent removal of the protecting group opens the possibility to modify the electrode through solid phase synthesis techniques (SPPS).[20,24]

Freshly polished GC electrodes were then modified with a uniform amine monolayer by cycling 5 times the potential of the electrode in the range 0.2 to 1.95 V vs Ag/AgCl, in a 20 mM solution of *N*-Boc-ethylenediamine (Boc-EDA) in acetonitrile with 0.1M tetrabutylammonium tetrafluoroborate (TBATFB) as supporting electrolyte, using the meniscus configuration.[25] Since no reduction peaks are present, the irreversible oxidation of the amine is evidenced, suggesting that the radical cations generated undergo to a very fast reaction, with the GC surface or with other radical cations to obtain oligomer molecules. The radical decreasing of the anodic current in the following cycles gives a response about the kind of reaction developed by the amine radical cation; indeed, since the amine covalently link the carbon surface and form a layer on the electrode, a passivation on the conductivity of the electrode occurs (Figure 3). After the functionalization, the electrodes were rinsed with bi-distilled water, acetonitrile and left dry in air.

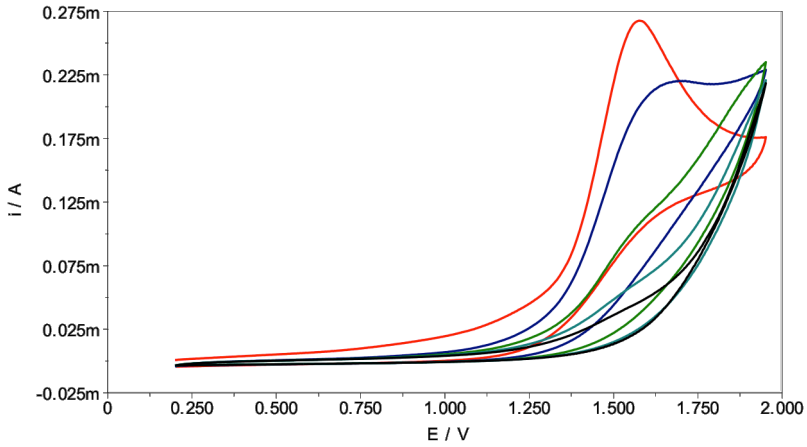


**Figure 3.** Cyclic voltammograms (5 scans) recorded in a 0.1 M TBATFB solution containing 20 mM Boc-EDA in $CH_3CN$, 5 scans from 0.2 to 1.95 V vs Ag/AgCl at a scan rate of 50 mV $s^{-1}$. First cycle (red), second cycle (blue), third cycle (green), fourth cycle (light blue) and fifth cycle (black) are displayed.

In order to generate reactive sites on the electrode organic layer, the Boc group of mono-grafted Boc- EDA was removed immersing the electrode in a 4M solution of HCl in 1,4-dioxane. After 1h stirring at room temperature, the electrode was rinsed

with water and acetonitrile. After the removal of the Boc group in acidic conditions, the electrode was available for further covalent functionalization using the diamine linker as anchoring point (Scheme 4). Among the possible covalent bonds that an amine function may form, the amide bond is the most robust and resistant; this functional group could be obtained reacting the mono-grafted EDA linker with a ω-carboxylic acid alkyl chain.

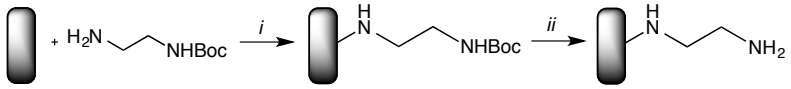


**Scheme 4.** Reagents and Conditions: *i*) 0.1 M TBATFB solution containing 20 mM Boc-EDA in $CH_3CN$, 5 scans from 0.4 to 1.95 V vs Ag/AgCl; *ii*) HCl 4M in 1,4-dioxane.

Since in the calix[6]arene wheel the two distincts domains able to actively bind viologen salts are at the upper rim, namely the three phenylureas and the electron-rich calixarene cavity, the insertion of three ω-undecanoic chains was established at the lower rim in order to favour the threading of the axle into the calix[6]arene annulus: the recognition sites need to be oriented toward the solution when the wheel is anchored to the electrode. Furthermore, long undecyl alkyl chains were selected as spacer between the electron-rich cavity and the electrode in order to avoid any possible effect of the GC surface on the formation/decomplexation processes of the pseudorotaxanes (Figure 4).

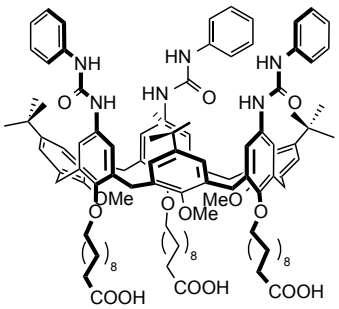


**15**

**Figure 4.** Calix[6]arene derivative (**15**) selected for the immobilization on GC electrode.

Wheel **15** was obtained with a synthetic strategy depicted in Scheme 5, starting from a tris(nitro) calix[6]arene (**5**) and 11-bromoundecanoic acid (**10**). Calix[6]arene derivative **12** was synthesised refluxing in acetonitrile **5** and alkylating agent **11**, obtained from the esterification of 11-bromoundecanoic acid with t-butanol in tetrahydrofuran using trifluoroacetic anhydride as activating agent. The three nitro groups of **12** were quantitatively reduced to amino using hydrazine monohydrate as reducing agent and Pd/C as catalyst in refluxing methanol. The resulting triamino derivative **13** was then reacted with an excess of phenylisocyanate in dry dichloromethane to insert the phenylureido moieties at the upper rim, yielding product **14**. Finally, product **15** was obtained, in an overall yield of 27%, by quantitatively hydrolysing the t-butyl esters with a large excess of trifluoroacetic acid in dichloromethane.

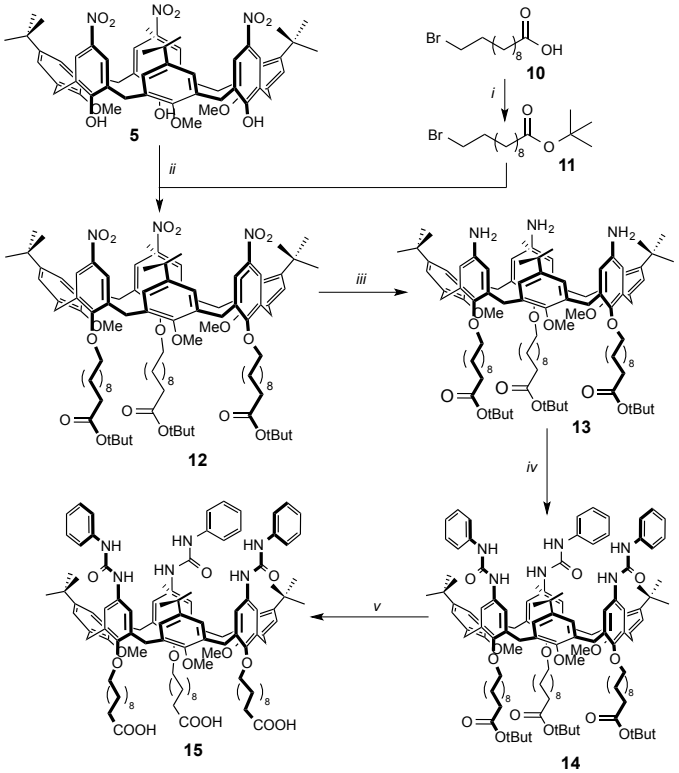


**Scheme 5.** Reagents and Conditions: *i*) trifluoroacetic acid, t-butanol, THF, 0°C to r.t., 16h, 87%; *ii*) $K_2CO_3$, $CH_3CN$, reflux, 72h, 54%; *iii*) $NH_2NH_2 \cdot H_2O$, Pd/C, MeOH, reflux, 6h, 98%; *iv*) $C_6H_5NCO$, $CH_2Cl_2$, r.t., 2h, 71%; *v*) TFA, $CH_2Cl_2$, r.t., 1h, 83%.

The structure of **15** was established through MS and NMR analysis. In particular, the $^1$H NMR spectrum, carried out in $CDCl_3$, showed that the calix[6]arene macrocycle adopts, on the NMR time-scale, a pseudo cone conformation in which the three alternate aromatic rings of the macrocycle decorated with the phenylureido groups define a trigonal prism, while the remaining phenolic units are tilted, orienting their relative methoxy groups inside the electron-rich cavity of the macrocycle. For this reason, in the $^1$H-NMR spectrum of **15** (Figure 5), the signal associated to the methoxy protons is characterised by a significant broadness and it is up-field shifted ($\delta$ = 2.9 ppm) compared to the expected chemical shift (ca. 3.8 ppm). Further diagnostic signals are the two doublets at $\delta$= 4.4 and 3.6 ppm ($J$ = 14.4 Hz) assigned to the bridging methylene units of the aromatic rings. Mass spectrometry experiments in the ESI-MS mode confirmed the identity of the molecule exhibiting a mass peak at 1825.7 m/z for the adduct formed by **15** and $Na^+$.

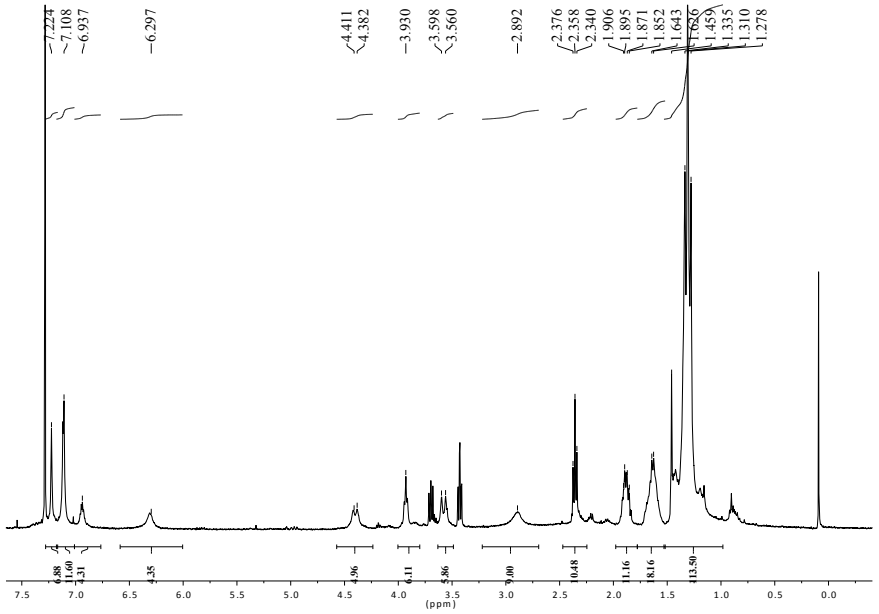


**Figure 5.** $^1$H NMR (400 MHz) of **15** in $CDCl_3$.

# 5.3 Modification of Glassy Carbon Electrodes with Pseudorotaxane Systems

The covalent binding of **15** onto GC electrodes, depicted in Scheme 6, was achieved dipping a series of amino modified electrodes in a solution of calixarene **15** in DMF with 1-Ethyl-3-(3-dimethylaminopropyl)carbodiimide (EDC) and *N*-Hydroxysuccinimide (NHS), very common coupling agents frequently used in the solid phase synthesis strategies.

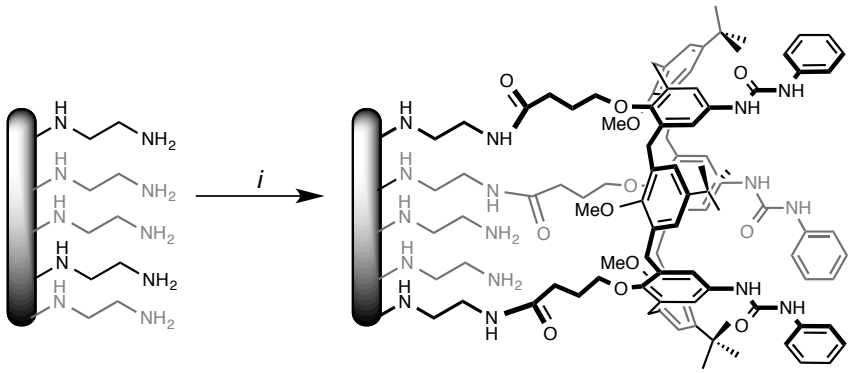


**Scheme 6.** Reagents and Conditions: *i*) **15**, EDC, NHS, DMF, r.t., 16h.

Since **15** is non-redox active, it resulted impossible to characterise and quantify the species at the surface by direct cyclic voltammetry. In order to monitor the interfacial changes occurring at the GC surface after the sequential modifications, a cyclic voltammogram in a 0.1 M KCl solution containing 5 mM $K_3[Fe(CN)_6]$ after each synthetic step was recorded. Figure 6 shows the comparison of the CVs recorded: the intensity of the redox peak at $E_{mp}$ = 0.2 V vs $Ag/Ag^+$, associated with the $Fe^{2+}/Fe^{3+}$ couple is highly affected by the variation of the thickness of the organic layer attached to the electrode surface. The decreasing of redox peak on the dot-dashed line, corresponding to the electrodes modified with compound **15**, suggested that the coupling reaction had worked and a full monolayer of the calix[6]arene was formed (Figure 6).[26]

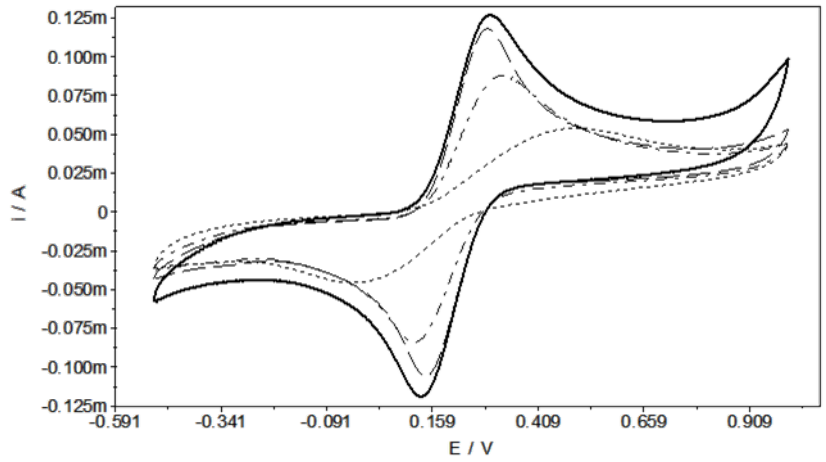


**Figure 6.** Cyclic voltammograms recorded at a scan rate of 100 mV $s^{-1}$ with the modified GC electrode in 0.1 M KCl solution containing 5 mM $K_3[Fe(CN)_6]/K_4[Fe(CN)_6]$ (1:1) for: bare GC electrode (solid), after electrochemical modification with EDA-Boc (dotted), after deprotection with HCl 4M in dioxane (dashed) and after attachment of calixarene **15** (dot-dashed).

A further proof of the successful electrode modification was obtained by electrochemical impedance spectroscopy (EIS) measurements.[27] The EIS response was analysed by means of a classical Randles equivalent circuit and fitted using the Autolab FRA software. Modifying the nature of the coating layer, a substantial alteration of the resistance inferred to the electrode was established (Figure 7). Starting with a resistance value of 258 Ω for a bare GC electrode, after the complete functionalization of the surface, we calculated an increased resistance value of 339 Ω for the modified electrode. The small variation of this value is probably due to the steric hindrance of derivative **15**, that prohibits to the calixarene to constitute a dense layer on the electrode.

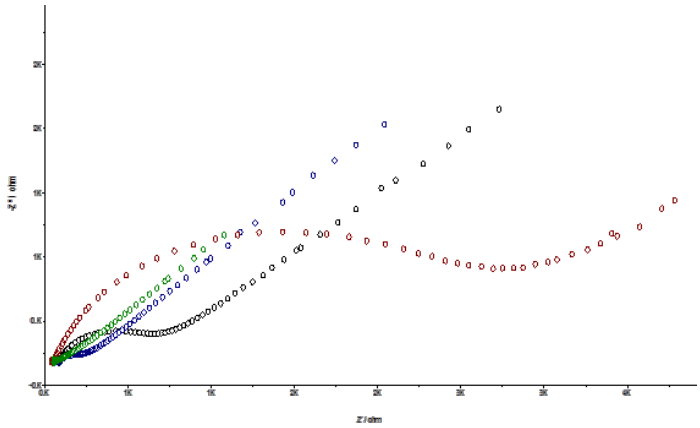

**Figure 7.** Nyquist plots of electrochemical impedance spectra obtained at glassy carbon electrode in the presence of 5 mM $K_3Fe(CN)_6$ electrochemical probe + 0.1 M KCl aqueous solution for: bare (green), EDA-Boc functionalised (red), Boc removed (blue) and calixarene **15** modified (black) electrode . Fixed potential of 220 mV ± 10 mV within the frequency range of 0.1 to $10^6$ Hz.

Electrochemical studies on the behaviour of pseudorotaxanes formed by tris(*N*-phenylureido) calix[6]arenes and dialkylviologen salts in solution have been previously reported in literature.[28] In order to have reference values for pseudorotaxanes and evaluate their behaviour in different experimental conditions, the CVs of free **DOV**•2TsO and **1⊃DOV**•2TsO in solution were first recorded (Figure 8).

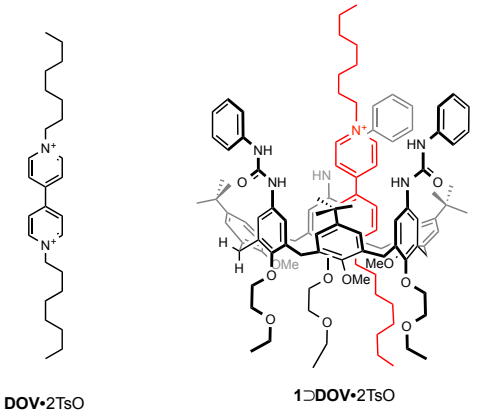

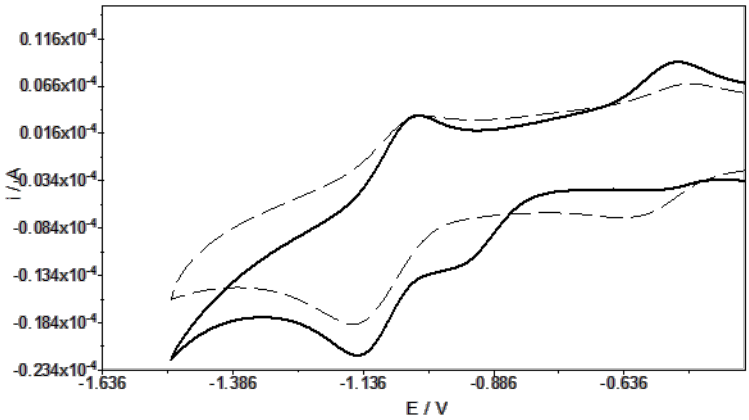


**Fig 8.** Cyclic voltammograms recorded at a scan rate of 100 mV $s^{-1}$ in a 0.1M $TBAPF_6$ solution in dichloromethane of a 5 mM solution of **DOV•**2TsO with (solid) or without (dashed) wheel **1**.

The middle peak potentials ($E_{1/2}$) associated to the redox peaks were calculated according to equation 1:

$$E_{1/2} = (E^a + E^c)/2 \quad \text{(Eq. 1)}$$

Consistently with previous results, the viologen included in the calix[6]arene cavity presented a shift of the $E_{1/2}$ of the first redox peak by about 160 mV to lower potentials compared to the free axle, due to the stabilization induced by the electron-rich cavity of **1**. The peaks associated to the second redox process present the same $E_{1/2}$ for both species, suggesting that there is no more interaction between the wheel and the axle after the first reduction step.

Once the anchoring of derivative **15** on GC electrode was confirmed, we decided to test its ability to generate pseudorotaxane with dialkyl viologen axles. The GC electrode modified with **15** was immersed in a 1 mM solution of **DOV•**2TsO in DCM/MeOH 95:5; the small percentage of methanol was required to solubilise the guest and to limit the amount of adsorbed material at the electrode during the complexation process. The properties of these systems formed at the surface were studied through cyclic voltammetry. The CVs recorded (Figure 9) revealed that

**DOV•**2TsO was included in the calixarene cavity, as indicated by the $E_{1/2}$' shifting to lower potentials by 100 mV compared to the free guest in solution. After the first reduction the radical cation specie of **DOV•**2TsO apparently dethreads from the cavity, since $E_{1/2}$'' is comparable to the value obtained performing CV to the free guest in solution.

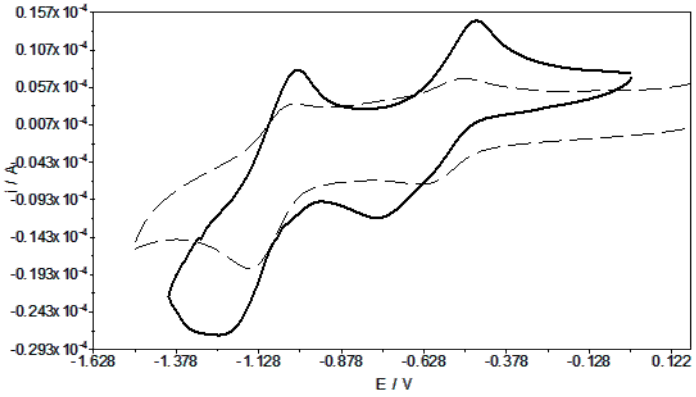


**Fig 9.** Cyclic voltammograms recorded at a scan rate of 100 mV $s^{-1}$ in a 0.1M $TBAPF_6$ solution in dichloromethane of a 5 mM solution of **DOV•**2TsO (dashed) and modified GC electrodes (solid).

The threading/dethreading process of the pseudorotaxane is only partially reversible, as suggested by the clear changes in the redox peaks, which occurred by increasing the scan number (see Figure 10). After four scans, the dissociation of the complex on the surface is complete, as demonstrated by the disappearance of its relative reduction peak in the CV, while the only reduction peaks present are relative to the free guest in solution. Such non reversibility of the pseudorotaxane formation could be explained by considering the diffusion processes occurring: the guest, after reduction and the consequent dethreading, is dispersed in the bulk solution and, once oxidised, the re-complexation process is not favoured.

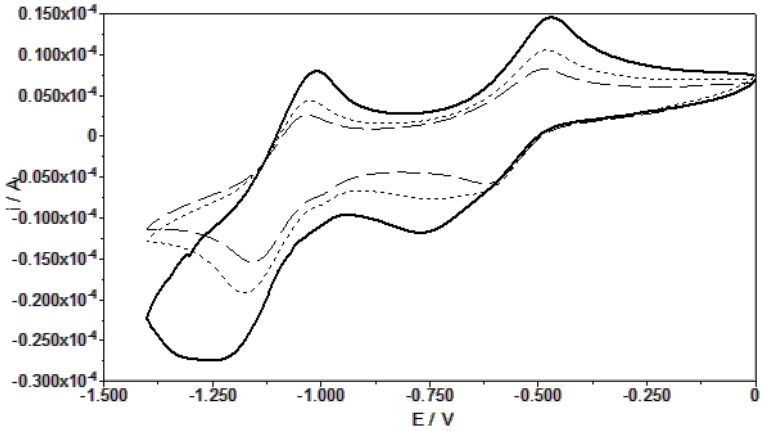


**Fig 10.** Cyclic voltammograms recorded at a scan rate of 100 mV $s^{-1}$ in 0.1M $TBAPF_6$ solution in dichloromethane GC electrodes modified by calixarene derivative **15** complexing **DOV•**2TsO. Second (solid), third (dotted) and fourth (dashed) scan are represented.

Analysing the redox peaks associated to **15⊃DOV•**2TsO covalently bound to the GC surface, it was possible to calculate its surface coverage (Γ). According to Faraday's law (Eq. 2):

$$\Gamma = Q/nFA\rho \quad \text{(Eq. 2)}$$

where $Q$ is the charge obtained from integration of the baseline-corrected area under the oxidation/reduction peaks, $F$ the Faraday constant, $A$ the geometric area of the electrode (0.071 $cm^2$), $n$=2 the number of electrons transferred, and $\rho$ is the roughness factor of the surface. According to literature, $\rho$ values lie between 4 and 8 for our type of electrode and polishing technique and 4 was used in these calculations.[29] The calculated surface coverage, $\Gamma$ = 139 pmol $cm^{-2}$, is about one order of magnitude smaller compared to previous results reported in literature for thick EDA-Boc monolayer electrografted on GC electrodes.[20] Several explanations may justify the lower amount of molecules attached to the surface: *a*) each molecule of wheel **15** covalently binds three molecule of amine on the surface, reducing considerably the theoretical number of possible pseudorotaxanes on the surface; *b*) the three carboxylic

groups of the calixarene may bind three amine functions distant in space, enabling several active site on the electrodes with the steric hindrance of its cavity; *c*) the redox active centre, represented by the guest axle, is not covalently attached to the electrode: it is plausible that certain host molecules appended to the electrode refuse to form pseudorotaxanes due to their wrong orientation toward the solution; *d*) since the calculations were performed on the second scan of the CV, they do not consider the amount of pseudorotaxane irreversibly dissociated during the first scan.

The success in the creation of a pseudorotaxane at the GC surface was an incentive to investigate the possibility to generate rotaxane systems in similar conditions. In this instance, the carbon surface played two different roles: not only it acted as supporting material for the functionalization, but it also acted as stopper for obtaining an organic monolayer composed by rotaxanes. To this purpose, we designed a viologen axle bearing a stopper group on one alkyl chain and a carboxylic function at the opposite side, suitable for the coupling to an amine monolayer. The axle needs to be taken up by wheel **1** to form the pseudorotaxane prior to attachment to the electrode surface (Scheme 7).

The synthesis of pseudorotaxane **1⊃17**•2X was carried out mixing wheel **1** and axle **17**•2X in apolar media. Compound **17**•2X was obtained refluxing known compound (**16**•Tos)[31] with an excess of 11-Bromoundecanoic acid in acetonitrile. Axle **17**•2X maintains all the necessary features to: *a)* perform unidirectional threading into wheel **1** only from the upper rim; *b)* react through a coupling reaction with deprotected EDA-Boc linked to the surface. The modification of the electrode was achieved with a similar solid-phase synthesis approach as presented previously (see Scheme 7). A slight excess of axle **17**•2X was added to a solution of wheel **1** in dichloromethane. After stirring for one hour, the solution went from colourless to deep red indicating the complete formation of the pseudorotaxane. The solution was filtered and the coupling agents were added. Following formation of the activated ester, an EDA modified GC electrode was dipped into the solution for four hours under magnetic stirring.

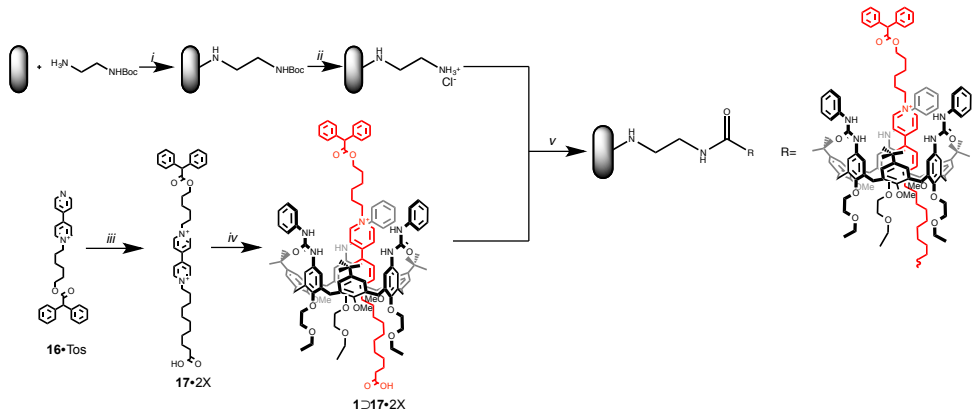


**Scheme 7.** Reagents and Conditions: *i*) a) 20 mM EDA-Boc solution in $CH_3CN$ with 0.1 M TBATFB, 5 cycles, potential range 0.5–2 V vs. Ag/AgCl at a scan rate of 50mVs-1; *ii*) 4.0 M HCl in 1,4- dioxane, r.t.; : *iii*) 11-Bromoundecanoic Acid, $CH_3CN$, reflux, 4 days, 50%; *iv*) **1**, $CH_2Cl_2$, r.t., 1h; *v)* EDC, NHS, DCM, 5h, r.t.

DCM was used instead of DMF as solvent for the coupling reaction, in order to: *a*) avoid the covalent binding of uncomplexed guest, insoluble in DCM, on the electrode, *b*) shift the equilibrium of the species in solution toward the pseudorotaxane formation, *c*) control the unidirectional threading of the axle, in low polarity solvents, selectively from the upper rim.[9] The modified electrodes were characterised by cyclic voltammetry in a 0.1 M solution of $TBAPF_6$ in dichloromethane. The CV (Figure 11) confirmed the successful anchoring of **1⊃17•**2X and the constant intensity of the relative redox peaks after 30 scans proved the stability of the system. The potential values of reduction and oxidation peaks confirm the inclusion of the viologen unit inside wheel **1**, showing a shift of the $E_{1/2}$' of about 200 mV to lower potentials compared to **DOV•**2Tos in solution. Although the peak resulted slightly shifted, determining the shift of the second redox peak ($E_{1/2}$'') resulted impossible, given the interference of molecular oxygen whose reduction occurred in the same potential window. Nonetheless, as expected, it resulted clear that the stopper prevented the de-threading of the axle, blocking the viologen unit in the macrocycle cavity even in its reduced form.

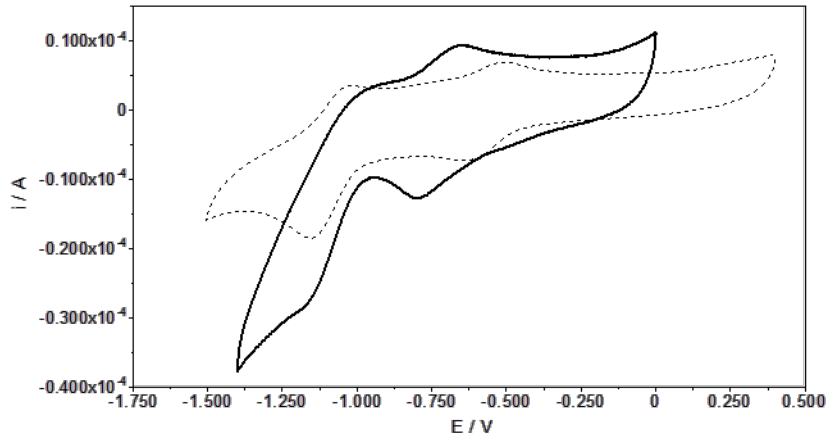


**Figure 11.** Cyclic voltammograms recorded at a scan rate of 100 mV $s^{-1}$ in a 0.1M $TBAPF_6$ solution in dichloromethane of (solid) a 5 mM solution of **DOV**•2TsO and (dotted) modified GC electrodes.

Calculating the charge obtained from integration of the baseline-corrected area under the oxidation or reduction peak, we were able to estimate the quantity of rotaxane linked to the electrode (Eq. 2): a value of $\Gamma$ = 79 pmol $cm^{-2}$ was obtained; this value is about half respect to the previous experiment, where calix **15** was directly attached to the electrode. The lower amount of material on the surface is probably due to the presence of the complex in solution, being the process governed by an equilibrium, the yield of the reaction was noticeably reduced.

Having optimised the conditions for the modification of GC electrodes with pseudorotaxanes and rotaxanes generated by calix[6]arenes and dialkylviologen salts and after demonstrating the partial reversibility of a pseudorotaxane when the calixarene host is anchored to the surface, we decided to further investigate on the threading/ de-threading process of these systems. Considering this, a pseudorotaxane comprising wheel **1** threaded by guest dialkylviologen axle **19**•2X was designed. Axle **19**•2X was synthesized following a linear synthetic route (Scheme 8). 1-octadecyl tosylate was refluxed in acetonitrile with an excess of 4,4'-bipyridyl to obtain **18**•Tos,

which, in turn, was refluxed in acetonitrile with an excess of 11-bromoundecanoic acid to yield final product **19**•2X as a yellow powder.

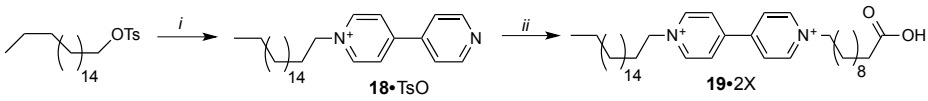


**Scheme 8.** Reagents and Conditions: *i*) 4,4'-bipyridyl, $CH_3CN$, reflux, 24h, 64%; *ii*) 11-bromoundecanoic acid, $CH_3CN$, reflux, 4 days, 62%.

The viologen unit presented a C11 alkyl chain substituent terminating in a carboxylic acid group suitable for the anchoring to the surface and a C18 alkyl chain substituent, which is expected to act as a kinetic stopper and avoid the de-threading of the wheel once the pseudorotaxane is anchored to the surface. It could be imagined that for this chain, due to its length, the loss of conformational freedom needed to pass through the calixarene annulus after the reduction of the viologen unit disfavours the dethreading of the axle. The activity of the C18 alkyl chain may be strongly dependent on the scan rate utilised during the CV experiments, since the dethreading of the axle may result as a slow process (see Scheme 9).

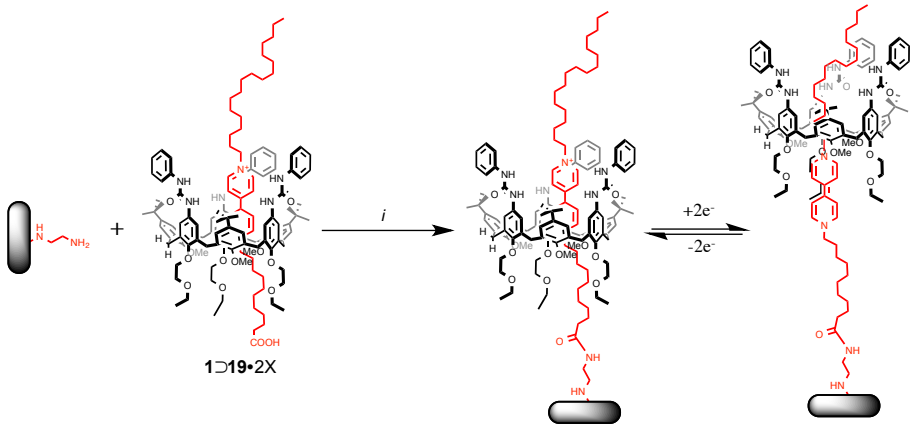


**Scheme 9.** Immobilization of pseudorotaxane **1⊃19**•2X and kinetic stopperage activity of C18 alkyl chain under electrochemical stimulus. Reagents and Conditions: *i*) EDC, NHS, DCM, 5h, r.t.

The **1⊃19**•2X pseudorotaxane formation and its immobilisation on the GC electrode were carried out following the same procedures previously described for pseudorotaxane **1⊃17**•2X. The modified surfaces were characterised by cyclic voltammetry in a 0.1 M solution of $TBAPF_6$ in dichloromethane. The CVs showed the typical pattern of signals relative to a rotaxane system[32,33], in which both the reduction potential peaks are shifted to lower potential compared to a free viologen derivative in solution (Figure 12).

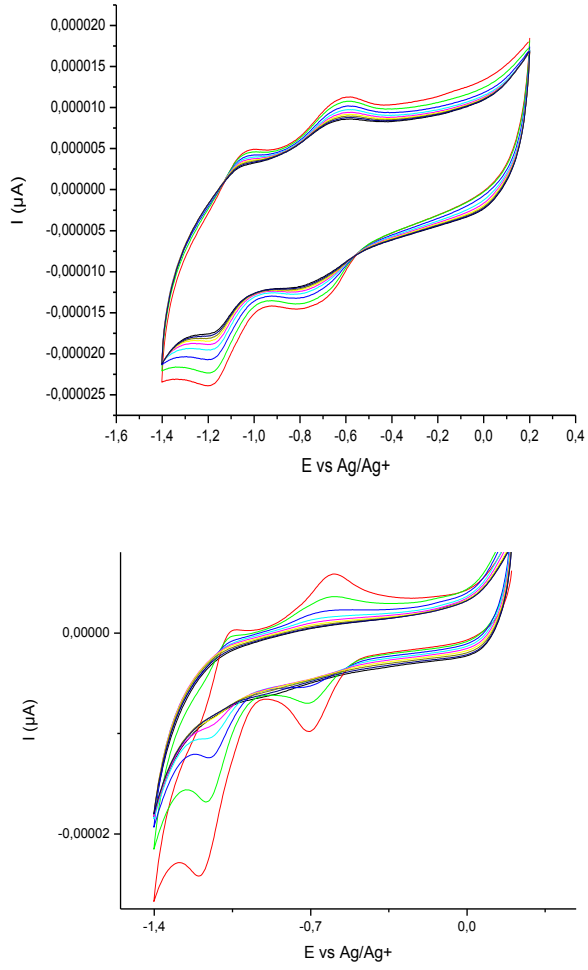


**Figure 12.** Cyclic voltammograms (10 scans) recorded in a 0.1M $TBAPF_6$ solution in dichloromethane of modified GC electrodes at a scan rate of: a) 100 mV $s^{-1}$; b) 50 mV $s^{-1}$.

The decreasing intensity of the current associated with the redox peaks of the specie at the surface by scanning the potential window several times, indicates that, despite the C18 chain presence, the wheel partially de-threads form the axle. Lowering the experiments scan rate to 50 mVs-1, the de-complexation process was complete after 6 scans. Such result would suggest that, upon reduction of the guest, the wheel de-threads it and within the time interval needed to re-oxidise the viologen unit, the host diffuses away from the electrode surface, rendering the regeneration of the pseudorotaxane impossible as seen in the initial experiment. Nonetheless, at a scan rate of 100 $mVs^{-1}$, the threading/dethreading process resulted reversible: we speculated that, the fast reduction/reoxidation process of the viologen, together with the steric effect of the octadecyl alkyl chain, avoided the total decomplexation of the wheel, favouring the re-inclusion of the viologen unit in the calixarene cavity once re-oxidised over diffusion processes (see Figure 13).

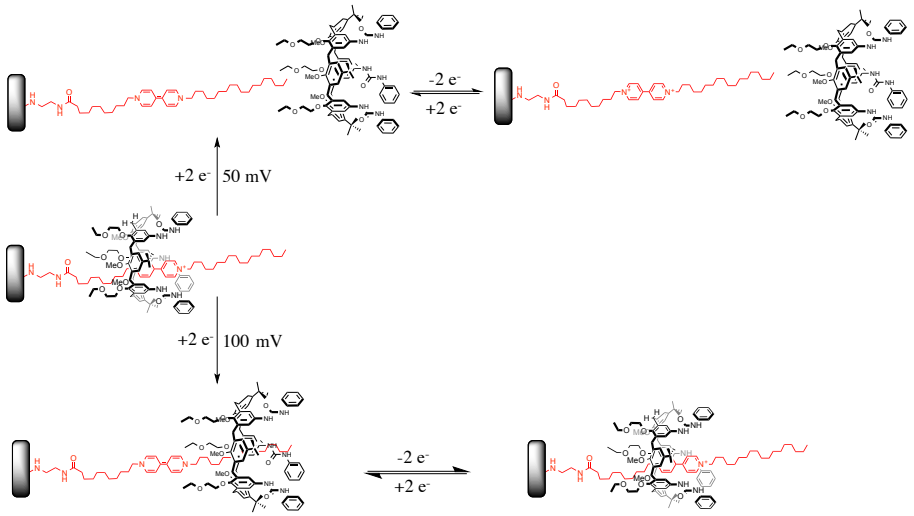


**Figure 13.** Different behaviour of the immobilised pseudorotaxane **1⊃19**•2X depending on the scan rate applied in the cyclic voltammetry.

With the purpose to compare the electrochemical behaviour of a dialkylviologen salt covalently linked to the surface without the presence of wheel **1** to the experimental results obtained with the anchoring of **1⊃17**•2X and **1⊃19**•2X, salt **17**•2X was coupled

to a free amine monolayer, following the standard procedures presented. DMF was used as solvent since **17**•2X is soluble in this solvent, while in DCM the viologen derivative is totally insoluble. The formation of the activated ester, using EDC as activating agent, resulted unsuccessful: the solution, after the addition of EDC, immediately turned from yellow to blue, suggesting the formation of the reduced form of viologen. We speculated that in this occasion, EDC acts as reducing agent instead of forming the activated ester needed for the coupling with the modified electrode. Such behaviour was not detected upon activation of the carboxylic acid group after the pseudorotaxane was formed: we supposed that the electron-rich cavity of the macrocycle acted as a sort of shield to the viologen unit against reduction.

An alternative method was then experienced by functionalizing GC electrode with free dialkylviologen salt derivatives. In this attempt, the viologen unit was decorated on one side with an alkyl chain terminating with an amine function, a functional group potentially available for the direct electrografting on GC. Final compound **22**•3X was obtained starting from tosylate **4**; this alkylating agent was refluxed in acetonitrile with an excess of 4,4'-dipyridil to obtain, through recrystallization, the monoalkyl-4,4'-bipyridinium salt **20**•TsO. An excess of pentyl tosylate was then refluxed with derivative **20**•TsO, to obtain the dialkyl-4,4'-bipyridinium salt **21**•2TsO. Removal of the Boc protecting group on the amine function of **21**•2TsO was obtained stirring a solution of the axle in trifluoroacetic acid, yielding final product **22**•3X.

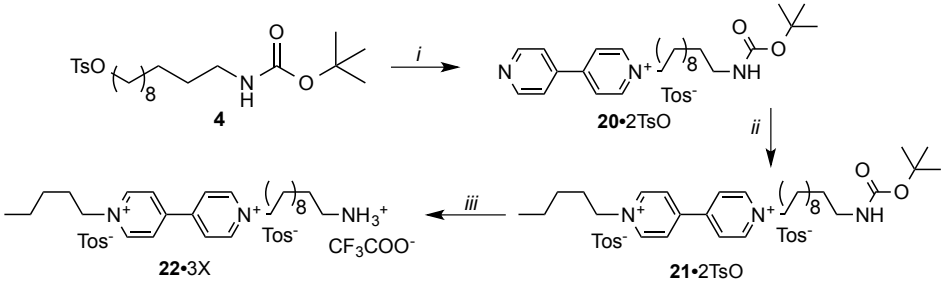


**Scheme 10.** Reagents and Conditions: *i*) 4,4'-bipyridyl, $CH_3CN$, reflux, 24h, 59%; *ii*) 1-Pentyl tosylate, $CH_3CN$, reflux, 72h, 60% *iii*) TFA, 0° C, 0.5h, 95%

With the aim to electrochemically graft this ammonium salt to GC electrode, a 20 mM solution of **22**•3X in 0.1M TBATFB and acetonitrile/water (10% $NaHCO_3$) 8:2 was prepared. Cyclic voltammetry was then carried out (5 scans from 0.2 to 1.95 V vs Ag/AgCl reference electrode). Voltammograms showed the presence of an irreversible oxidation single broad irreversible peak starting from +1.1 V and reaching a maximum at about +1.3 V versus Ag/AgCl. The intensity of the cathodic tends to gradually disappear in the next cycles (Figure 14); this signal could be assigned to the oxidation of a functional group from amino to radical-cation specie. The solution also showed a blue color, typical of the viologen radical-cation specie, in the proximity of the GC electrode and the Pt counter electrode during the oxidation process. It's plausible that high voltage is not selective for the oxidation of amine function and could affect the oxidation/reduction process of a viologen unit.

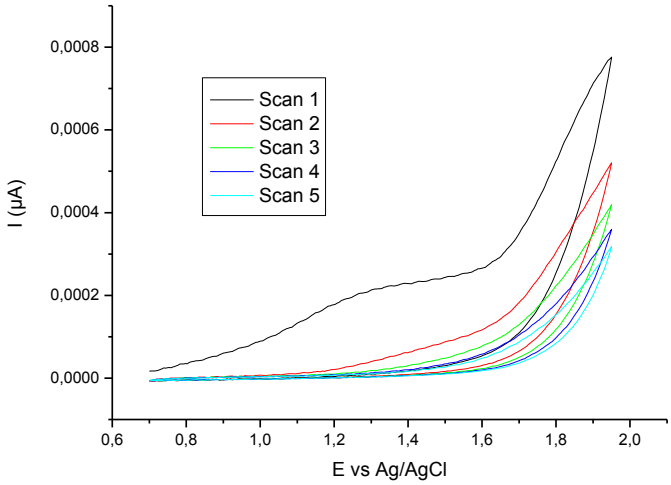


**Figure 14**. Cyclic voltammogram recorded at a scan rate of 50 $mVs^{-1}$ for 3 mm diameter GC electrode in 10 mM of **22**•3X in acetonitrile/water (10% $NaHCO_3$) 8:2 with 0.1m TBATFB.

Running cyclic voltammetry on the modified electrodes, a typical pattern of redox signals assignable to a viologen derivative was observed. The main differences are that the values of the redox potential are extremely shifted to lower voltage vs $Ag/Ag^+$ reference electrode (Figure 15); our supposition is that interactions between the

viologen station and the GC surface during the oxidation process may affect the electrografting of derivative **22•**3X to the electrode.

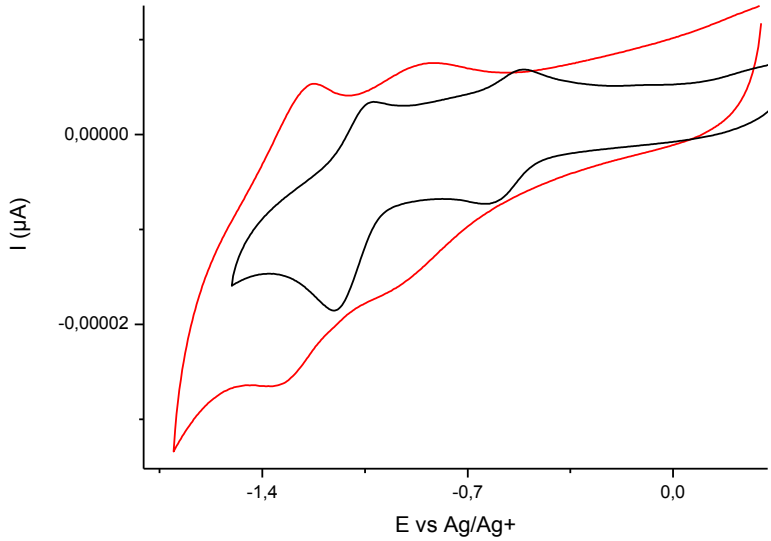


**Fig 15.** Cyclic voltammograms recorded at a scan rate of 100 mV $s^{-1}$ in a 0.1M $TBAPF_6$ solution in dichloromethane of (black) a 5 mM solution of DOVx2Ts and (red) **22•**3X modified GC electrodes.

To support our hypothesis, CVs in a 5mM solution of wheel **1** in 0.1M $TBAPF_6$ and dichloromethane were performed: with the presence of the calixarene, no differences were noticed in the voltammograms, indicating that no pseudorotaxane formation occurs on the surface of the electrode, probably due to interactions between the cationic unit of the salt and the GC surface.

## 5.4 Conclusions and Perspectives

In this chapter, a new approach to the covalent modification of GC electrodes with calix[6]arene and dialkylviologen based pseudorotaxanes and rotaxanes using solid-phase synthesis techniques was reported. Initially, the surfaces were modified with a tris(*N*-phenylureido)calix[6]arene derivative: such functionalization conferred to the electrode the ability to take up *N,N*-dialkylviologen salts in low polarity media such as DCM and to assemble pseudorotaxane systems. In these conditions, the threading/de-threading processes of the viologen-based axle into the calix[6]arene-based wheel could be controlled by electrochemical stimuli generated by the same electrode on which the pseudorotaxane was anchored. Next, we designed two solution generated pseudorotaxane-like structures that could be anchored at the surface through the axle, showing different behaviour under electrochemical stimuli. In the first example, a bulky group present at one extremity of the axle inhibited its de-threading from the wheel after the reduction of the viologen unit, generating a rotaxane, while in the second, the axle was characterised by a long C18 alkyl chain whose ability to act as a kinetic stopper was strongly dependant on the scan rate of the electrochemical experiment. These studies gave further insight on the behaviour and stability of calix[6]arenes based pseudorotaxanes and rotaxanes covalently bound to electrode surfaces. Our results represent a step further toward the creation of electrochemically controlled molecular machines confined on GC surfaces for the development of smarter devices. Future studies could involve the insertion of a secondary recognition site on the axle, able to stabilise the mono-reduced form of the viologen axle: using this work as inspiration it would be possible to design molecular elevators, shuttles or other switchable Host-Guest systems.

# Experimental Section

**Reagents and Methods.** All solvents were dried using standard procedures; all other reagents were of reagent grade quality obtained from commercial suppliers and were used without further purification. NMR spectra were recorded at 400 or 300 MHz for $^{1}H$ and 100 or 75 MHz for $^{13}C$. Melting points are uncorrected. Chemical shifts are expressed in ppm ($\delta$) using the residual solvent signal as internal reference (7.26 ppm for $CHCl_3$, 3.31 for $CH_3OH$ and 2.50 for DMSO). Mass spectra were recorded in ESI mode. Calix[6]arenes **2**[23] and **7**[30] , alkylviologen salt **16**•TsO[31], 11-aminoundecan-1-ol (**2**)[22] and octadecyl 4-methylbenzenesulfonate[10] were synthesised according to published procedures.

**Electrochemical Measurements.** Electrochemical experiments were performed in a conventional three electrode cell using an Autolab PGSTAT30 Potentiostat/Galvanostat. An Ag/AgCl was used as the reference electrode, and about 1 $cm^2$ platinum gauze as the counter electrode. Ferrocene was used as internal standard. The working electrode was a 3 mm diameter (0.071 $cm^2$) glassy carbon disc (RA3-100, Tokai Carbon, Japan) sealed in glass tube and wired up with copper wire by using melted indium (Aldrich). Prior to modification, the working electrodes was polished with silicon carbide polishing paper (grade 1200) and rinsed with deionized water followed by sonication for 5 min in acetonitrile.

## Synthetic procedures

***tert*-butyl (11-hydroxyundecyl)carbamate (3).** In a 100 ml round bottom flask, under inert atmosphere, di-tert-butyl dicarbonate (1.0 g, 4.8 mmol) and triethylamine (0.8 g, 4.8 mmol) were added to a solution of 11-aminoundecan-1-ol (0.9 g, 4.8 mmol) in THF (50 mL). The reaction mixture was stirred overnight at room temperature. Afterwards, the solvent was removed under reduced pressure and the residue was portioned

between ethyl acetate and water. The separated organic phase was dried over $Na_2SO_4$ and evaporated under reduced pressure to afford 1.3 g of **3** as a white solid in 94% yield. M.p. = 33-35°C; $^1$H NMR ($CDCl_3$, 300 MHz) $\delta$= 3.68 (t, 2H, $J$ = 6.6 Hz), 3.14 (t, 2H, $J$ =7.0 Hz), 1.54 (m, 2H), 1.46 (s, 11H), 1.29 (m, 14H); $^{13}$C NMR (75 MHz) $\delta$= 158.0, 63.0, 40.8, 32.8, 30.0, 29.5, 29.4, 29.2, 28.4, 26.8, 25.7; MS (ES): m/z: 288.3 $[M+ H]^+$.

**11-((*tert*-butoxycarbonyl)amino)undecyl 4-methylbenzenesulfonate (4).** A solution of *p*-toluenesulfonyl chloride (3.0 g, 15.8 mmol) in anhydrous $CH_2Cl_2$ (100 mL) was slowly added to a solution of **3** (3.5 g, 12.2 mmol) in 50 mL of anhydrous $CH_2Cl_2$. Triethylamine (2.3 g, 24.4 mmol) and a catalytic amount of DMAP were added. After stirring at room temperature for 5 hours, the reaction was quenched with water (100 mL) and the organic phase was separated, dried over anhydrous $CaCl_2$ and filtered. The solvent was removed under reduced pressure and the residue was purified by column chromatography (*n*-hexane/ethyl acetate 85:15) to afford 3.9 g of **4** as a white solid in 72% yield. M.p. = 52-53°C; $^1$H NMR ($CDCl_3$, 400 MHz) $\delta$ = 7.82 (d, 2H, $J$ = 8.0 Hz), 7.37 (d, 2H, $J$ = 8.0 Hz), 4.51 (bs, 1H), 4.05 (t, 2H, $J$ = 6.6 Hz), 3.11 (bs, 2H), 2.47 (s, 3H), 1.67 (m, 2H), 1.46 (s, 11H), 1.29 (m, 14H); $^{13}$C NMR (100 MHz): $\delta$=158.0, 144.6, 133.3, 129.8, 127.9, 70.7, 40.6, 30.1, 29.5, 29.4, 29.2, 29.3, 28.9, 28.8, 28.4, 26.8, 25.3, 21.6; MS (ES): m/z: 464.4 $[M+ Na]^+$.

**Calix[6]arene 6.** In a 100 ml sealed glass autoclave, a heterogeneous mixture of compounds **5** (1.0 g, 1.1 mmol), **4** (2.4 g, 5.4 mmol) and $K_2CO_3$ (0.7 g, 5.1 mmol) in $CH_3CN$ (60 ml) was refluxed under vigorous stirring for 72 h. After cooling to room temperature, the solvent was evaporated to dryness under reduced pressure. The solid residue was taken up with ethyl acetate (80 ml) and the resulting organic phase washed with water (2x 80 ml). The separated organic phase was dried over anhydrous sodium sulfate, filtered to remove the drying agent and the solvent evaporated under reduced pressure. The residue was purified by column chromatography on silica gel (dichloromethane/ethyl acetate 97:3) to yield 0.6 g of **6** as a pale yellow solid in 32%

yield. M.p. = 89°C; $^{1}$H NMR ($CDCl_3$, 400 MHz) $\delta$ = 7.70 (bs, 6H), 7.24 (bs, 6H), 4.52-4.37 (bs,9H), 3.85-3.57 (bs, 12H), 3.11 (t, 6H, $J$ = 6.8 Hz), 2.88 (s, 9H), 1.87 (bs, 6H), 1.65-1.29 (m, 124 H); $^{13}$C NMR (100 MHz): $\delta$= 156.0, 146.8, 143.6, 135.7, 132.2, 127.3, 123.2, 79.0, 74.0, 60.2, 59.9, 40.7, 34.3, 31.5, 30.3, 30.1, 29.7, 29.5, 29.3, 28.4, 26.9, 26.2; MS (ES): m/z: 1813.3 $[M+ Na]^+$.

**Calix[6]arene 7**. In a 100 ml round bottom flask kept under nitrogen atmosphere, a tip of spatula of Pd/C catalyst was cautiously added to a suspension of compound **6** (0.57 g, 0.32 mmol) in methanol (50 ml), then hydrazine monohydrate (1.53 g, 30 mmol) was added dropwise. The resulting heterogeneous mixture was refluxed for 6 h, cooled to room temperature and then filtered, under nitrogen atmosphere, through a celite pad to remove the Pd/C catalyst. The filtered solution was evaporated to dryness under reduced pressure to yield 0.52 g of **7** as a white solid in 98% yield. Because of its instability to air, compound **7** was employed in the following synthetic step without any further purification.

**Calix[6]arene 8.** In a 50 ml round bottom flask, at a solution of compound **7** (520 mg, 0.31 mmol) in dichloromethane (25 ml) under nitrogen atmosphere, phenylisocyanate (0.21 mg, 1.8 mmol) was added dropwise. The reaction mixture was stirred for two hours at room temperature. The solvent was removed under reduced pressure and the mixture was purified by silica gel chromatography column, using dichloromethane/ethyl acetate (93:7) as eluent to yield 0.28 g of **8** as a pale yellow solid in 69% yield. M.p. = 118-120°C; $^{1}$H NMR ($CDCl_3$, 400 MHz) $\delta$ = 7.21 (m, 6H), 7.11 (d, 12H, $J$ = 5.6 Hz), 6.94 (m, 4H), 6.3 (s, 6H), 4.55 (s, 3H), 4.41 (d, 6H, $J$ = 15.6 Hz), 3.91 (t, 6H, $J$ = 6.3 Hz), 3.59 (d, 6H, $J$ = 15.3 Hz), 3.10 (m, 6H, $J$ = 6.3 Hz), 2.86 (s, 9H), 1.90 (m, 6H, $J$ = 6.9 Hz), 1.6-1.1 (ms, 75H). $^{13}$C NMR (100 MHz): $\delta$= 156.0, 155.0, 154.5, 152.3, 138.2, 135.7, 133.0, 132.4, 128.8, 128.7, 127.7, 123.5, 122.9, 120.6, 79.1, 73.1, 60.2, 40.6, 34.2, 31.5, 31.4, 31.0, 30.5, 30.1, 29.6, 29.5, 29.3, 28.4, 26.8, 26.3. MS (ES): m/z: 2080.1 $[M+ Na]^+$.

**Calix[6]arene 9.** In a 10 ml round bottom flask, at a solution of **8** (20 mg, 0.01 mmol) in dichloromethane (2 ml), under nitrogen atmosphere, trifluoroacetic acid (0.30 g, 1.00 mmol) was added dropwise. The reaction mixture was stirred for one hour at room temperature. The solvent and the acid in excess were removed under reduced pressure. The solid residue was taken up with ethyl acetate (20 ml) and the resulting organic phase washed with a saturated $K_2CO_3$ solution in water (2x 25 ml). The separated organic phase was dried over anhydrous sodium sulfate, filtered to remove the drying agent and the solvent evaporated under reduced pressure to yield 20 mg of impure product **9** as a pale yellow solid. $^1$H NMR ($CDCl_3$, 400 Hz) $\delta$: 7.3 (bs, 6H), 7.0 (s, 6H), 6.8 (bs,9H), 6.2 (bs, 6H), 5.3 (bs, 6H), 4.4 (bs, 6H), 3.8 (bs, 17H), 3.5 (bs, 6H), 2.7 (bs, 6H), 1.9 (bs, 12H), 1.6-1.2 (m, 78H). MS (ES): m/z: 1879.8 $[M+ 2H]^{2+}$.

***tert*-butyl 11-bromoundecanoate (11).** In a 250 ml round bottom flask, at a solution at 0° C of 11- bromo- undecanoic Acid (**10**) (5.0 g, 18.9 mmol) in freshly distilled tetrahydrofuran (100 ml), under nitrogen atmosphere, trifluoroacetic anhydride (5.2 ml, 37.8 mmol) was added dropwise. The reaction mixture was stirred for two hours at 0° C, then tert-butanol was added (7.0 g, 94.5 mmol). The reaction was stirred at room temperature for 16h. The solvent was then removed under reduced pressure and the mixture was dissolved in ethyl acetate (100 ml) and washed with a solution of $NaHCO_3$ (o.1 M, 100 ml) and water (2x 100 ml). The organic phase was dried with anhydrous sodium sulfate, filtrated and the solvent was removed under reduced pressure to yield 5.2 g of product **11** as a colorless oil in 87% yield. $^1$H NMR ($CDCl_3$, 400 MHz) $\delta$: 3.41 (t, 2H, $J$ = 6.9 Hz), 2.20 (t, 2H, $J$ =7.5 Hz), 1.85 (m, 2H, $J$ =7.2 Hz), 1.58 (m, 2H, $J$ =7.2 Hz), 1.45 (s, 9H), 1.29 (m, 14H); $^{13}$C NMR (100 MHz) 173.3, 79.9, 77.5, 77.0, 76.6, 35.6, 34.0, 32.8, 29.3, 29.2, 29.0, 28.7, 28.1, 25.1; MS (ES): m/z: 343.2-345.2 $[M+ Na]^+$.

**Calix[6]arene 12.** In a 100 ml sealed glass autoclave, a heterogeneous mixture of three nitro calixarene **5** (1.0 g, 1.1 mmol), **11** (2.0 g, 6.0 mmol) and $K_2CO_3$ (0.7 g, 5.1 mmol) in $CH_3CN$ (60 ml) was refluxed under vigorous stirring for 72 h. After cooling to room

temperature, the solvent was evaporated to dryness under reduced pressure. The solid residue was taken up with ethyl acetate (80 ml) and the resulting organic phase washed with a 10% w/v solution of HCl (80 ml) and water (2x 80 ml). The separated organic phase was dried over anhydrous sodium sulphate, filtered to remove the drying agent and the solvent evaporated to dryness under reduced pressure. The residue was purified by column chromatography on silica gel (hexane/ethyl acetate 8:2) to yield 0.92 g of **12** as a pale yellow solid in 54% yield. M.p. = 78-79°; $^{1}$H NMR ($CDCl_3$, 400 MHz) $\delta$ = 7.69 (s, 6H), 7.23 (s, 6H), 4.4 (bs, 6H), 3.8 (m, 6H), 3.6 (bs, 6H), 2.88 (s, 9H), 2.21 (t, 6H, , $J$ =7.6 Hz), 1.7-1.3 (m, 96H); $^{13}$C NMR (100 MHz): $\delta$=173.3, 159.9, 154.3, 146.8, 143.6, 135.6, 132.2, 127.4, 123.1, 79.9, 74.0, 60.0, 35.6, 34.3, 31.5, 31.3, 30.9, 30.3, 29.5, 29.3, 29.1, 28.1 26.0, 25.1 ; MS (ES): m/z: 1726.6 $[M+ Na]^+$.

**Calix[6]arene 13.** In a 100 ml round bottom flask kept under nitrogen atmosphere, a tip of spatula of Pd/C catalyst was cautiously added to a suspension of compound **12** (0.52 g, 0.31 mmol) in methanol (50 ml), then hydrazine monohydrate (1.53 g, 30 mmol) was added dropwise. The resulting heterogeneous mixture was refluxed for 6 h, cooled to room temperature and then filtered, under nitrogen atmosphere, through a celite pad to remove the Pd/C catalyst. The filtered solution was evaporated to dryness under reduced pressure to yield 0.48 g of 3 as a white solid in 98% yield. Because of its instability to air, compound **13** was employed in the following synthetic step without any further purification.

**Calix[6]arene 14.** In a 50 ml round bottom flask kept under nitrogen atmosphere, to a solution of **13** (0.48 g, 0.30 mmol) in dichloromethane (20 ml), phenyl isocyanate (0.17 g, 1.44 mmol) was added dropwise. The reaction mixture was stirred for two hours at room temperature, then the solvent was evaporated to dryness under reduced pressure and the residue was purified by column chromatography on silica gel (hexane/ethyl acetate 7:3) to yield 0.42 g of **14** as a pale yellow solid in 71% yield. M.p. = 111-112°. $^{1}$H NMR ($CDCl_3$, 400 MHz) $\delta$ = 7.22 (s, 6H), 7.12 (s, 6H), 6.94 (s, 6H), 6.31 (s, 6H), 4.42 (d, 6H, $J$ =13.2 Hz), 3.93 (s, 6H), 3.58 (d, 6H, 14.4 MHz), 2.85 (s, 9H), 2.22 (s,

6H), 1.91 (s, 6H), 1.59 (s, 12H) ), 1.47 (s, 54H), 1.32 (s, 36H). $^{13}$C NMR (100 MHz): $\delta$ = 173.4, 155.0, 154.6, 152.3, 146.8, 138.3, 135.7, 133.1, 132.4, 128.9, 127.7, 123.4, 123.1, 120.5, 79.9, 73.1, 60.2, 35.6, 34.2, 31.5, 31.0, 30.6, 29.6, 29.5, 29.3, 29.1, 28.1, 26.3, 25.1. MS (ES): m/z: 1994.1 $[M+ Na]^+$.

**Calix[6]arene 15.** In a 10 ml round bottom flask, at a solution of **14** (20 mg, 0.01 mmol) in dichloromethane (2 ml), under nitrogen atmosphere, trifluoroacetic acid (0.30 g, 1.00 mmol) was added dropwise. The reaction mixture was stirred for one hour at room temperature. The solvent and the acid in excess were removed under reduced pressure to yield 15 mg of impure product **15** as a pale yellow solid in 83% yield. $^1$H NMR ($CDCl_3$, 400 Hz) $\delta$: 7.2 (bs, 6H), 7.1-7.0 (m, 15H), 6.94 (m, 6H, J= 4.4 Hz), 6.31 (s, 6H), 4.39 (d, 6H, *J* =13.2 Hz), 3.93 (t, 6H, *J* = 6.4 Hz), 3.58 (d, 6H, 14.4 Hz), 2.89 (s, 9H), 2.36 (t, 6H, *J* = 7.2 Hz), 1.89 (m, 12H, *J* = 7.2 Hz ) ), 1.64 (bs, 12H), 1.5-1-4 (m, 36H) ), 1.3-1.2 (ms, 54H). $^{13}$C NMR (100 MHz): $\delta$=179.1, 168.5, 155.0, 154.6, 152.3, 146.8, 138.3, 135.7, 133.8, 133.1, 132.2, 128.9, 127.7, 123.4, 123.1, 120.5, 73.0, 60.3, 34.2, 31.5, 31.0, 30.6, 29.6, 29.5, 29.3, 29.1, 28.1, 26.3, 25.1. MS (ES): m/z: 1825.7 $[M+ Na]^+$.

**Axle 17•**2X**.** In a sealed 100 ml glass autoclave, a solution of **16•**TsO (0.5 g, 0.8 mmol) and 11- Bromoundecanoic Acid (0.7 g, 2.6 mmol) in $CH_3CN$ (40 ml) was refluxed for 4 days. Afterwards, the solution was evaporated to dryness under reduced pressure. The solid residue was triturated with $CH_3CN$ to afford 0.4 g of product **17•**2X as a yellow solid in 50% yield. M.p. = 240-243°; $^1$H NMR (DMSO-$d_6$, 400 MHz) $\delta$ = 12.0 (bs, 1H) 9.4 (m, 4H), 8.83 (d, 4H, *J* = 6.8 Hz), 7.49 (d, 0.5H, *J*= 8.0 Hz), 7.3-7.1 (m, 10H), 7.11 (d, 0.5H, *J*= 8.0 Hz), 5.18 (s, 1H), 4.7 (m, 4H), 4.11 (t, 2H, *J*= 6.8 Hz), 2.20 (s, 1H), 2.18 (t, 2H, *J* = 7.6 Hz), 2.0-1.9 (m, 4H), 1.6-1.4 (m, 4H), 1.3-1.2 (m, 16H). $^{13}$C NMR (100 MHz): $\delta$ = 174.9, 172.4, 149.0, 146.2, 146.1, 139.5, 138.1, 129.0, 128.9, 128.5, 127.5, 127.1, 125.9, 64.9, 61.3, 61.2, 56.3, 34.1, 31.2, 31.0, 29.2, 29.1, 29.0, 28.8, 28.2, 25.9, 25.3, 25.0, 24.9, 21.2. MS (ES): m/z: 635.5 $[M- H]^+$.

**Salt 18•**TsO**.** In a 100 ml round-bottomed flask octadecyl 4-methylbenzenesulfonate (1.0 g, 2.4 mmol) and 4,4'-dipyridyl (1.1 g, 7.1 mmol) were dissolved in $CH_3CN$ (50ml) and the solution was refluxed for 24h. Then the solvent was evaporated at reduced pressure and the residue obtained was triturated with EtOAc (3x 20 ml) until the product precipitated as a solid compound and was recovered by suction filtration to afford 1.0 g of product **18•**TsO as a white solid in 64% yield. M.p. = 97-99°; $^1$H NMR (400MHz, $CD_3OD$) $\delta$ = 9.12 (d, 2H, *J* = 6.0 Hz), 8.85 (d, 2H, *J* = 6.8 Hz), 8.52 (d, 2H, *J*= 5.6 Hz), 7.99 (d, 2H, *J*= 6.4 Hz), 7.72 (d, 2H, *J*= 7.6 Hz), 7.24 (d, 2H, *J*= 8.0 Hz), 4.68 (t, 2H, *J* = 7.6 Hz), 2.37 (s, 3H), 2.18 (t, 2H, *J* = 6.8 Hz), 1.4-1.3 (m, 30H), 0.92 (t, 3H, *J* = 6.0 Hz). $^{13}$C NMR (100 MHz) $\delta$ = 153.9, 150.4, 142.3, 142.2, 140.2, 128.4, 125.7, 125.6, 122.1, 61.4, 31.7, 31.1, 29.4, 29.3, 29.2, 29.1, 28.7, 25.8, 22.3, 19.9, 13.0. MS (ES): m/z: 409.3 $[M- Tos]^+$.

**Axle 19•**2X**.** In a sealed 100 ml glass autoclave, a solution of **18•**TsO (0.5 g, 0.9 mmol) and 11- bromoundecanoic acid (0.6 g, 2.7 mmol) in $CH_3CN$ (40 ml) was refluxed for 4 days. Afterwards, the solution was evaporated to dryness under reduced pressure. The solid residue was triturated with $CH_3CN$ to afford 0.6 g of product **19•**2X as a yellow solid in 62% yield. M.p. = 250-253°. $^1$H NMR (DMSO-d6, 400 MHz) $\delta$ = 12.0 (bs, 1H) 9.39 (d, 4H, *J* = 6.2 Hz), 8.79 (d, 4H, *J* = 6.2 Hz), 7.49 (d, 1H, *J*= 8.0 Hz), 7.12 (d, 1H, *J*= 8.0 Hz), 4.69 (t, 2H, *J* = 7.2 Hz), 2.38 (s, 2H), 2.18 (t, 2H, *J* = 7.6 Hz), 2.0 (bs, 4H), 1.5 (bs, 2H), 1.3-1.2 (m, 42H), 0.85 (t, 3 H, *J* = 6.0 Hz). $^{13}$C NMR (100 MHz) $\delta$ = 175.0, 149.1, 146.2, 146.0, 138.2, 128.5, 127.1, 125.9, 61.4, 40.5, 40.3, 40.1, 39.9, 39.7, 39.5, 39.3, 34.1, 31.7, 31.2, 29.5, 29.4, 29.1, 29.0, 28.8, 25.9, 24.9, 22.6, 21.2, 14.4. MS (ES): m/z: 593.6 $[M-H^+]^+$.

**Salt 20•**TsO**.** A solution of **4** (1.0 g, 2.3 mmol) and 4,4'-bipyridyl (1.1 g, 6.8 mmol) in $CH_3CN$ (150 mL) was refluxed with stirring for 24 h. After cooling to room temperature, the solvent was completely evaporated under reduced pressure and the sticky residue was taken up with hot ethyl acetate. After cooling to room temperature, 0.8 g of the desired pure monotosylate salt **20•**TsO was recovered as a white solid by

suction filtration in 59% yield. M.p. = 72-73°C; $^1$H NMR (MeOD, 400 MHz) $\delta$ = 9.13 (d, 2H, $J$ = 7.2 Hz), 8.85 (d, 2H, $J$ = 6.4 Hz), 8.53 (d, 2H, $J$ = 6.8 Hz), 8.00 (d, 2H, $J$ = 6.4 Hz), 7.24 (d, 2H, $J$ = 8.0 Hz), 7.25 (d, 2H, $J$ = 8.0 Hz), 4.69 (t, 2H, $J$ = 7.6 Hz), 3.02 (t, 2H, $J$ = 7.0 Hz), 2.38 (s, 3H), 2.08 (bs, 2H), 1.45 (bs, 16H), 1.33 (s, 9H); $^{13}$C NMR (100 MHz): $\delta$= 153.7, 150.4, 145.1, 142.2, 140.2, 128.4, 125.7, 125.5, 122.1, 61.4, 39.9, 31.0, 29.6, 29.2, 29.1, 29.0, 28.7, 27.4, 26.4, 25.8, 19.9. MS (ES): m/z: 426.5 $[M- TsO]^+$.

**Axle 21•**2TsO. In a sealed glass autoclave, a solution of **20•**TsO (0.7 g, 1.2 mmol) and 1-pentyl tosylate (0.8 g, 3.5 mmol) in $CH_3CN$ (50 mL) was refluxed for 72h. After cooling to room temperature, the reaction mixture was evaporated to dryness under reduced pressure. Recrystallization of the solid residue from $CH_3CN$ afforded **21•**2TsO as a white solid in 60% yield. M.p. = 135-136°C; $^1$H NMR (MeOD, 400 MHz) $\delta$ = 9.27 (d, 4H, $J$ = 5.6 Hz), 8.68 (d, 4H, $J$ = 6.4 Hz), 7.71 (d, 4H, $J$ = 8.0 Hz), 7.25 (d, 4H, $J$ = 8.0 Hz), 4.74 (t, 4H, $J$ = 7.6 Hz), 3.02 (t, 2H, $J$ = 7.0 Hz), 2.83 (s, 6H), 2.08 (bs, 4H), 1.45-1.33 (m, 29H), 0.98 (t, 3H, $J$ = 6.8 Hz); $^{13}$C NMR (100 MHz): $\delta$= 149.9, 145.7, 143.1, 142.2, 140.3, 128.4, 126.9, 125.5, 61.9, 39.9, 31.2, 30.8, 29.2, 29.1, 29.0, 28.7, 27.9, 27.4, 26.5, 25.8, 21.8, 19.9, 12.7. MS (ES): m/z: 668.3 $[M- TsO]^+$.

**Axle 22•**3X. Solid **21•**2TsO (50 mg, 0.06 mmol) was added to trifluoroacetic acid (5 ml) at 0° C; the solution was stirred for 30 minutes, then trifluoroacetic acid was evaporated under reduced pressure; recrystallization from acetonitrile afforded **22•**3X as a yellow solid in 95% yield. M.p. = 101-102°C; $^1$H NMR (MeOD, 400 MHz) $\delta$ = 9.24 (d, 4H, $J$ = 6.4 Hz), 8.65 (d, 4H, $J$ = 6.4 Hz), 7.69 (d, 6H, $J$ = 8.0 Hz), 7.24 (d, 6H, $J$ = 8.0 Hz), 4.72 (t, 4H, $J$ = 7.6 Hz), 2.91 (t, 2H, $J$ = 7.8 Hz), 2.38 (s, 9H), 2.07 (bs, 4H), 1.65 (bs, 2H), 1.4-1.3 (m, 18H), 0.98 (t, 3H, $J$ = 6.8 Hz); $^{13}$C NMR (100 MHz): $\delta$= 145.6, 142.2, 140.3, 128.4, 126.9, 125.5, 61.9, 39.4, 31.2, 30.8, 29.2, 29.1, 28.8, 27.9, 27.2, 26.1, 25.9, 21.8, 19.9, 12.7. MS (ES): m/z: 740.6 $[M- TsO]^+$

**Modification of GC Electrodes with Calixarene 1.** In a 10 ml beacker, at a solution of calixarene **15** (90 mg, 0.05 mmol) in DMF (5 ml), EDC (27 mg, 0.21 mmol) and NHS (24 mg, 0.21 mmol) were added. The solution was stirred for 1h and then the electrodes were dipped in the solution for 4h. The electrodes were then rinsed with water (5 ml), acetonitrile (5 ml) and left to dry in air.

**General Procedure for the Modification of GC Electrodes with Pseudorotaxane.** In a 10 ml beacker, at a solution of **1** (73 mg, 0.05 mmol) in $CH_2Cl_2$ (5 ml) a slight excess of **Axle•**2X (0.07 mmol) was added; the solution was stirred at r.t. for 1 hour and then filtered to remove the excess of the salt; after EDC (9 mg, 0.07 mmol) and NHS (8 mg, 0.07 mmol) were added, the solution was stirred for 1h and then the electrodes were dipped in the solution. After 4h, the electrodes were rinsed with water (5 ml), acetonitrile (5 ml) and left to dry in air for five minutes.

## References


(1) Fahrenbach, A. C.; Warren, S. C.; Incorvati, J. T.; Avestro, A. J.; Barnes, J. C.; Stoddart, J. F.; Grzybowski, B. A. *Adv. Mater.* **2013**, *25* (3), 331–348.

(2) Yang, Y.-W.; Sun, Y.-L.; Song, N. *Acc. Chem. Res.* **2014**, *47* (7), 1950–1960.

(3) Balzani, V.; Credi, A.; Venturi, M. *Chemphyschem* **2008**, *9* (2), 202–220.

(4) Cooke, G. *Angew. Chem. Int. Ed. Engl.* **2003**, *42* (40), 4860–4870.

(5) Bryce, M. R.; Cooke, G.; Duclairoir, F. M. A.; John, P.; Perepichka, D. F.; Polwart, N.; Rotello, V. M.; Fraser Stoddart, J.; Tseng, H.-R. *J. Mater. Chem.* **2003**, *13* (9), 2111.

(6) Bayly, S. R.; Gray, T. M.; Chmielewski, M. J.; Davis, J. J.; Beer, P. D. *Chem. Commun. (Camb).* **2007**, No. 22, 2234–2236.

(7) Evans, N. H.; Rahman, H.; Leontiev, A. V.; Greenham, N. D.; Orlowski, G. A.; Zeng, Q.; Jacobs, R. M. J.; Serpell, C. J.; Kilah, N. L.; Davis, J. J.; Beer, P. D. *Chem. Sci.* **2012**, *3* (4), 1080.

(8) Arduini, A.; Ferdani, R.; Pochini, A.; Secchi, A.; Ugozzoli, F. *Angew. Chemie, Int. Ed.* **2000**, *39* (19), 3453–3456.

(9) Arduini, A.; Calzavacca, F.; Pochini, A.; Secchi, A. *Chem. - A Eur. J.* **2003**, *9* (3), 793–799.

(10) Boccia, A.; Lanzilotto, V.; Zanoni, R.; Pescatori, L.; Arduini, A.; Secchi, A. *Phys. Chem. Chem. Phys.* **2011**, *13* (10), 4444–4451.

(11) Boccia, A.; Lanzilotto, V.; Di, C. V.; Zanoni, R.; Pescatori, L.; Arduini, A.; Secchi, A. *Phys. Chem. Chem. Phys.* **2011**, *13* (10), 4452–4462.

(12) Boccia, A.; Lanzilotto, V.; Di, C. V.; Zanoni, R.; Arduini, A.; Pescatori, L.; Secchi, A. *J. Nanosci. Nanotechnol.* **2011**, *11* (10), 9333–9339.

(13) Boccia, A.; D'Orazi, F.; Carabelli, E.; Bussolati, R.; Arduini, A.; Secchi, A.; Marrani, A. G.; Zanoni, R. *Chemistry* **2013**, *19* (24), 7999–8006.

(14) Li, Y.; Lin, X. *Sensors Actuators B Chem.* **2006**, *115* (1), 134–139.

(15) Cui, K.; Song, Y.; Yao, Y.; Huang, Z.; Wang, L. *Electrochem. commun.* **2008**, *10* (4), 663–667.

(16) Mattiuzzi, A.; Jabin, I.; Mangeney, C.; Roux, C.; Reinaud, O.; Santos, L.; Bergamini, J.-F.; Hapiot, P.; Lagrost, C. *Nat. Commun.* **2012**, *3*, 1130.

(17) Cannizzo, C.; Wagner, M.; Jasmin, J.-P.; Vautrin-Ul, C.; Doizi, D.; Lamouroux, C.; Chaussé, A. *Tetrahedron Lett.* **2014**, *55* (31), 4315–4318.

(18) Toumi, N.; Bonnamour, I.; Joly, J.-P.; Finqueneisel, G.; Retailleau, L.; Kalfat, R.; Lamartine, R. *Mater. Sci. Eng. C* **2006**, *26* (2-3), 490–494.

(19) Bélanger, D.; Pinson, J. *Chem. Soc. Rev.* **2011**, *40* (7), 3995–4048.

(20) Ghanem, M. A.; Chrétien, J.-M.; Pinczewska, A.; Kilburn, J. D.; Bartlett, P. N. *J. Mater. Chem.* **2008**, *18* (41), 4917.

(21) Kates, A. S. . A. F. *Solid-Phase Synthesis: A Practical Guide*; 2000.

(22) Niwa, M.; Morikawa, M.; Nabeta, T.; Higashi, N. *Macromolecules* **2002**, *35* (7), 2769–2775.

(23) Casnati, A.; Domiano, L.; Pochini, A.; Ungaro, R.; Carramolino, M.; Oriol Magrans, J.; M. Nieto, P.; López-Prados, J.; Prados, P.; de Mendoza, J.; G. Janssen, R.; Verboom, W.; N.Reinhoudt, D. *Tetrahedron* **1995**, *51* (46), 12699–12720.

(24) Ghanem, M. A.; Chrétien, J.-M.; Kilburn, J. D.; Bartlett, P. N. *Bioelectrochemistry* **2009**, *76* (1-2), 115–125.

(25) Groppi, J.; Bartlett, P. N.; Kilburn, J. D. **2015**, 1–8.

(26) Fernández, I.; Araque, E.; Martínez-Ruiz, P.; Di Pierro, P.; Villalonga, R.; Pingarrón, J. M. *Electrochem. commun.* **2014**, *40*, 13–16.

(27) Orazem, M. E.; Tribollet, B. *Electrochemical Impedance Spectroscopy*; John Wiley & Sons, Inc.: Hoboken, NJ, USA, 2008.

(28) Credi, A.; Dumas, S.; Silvi, S.; Venturi, M.; Arduini, A.; Pochini, A.; Secchi, A. *J. Org. Chem.* **2004**, *69* (18), 5881–5887.

(29) Ranganathan, S.; McCreery, R. L. *Anal. Chem.* **2001**, *73* (5), 893–900.

(30) Gonzalez, J. J.; Ferdani, R.; Albertini, E.; Blasco, J. M.; Arduini, A.; Pochini, A.; Prados, P.; De Mendoza, J. *Chem. - A Eur. J.* **2000**, *6* (1), 73–80.

(31) Arduini, A.; Ciesa, F.; Fragassi, M.; Pochini, A.; Secchi, A. *Angew. Chemie, Int. Ed.* **2005**, *44* (2), 278–281.

(32) Arduini, A.; Bussolati, R.; Credi, A.; Pochini, A.; Secchi, A.; Silvi, S.; Venturi, M. *Tetrahedron* **2008**, *64* (36), 8279–8286.

(33) Arduini, A.; Bussolati, R.; Masseroni, D.; Royal, G.; Secchi, A. *European J. Org. Chem.* **2012**, *2012* (5), 1033–1038.

# The Author

Guido Orlandini studied chemistry at Università degli Studi di Parma, where he reached the graduation (110/100 cum laude), under the supervision of Prof. Arturo Arduini and Prof. Andrea Secchi, in 2012 with a thesis entitled "Synthesis of new Calix[6]arene derivatives for the modelling of supramolecular devices". Since 2013, he is carrying out his Ph.D. at the University of Parma under the supervision of Prof. A. Arduini. His PhD thesis is focusing on the design, synthesis, and characterization of calix[6]arene-based pseudorotaxanes and molecular machine prototypes. During this period he joined for five months (September 2014 – February 2015) as a Ph.D. visiting student the group of Prof. Jeremy Kilburn at the School of Biologic and Chemical Sciences of "Queen Mary University of London", London (UK). The results of the research conducted during its Ph.D. period are described in this thesis.

## List of Publications

1. Arduini, A.; Orlandini, G.; Secchi, A.; Credi, A.; Silvi, S. and Venturi, M. (**2014**) *Calix-Based Molecular Machines and Devices*. In: Reedijk, J. (Ed.) Elsevier Reference Module in Chemistry, Molecular Sciences and Chemical Engineering. Waltham, MA: Elsevier

2. "Synthesis by Ring Closing Metathesis and Properties of an Electroactive Calix[6]arene [2]Catenane", Guido Orlandini, Valeria Zanichelli, Andrea Secchi, Arturo Arduini, Giulio Ragazzon, Alberto Credi, Margherita Venturi, and Serena Silvi; published online on *Supramolecular Chemistry*.

3. "Constitutionally Isomeric Oriented Calix[6]arene-Based Rotaxanes: Synthesis, Characterization and Dynamic Properties", Valeria Zanichelli, Giulio Ragazzon, Guido Orlandini, Serena Silvi, Margherita Venturi, Alberto Credi, Andrea Secchi, Arturo Arduini, Paola Franchi, Marco Lucarini; published online on *European Journal of Organic Chemistry*.

## *Acknowledgements*

*I would like to express my special appreciation and thanks to my supervisor Prof. Arturo Arduini, who has been a tremendous mentor for me. I would like to thank you for all the enthusiasm you put in giving me advices on my projects and on my Ph.D. career. I would also like to thank Prof. Andrea Secchi for all the teaching on theoretical and practical organic chemistry, and for the assistance during the NMR experiments.*

*A special thanks to Prof. Alberto Credi and his research group at University of Bologna, especially Ph.D. student Giulio Ragazzon, for their valuable contribution for the study of the photo- and electrochemical properties of the molecules described in this thesis.*

*I would especially like to thank Prof. Jeremy Kilburn for hosting me as Ph.D visiting student at Queen Mary University of London; I felt like I was a real member of Prof. Kilburn's research group. A special thanks to Dr. Jessica Groppi for introducing me in the laboratories and for all the teachings on the electrochemical techniques.*

*A remarkable thank to my Ph.D. student colleagues Francesco and Valeria and to all the students who attended Lab.49 for their thesis period and helped me to develop my projects: Francesco, Alessandro, Margherita, Guido and Andrea.*

*Finally, a special thank to my family; words can not express how grateful I am to my father Giuseppe, my mother Sandra, my brother Pietro, my aunt Giancarla for supporting me for everything, and especially I can't thank you enough for encouraging me throughout this experience. Thank you Maria Elena for always be so kind and cheering me up. Thank you to my nephew Tommaso for always smiling at me.*

*Guido*